A COMPUTER SIMULATION OF THE PULMONARY MICROVASCULAR EXCHANGE SYSTEM - ALVEOLAR FLOODING

By

FRANCISCUS R. C. HEIJMANS

B.E.Sc., University of Western Ontario, London, 1982

A THESIS SUBMITTED IN PARTIAL FULFILLMENT OF

THE REQUIREMENTS FOR THE DEGREE OF

MASTER OF APPLIED SCIENCE

in

THE FACULTY OF GRADUATE STUDIES

(Department of Chemical Engineering)

We accept this thesis as conforming

to the required standard

THE UNIVERSITY OF BRITISH COLUMBIA

April 1985

In presenting this thesis in partial fulfilment of the requirements for an advanced degree at the University of British Columbia, I agree that the Library shall make it freely available for reference and study. I further agree that permission for extensive copying of this thesis for scholarly purposes may be granted by the head of my department or by his or her representatives. It is understood that copying or publication of this thesis for financial gain shall not be allowed without my written permission.

Department of Chemical Engineering

The University of British Columbia
1956 Main Mall
Vancouver, Canada
V6T 1Y3

Date 12/4/85

ABSTRACT

Previous models of the pulmonary microvascular exchange system (28,29) have been restricted to the study of fluid and solute exchange between the pulmonary microcirculation, interstitial tissue space, and lymphatics. In severe pulmonary edema the capacities of the lymphatics and tissue space are exceeded. The fluid and solutes entering the interstitium from the circulation will, then, be transported into the air space. The accumulation of fluid in the air space impairs the diffusion of gas (oxygen and carbon dioxide) between the air space and blood circulation; if this fluid accumulation is excessive a patient's health may be compromised.

In this thesis severe pulmonary edema is studied by including the air space as a fourth compartment into the interstitial model developed by Bert and Pinder (29).

A computer simulation of the four compartment (alveolar) model was developed on a digital computer. Tests of the model were made to study the effect of the parameters which were introduced into the alveolar model. These parameters include: a filtration coefficient that describes the alveolar membrane fluid conductivity, an extravascular fluid volume that represents the point at which fluid enters the air space, the alveolar fluid pressure at the onset of fluid flow into the air space, and the rate of alveolar fluid pressure

change relative to an alveolar fluid volume change. For each case the dynamic response of the exchange system was recorded. In addition, two types of pulmonary edema were simulated: 1) hydrostatically induced edema, and 2) edema induced by changes to the fluid and solute permeability of the porous membrane separating the circulatory and interstitial compartments.

Due to the limited data available on the interaction of the air space with the other three compartments of the pulmonary microvascular exchange system, only partial verification of the appropriate range of values of the alveolar model parameters and the predictions of the simulations was possible. The alveolar model developed in this thesis is an initial approximation but appears to provide a satisfactory approach for the inclusion of the air space in the pulmonary microvascular exchange system.

TABLE OF CONTENTS

TABLE OF CONTENTS (Cont.d)

TABLE OF CONTENTS (Cont.d)

TABLE OF CONTENTS (Cont.d)

LIST OF TABLES

LIST OF TABLES (Cont'd.)

LIST OF FIGURES

LIST OF FIGURES (Cont.d)

LIST OF FIGURES (Cont.d)

LIST OF FIGURES (Cont.d)

ACKNOWLEDGEMENTS

I would like to thank my supervisors, Dr. J.L. Bert and Dr. K.L. Pinder, for their guidance throughout the course of this work.

Thanks are also due to Dr. P. Paré and Dr. P. Dodek of the Pulmonary Research Unit at St. Paul's Hospital, who provided the medical perspective in this work.

The manuscript was typed by Mrs. M. Woschee and Mrs. K. Leslie, whose work is much appreciated.

The computer subroutines DLINE and BBLINE were generously provided by Dr. B. Bowen.

Finally, I would like to thank the Natural Sciences and Engineering Research Council of Canada for their financial support.

BACKGROUND

1.1 Introduction

Biological systems, because of their complex interactions and non-linear nature, are sometimes studied by a combination of experimental models and computer simulations. In this thesis the behaviour of the fluid and solute exchange system of the lungs is investigated by means of a computer simulation.

Figure 1 shows a schematic of the pulmonary microvascular exchange system (PMVES). It involves the exchange of fluid and solute between the main compartments of the lung, that is, the blood circulation, air space, tissue space (or interstitium), and lymphatics. The term microvascular refers to the circulating system of the small blood vessels. The interstitial compartment interacts directly with the other three compartments, which are assumed not to interact directly with each other. Separating the compartments are the vascular membrane - between the circulation and interstitium - the alveolar barriers - between the interstitium and air space - and the lymphatic capillary membrane - between the interstitium and lymph channel.

The pulmonary microvascular exchange system operates in conjunction with other physiological and biochemical systems to carry out the functions of the lung. The primary function of the lung is that of gas exchange, involving the countercurrent transfer of oxygen and carbon dioxide between the blood and air space.

Figure 1: Schematic of the Pulmonary Microvascular Exchange System: Illustrates Fluid-flow pathways (50)

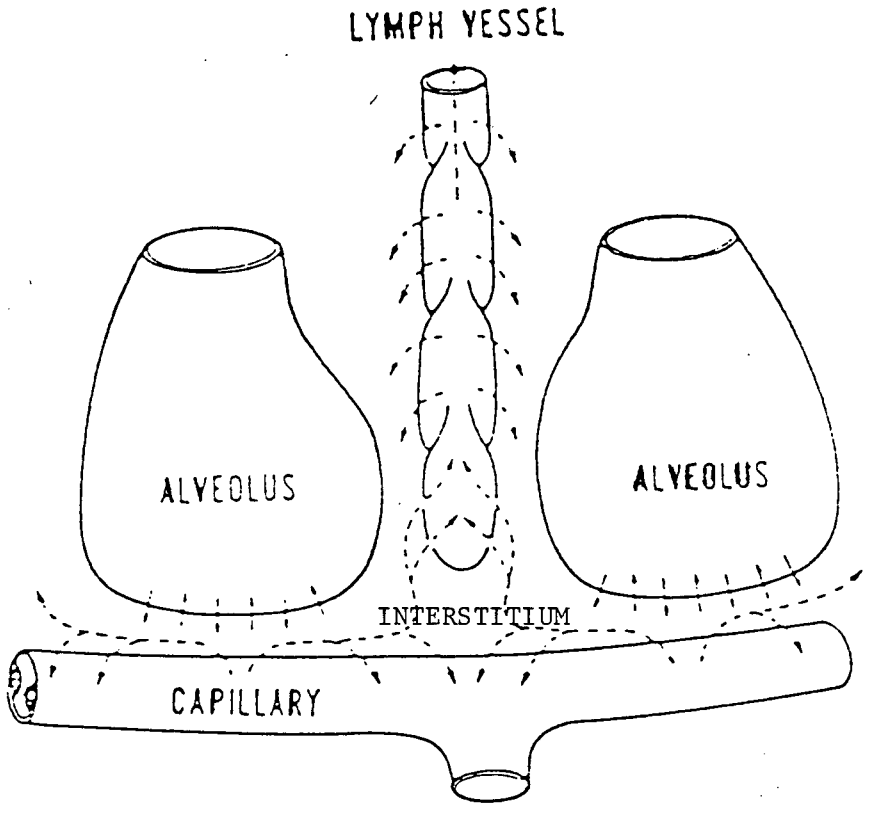

The following sections discuss the lung compartments, their components, and the barriers to flow of the pulmonary microvascular exchange system. A section outlining the exchange of fluid and solute between the compartments and the clinical importance of studying pulmonary fluid and solute exchange will also be presented.

1.2 The Circulation

1.2.1 The Pulmonary and Systemic Circulatory Systems

Circulation of blood in the body takes place in the pulmonary and systemic vascular systems. Figure 2 illustrates these two systems. The systemic circulation refers to the vascular network of the whole body where the blood is deoxygenated, while the pulmonary circulation is confined to the lungs where the blood is oxygenated. The heart combines the two circulatory systems to form a loop of continuous blood flow. The heart is composed of two halves with each half containing two chambers - an atrium and a ventricle. The right atrium of the right heart receives blood from the systemic circulation. The right ventricle then pumps the blood into the pulmonary vasculature. The oxygenated blood of the pulmonary system enters the left atrium of the left heart and is subsequently pumped through the systemic circulation by the left ventricle.

The primary function of the systemic circulation is to transport nutrients and oxygen to the body tissues, and remove the wastes, such as carbon dioxide.

Figure 2: Illustration of Pulmonary and Systemic Circulatory Systems (54)

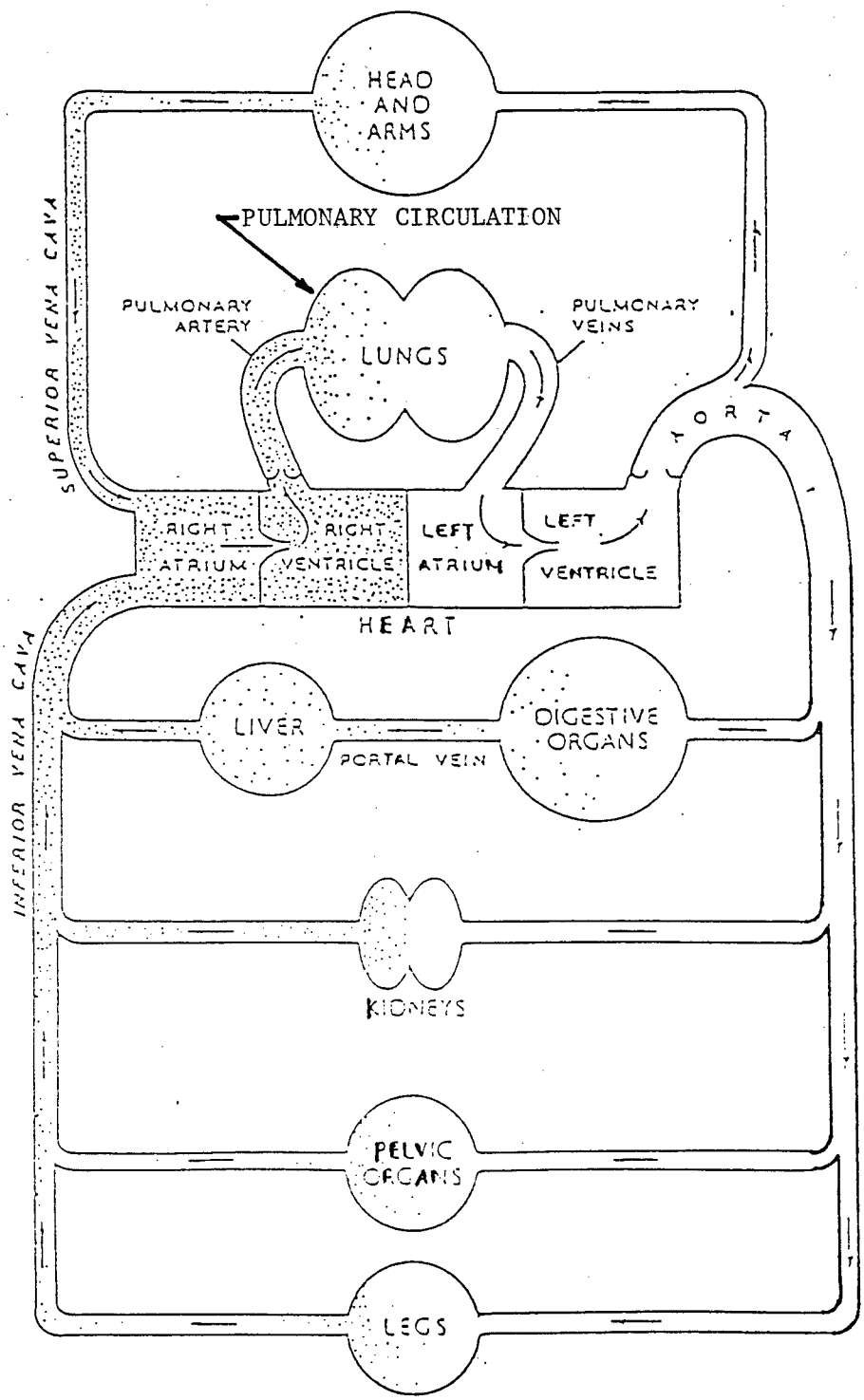

The pulmonary microvasculature (a network of small blood vessels), while supplying nutrients to the surrounding tissue, is also in intimate contact with the air spaces of the lungs. One of the purposes of this unique arrangement is to exchange the carbon dioxide of the incoming (oxygen deficient) blood for the oxygen present in the air space.

This thesis is concerned with the exchange of fluid and solute in the pulmonary microvasculature.

1.2.2 Physical Characteristics of Blood

Circulating through the vascular systems is blood: "a viscous fluid composed of cells and plasma" (1). The blood cells may be divided into two classes: the red blood cells which make up 99% of the cells, and the white blood cells. The primary function of these red blood cells is to transport hemoglobin, which in turn carries oxygen from the lungs to the tissues (1).

The plasma medium of the blood is almost identical in electrolyte composition to the lung interstitial fluid. The watery fluid contains electrolytes, nonelectrolytes and proteins. Figure 3 illustrates the composition of plasma and interstitial fluid. The electrolytes include the cations - sodium, potassium, calcium, and magnesium - and the anions - chloride, bicarbonate, phosphate, sulfate, and organic acid ions. Blood plasma and lung interstitial fluid differ from each other in their protein content which is greater in the blood plasma. Three major classes of proteins exist, based on

Figure 3: Composition of Blood Plasma and Interstitial Fluid (1)

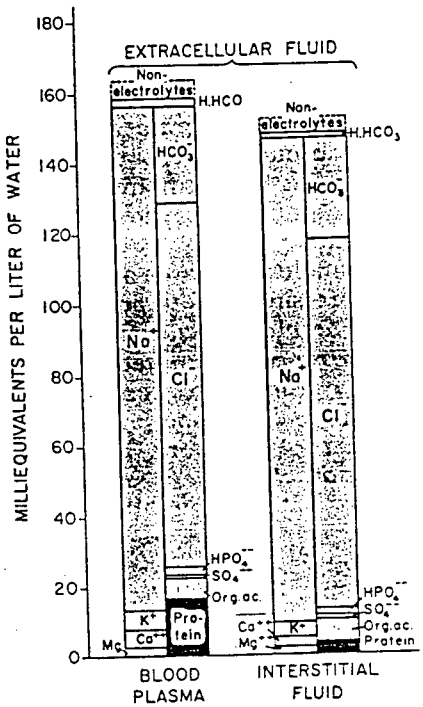

their molecular weights and functions; these classes are albumins, globulins and fibrinogen. The protein composition of blood plasma and lung interstitial fluid are given in Table 1. The content of the globulins and albumin exceeds that of fibrinogen. The primary function of albumin is to cause a colloid osmotic pressure at cell membranes (1).

1.2.3 The Pulmonary Circulation

The pulmonary circulation is composed of a branching network of blood vessels, as shown in Figure 4. Blood that enters the right heart is pumped through the pulmonary artery. The pulmonary artery branches into vessels of smaller diameter, eventually reaching the size of the arterioles - less than 100 μ in diameter - and then the capillaries - approximately 7 μ in diameter. At the level of the capillaries oxygen and carbon dioxide are exchanged between the blood in the capillaries and the gas of the air space. The capillary surface area available for exchange is 50 to 70 m^2, while that of the air space is about 20% larger (2). The capillaries then unite to form the venules - less than 200 μ in diameter. The venules combine further until they form the pulmonary vein which delivers the blood to the atrium of the left heart.

The vessels of the microvasculature are thought to be composed of arterial, capillary, and venous segments. As blood flows from the arterial to the capillary and then to the venous segments of the vessel, the fluid hydrostatic pressure decreases. The longitudinal

Table 1

Table 1: The Protein Composition of the Blood and Interstitial Fluid (29)

Protein	Blood (g/ml)	Interstitial Fluid (g/ml)
Albumin	.042	.025
Globulins	.027	.011
Fibrinogen(55)	0.003	N.A.
Total Protein	0.073	

N.A. - not available

Figure 4

a) Branching Network of Circulation (54)

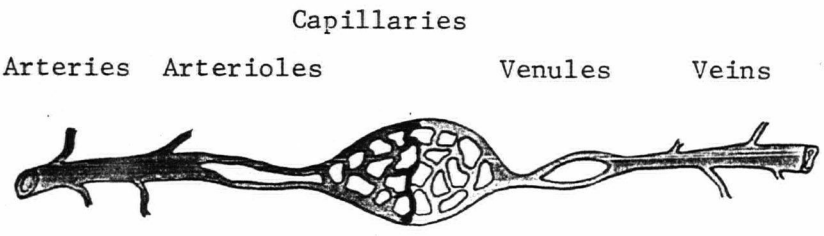

b) Pulmonary Circulation at level of Alveolus (54)

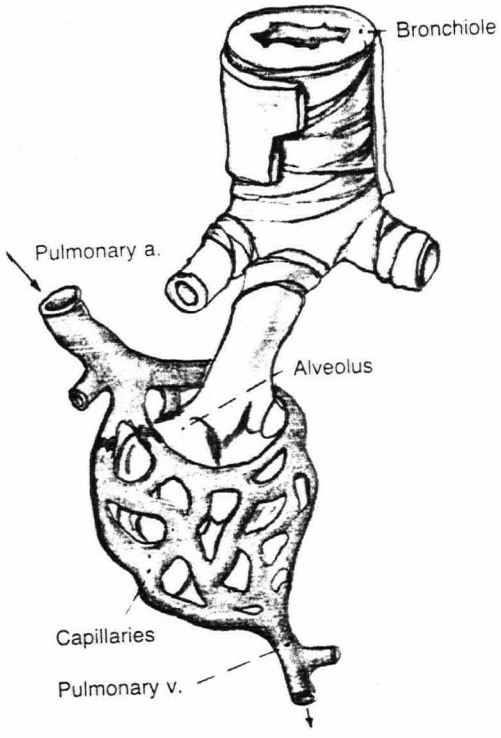

pressure profile of the blood vessel may be simply illustrated by assigning a hydrostatic pressure to the fluid of each vascular segment: PA for the arterial end, PMV for the capillary, and PV for the venous end. The pressures in descending order of value are PA > PMV > PV.

The capillary segment is in close contact with the air space, while the arterial and venous ends are less so; the diagrams of Figure 5a show the location of the three segments in relation to the air space. West, Dollery, and Naimark (3) proposed a Zone Model for the lungs, based on measurements of the relative values of PA, PV and the hydrostatic pressure of the gas in the air space PALV. In zone I, the air space pressure is greater than the arterial and venous pressures:

$$PALV > PA > PV \tag{1}$$

Figure 5a illustrates zone I. Under these conditions the capillary segment of the blood vessel will be collapsed; the capillary fluid pressure, PMV, will assume a value approximately equal to PALV. Therefore blood will not flow through the capillary since the pressure gradient that causes flow (PA - PALV) is negative. In zone II the air space pressure is between the arterial and venous pressures:

$$PA > PALV > PV \tag{2}$$

Figure 5b (i) shows the case when PALV is much larger than PV. At the downstream end of the capillary the capillary pressure will assume a value approximately equal to PALV. The pressure gradient causing

Figure 5: Illustration of Zone Model as Developed by West, Dollery and Naimark (3) (PA=arterial pressure; PV=venous pressure; PALV=alveolar pressure)

a) Zone I: PALV > PA > PV
·capillary collapsed

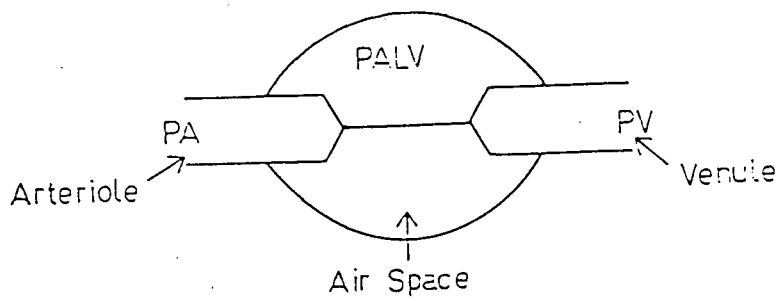

b) Zone II: PA > PALV > PV
·constriction at downstream end of vessel

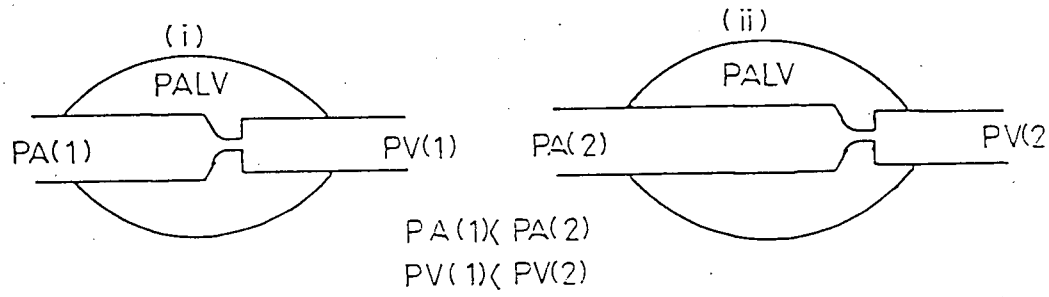

c) Zone III: PA > PV > PALV
·vessel held open

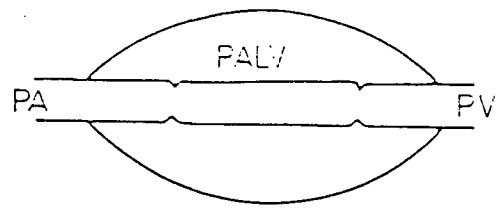

blood flow through the capillary becomes (PA - PALV). The capillary will be constricted at the downstream end. If PA and PV are elevated, such that PV approaches PALV, the condition shown in Figure 5b (ii) results. The pressure gradient causing blood flow will remain (PA - PALV) since PMV is approximately equal to PALV, but the constriction moves further downstream. The final zone, zone III, has the following relationship:

$$PA > PV > PALV \tag{3}$$

The pressure gradient causing blood flow now becomes (PA - PV). The capillary fluid pressure, PMV, will be between PA and PV, and therefore exceed PALV. The greater PVM is above PALV the more the vessel will distend. Figure 5c shows the vessel under zone III conditions.

West, Dollery and Naimark (3) have suggested that the human lung may be horizontally divided into zones. The blood circulation is affected by gravity. In the upper section of the lung under normal conditions zone I conditions prevail; there is no blood flow through the vessels. Zone II conditions prevail in the middle section of the lung. At the junction of zone I and zone II PALV equals PA. At horizontal positions of the lung lower than this junction of zones I and II the hydrostatic pressure of the blood rises due to gravity. Therefore, at vertical positions lower than the junction of zones I and II PA and PV increase; (PA - PALV) increases and (PALV - PV) decreases. The blood flow increases as the driving force causing flow

(PA - PALV) increases. When PV equals PALV there is no circulatory constriction and the pressure gradient causing flow becomes (PA - PV). Zone III conditions prevail in the lower section of the lung. At lower positions in zone III the blood flow rises due to the distension of the vessels. Figure 6 illustrates the Zone Model, showing how blood flow changes at different positions in the lung.

1.3 The Vascular Membrane

1.3.1 Structure of the Vascular Membrane

The vascular membrane, shown in Figure 7, separates the blood circulation from the interstitium. The membrane is composed of an endothelial cell layer that is in contact with the circulation, and an underlying basement membrane.

"Whenever the endothelial cells come into contact, there are junctions that are continuous along the line of contact. These vary from "tight" junctions to "gap" junctions, which themselves vary from the tight to the "leaky" type, the particular condition depending on the width of the junction." (4)

Wissig and Charonis (5) suggest that the basement membrane functions as a "supportive role for the endothelial lining of the capillaries". The basement membrane may "stabilize the wall, assisting it to withstand the hydrostatic pressure of the perfusing blood".

Figure 6: Illustration of Blood Flow at Different Heights of the Lung (Pa = arterial pressure, P_A = Air Pressure, P_v = venous pressure)(3)

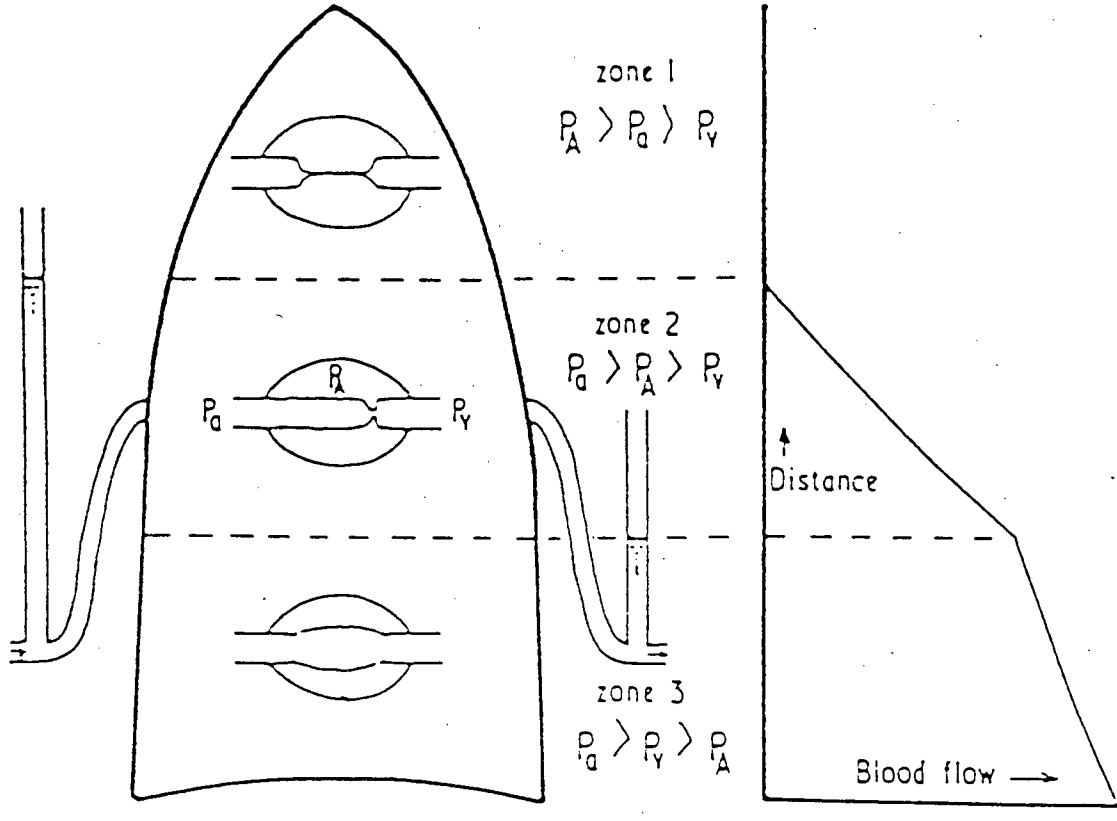

Figure 7: Illustration of vascular membrane separating Interstitium and Circulation: Values of hydrostatic (PMV, PPMV) and oncotic (PIMV, PIPMV) pressures at normal conditions.

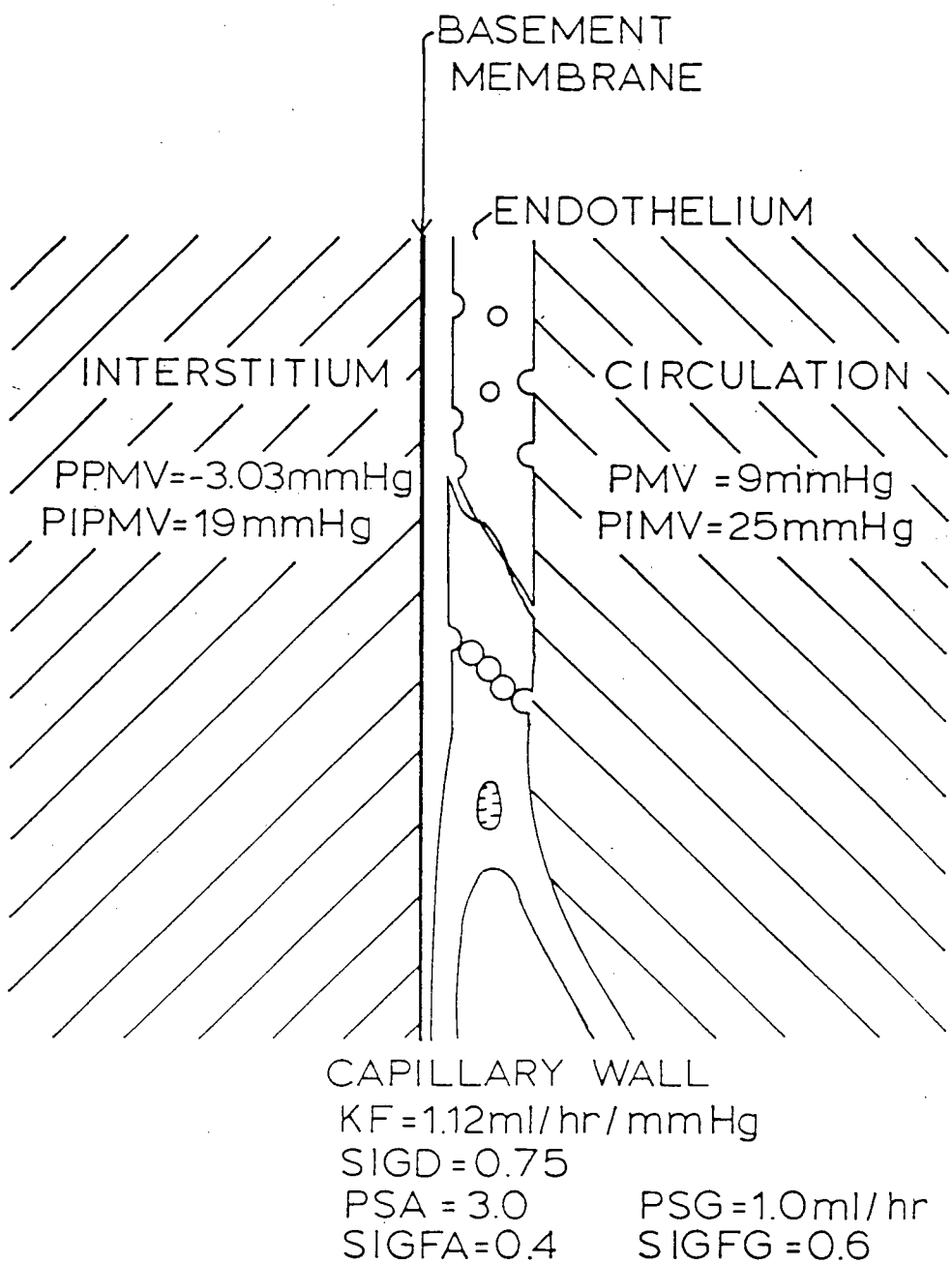

1.3.2 Physical Properties of the Vascular Membrane

Studies of the permeability of the vascular membrane to fluid and solute rarely differentiate between the permeabilities of the endothelial cell layer and the basement membrane. In the remainder of this thesis the cell layer and basement membrane will be lumped together, and referred to as either the vascular or endothelial membrane.

The vascular membrane of the pulmonary microvasculature is classified as being "leaky" (6); fluid and solute are transported across the membrane, generally from the circulation to the interstitium. Among the factors that determine the ability of a solute to cross the endothelium are the solute size, electrical charge of the solute (2), distribution of the size of the membrane openings and the population of these openings. In the case of globulins and albumin - with an average radius of about 5.2 and 3.7 nm, respectively - a larger fraction of albumins cross the vascular membrane as compared to globulins.

The fraction of solute crossing the vascular membrane may be obtained experimentally by comparing the solute concentration in the interstitium to that of the plasma. The solute concentration of the interstitium is generally approximated by the solute concentration in lung lymph, since interstitial samples are difficult to obtain experimentally. Yoffey and Courtice (7) have obtained estimates of the concentration ratios: the ratio of the interstitial concentration of albumin to the plasma albumin concentration was 0.80, while the

interstitial-to-plasma concentration ratio for globulin was 0.55. These results indicate that a greater fraction of plasma albumin crosses the vascular membrane than plasma globulins.

1.4 The Interstitium

1.4.1 Structure and Composition of the Interstitium

The interstial space of the lung is that space which is between the vascular membrane and the alveolar membrane. The components of the interstitium are numerous. Figure 8 shows a section of the interstitium. The basic structure involves a "skeleton of collagen fibres"; the space between the fibres is an interstitial matrix of water, salts, plasma proteins and glycosaminoglycans (8).

The collagen fibres range in diameter from 0.5 μ to 1.0 μ. The actual arrangement of the fibres in tissue is not well known. Bert and Pearce (9) state that the fibres in many tissues are organized into bundles of parallel fibres; these "bundles may be assembled into highly ordered arrays, as in cornea, or into felt-like mats randomly oriented parallel to the surface, as in dermis" (10). "The main functional effects of the collagen fibres are that they resist changes in tissue configuration and volume, they exclude proteins, and they immobilize the glycosaminoglycans (see below) of the interstitial matrix" (8).

The interstitial matrix may be described with two major phases in the interstitium: one a free fluid and the other a complex gel structure. The free fluid phase is comparable to the plasma fluid of the blood, except that the interstitial protein concentration differs.

Figure 8: Cross-sectional View of Interstitium and Contents, Epithelial and Endothelial Membranes (RBC-red blood cell; WBC-white blood cell)(55)

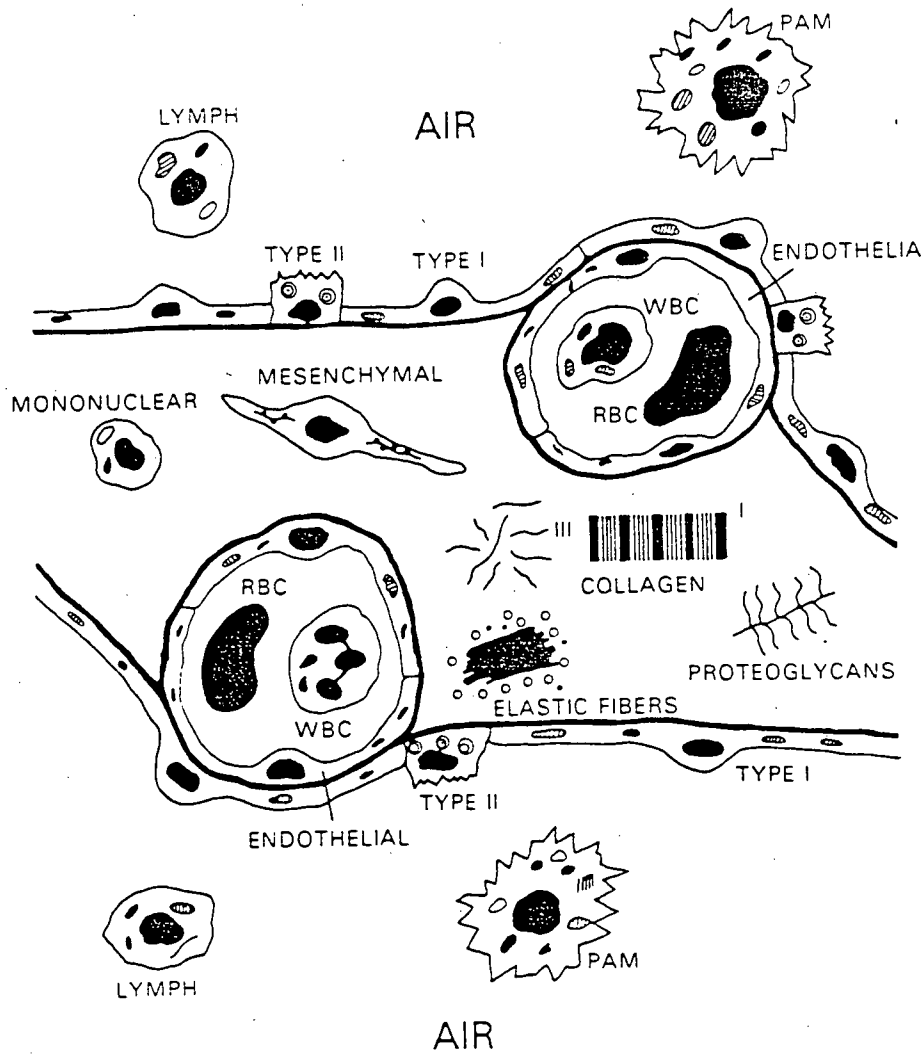

The gel phase is composed of macromolecules called glycosaminoglycans or GAGs. The primary GAG is hyaluronic acid. Hyaluronic acid is an unbranched, random coil macromolecule. In tissue, hyaluronic acid occupies a volume 1000 times that of its own unhydrated structure (8). Other GAGs, such as chondroitin sulphate, are present in smaller quantity; they are attached as side branches to a protein backbone, forming proteoglycans. The GAGs show noticeable "internal entanglement" (8). The collagen fibres are entangled with the GAGs, and immobilize the mass. Thus, a gel-like structure results which exhibits solid-like behaviour (9).

1.4.2 Volume Exclusion

"Volume exclusion refers to a property of matter that prevents two materials from occupying the same space at the same time" (10). The interwoven latticework of the fibres, primarily collagen, in conjunction with hyaluronate, contribute to the exclusion phenomenon by limiting the "extravascular-extracellular space accessible to a plasma protein" (9). Therefore, the volume of the interstitial space available to proteins is reduced, which results in an increase in the effective protein concentration.

The exclusion phenomenon may be explained by: 1) the rod and sphere model, and 2) the sphere in a random network of rods model. In the former model, shown in Figure 9a, the rod represents an isolated collagen bundle in the tissue while the protein is approximated by the sphere. The protein will be excluded from the volume occupied by the rod, and the volume that is one protein radius from the rod - shown by

Figure 9: Models of Volume Exclusion in the Interstitial Space (9)

a) Rod and Sphere Model (thatched area is excluded space)

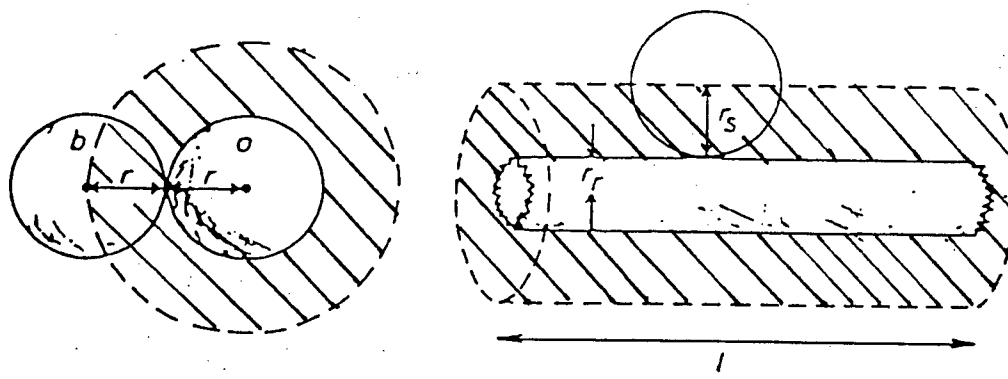

b) Sphere in a Random Network of Rods Model (thatched area is excluded space)

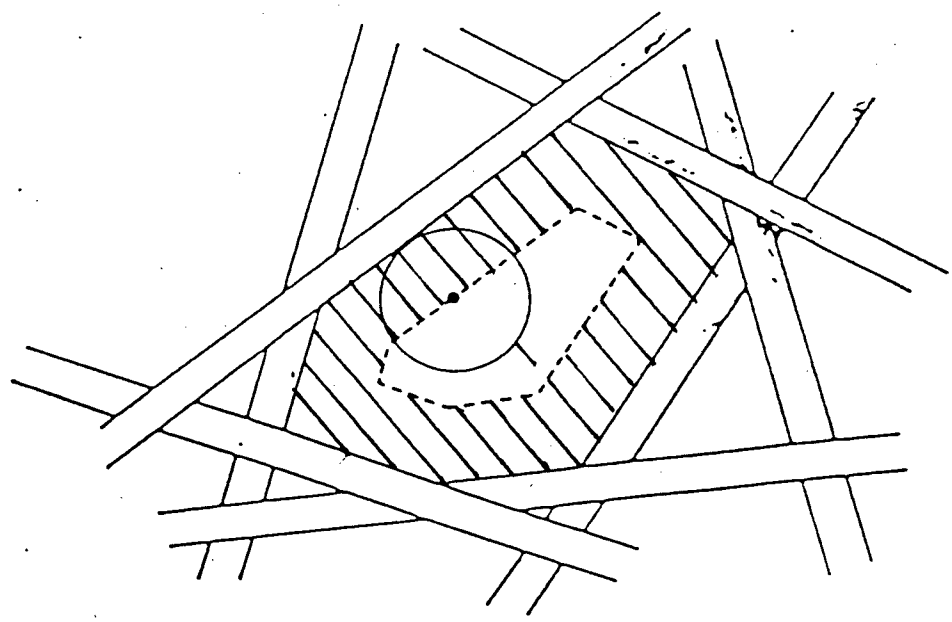

the shaded area in the side and front view given in Figure 9a. The collagen bundles may be arranged into felt-like mats, with the bundles randomly oriented. In this case the bundles may be represented as a random network of rods, hence, the sphere in a random network of rods model. Figure 9b shows the sphere in a random network of rods model - the centre of the sphere (protein) is excluded from the shaded area. In both models the excluded space (volume) is dependent on the size of the protein. Thus in either model, globulins, with an average diameter of 5.2 nm will be excluded from a larger volume than albumins having an average diameter of 3.7 nm.

The effective concentrations of the proteins may be calculated from the interstitial protein weights and the volumes available to the proteins. The colloid osmotic pressure calculated from the effective protein concentration will be greater than that determined from the protein concentration that does not account for the excluded volume of the proteins, i.e., in the latter case, the concentration uses the interstitial volume, while in the former case the volume is the interstitial volume less the excluded volume.

1.4.3 The Alveolar and Extra-alveolar Tissue Sub-compartments

The interstitium is subdivided into alveolar and extra-alveolar sub-compartments, as shown in Figure 10. The sub-compartments are distinguished by at least two factors: 1) the effect of lung inflation (or a rise in the hydrostatic pressure of the air space) on the tissue hydrostatic pressure, and 2) the tissue compliance curves of the two sub-compartments.

Figure 10: Schematic of Pulmonary Microvascular Exchange System showing sub-compartments of Interstitium and Circulation and surfactant layer lining air space (PALV-alveolar (gas) pressure; PAS=alveolar fluid pressure; PPMV=pressure of alveolar interstitial fluid; PEA=pressure of extra-alveolar interstitial pressure; PMV=microvascular pressure) (2)

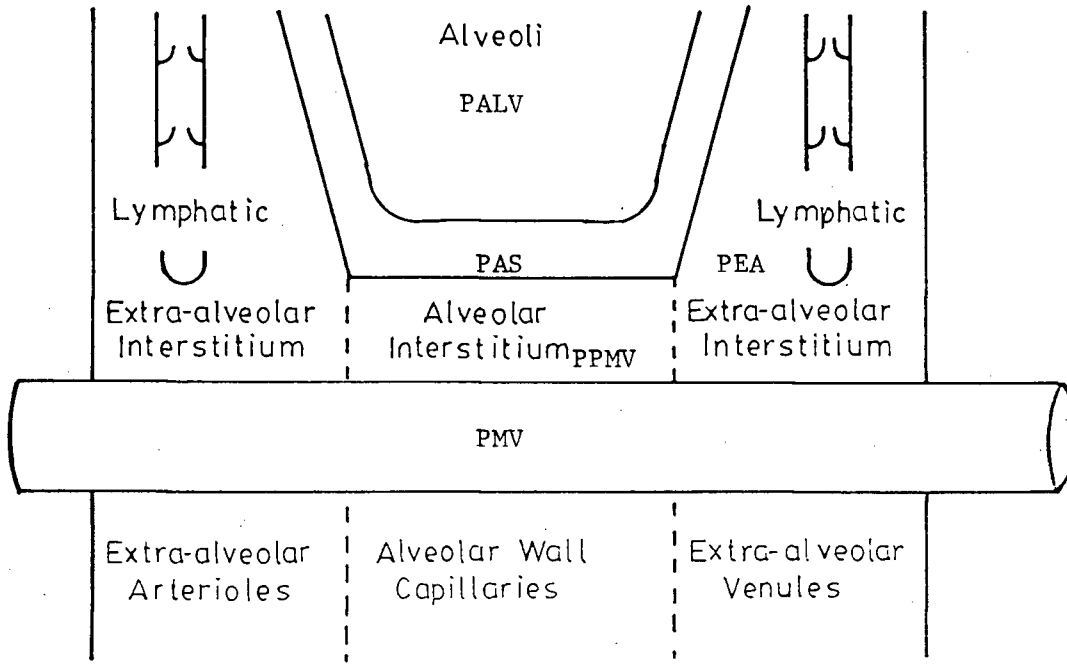

First, the alveolar tissue sub-compartment lies in close proximity to the alveoli (or air sacs) of the air space. The extra-alveolar interstitium is not necessarily adjacent to the air space. The result of this arrangement is the different responses of the hydrostatic pressures of the sub-compartments to an increase in the air pressure of the air space. Lai-Fook (11), and Parker, Guyton and Taylor (12) have suggested that the alveolar tissue hydrostatic pressure (PPMV) assumes a value related to the air pressure (PALV). The air space is lined with a surfactant fluid that produces an alveolar tissue pressure slightly less than PALV (see section 1.7.2). The hydrostatic pressure of the extra-alevolar tissue (PEA) is less than the pressure of the alveolar tissue (13). Howell, et al. (14), Hida, et al. (15) and Goldberg (16) have observed experimentally that PEA decreases with a rise in PALV; reasons for this decrease have been related to the configuration of the air space and blood vessels (14), but generally remain unclear. The effect of a rise in the air pressure, PALV, is, then, an equivalent rise in the alveolar tissue hydrostatic pressure, PPMV, and a drop in the extra-alveolar hydrostatic pressure, PEA.

Second, the tissue compliance curves of the two subcompartments differ in shape and value. Tissue compliance is defined as the change in extravascular-extracellular (EVEA) fluid volume relative to the change in tissue fluid pressure, i.e. ($\Delta V/\Delta P$). Prichard (17) gives hypothetical complicance curves for the alveolar and extra-alveolar tissue spaces, as shown in Figure 11. Figure 11 illustrates that for any tissue fluid volume less than point D the alveolar tissue

Figure 11: Compliance Curves of Alveolar and Extra-alveolar Tissue Sub-compartments - Alveolar Flooding Occurs When Point C' is reached. (17)

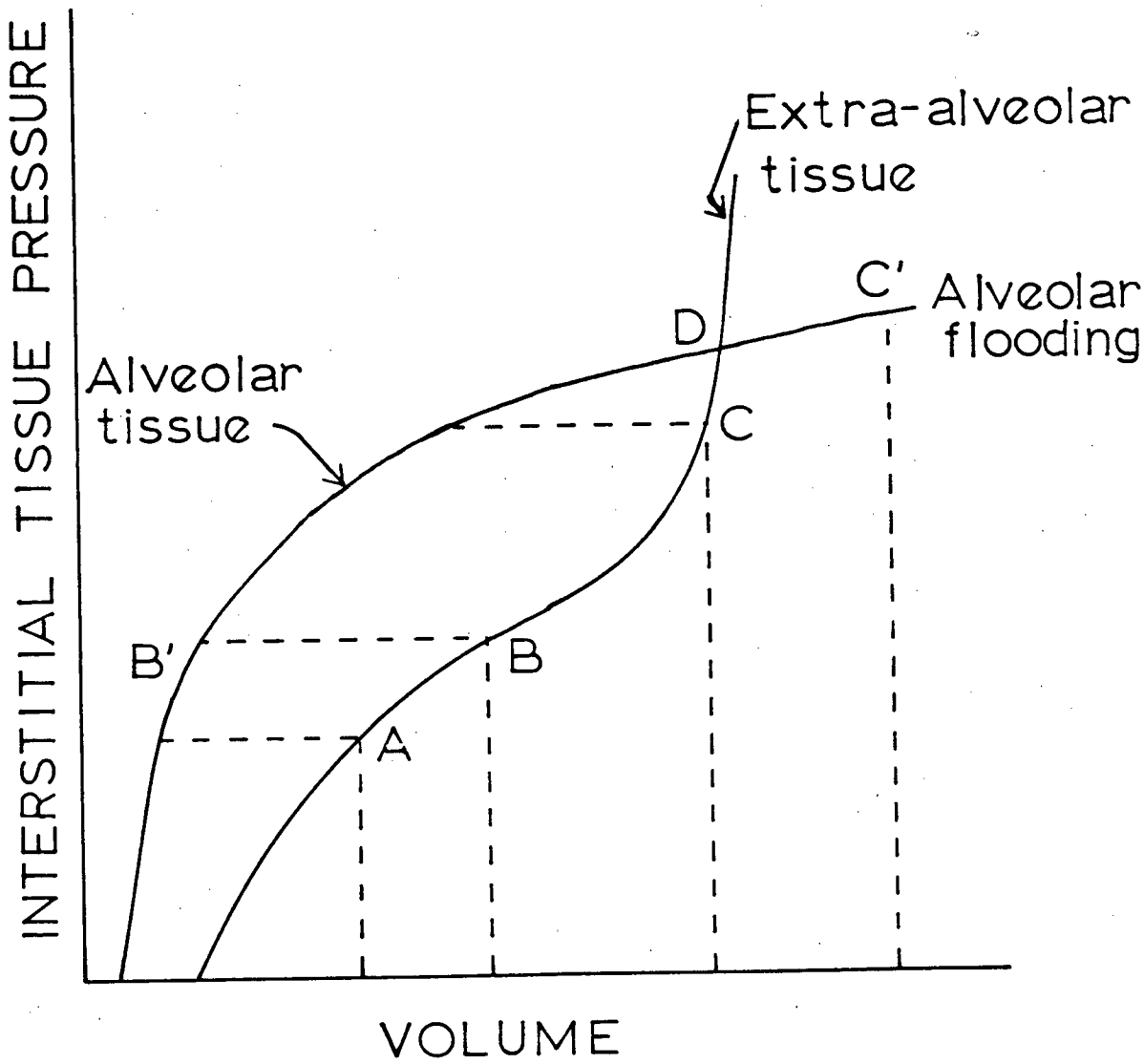

hydrostatic pressure (PPMV) is greater than the extra-alveolar tissue hydrostatic pressure (PEA). The pressure gradient that results will cause fluid to drain preferentially from the alveolar tissue to the extra-alveolar tissue.

The tissue compliance for each sub-compartment varies as fluid accumulates in the tissue. Both hypothetical curves in Figure 11 illustrate a low compliance (low $\Delta V/\Delta P$) for volumes less than that at point A on the extra-alveolar tissue compliance curve and point B^1 on the alveolar tissue compliance curve. In this low compliance region it is postulated (18) that the gel phase - of glycosaminoglycans (GAGs) - is compressed, such that as the fluid volume rises in the low compliance region the gel is returning to its neutral states. As fluid volume increases from points A and B^1 the compliance curves of the extra-alveolar and alveolar tissues, respectively, undergo a transition to a higher compliance. In the region of high compliance it is hypothesized (18) that the GAGs fragment as the tissue expands; the fluid volume rises sharply with little change in the tissue fluid pressure. In the extra-alveolar tissue the high compliance proceeds until the fluid volume reaches point C, whereupon maximum expansion of tissue elements has occurred. The extra-alveolar tissue returns to a low compliance, and the rise in tissue fluid pressure is high for further increases in fluid volume. The alveolar tissue continues to expand under a high compliance for fluid volumes beyond point B^1. When the tissue elements are stretched to their upper limit the fluid empties into the air space which has a large capacity; thus enabling the alveolar tissue compliance to remain high.

1.5 The Lymphatics

1.5.1 Structure of the Lymphatics

The lymphatics provide drainage channels for the fluid that enters the interstitium. Figure 10 illustrates that the terminal lymphatic capillaries are situated in the extra-alveolar interstitium, but not the alveolar interstitium. The fluid and solute that is transported across the vascular membrane into the alveolar tissue space must, therefore, flow through the tissue space to reach the lymphatics; as noted in the previous section a pressure gradient from the alveolar to extra-alveolar interstitium causes this flow of fluid.

The lymphatic capillary membrane is assumed to be extremely permeable to fluid and solute (19). The membrane is composed of an endothelial cell layer and an underlying basement membrane. The basement membrane is "poorly developed, and is commonly absent, or at best, discontinuous" (19) and therefore, does not provide significant resistance to solute and fluid flow. Figure 12 shows that anchoring filaments are attached to the cellular wall, and embedded in the surrounding tissue. When the perilymphatic tissue expands, due to fluid accumulation, the filaments maintain the cellular junctions open, and the vessel does not collapse (17,18). The tissue fluid is then able to continue flowing into the lymphatic vessel. As the fluid moves downstream through the lymph vessel it is prevented from returning to the terminal lymphatic end by lymphatic valves (Figure 12).

Figure 12: Structrual Features of a Terminal Lymphatic (18)

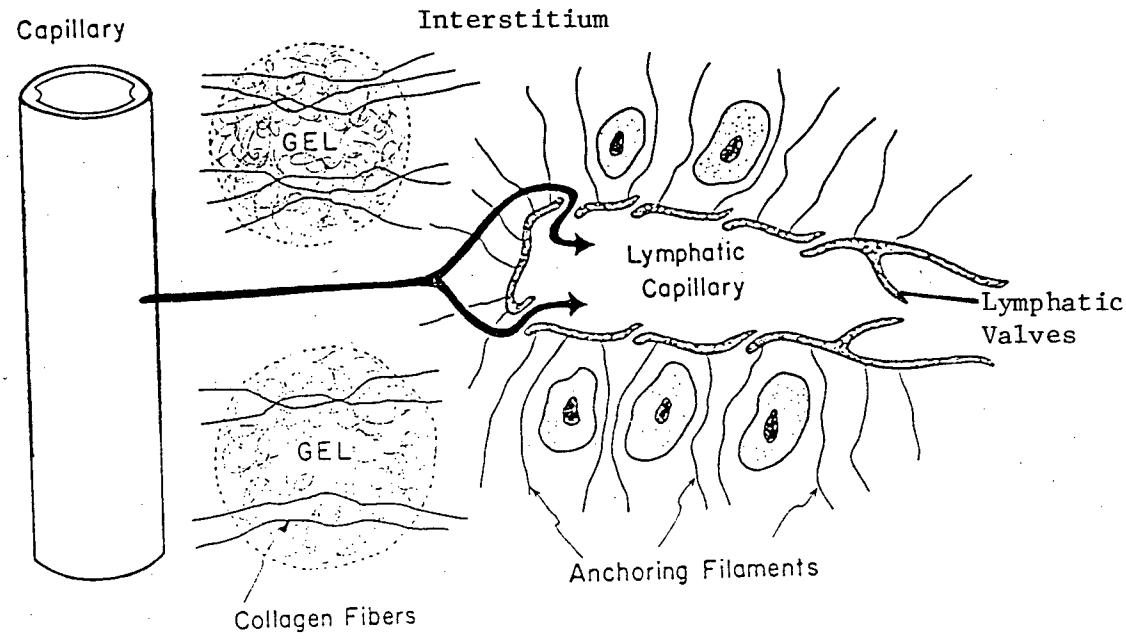

1.5.2 Contractility and Pumping in Lymphatic Vessels

To further facilitate the drainage of fluid and solutes there is a contractile and pumping motion of the lymphatic capillaries produced by muscular contractions, respiration, tissue movements, and an intrinsic pumping mechanism (17,19).

The operation of the intrinsic pumping mechanism is not clearly understood. Guyton (18) suggested the following explanation of the mechanism: "As fluid accumulates in the tissue space it expands the tissue. The anchoring filaments of the lymphatic capillaries, embedded in the tissue, become expanded along with the expansion of the tissues, thereby creating a suction inside the lymphatic capillaries. This suction pulls fluid inward through the (openings) of the lymphatic capillary, the inward movement of fluid causing the flap valves of the lymphatic membrane cells (see Figure 12) to open inward". Guyton then postulates that the fluid-filled lymphatic capillary will be compressed by the fluid in the surrounding tissue, raising the pressure at the capillaries end, and forcing the fluid forward into the collecting lymphatic.

The force that propels the fluid forward into the collecting lymphatic may alternatively be the respiration movements or muscular contractions.

1.6 The Air Space

1.6.1 Arrangement of the Air Space

Figure 13a illustrates that the air space is composed of a branching network of air ducts (or airways). Air enters via the mouth or nose and passes through the trachea. The trachea continues to the hilum of the chest, whereupon the duct bifurcates into the left and right main bronchial ducts (bronchi); the main bronchi lead to the left and right lung units. The left and right lung units are composed of individual lung segments or lobes (Figure 13b). Lobar bronchi branch from the left and right main bronchi to each lobe. Each lobar bronchi branches into terminal bronchioles and then respiratory bronchioles (Figure 13a). The respiratory bronchioles divide into alveolar ducts. At the periphery of the alveolar ducts are air sacs or alveoli. There are about 300 million alveoli, each having an equivalent diameter of 25 to 30 μ (17). It is at the level of the alveolus that the gas exchange occurs between the air space and blood circulation.

The major sites for fluid and solute exchange are located at the level of the respiratory units, that is, the respiratory bronchiole, alveolar ducts and alveoli.

Figure 13a: Branching Network of Air Space (54)

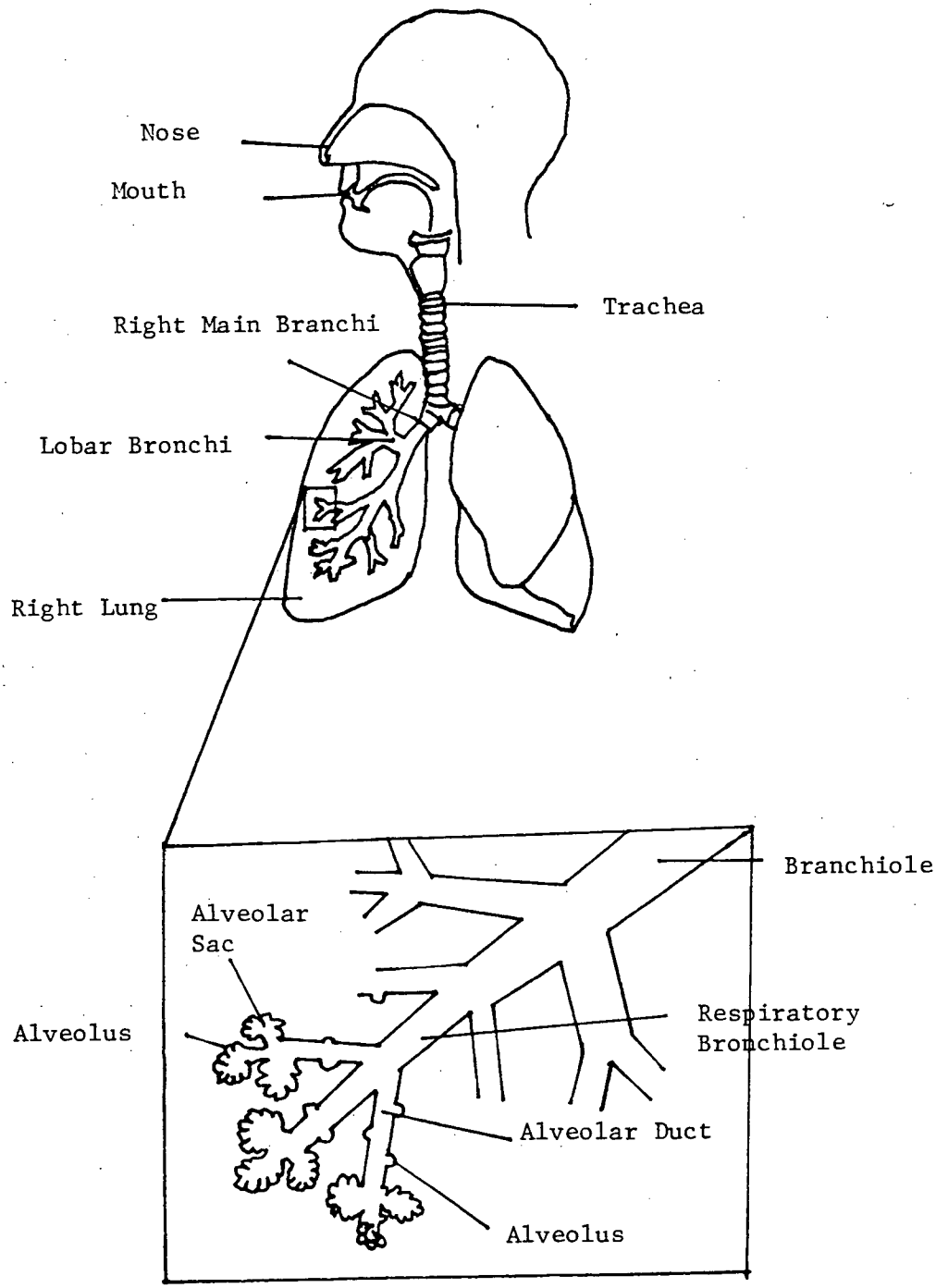

Figure 13b: Lobes, lobules and bronchopulmonary segments of the Lungs (54)

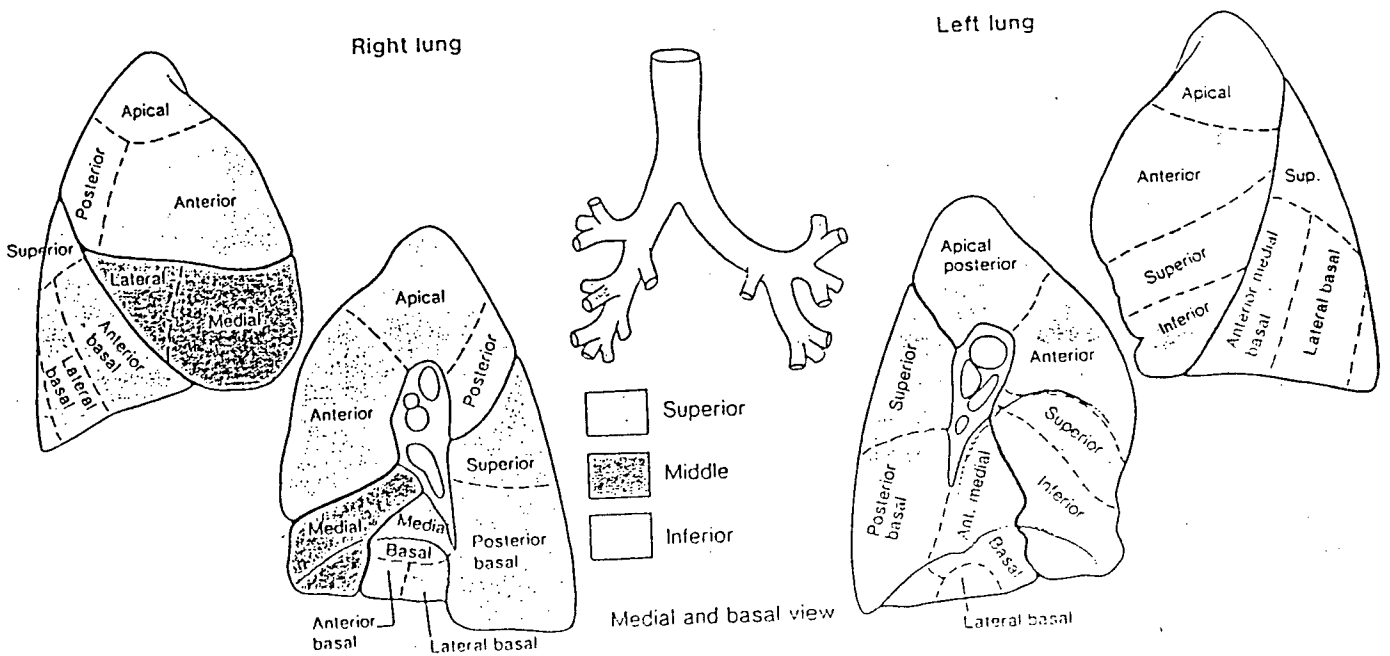

1.7 Barriers Between the Interstitial Space and Air Space

1.7.1 Alveolar Membrane

The alveolar membrane is composed of a cellular layer and a basement membrane. The cells of the membrane, primarily of squamous type I, normally form continuous tight junctions. The membrane behaves functionally as though it contained water-filled pores having a radius between 0.6 and 1.0 nm (6,20). Therefore the transport of water across the alveolar membrane is possible.

Although water crosses the epithelium, it does not accumulate in excess in the air space; there must be mechanisms to remove the water. The action of the surfactant lining the epithelium functions as one possible means to prevent fluid accumulation (see sections 1.7.2 and 3.6). Another mechanism to remove the water is evaporation to the inspired air. However, the inspired air becomes completely humidified in the upper airways; therefore, only a small amount of water will be removed by evaporation (17).

1.7.2 Surfactant Lining the Wall of the Air Space

Two secretions line the walls of the respiratory unit: the alveolar wall (of the alveoli) is covered with a surfactant, while the walls of the respiratory bronchiole are lined with the secretions of the mucous glands, goblet cells, and Clara cells (17).

It is the surfactant lining of the alveolar wall that is believed to play an important role in the mechanics of the lung and in pulmonary microvascular exchange (21). The surfactant is a surface

active lipoprotein - primarily composed of dipalmitoly lecithin (DPL) - that has a low surface tension of 24-34 dynes/cm (21); water characteristically has a surface tension of 68 dynes/cm. The advantage of the lower surface tension is illustrated by the Laplace equation developed for a spherical gas bubble

$$\Delta P = PG - PL = \frac{2\tau}{r} \qquad (4)$$

where PG = hydrostatic pressure of gas in bubble

PL = liquid hydrostatic pressure

τ = surface tension

r = radius of curvature

Figure 14a shows the location of the pressures, PG and PL, and the radius of curvature, r. In the adjacent diagram, Figure 14b, a schematic of the alveolus is shown and the variables of the Laplace equation indicated. Assuming a constant radius of curvature, one can see from equation (4) that the lower the surface tension (τ), the smaller the pressure differential (PG - PL). Therefore, in comparing the lung surfactant to water, the lower surface tension of DPL reduces the pressure differential, (PG - PL), needed in the alveolus to maintain a stable air sac.

DPL is a cationic surfactant which has two structural features that aid in maintaining the alveoli virtually dry. First, DPL has a positive charge from the quaternary nitrogen ion that may firmly attach to the negative charges that abound in the alveolar membrane. These bonds may be compared to those between cationic surfactants and

Figure 14a: Illustration of Gas Bubble Surrounded by Liquid: To Illustrate Variables of Laplace's Equation (PG=gas pressure; PL=liquid pressure; r=radius of curvature)

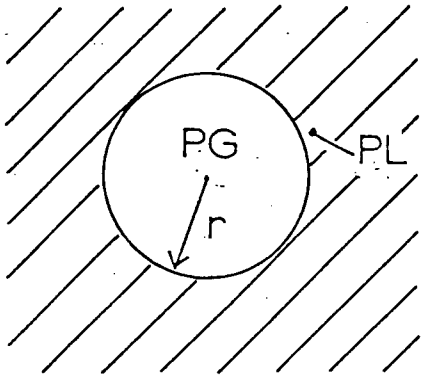

Figure 14b: Illustration of an Ideal Alveolus with Surfactant Lining

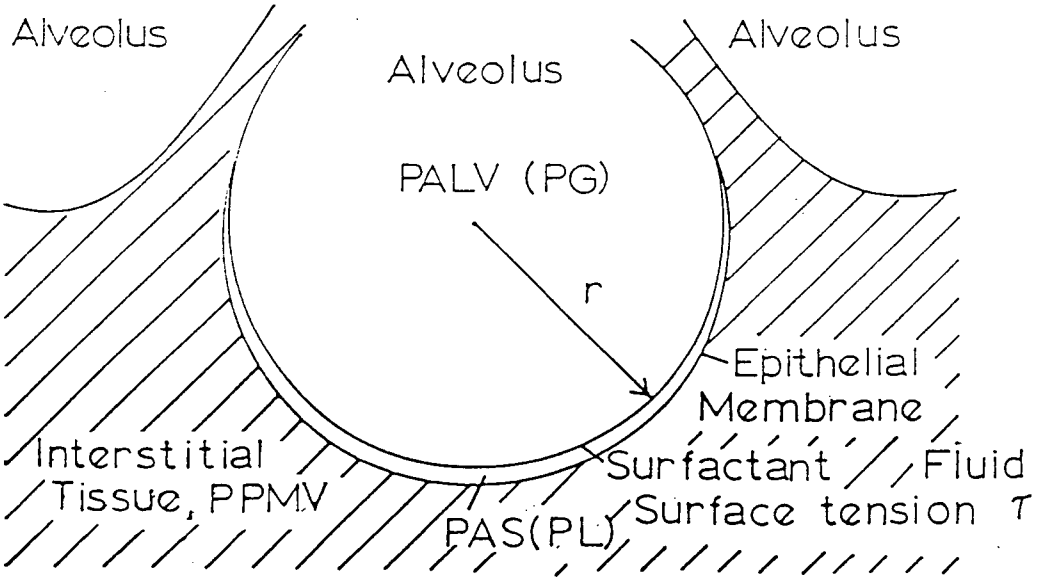

textiles. The surfactants applied to textiles have been shown to raise the "water entry pressure" to over 760 mm Hg, which is the pressure needed on the convex side of the liquid surface to break through the barrier. Although the DPL surfactant may only have a fraction of one percent efficiency in comparison to the textile surfactants, it does serve as an "appreciable protection" against acute fluid accumulation in the air space (21).

Second, DPL has "long hydrocarbon chains which are oriented outwards to provide a hydrophobic surface with a consequent lack of wettability" (21). Wettability is the ability of a liquid to adhere to a surface - the greater the surface area a given volume of liquid covers, the greater the wettability. The lung surfactant has a low wettability; water is repelled by the surfactant. Thus liquid water is prevented from crossing the surfactant lining.

The surfactant is produced by type II epithelial cells that are interspersed throughout the predominantly type I epithelial cellular membrane. Any minor breaks in the surfactant layer may be quickly eliminated by replenishing the surface with the newly-secreted surfactant.

1.8 The Normal Fluid Pathways in the Pulmonary Microvascular Exchange System

Figure 1 shows the arrangement of the pulmonary microvascular exchange system, and the normal pathways for fluid and solute. The endothelium is permeable to fluid and solutes. A net flow of fluid and solutes is generally observed to occur from the circulation to the interstitium. Once in the alveolar interstitium the fluid and solute flow along a pressure gradient to the extra-alveolar interstitium. The lymphatics drain the extra-alveolar tissue space. If steady state is achieved the flow of fluid and solutes across the endothelium is equivalent to the flow of fluid and solutes leaving the tissue space through the lymphatics.

Under normal conditions fluid may traverse the epithelium between the interstitium and air space. However fluid entering the air space may be evaporated (a minor amount) or return to the interstitium. Therefore the net flow is negligible, and the air space is assumed to be virtually dry.

1.9 Pulmonary Edema

1.9.1 Definition of Pulmonary Edema

Edema is defined as "a swelling due to an effusion of watery fluid into the intercellular spaces of connective tissue" (17). Prichard (17) presented a further definition of pulmonary edema: "a pathologic state in which there is abnormal water storage in the lungs".

Pulmonary edema may be initiated from the circulation compartment by elevated circulatory fluid pressure and/or changes in the permeability of the endothelium. Alternatively, edema may be induced by changes to the permeability of the epithelium. The following discussion on the sequence of events during pulmonary edema will be for edema initiated from the circulation compartment.

A rise in the circulatory hydrostatic pressure, or a change in the permeability of the vascular membrane will lead to increased fluid filtration from the circulation to the interstitium. The blood capillary segment because of its larger surface area and higher fluid and solute permeability, in comparison to the arterial and venous segments, is the major site of fluid and solute transudation (22,23). The fluid and solute enter the alveolar interstitium, and flow towards the extra-alveolar tissue space along the pressure gradient between the two tissue sub-compartments. The lymphatics drain the fluid that flows into the extra-alveolar tissue space. As the fluid volume rises in the tissue space the lymph flow also rises. If the edema is moderate the lymph flow may equalize with the transendothelial flow, and a new steady state will be established.

However, in severe pulmonary edema the transendothelial flow exceeds the flow capacity of the lymphatics. The fluid pressure in the extra-alveolar tissue space rises as fluid accumulates in this sub-compartment. This results in a decreased alveolar to extra-alveolar tissue fluid flow, and an increase in alveolar tissue fluid volume. Eventually the capacity of the interstitium is exceeded and

breaks in the epithelium develop. Fluid may then flow from the circulation into the air space, as well as into the lymphatics.

The location of the epithelial breaks is not well-known. Staub and Gee (24), and Zumsteg et al. (23) suggest that the breaks are present at the level of the terminal bronchioles; these epithelial breaks are possibly present under normal conditions, but the pressure gradient does not normally favour interstitial to alveolar fluid transport. Egan (25) proposes that the breaks may develop between the normally tight junctions between the epithelial cells. In both cases, the openings are not considered to be uniformly spread over the epithelium, but occur at a relatively few discrete sites. The protein flow into the air space occurs through these openings.

The fluid accumulation in the air space is spotty and the alveoli fill under an all or nothing phenomena. This individual filling is described in more detail in section 3.6.

1.9.2 Clinical Causes of Pulmonary Edema

"Pulmonary edema may arise from a number of causes and in a wide variety of diseases" (17). In most cases the cause of edema will be an increase in the pulmonary microvascular hydrostatic pressure and/or an increase in the fluid and solute permeability of the vascular and/or epithelial membranes.

1.9.2.1 Hydrostatic pulmonary edema.

The elevation of the microvascular hydrostatic pressure raises the driving force that causes fluid flow from the circulation to the interstitium. If the high transmembrane flow of fluid overwhelms the

safety factors of the exchange system - that are trying to regulate the flow - then the progression of edema may proceed through the interstitial and alveolar stages.

Hydrostatic edema may result from upsets to the cardiac system. For example, if the heart malfunctions, and the rate of fluid pumped from the right ventrical is greater than the rate of fluid pumped from the left ventrical, fluid will accumulate in the pulmonary circulation. As the blood volume of the circulation rises, the vascular hydrostatic pressure will also rise. The result will be an increased transendothelial flow of fluid and solutes. The major causes of cardiogenic pulmonary edema are listed in Table 2.

1.9.2.2 Permeability pulmonary edema.

Permeability changes to the endothelial and/or epithelial membranes will also result in the formation of edema. Endothelial permeability to fluid and solute may be altered by intravenous injections of excessive doses of drugs, such as heroin (diamorphine) or methadone. Moderate edema will result in the accumulation of fluid interstitially. In severe pulmonary edema alveolar flooding will occur as the interstitial and lymphatic fluid capacities are exceeded.

The permeability of the epithelium to fluid and solute may be affected by the inhalation of smoke or volatile toxins, such as nitrogen oxides. Increasing the epithelial permeability will initiate alveolar edema; the fluid leaving the interstitium may then enter either the air space or the lymphatics.

Table 2

Table 2: Major Causes of Cardiogenic (Hydrostatic) Pulmonary Edema (17)

Left vetricular failure
Cardiomyopathy
Mitral stenosis
Mitral regurgitation
Left atrial thrombi
Left atrial myxoma
Cor triatriatum
Loculated constrictive pericarditis

In either of the above cases, the other membrane may also be injured by the insult. Therefore the permeability of the endothelium and the epithelium will be changed, resulting in a more severe case of pulmonary edema.

INTERSTITIAL MODEL

2.1 Introduction

Modelling of the complex, nonlinear interactions of the pulmonary microvascular exchange enables the study of the effect of perturbations to this system. Pulmonary edema is the pathophysiological disease that is most commonly studied (13,17). Moderate pulmonary edema, induced by perturbations to the circulation and/or permeability of the vascular membrane, will result in the accumulation of fluid in the interstitium. The tissue between the circulation and air space will expand, thereby impairing the diffusion of oxygen and carbon dioxide between the two compartments.

The two classes of computer models used to study the interstitial phase of moderate pulmonary edema are the Pore Models (Blake and Staub (26); Harris and Roselli (27); Roselli, Parker and Harris (28)) and the Lumped Compartment Models (Bert and Pinder (29); Prichard, Rajagopalan and Lee (30)). Both types of models have been developed to provide transient and steady state responses. The pore model assumes that the vascular membrane is composed of a population of pores; the pores are of uniform or different sizes. The fluid and solute are assumed to be transported across the membrane through these pores. The parameters employed to define the membrane transport properties to fluid and solute are expressed in terms of the pore dimensions. To simulate the transient responses of the pulmonary microvascular exchange with the Pore Model, the pore structure should be established initially, with the help of experimental data obtained

under steady state conditions (28). The lumped compartment model, on the other hand, does not interpret the physical structure of the membrane. The parameters used to define the membrane transport properties are obtained from experimental data.

The lumped compartment model developed by Bert and Pinder (29) to study interstitial edema forms the basis for the work done in this thesis on alveolar edema. Their three compartment model, titled the Interstitial Model, will be discussed first. Incorporation of the air space will lead to the development of the Alveolar Model.

2.2 Modelling of the Pulmonary Microcirculation

The circulating compartment interacts directly with the interstitial compartment in the pulmonary microvascular exchange system. To develop a lumped compartment for the circulation, assumptions and simplifications are needed in defining its macroscopic properties - the hydrostatic and colloid osmotic pressures, and the protein concentrations.

At different levels of the lung's circulation the value of the hydrostatic pressure changes. West, Dollery and Naimark (3) have identified three zones along the height of the lung - see section 1.2.3. The third zone was identified as a region where PA > PV > PALV. In this region all the blood capillaries are recruited, and thus, involved in fluid and solute exchange. The interstitial model assumes zone III conditions prevail.

The hydrostatic pressure of the blood circulation also varies axially along the length of the blood vessel from the arterial to venous ends. The blood vessel was divided into arterial, venous and capillary segments. If the circulation is divided into three sub-compartments, then hydrostatic pressures would be assigned to each segment. Additional information would be needed because of the vessel sub-division. (1) The surface area of the wall of each segment would be needed in order to determine the available area for fluid filtration. (2) The permeability characteristics of the membrane of each segment to fluid and solute would be required. And (3) there would be a preference to divide the interstitium into an alveolar sub-compartment - interacting with the capillary segment - and an extra-alveolar sub-compartment - interacting with the venous and arterial segments. The physical properties of these interstitial sub-compartments would then be required. However, sufficient information is not available to define the interstitial sub-compartments and vascular segments. Therefore, the division of the circulation into segments was not carried out. In the interstitial model, the pulmonary circulation was represented as a lumped compartment with one circulatory hydrostatic pressure (PMV).

The microvascular hydrostatic pressure representing the circulatory compartment, in zone III conditions, may be calculated from the left atrial and pulmonary arterial hydrostatic pressures (3):

$$PMV = PLA + 0.4\ (PPA - PLA) \qquad (5)$$

where PMV, PLA, PPA = the capillary, left atrial, and pulmonary arterial hydrostatic pressures, respectively.

The proteins of the microvascular exchange system were assumed to be represented by albumin and globulins. Albumin is the most abundant protein in the exchange system, and the most osmotically active macromolecule. Globulins represent the class of larger proteins, and are the second most abundant proteins.

The contents of the circulation compartment were assumed to be well-mixed. As a result the concentrations of albumin (CMVA) and the globulins (CMVG) are uniform. Intracompartmental solute diffusive flow is therefore eliminated.

The presence of proteins in the circulation generates a compartmental colloid osmotic pressure, PIMV. Combining the concentrations of albumin and the globulins provides the total protein concentration CPMV:

$$CPMV = CMVA + CMVG \qquad (6)$$

The colloid osmotic or oncotic pressure may then be calculated from the total protein concentration by the Landis and Pappenhiemer Equation (7), with concentration changed to units of g/ml:

$$PI = 210\ CP + 1600\ CP^2 + 9000\ CP^3 \qquad (7)$$

where PI = oncotic pressure,

CP = total protein concentration.

In the case of the circulation compartment CP is equated to CPMV and PI to PIMV.

The macroscopic properties of the lumped circulation compartment are: the hydrostatic pressure (PMV), the colloid osmotic pressure (PIMV), and the protein concentrations for albumin (CMVA) and globulins (CMVG).

2.3 Modelling of the Interstitium

Previous discussion of the interstitium suggested the presence of an alveolar sub-compartment and an extra-alveolar sub-compartment. Each sub-compartment would have its own macroscopic properties. However, values of the properties for each sub-compartment are difficult to obtain. The approach taken in the interstitial model was to assume one interstitial compartment.

The interstitial compartment was composed of two phases - a free fluid phase and a gel phase. The fluid present in both phases would be of a volume VIS - the interstitial fluid volume. However, solutes would have access to only a fraction of the interstitial fluid volume, or conversely would be excluded from a fraction of the interstitial fluid volume. This "excluded" volume is generally found in the gel phase, and the fraction of the interstitial volume from which the solute is excluded is dependent on the diameter of the solute. Albumin representing the smaller class-size of proteins is excluded from a fluid volume (VEXA) of 75.5 ml (29), while globulin,

representing the larger class-size of proteins is excluded from a fluid volume (VEXG) of 150 ml (29). In the interstitial model neither of these excluded volumes are assumed to rise as fluid accumulates in the interstitium (29). An available volume accessible to albumin and globulin results:

$$VAVA = VIS - VEXA \tag{8}$$

$$VAVG = VIS - VEXA \tag{9}$$

where VAVA, VAVG = the fluid volume available to albumin and globulin, respectively.

VEXA, VEXG = the fluid volume excluded from albumin and globulin, respectively.

VIS = interstitial fluid volume.

The available volumes for albumin and globulin are used in the evaluation of the protein concentration of the available spaces. These protein concentrations are the effective concentrations of the proteins:

$$CAVA = \frac{QA}{VAVA} \tag{10}$$

$$CAVG = \frac{QG}{VAVG} \tag{11}$$

where CAVA, CAVG = the effective interstitial concentration of albumin and globulin, respectively.

QA, QG = the weight of albumin and globulin, respectively, in the interstitium.

The oncotic pressure actually exerted in the interstitium is calculated from the summation of the effective interstitial concentrations:

$$CPPMV = CAVA + CAVG \tag{12}$$

where CPPMV = total effective protein concentration in the interstitium

The interstitial oncotic pressure PIPMV may then be calculated by using the Landis and Pappenhiemer expression by setting CP in equation (7) equal to CPPMV.

The interstitium is assumed to be drained by nonsieving lymph ducts. These ducts collect the fluid that passes through the interstitial space, that is, both the space which excludes the proteins and the space which is accessible to the proteins. The volume of this fluid space is VIS. Albumin and globulin have protein weights in the interstitium of QA and QG, respectively. Assuming the lymphatics are well mixed, the protein concentrations of the fluid entering the lymphatics are given by:

$$CTA = \frac{QA}{VIS} \tag{13}$$

$$CTG = \frac{QG}{VIS} \tag{14}$$

where CTA, CTG = the tissue concentration of albumin and globulin, respectively.

Under normal steady state conditions the lymph flow is equivalent to the transendothelial flowrate; no fluid accumulates in the interstitium. However, a perturbation to the fluid exchange system where the transendothelial flow exceeds the lymph fluid flow will lead to an accumulation of fluid in the interstitium. In the interstitium the hydrostatic pressure rises with the rise in fluid volume according to the relationship provided by the tissue compliance curve. Although a compliance curve should exist for each of the tissue sub-compartments - alveolar and extra-alveolar - uniting these sub-compartments into one compartment allows for the assumption of one tissue compliance curve. Bert and Pinder (29) have recalculated the compliance curve of Parker et al. (31) to account for the dimensions of a human lung; the extravascular-extra-alveolar (EVEA) fluid volume, VIS1, is used instead of the interstitial volume, VIS. These two volumes are related by the expression:

$$VIS1 = VIS + VCELL \tag{15}$$

The cellular volume, VCELL, is assumed to be constant. The hydrostatic pressure - EVEA fluid volume relationship is shown in Figure 15. At fluid volumes less than 380 ml the tissue compliance is low and the relationship is given by:

$$PPMV = 0.227\ VIS1 - 89.0 \tag{16}$$

where PPMV = interstitial hydrostatic pressure.

Figure 15: Tissue Compliance Curve used in Models (29)

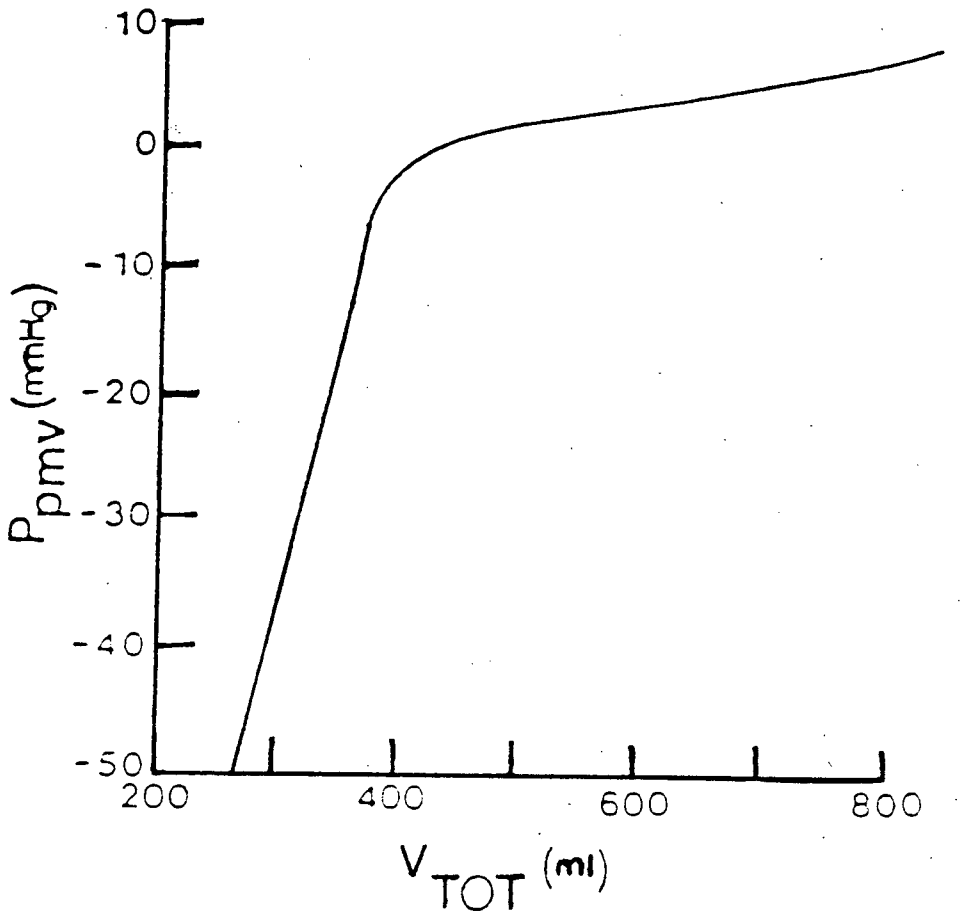

If the EVEA fluid volume exceeds 460 ml a high tissue compliance is present, the expression is given by:

$$PPMV = .017\ VIS1 - 6.73 \qquad (17)$$

The smooth transition zone between the low and high compliance curves is represented by a series of points approximating the smooth curve - see Table 3. An interpolation routine is used to relate interstitial hydrostatic pressure to the EVEA fluid volume in this region.

2.4 Modelling the Vascular Membrane

The circulation and interstitial compartments are separated by the vascular membrane. Fluid and solute exchange occurs between these two compartments across this barrier. The barrier is composed of a cellular layer and basement lamina, each component having a specific resistance to fluid and solute flow. The model combines these resistances to fluid and solute flow, and assumes that the vascular membrane may be represented by a resistance to fluid and solute that is uniform throughout the membrane.

2.5 Starling's Hypothesis: Transendothelial Fluid Flow

Starling's Hypothesis has been used to represent the transendothelial flow from the circulation compartment to the interstitial compartment (8,29,32).

Table 3

Table 3: PPMV versus VIS1 for transition region of interstitial compliance curve.

VIS1 (ml)	PPMV (mmHg)
380	-2.74
390	-2.4
400	-1.9
410	-1.3
420	-0.8
430	-0.3
440	0.15
450	0.6
460	1.09

$$JV = KF[(PMV-PPMV) - SIGD(PIMV-PIPMV)] \qquad (18)$$

where JV = transendothelial fluid flowrate (ml/hr)

KF = endothelial filtration coefficient (ml/hr/mm Hg)

SIGD = solute reflection coefficient (σ_d)

PMV, PPMV = circulation and interstitial hydrostatic pressures, respectively (mm Hg)

PIMV, PIPMV = circulatory and effective interstitial oncotic pressures, respectively (mm Hg).

This hypothesis assumes that the flow of fluid across the endothelium may be defined by two driving forces: 1) the hydrostatic pressure gradient between the interstitial and circulation compartments (PMV - PPMV), and 2) the colloid osmotic pressure gradient (PIMV - PIPMV). The parameter KF characterizes the permeability of the endothelial membrane to fluid transport, while SIGD characterizes an effective oncotic pressure gradient across the endothelium. Figure 7 shows a schematic of the circulation and tissue space separated by the endothelium; the normal values of the circulation and interstitial hydrostatic (PVM, PPMV) and oncotic (PIMV, PIPMV) pressures, and of the parameters KF and SIGD are indicated. These are the values assumed by Bert and Pinder (29) to be representative of existing experimental data. The hydrostatic pressure difference (PMV - PPMV) of 12.3 mm Hg will force fluid from the circulation to the interstitium.

Equation (7) showed that oncotic pressure may be calculated from the total protein concentration of a compartment, the total protein concentration of the circulation compartment is 69 g/litre - assuming an albumin concentration of 42 g/l and a globulin concentration of 27 g/l. The total protein concentration of the available interstitial space was 36 g/l. The albumin concentration (25 g/l) and the globulin concentration (11 g/l) of the available interstitial space were calculated by equations (10) and (11), respectively - VAVA and VAVG were evaluated from known (or assumed) values of VISl, VCELL, VEXA and VEXG. The resultant oncotic pressures are 25 mm Hg for the circulation and 18.9 mm Hg for the interstitium, which gives an oncotic pressure difference (PIMV-PIPMV) of 6.1 mm Hg. Contrary to the effect of a hydrostatic pressure gradient - causing fluid movement from a high to a low hydrostatic pressure - an oncotic pressure gradient will force fluid from the lower oncotic pressure to the higher oncotic pressure. The transport of fluid to the compartment of higher protein concentration results in the dilution of the receiving compartment's proteins, and concentration of the proteins of the compartment losing fluid. Therefore the oncotic pressure gradient forces fluid from the interstitium to the circulation. If the membrane separating the compartments is permeable to proteins, the proteins will also be able to move from the circulation to the interstitium; the magnitude of the oncotic pressure driving force will be reduced. The solute reflection coefficient (SIGD) measures the ability of the proteins to pass through a membrane. If the membrane is semi-permeable, only

water can flow across the membrane and the solutes are restricted to the compartments on either side of the membrane. In this case the solute reflection coefficient equals one (SIGD = 1) and the oncotic pressure driving force is (PIMV-PIPMV). However, if the solutes are able to freely pass across the membrane then the solute reflection coefficient would equal zero (SIGD = 0) and the oncotic pressure driving force is non-existent. In the case of the plasma proteins - albumin and globulins - a fraction of the proteins may cross the endothelial membrane, while the remaining fraction does not - the membrane sieves the proteins. For the interstitial model the solute reflection coefficient for the endothelium is 0.75 (29). Therefore, the effective oncotic pressure driving force between the circulation and interstitium is 0.75 (PIMV-PIPMV).

The fluid filtration coefficient of the endothelium, KF, represents the permeability of the membrane to fluid. KF is the product of the membrane's fluid conductivity (the inverse of the membrane's resistance to fluid flow) and the surface area of the membrane (33):

$$KF = LF(SA) \tag{19}$$

where LF = the fluid conductivity coefficient of the membrane

SA = the surface area of the membrane

By maintaining the circulation pressure above the alveolar (gas) pressure, i.e. zone III conditions, all the capillaries are assumed to be recruited. In zone III conditions the membrane surface area is assumed to remain relatively constant, so that the increase in the

fluid filtration coefficient is primarily due to an increase in the endothelial fluid conductivity (all capillaries are recruited and the surface area increases only slightly because of vessel distension). Bert and Pinder (29) reviewed the data and made appropriate selection of the values for KF (1.12 ml/hr) and SIGD (0.75).

The driving force for fluid flow across the endothelium is the difference [(PMV-PPMV) - SIGD(PIMV-PIPMV)]. The fluid filtration rate across the membrane, JV, is the product of the fluid filtration coefficient, KF, and the driving force noted above, i.e., JV is calculated by equation (18), Starling's Hypothesis.

2.6 Kedem-Katchalsky Solute Flux Equation: Transendothelial Solute Flow

The Kedem-Katchalsky (K-K) solute flux equation has been used to describe solute flow across the endothelial membrane:

$$(JS)i = (PS)i((CMV)i-(CAV)i) + (1-(SIGF)i)[\frac{(CMV)i + (CAV)i}{2}]JV \quad (20)$$

diffusive term convective term

(JS)i = the flowrate of the solute 'i' across the membrane (g/hr)

(PS)i = the permeability - surface area product of the membrane to solute 'i' (ml/hr)

(SIGF)i = the solvent drag reflection coefficient of the membrane to solute 'i'

(CMV)i,(CAV)i = the concentration of solute 'i' in the circulation and available tissue space, respectively (g/ml)

JV = the fluid filtration rate (ml/hr)

The K-K solute flux equation is separated into a diffusive term and a convective term. The diffusive term is the product of a concentration gradient ((CMV)i-(CAV)i) for solute 'i' - albumin or globulins - and the permeability-surface area product (PS)i. The direction of solute flow is from the higher concentration to the lower concentration. In the interstitial model the diffusive flow of albumin and globulin across the endothelium is from the circulation to the interstitial free fluid phase that is available to proteins. The protein concentration of this interstitial fluid space accessible to proteins is CAVA (albumin) and CAVG (globulin). It is these available concentrations that represent the interstitial protein concentrations used in the K-K solute flux equation. The permeability surface area products, PSA and PSG, illustrate the permeability of the endothelial membrane to the specified solute. Bert and Pinder (29) reviewed the data on these parameters and made appropriate selections. They have assumed a PSA for albumin of 3.0 ml/hr; a value within the range of PSA derived for canine and sheep models. The permeability-surface area product for globulin, PSG, was set at one-third the value for albumin, i.e., PSG was assumed to be 1.0 ml/hr (29).

The convective term of the K-K solute flux equation is assumed to represent the flow of solute that is coupled with the fluid flow. The arithmetic mean of the solute concentration is a simplified expression of the mean logarithmic solute concentration that results from the analytical derivation of the convective term of the K-K solute flux equation. The product of the arithmetic mean of the solute concentration and the transendothelial fluid filtration rate yields the rate of convective solute flow that crosses an endothelial membrane that is highly permeable to solute 'i'. A solvent drag reflection coefficient for solute 'i' of zero, (SIGF)i = 0, is assumed to represent an endothelium highly permeable to the solute. If the endothelium is semi-permeable to solute 'i', then solute 'i' is not transported across the membrane and the solvent drag reflection coefficient for solute 'i' equals one, (SIGF)i = 1. Therefore the solvent drag reflection coefficient indicates the ability of the fluid to 'drag' solute 'i' across the membrane. After reviewing the data in literature, Bert and Pinder (29) selected the value of the solvent drag reflection coefficient for albumin, SIGFA, to be approximately 0.4; near the midrange of values determined in dogs as JV varied. The solvent drag reflection coefficient for globulin, SIGFG, would be expected to be greater than SIGFA, since its diameter is larger. Bert and Pinder (29) selected a value of 0.6 for SIGFG.

Table 4 lists all the input parameters discussed in the interstitial model. The estimates used by Bert and Pinder (29) are shown.

Table 4

Table 4: Input Parameters to the Interstitial Computer Simulation for Normal Conditions (29)

	Bert & Pinder
PMV	9 mmHg
PIMV	25 mmHg
KF	1.12 ml/hr mmHg
SIGD	0.75
VCELL	150 ml
VIS1	379. ml
Albumin	
PSA	3.0 ml/hr
SIGFA	0.4
VEXA	73.5 ml
QA	5.38 g
CMVA	0.042 g/ml
Globulin	
PSG	1.0 ml/hr
SIGFG	0.6
VEXG	115.5 ml
QG	2.48 g
CMVG	0.0271 g/ml

2.7 Modelling of the Lymphatics

The lymphatics function, in part, as drainage channels for fluid and solute leaving the interstitium. Although an intrinsic pumping mechanism within the lymphatics is thought to actively drain the tissue (17,18), in the interstitial model the lymphatics assume a passive role. The lymph fluid flow has been expressed as a function of total extravascular fluid volume (VTOT), interstitial pressure (PPMV), and also circulation hydrostatic pressure (PMV) (34,35,36, 37). An increase in either of the variables - VTOT, or PPMV, - or parameter PMV - is equivalent to a rise in the interstitial (+ cellular) fluid volume, VIS1 (= VIS + VCELL). Bert and Pinder (29) have replotted and recalculated the data of Erdmann et al. (35) to develop a relationship for the lymph fluid flow, JL as a function of the interstitial (+ cellular) fluid volume, VIS1, for the dimensions of human lungs. Accounting for experimental and clinical trends, the relationship is:

$$JL = 0.17\ VIS1 - 55.6 \qquad (21)$$

where JL = lymph fluid flow (ml/hr)

VIS1 = interstitial (+ cellular) or extravascular -extra-alveolar (EVEA) fluid volume (ml)

Therefore, any rise in interstitial fluid volume will cause JL to increase.

The solutes are also assumed to passively leave the interstitium and enter the lymphatics. The lymphatic capillary membrane is assumed to be highly permeable to the proteins. The protein concentration of the lymph is thus assumed to be equivalent to the tissue protein concentration:

$$(CL)_i = (CT)_i \tag{22}$$

where $(CL)_i$ = concentration of protein 'i' in lymph

$(CT)_i$ = tissue concentration of protein 'i'

The solute flow into the lymphatics is assumed to be completely convective, that is:

$$\text{(Solute Flowrate into the Lymphatics)} = JL(CT)_i \tag{23}$$

2.8 Fluid and Solute Material Balances

2.8.1 Fluid Material Balance

The fluid flows previously described in section 2.5 and 2.7 were of the fluid entering and exiting the interstitium; fluid enters from the circulation and exits through the lymphatics. In steady state conditions the fluid flows into and out of the interstitium, JV and JL respectively, are assumed equal. If unsteady state conditions prevail in the three-compartment model, and JV exceeds JL, there is an

accumulation of fluid in the interstitium. A statement of the fluid material balance around the interstitium is:

Fluid Flowrate into the Interstitium	=	Rate of Fluid Accumulation in the Interstitium	+	Fluid Flowrate out of the Interstitium	(24)

Using the appropriate nomenclature results in:

$$JV = JNET1 + JL \tag{25}$$

where JNET1 = rate of fluid accumulation in the interstitium

The material balance of equation (25) applies to the three-compartment interstitial model. Figure 16a illustrates the three compartment model and the fluid flows. Equation (25) illustrates that if the fluid flow into the interstitium, JV, and out of the interstitium, JL, are known, then the rate of accumulation of fluid in the interstitium is simply the difference (JV-JL). The integral of JNET1 with time will yield the difference between the fluid volume in interstitial (+ cellular) space at time zero and time t:

$$VIS1 - VIS10 = \int_0^t JNET1 \, dt \tag{26}$$

In the interstitial model fluid does not accumulate in the air space; the EVEA or interstitial (+ cellular) fluid volume, VIS1, will be equivalent to the total extravascular fluid volume, VTOT.

Figure 16a: Schematic of the Three Compartment Interstitial Model Illustrating Fluid Flows and Accumulation

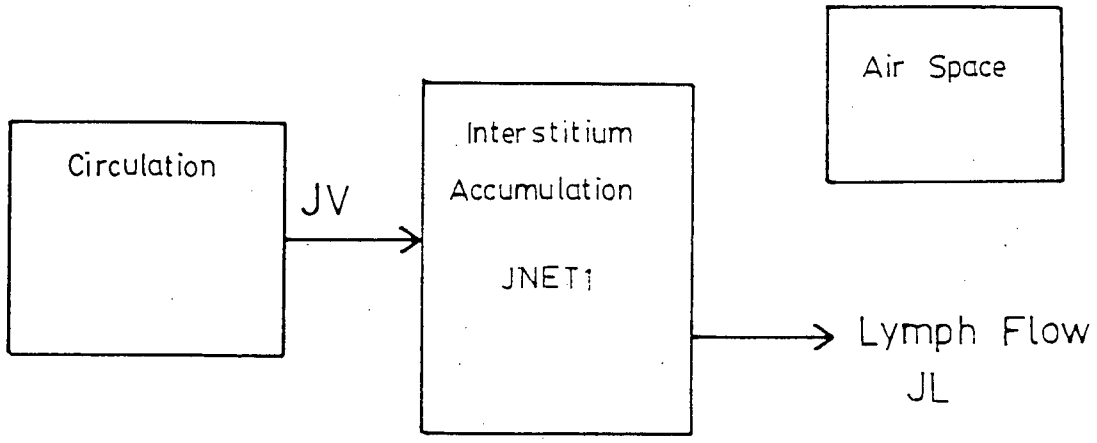

Figure 16b: Schematic of the Three Compartment Interstitial Model Illustrating Solute Flows and Accumulation

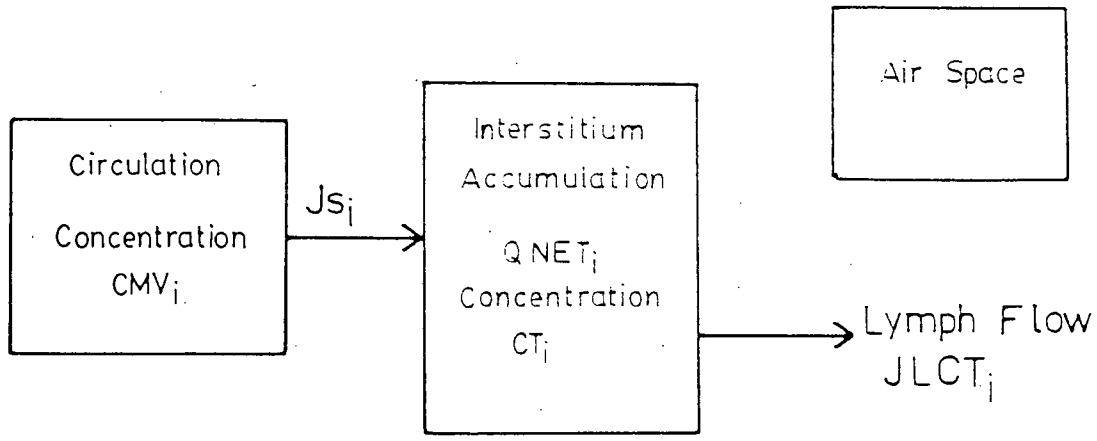

2.8.2 Solute Material Balance

The material balance for the proteins - albumin and globulin - around the interstitium may be stated as follows:

Flowrate of Solute 'i' into the Interstitium	=	Rate of Accumulation of Solute 'i' in the Interstitium	+	Flowrate of Solute 'i' out of the Interstitium	(27)

The solute material balance may be rewritten, with the solute flow variables inserted:

$$(JS)_i = (QNET)_i + JL(CT)_i \qquad (28)$$

where $(QNET)_i$ = rate of accumulation of solute 'i' in the interstitium

The solute flows are illustrated in Figure 16. Equation (28) illustrates that if the solute flow into the interstitium, $(JS)_i$, and out of the interstitium, $(QNET)_i$, are known, then the rate of accumulation of solute in the interstitium is simply the difference $((JS)_i - JL(CT)_i)$. The integral of $(QNET)_i$ with time will yield the difference between the solute weight in the interstitium at time zero and time t:

$$Q_i - (QO)_i = \int_o^t (QNET)_i \, dt \qquad (23)$$

where $Q_i, (QO)_i$ = the weight of solute 'i' at time t and zero, respectively (gm).

ALVEOLAR MODEL

3.1 Introduction

Previous models (28,29) of pulmonary microvascular exchange were developed to study the exchange of fluid and solutes between the interstitial, circulation, and lymphatic compartments. The air space was not included as a fourth compartment since the experimental data needed to include it were not available.

This thesis reports one way of integrating the air space into the interstitial model developed by Bert and Pinder (29), and previously described in section 2. The four compartment model that results is referred to as the alveolar model. The limited data which are available on the involvement of the air space in the pulmonary microvascular exchange were combined with assumptions - in areas of the model lacking experimental evidence - to integrate the air space with the lumped compartment model.

3.2 Modelling of the Air Space

The major regions for fluid and solute exchange are at the level of the respiratory units, that is, the respiratory bronchiole, alveolar ducts, and alveoli. Each lung lobe is composed of many respiratory units.

In experimental studies of the pulmonary microvascular exchange it was found that the air space of a lobe or segment of a lobe may be filled with fluid (12,38). The effects of filling these air spaces with fluid remain localized, i.e., other lung sections would continue

to operate normally. In severe pulmonary edema the accumulation of fluid in the air space may also be confined to isolated sections of the lung (39).

During severe pulmonary edema Staub et al. (39) proposed that the accumulation of fluid in the air space was not uniform. They proposed that an alveolus would not remain partially filled, but when fluid started to accumulate in the alveolus it would fill rapidly and independently of the neighbouring alveoli.

Ideally, modelling of the air space should incorporate the concept of individual alveoli filling independently. The air space would then be modelled as a compartment composed of millions of sub-compartments that represent the alveoli. As the fluid accumulates in the air space the number of small sub-compartments filled would increase. However, as a first approximation in the development of the alveolar model it is unreasonable to incorporate this degree of complexity. Consequently in this model the air space compartment is represented as a reservoir with a capacity of several litres.

During normal conditions the base of the compartment is lined with a thin layer of surface active fluid. Macklin (40) estimated that the total fluid volume in the air space under normal conditions is 20 ml; a volume that is negligible in comparison to the large capacity of the air space. At normal conditions the compartment will be filled primarily with gas (or air).

The fluid that accumulates in the air space will be assumed to be well-mixed. Therefore, the compartment will have a uniform protein concentration.

3.3 Modelling of the Alveolar Membrane

Figure 8 illustrates that the air space is separated from the other compartments of the pulmonary microvascular exchange by the alveolar wall composed of a cellular and a basement membrane. For simplicity, the individual resistances of each membrane to fluid and solute flow are represented in the alveolar model by a single resistance. Hence the alveolar wall will be taken as being uniformly permeable to fluid and solutes throughout its thickness and surface area.

In the alveolar model the exchange of fluid and solutes across the alveolar membrane will be assumed to occur between only the interstitial and alveolar compartments. Structurally, the alveolar wall separates the air space and interstitium. At other sites the basement membrane of the alveolar wall is fused to the basement membrane of the vascular wall (Figure 8). Fluid and solute may also be transported across this vascular-alveolar wall, between the circula- tion and air space. However, if fluid and solutes could leave the circulation across the vascular wall (to the interstitium) and the vascular-alveolar membrane (to the air space) a factor would be required to indicate the proportion of fluid and solutes leaving the circulation for the interstitium, and for the air space. Furthermore, the permeability to fluid and solute of the vascular-alveolar membrane would be needed. Neither the proportionality factor nor the vascular-alveolar permeability to fluid and solute are available in literature. Therefore, to simplify the matter, the circulation was assumed to interact with only the interstitium, which then interacts with the air space.

3.4 The Onset of Alveolar Flooding

During interstitial pulmonary edema, fluid and protein are exchanged between the circulation, interstitial, and lymphatic compartments. The air space remains virtually dry, and is assumed to not participate in the pulmonary microvascular exchange. Following the onset of alveolar flooding the air space receives fluid and protein from the interstitial compartment.

The onset of alveolar flooding is assumed to occur at a specific extravascular-extra-alveolar (EVEA) fluid volume, VTONS. Preceding alveolar flooding the extravascular-extra-alveolar fluid volume (VIS1) is equivalent to the total extravascular fluid volume (VTOT). In the alveolar model, when the fluid volume VIS1 (or VTOT) reaches VTONS alveolar flooding begins. The subsequent progression of the alveolar edema will depend on other factors introduced in later sections (3.5, 3.6).

The value of VTONS is dependent on the cause of the edema. Edema may be caused by a perturbation that originates from the vascular compartment, and augments the transendothelial flow - through an elevated PMV, or change in endothelial permeability. Fluid will accumulate in the interstitial space until the EVEA fluid volume (VIS1) exceeds VTONS, at which point alveolar edema begins. A number of values of VTONS have been suggested under these circumstances: Iliff (41) has suggested that alveolar flooding occurs after a 30% increase in VTOT from the normal total extravascular fluid volume; i.e., for a VTOT of approximately 379 ml under normal conditions VTONS would be 490 ml.

Prichard (17) has stated that alveolar flooding occurs at a total extravascular fluid volume (VTOT) equivalent to twice the interstitial fluid volume (VIS = VTOT - VCELL) at normal conditions; for an interstitial fluid volume of approximately 229 ml (= 379 - 150 ml) under normal conditions, VTONS would be 458 ml.

Finally, Staub (13) has stated that alveolar flooding occurs after a 30% increase in lung weight from normal conditions; for a wet lung weight of approximately 672 ml under normal conditions, VTONS would be 585 ml (VTONS = (1.3(672) - 195 - 94): Blood content = 195 g; Blood-free dry lung weight = 94 g; Density of fluid = 1 g/ml). Therefore, in alveolar edema caused by a transendothelial flow greater than normal, the range of VTONS lies between 450 ml and 600 ml.

Severe pulmonary edema may also arise from permeability changes to the epithelial membrane induced by an irritant introduced intravenously, or from the air side. The parameter VTONS may still be used to indicate the onset of alveolar flooding. If the irritant is introduced from the air side VTONS will assume the extravascular fluid volume at normal conditions, 379 ml, since no interstitial accumulation of fluid will have occurred. If the irritant is introduced intravenously it may alter the epithelial permeability to fluid and solute after it changes the endothelial permeability; the length of time before the epithelium is injured may depend on the dosage of the irritant. Introduction of a large dose may cause injury to the epithelium immediately after the irritant damages the endothelium; in this case VTONS will be just above 379 ml (normal extravascular fluid volume). On the other hand, the epithelial

permeability may change at a longer period of time after the endothelium is injured by a small dosage of the irritant. During this period of time, before the epithelium is injured, the EVEA fluid volume (VISl) will rise, and the value of VTONS will then be above 379 ml - the upper value of VTONS will be that EVEA fluid volume at which edema is induced by an elevated circulation hydrostatic pressure or a permeability change to only the endothelium.

The estimates provided for VTONS were determined by experimental measurements on the lungs of animals (41,42), and then recalculated for the dimensions of human lungs. Using these estimates to approximate the value of VTONS for human lungs may provide erroneous results. Acquiring the measurements for the animal lungs in vitro will also affect the values of VTONS (P. Dodek, personal communication). The expansion of lungs in vivo will be restricted by the chest wall, while in vitro expansion of the lungs will not be restricted. Therefore the estimates obtained with the lungs in vitro (41,42) may be unusually high.

A series of computer simulations of the alveolar model were performed to study the effect of different values of VTONS. In other simulations where the purpose was to study the effect of different values of other parameters VTONS was set at approximately 460 ml. This value of VTONS is close to the fluid volume equal to twice the interstitial fluid volume, 458 ml.

3.5 Modelling of Fluid and Solute Transport Across the Alveolar Membrane

During alveolar flooding fluid and solute are transported across the alveolar membrane from the interstitium into the air space. Modelling the fluid flow across the alveolar membrane may be approached in a manner similar to that used in the modelling of fluid movement across the endothelium. The driving forces are the hydrostatic and colloid osmotic pressure gradients, while the epithelial conductivity to fluid flow is described by an epithelial filtration coefficient. The form of the expression is similar to Starling's Hypothesis:

$$JAS = KAS[(PPMV-PAS) - SIGDAS(PIPMV-PIAS) \quad (24)$$

where JAS = transepithelial fluid filtration rate

KAS = epithelial filtration coefficient

PPMV,PAS = fluid hydrostatic pressure of interstitial space and alveolar fluid space, respectively

PIPMV,PIAS = colloid osmotic pressure of interstitial space and alveolar fluid space, respectively

SIGDAS = solute reflection coefficient of epithelium

To insure that the transepithelial fluid flow is zero before the onset of alveolar flooding the epithelial filtration coefficient - representing the fluid conductivity of the epithelium - will be set equal to zero. Following the onset of alveolar flooding KAS will be greater than zero. The actual value depends on the expression used for KAS.

Vreim et al. (43,44) have illustrated with dog lung experiments exposed to conditions that caused severe pulmonary edema with alveolar flooding (induced hydrostatically or by permeability changes to the vascular and alveolar membranes), that the protein concentrations in the alveolar fluid, interstitial fluid and lymph were similar - with no statistically significant differences. The protein concentration of the interstitial fluid refers to the tissue concentration (CTA, CTG). In hydrostatically induced edema the protein concentration of the tissue fluid was less than in the plasma. If the edema was induced by permeability changes to both membranes the protein concentration of the alveolar, interstitial, lymphatic and circulation compartments was similar. The similarity in protein concentration between the tissue and alveolar fluid suggests that the alveolar membrane was highly permeable to proteins. This situation would permit the assumption that during alveolar flooding the solute reflection coefficient of the epithelium (SIGDAS) is equal to zero. Therefore, during alveolar flooding, the expression for transepithelial fluid flow reduces to:

$$JAS = KAS(PPMV-PAS) \tag{25}$$

Preceeding alveolar flooding KAS is set equal to zero, so that there is no need to define the solute reflection coefficient of the epithelium and the colloid osmotic pressure of the alveolar fluid. The variables PAS and KAS will be defined in sections 3.6 and 3.7, respectively.

The observation by Vreim et al. (43,44) that solute concentration in the tissue space and alveolar fluid were similar during alveolar flooding supports a convective non-sieving flow of solutes across the epithelium:

$$\begin{matrix}\text{Flowrate of} \\ \text{Solute 'i' across} \\ \text{the epithelium}\end{matrix} = JAS(CT)i \qquad (26)$$

The fluid that enters the air space will be the fluid that passes through the free-fluid channels of the interstitium which are accessible to proteins and also the gel phase of the interstitial space which is not available to the proteins. As a result the protein concentration of fluid entering the air space is assumed to be the tissue concentration (CTA,CTG).

3.6 Pressure-volume Relationship of the Alveolar Fluid

3.6.1 Fluid Pressure-volume Relationship of an Individual Alveolus

(i) Normal Conditions

A schematic of an alveolus and its surrounding tissue is shown in Figure 14b. Lining the alveolus is the surfactant fluid. The pressures assigned to this schematic are the air pressure (PG), the alveolar fluid pressure (PL), and the interstitial hydrostatic pressure (PPMV). The average radius of curvature of the air-liquid interface is r. As mentioned in section 1.7.2, Laplace's equation, equation (4), has been applied to the alveolus. The pressure

differential (PG-PL) is equal to $2\tau/r$ (τ = surface tension of the surfactant). To ensure a stable alveolus, Laplace's expression should hold.

The epithelial cellular membrane is water porous. If the fluids on both sides of the membrane reach equilibrium under normal conditions then the hydrostatic pressures of fluid on each side on the membrane should be equal, i.e., PL = PPMV (45). Under normal conditions the net exchange of fluid across the epithelium should be essentially zero. A schematic of the alveolus under normal conditions is shown in Figure 17.

(ii) Fluid Filling of the Alveolus

The filling of an alveolus with fluid may be divided into three phases (17,39). First, if the interstitial hydrostatic pressure is elevated slightly (because of a perturbation to the microvascular exchange system) a hydrostatic pressure gradient from the interstitium to the air space develops. Fluid will flow along this gradient into the alveolus. If a steady state is achieved at this new interstitial pressure, the alveolar fluid pressure will have risen to equal the interstitial pressure. To maintain Laplace's equation (and a stable alveolus) the extra fluid in the alveolus must increase the radius of curvature (Figure 17). The affect of the fluid entering the alveolus on the surface tension at the air-liquid interface is unclear. If the surfactant is diluted, the surface tension will rise; Laplace's equation will be maintained by a greater rise in the radius of

Figure 17: Schematic Representation of Fluid Filling an Alveolus During Acute Pulmonary Edema. Phase 1: radius of curvature(r) increases during initial phase of filling. Phase 2: radius of curvature(r) decreases during filling. Phase 3: radius of curvature increases during final phase of filling. (Modified from (39))

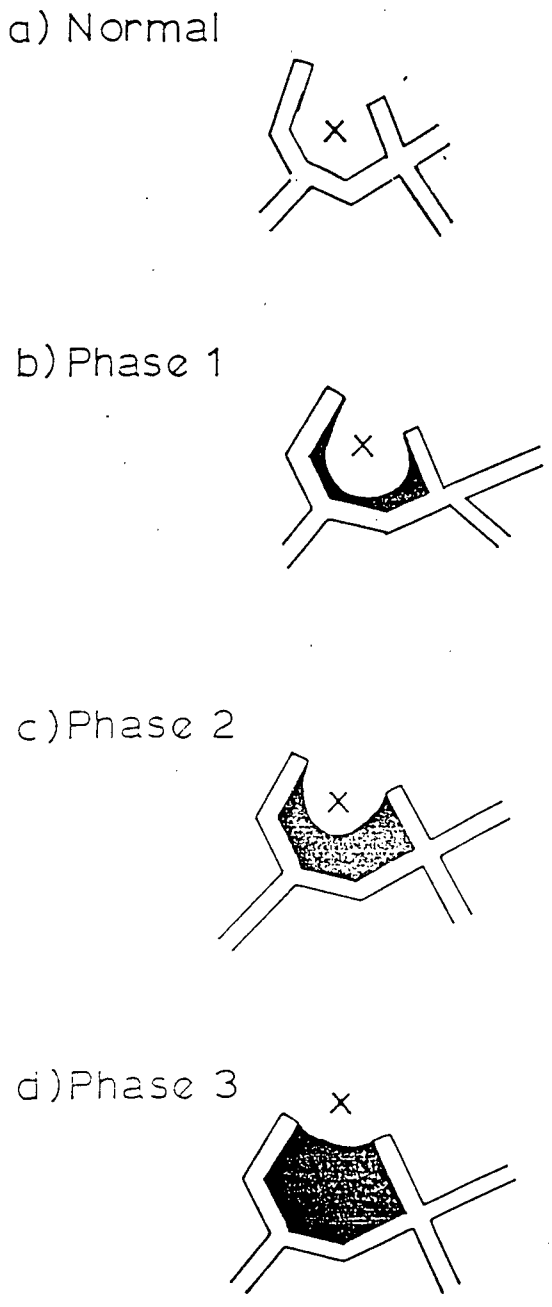

curvature. Tierney and Johnson (46) have performed experiments in which plasma fluid was slowly introduced under a surfactant lining; the surface tension at the air-liquid interface remained at its normal value. Nonetheless, in this first phase the alveolar fluid pressure rises with alveolar fluid volume.

Guyton and co-workers (45,47) have suggested that this first phase of filling may continue up to a slightly positive interstitial hydrostatic pressure (+1 or +2 mm Hg).

Secondly, if the interstitial hydrostatic pressure increases beyond this slightly positive interstitial pressure the alveolus will become unstable and fluid will rush into the air sac. During this second phase the radius of curvature, r, decreases (Figure 17). Laplace's equation (4) illustrates that if r is decreasing then (PG-PL) must increase; assuming that PG remains constant, PL must decrease. The transepithelial fluid pressure gradient that is formed causes further fluid flow into the alveolus. The surface tension at the air-liquid interface is assumed to rise to that of water and remain constant (17). Therefore, in this second phase the alveolar fluid pressure is inversely proportional to the alveolar fluid volume.

Thirdly, the radius of curvature of the air-liquid interface reaches a second critical value whereafter further increase in alveolar fluid volume causes the radius of curvature to increase (Figure 17). Applying Laplace's equation to the alveolus indicates that (PG-PL) will begin to decrease once again; the alveolar fluid

pressure PL will rise. In this third phase the alveolar fluid pressure rises, once again, with the alveolar fluid volume.

3.6.2 Fluid Pressure-volume Relationship for the Air Space Compartment

In the alveolar model a fluid pressure-volume relationship will be developed for the alveolar fluid of the air space compartment. As fluid enters the air space a pressure head develops in the compartment. As a first approximation for the compartment a straight-line relationship of pressure as a function of volume is assumed. The equation will take the following form:

$$PAS = SL\ VAS + B \tag{27}$$

where PAS = alveolar fluid hydrostatic pressure

VAS = fluid volume of air space

SL = slope of PAS-VAS curve

B = PAS at the onset of alveolar flooding

The pressure PAS will be the pressure resisting fluid transport into the air space.

Preceding the onset of alveolar flooding transepithelial flow is assumed to be equal to zero. The value of the alveolar fluid pressure, PAS, is not needed during the pre-alveolar edema phase. At the onset of alveolar flooding the value of the alveolar fluid pressure is required; it will be given by B. No estimates of B have been documented. As a result, a range of estimates of B will be investigated in this thesis. For an initial estimate B shall be taken

as the value of the alveolar fluid pressure at normal conditions, i.e. B will be equivalent to the interstitial hydrostatic pressure at normal conditions.

The slope of the PAS-VAS relationship is the parameter SL. As with B, no estimates of SL have been documented. In this thesis the effect of the parameter SL on the microvascular exchange system will also be investigated. An initial estimate of SL shall be a value of $.25 \times 10^{-2}$ mm Hg/ml.

3.7 Representation of the Epithelial Filtration Coefficient, KAS

The epithelial filtration coefficient represents the fluid conductivity of the alveolar barrier. Preceding the onset of alveolar flooding the parameter is set equal to zero. Following the onset of alveolar flooding the value of KAS may be a function of time or some other variable, or KAS may assume a constant value. In this thesis two proposals for the value of KAS will be investigated.

3.7.1 Representation of KAS as a Variable:

$$KAS = NK(VIS1-VTONS) \text{ for } VIS1 > VTONS \qquad (28)$$

In this circumstance the epithelial filtration coefficient is proportional to the EVEA fluid volume, VIS1, less the fluid volume at the onset of alevolar flooding VTONS. The parameter NK may be considered a sensitivity parameter: as NK rises, the epithelial

filtration coefficient will be more sensitive to a given (VIS1-VTONS). The fluid volume difference (VIS1-VTONS) gives an indication of the effect of the expansion of the extra-vascular-extraalveolar fluid space above its fluid volume at the onset of alveolar flooding, on KAS.

A range of magnitude of NK will be examined in this thesis.

3.7.2 Representation of KAS as a Constant:

$$KAS = KASO \text{ for } VTOT > VTONS \tag{29}$$

Preceding alveolar flooding the total extravascular fluid volume (VTOT) is equivalent to the extravascular-extra-alveolar fluid volume (VIS1). When VTOT reaches the fluid volume VTONS the epithelial filtration coefficient rises instantly to a constant value of KASO. The fluid volume VTOT is then composed of VIS1 and the alveolar fluid volume, VAS; provided VTOT exceeds VTONS KAS will remain at a value of KASO. The EVEA fluid volume VIS1 may become greater or less than the fluid volume VTONS.

In this study simulations were conducted to determine the response of the pulmonary microvascular exchange system to different values of KASO.

3.8 Integration of the Air Space Compartment with Pulmonary Microvascular Exchange Model

In the interstitial model the material balances for the interstitium involved an influx of fluid and solute from the circulation and an efflux of fluid and solute through the lymphatics. The addition of the air space compartment to the interstitial model presents few difficulties. During alveolar flooding, fluid and solute cross the epithelium from the tissue space into the air space. The fluid material balance denoted by equation (24) is still applicable, but in this case:

$$\begin{matrix}\text{Rate of Fluid} \\ \text{Flow out of} \\ \text{the Interstitium}\end{matrix} = JL + JAS \qquad (30)$$

Similarly, the flow rate of solute 'i' out of the interstitium is:

$$\begin{matrix}\text{Flow rate of} \\ \text{solute 'i' out} \\ \text{of the Interstitium}\end{matrix} = JL(CT)i + JAS(CT)i \qquad (31)$$

The material balances of the alveolar model, around the interstitium, are:

Fluid Material Balance

$$JNET1 = JV - JL - JAS \qquad (32)$$

Material Balance for Solute 'i'

$$(QNET)i = (JS)i - JL(CT)i - JAS(CT)i \qquad (33)$$

where i = albumin or globulins.

Figure 18 illustrates the material balances of the alveolar model. The material balances shown in equations (32) and (33) are applicable before and after the onset of alveolar flooding. Preceeding the onset of alveolar flooding there is no transepithelial fluid or solute flow, since KAS, and therefore JAS, in equation (25) are equal to zero.

The time integrals of JNET1, QNETA, QNETG, and JAS yield the variables VIS1, QA, QG, and VAS, respectively, which are needed in the evaluation of the fluid and solute flows of the material balances shown in equations (32) and (33). JV, JL and JAS of the fluid material balance are evaluated by equations (18), (21) and (25), while (JS)i of the solute material balance is determined by equation (20). The solute concentrations CTA and CTG are evaluated by equations (13) and (14).

Figure 18a: Schematic of Four Compartment Alveolar Model Illustrating Fluid Flows

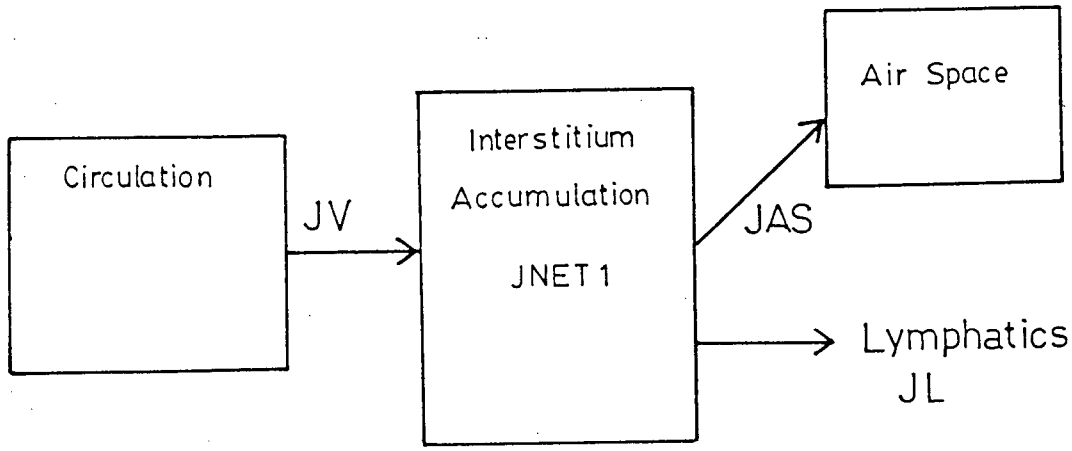

Figure 18b: Schematic of Four Compartment Alveolar Model Illustrating Solute Flows

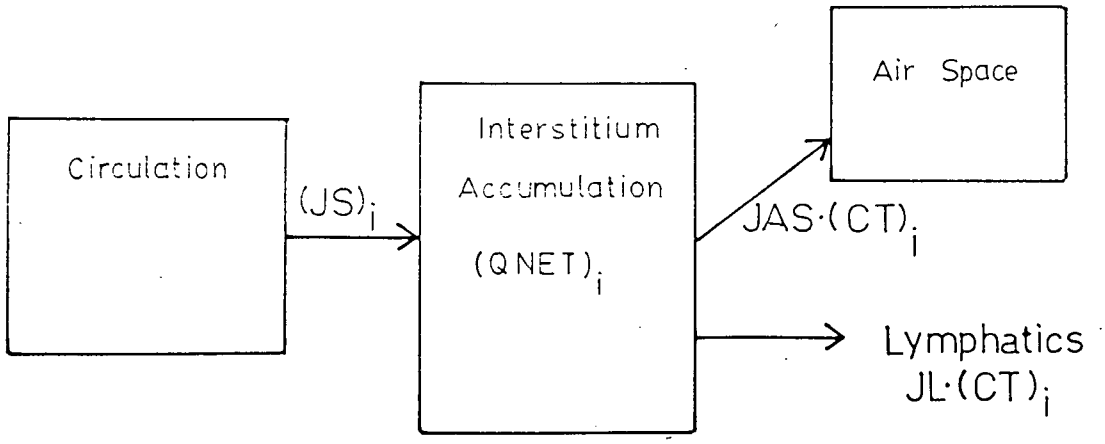

COMPUTER SIMULATION OF ALVEOLAR MODEL

4.1 Introduction

Traditionally, the study of biological models involved the use of human and/or animal experiments. Recently, computer simulations have provided an additional method for testing the biological models. Due to the complexities that arise from the interactions of a physiological system, numerous simplifications are necessary when developing a computer model. In spite of this, a simplified model of a biological system examined with a computer may provide:
1) biological scientists and health care professionals with an estimate of the progress of a pathophysiological state and the effects of clinical management, and 2) pulmonary researchers with an alternate tool with which to test their experimental findings. The model may provide suggestions on the essential variables and parameters that should be measured to validate the model.

Bert and Pinder (29) first developed the interstitial model on an AD-80 analog computer. This initial step in the modelling allowed a clear visualization of the interrelationships between variables. Thus, the analog computer was a useful tool while developing the model and its solution. However, due to problems in scaling, amplifer instability, and the limited capacity of the AD-80 analog computer the interstitial model was translated into digital form, using FORTRAN.

The solution for the alveolar model was also initiated on the AD-80 analog computer. However, due to the limited capacity of the

analog computer, the solution to the Alveolar Model was completed on a digital computer using FORTRAN. The digital computer system employed for this task was the AMDAHL 4TOV-12 of the University of British Columbia. A benefit of using the university facilities was the access to a variety of library subroutines.

The following sub-sections describe the computer program developed for the solution of the alveolar model, and the simulations that were performed to study the operation of the alveolar model.

4.2 The Computer Program

The computer program of the Alveolar Model may be divided into three sections: 1) the input data files EDA and PDA, 2) the main program UBCEDEMA, and 3) the output of results - tabulated and/or plotted. In Appendix A some additional information on the computer program will be discussed.

4.2.1 Input Data Files EDA and PDA

The parameters listed in the two data files are defined in Tables 5 and 6. File EDA (listed in Table 5) contains parameters that were introduced with the interstitial and alveolar models, such as the plasma protein concentrations (CMVA,CMVG) and the cellular fluid volume (VCELL). File PDA (listed in Table 6) includes four parameters that were introduced with the interstitial and alveolar models - PMV, SL, NK, and KASO.

The remaining parameters of file PDA pertain to the operational aspect of the simulation. The first two input parameters indicate

Table 5: Content of Input File EDA

VTOTO	: Initial value of total extravascular fluid volume (ml)
VASO	: Initial value of alveolar fluid volume (ml)
QAO	: Initial value of interstitial albumin weight (g)
QGO	: Initial value of interstitial globulin weight (g)
PIMV	: Microvascular colloid osmotic pressure (mmHg)
VCELL	: Cellular fluid volume (a constant)(ml)
VEXA	: Excluded volume for albumins (ml)
VEXG	: Excluded volume for globulins (ml) (EVEA)
VTONS	: Extravascular extraalveolar (EVEA) fluid volume at the onset of alveolar flooding (ml)
VLMPH	: EVEA fluid volume that corresponds to the maximum lymph flow (ml)
B	: Alveolar fluid pressure at the onset of alveolar flooding (mmHg)
CMVA	: Microvascular albumin concentration (g/ml)
CMVG	: Microvascular globulin concentration (g/ml)
FPPMV(1)-FPPMV(9)	: Interpolation values for tissue compliance curve (mmHg)

Continued....

Table 5: Content of Input File EDA (Continued)

KF	: Endothelial fluid filtration coefficient (ml/hr/mmHg)
SIGD	: Endothelial osmotic reflection coefficient for fluid flow
PSA	: Permeability times surface area of vascular membrane for albumins (ml/hr)
PSG	: Permeability times surface area of vascular membrane for globulins (ml/hr)
SIGFA	: Endothelial reflection coefficient for albumins
SIGFG	: Endothelial reflection coefficient for globulins

Table 6: Variables in Input File PDA

PLOTS (Y=1,N=2)	Calls plot routine (Yes or No) sets NN
TABLES 1 (Y=1,N=2)	Calls table routine (Yes or No) sets NNN
TAUMX1	Maximum time for output of printing interval SUBNT1 (hr)
SUBNT1	Time interval for printing output up to TAUMX1. Must divide evenly into TAUMX1. (hr)
TAUMX2	Maximum time for calculations (hr)
SUBNT2	Time interval for printing output between TAUMX1 and TAUMX2. Must divide evenly into TAUMX1 and TAUMX2. (hr)
STEPSZ	Initial stepsize to be used in calculations involving UBC Computing Centre subroutine "DRKC" (hr)
HMIN	Minimum value of stepsize to be used in subroutine "DRKC" (hr)
TOL	Maximum tolerance level allowed in calculations of subroutine "DRKC"
KAS0	Constant value of epithelial filtration coefficient (ml/hr/mmHg)
NK	Sensitivity parameter for variable epithelial filtration coefficient (hr/mmhg)
SL	Slope of alveolar fluid pressure-volume curve (mmHg/ml)
PMV	Circulatory hydrostatic pressure (mmHg)
XS(1),XS(2)	X coordinates of legend curve representations (left and right values) for plots (inches)

Continued....

Table 6: Variables in Input File PDA (Continued)

YS(1)-YS(4)	Y coordinates of legend curve representations for plots (inches)
SFT	Value of increments on abscissa (time)(hr/inch)
SFX	Value of increments on ordinate for fluid flow ((ml/hr)/inch)
SFY	Increments on ordinate for fluid volume (ml/inch)
ZMN	Minimum value of hydrostatic and colloid osmotic pressure for ordinate (mmHg)
SFZ	Increments on ordinate for hydrostatic and colloid osmotic pressure (mmHg/inch)
SFK	Increments on ordinate for epithelial filtration coefficient ((ml/hr/mmHg)/inch)
SFR	Increments on ordinate for solute weights (g/inch)
SFU	Increments on ordinate for solute concentrations ((g/ml)/inch)

whether plots and/or tables are desired. The parameters from TAUMX1 through to TOL apply to the time integration steps and the time intervals for printing. The parameters from XS(1) through to SFU pertain to the plotting of the transient responses.

Preceding each simulation it will generally be necessary to adjust the parameters in files EDA and PDA to the desired values.

4.2.2 The Main Program UBCEDEMA

The main program may also be divided into three sections. In the first section the parameter values listed in Tables 5 and 6 are read into the computer. In addition, a number of variables and counters are initialized.

The second section of UBCEDEMA involves the solution of the equations over the time intervals specified in file PDA. The equations solved are listed in Table 7. The stepout in time for the integrations is made using the Runge-Kutta-Merson technique as packaged by the UBC Computing Centre; the technique is provided through the subroutine "DRKC". The beginning and end values of a time interval must be specified for the subroutine. DRKC uses an externally declared subroutine FUNC to calculate the values of the differentials JNET1, JAS, QNETA and QNETG; FUNC contains the equations listed in Table 7. After integration over the time interval subroutine "DRKC" provides the values of the integrals VIS1, VAS, QA and QG (whose differentials are JNET1, JAS, QNETA and QNETG respectively). The series of equations are then solved with the new values of the integrals to yield the desired variables; when a

Table 7: Equations used in the Alveolar Model

1) $JV = KF[(PMV-PPMV)-SIGD(PIMV-PIPMV)]$

2) a) $JSA = PSA(CMVA-CAVA) + (1-SIGFA)(CMVA + CAVA)JV/2.$
   b) $JSG = PSG(CMVG-CAVG) + (1-SIGFG)(CMVG + CAVG)JV/2.$

3) $JL = 0.17\ VIS1-55.6$

4) $JAS = KAS(PPMV-PAS)$

5) $JNET1 = JV-JL-JAS$

6) $VIS1 = {}_0\int^t JNET1\ \delta t + VIS10$

7) $VAS = {}_0\int^t JAS\ \delta t + VASO$

8) a) $QNETA = JSA-JL\ CTA-JAS\ CTA$
   b) $QNETG = JSG-JL\ CTG-JAS\ CTG$

9) a) $QA = {}_0\int^t QNETA\ \delta t + QAO$
   b) $QG = {}_0\int^t QNETG\ \delta t + QGO$

10) $VTOT = VIS1 + VAS$

11) $VIS = VIS1 - VCELL$

12) a) $VAVA = VIS-VEXA$
    b) $VAVG = VIS-VEXG$

13) a) $CTA = QA/VIS$
    b) $CTG = QG/VIS$

14) a) $CAVA = QA/VAVA$
    b) $CAVG = QG/VAVG$

15) $PIPMV = 210\ CP + 1600\ CP^2 + 9000\ CP^3$

Continued....

Table 7: Equations used in the Alveolar Model (Continued)

16) PPMV = fn(VIS1) (by interpolation)

17) PAS = SL VAS + B

18) a) KAS = 0 for VIS1 < VTONS
KAS = NK(VIS1-VTONS) for VIS1 > VTONS

or

b) KAS = 0 for VTOT < VTONS
KAS = KASO for VTOT > VTONS

19) CP = CAVA + CAVG

printing interval is reached the variables are stored in array form for use in the table and plotting sections. When TAUMX2, the maximum time for calculations is reached, tabulation begins as described in the third section.

4.2.3 Tabulated and graphical output of variables from the computer program

Table 8 lists the variables that are tabulated and/or graphically illustrated. The transient response of these variables is recorded. The conditions of the simulation are listed before the output of the tables; the conditions listed consists of most of the variables in the data files EDA and PDA. The value of variables at several characteristic points along the transient response were also recorded. The characteristic points and the variables recorded at these points are shown in Table 9.

4.3 Characteristic Points Along the Transient Response of Variables

The characteristic points chosen to represent the transient responses of the PMVES simulation are listed in Table 9.

4.3.1 The onset of alvaeolar flooding

This first characteristic point represents the point of transition in a simulation from interstitial edema to alveolar edema. At the onset of alveolar flooding the variables recorded will be:
1) the time to reach the onset of alveolar flooding (t(onset)), and
2) the ratio of the tissue albumin concentration to the plasma albumin concentration - CTA/CMVA.

Table 8: Variables Tabulated and/or Plotted by Main Program UBCEDEMA

Variable	Tabulated	Plotted
JV	✓	✓
JL	✓	✓
JAS	✓	✓
JNET1	✓	✓
VTOT	✓	✓
VIS1	✓	✓
VAS	✓	✓
VIS	✓	✓
PPMV	✓	✓
PAS	✓	✓
(PPMV-PAS) or (PDIF)	✓	
PIPMV	✓	✓
KAS	✓	✓
QA	✓	✓
QG	✓	✓
VAVA	✓	
VAVG	✓	
CTA	✓	✓
CTG	✓	✓
CAVA	✓	
CAVG	✓	
QNETA	✓	
QNETG	✓	

Table 9: Characteristic Points along Transient Response and Variables Recorded

Characteristic Point	Variables Recorded
1) Onset of alveolar flooding	time CTA/CMVA
2) Maximum Transepithelial Flow	JAS time VIS1 VTOT CTA/CMVA
3) Total Extravascular Fluid Volume of 1000 ml.	JAS time VIS1 CTA/CMVA

4.3.2 The point of maximum transepithelial flow

In the simulations of the PMVES discussed in this thesis the transient response of the transepithelial flow (JAS) has a maximum value. The variables recorded at this characteristic point are: 1) the maximum value of the transepthelial flow JAS(max), 2) the time to reach a maximum JAS, 3) the EVEA and total extravascular fluid volumes, VIS1 and VTOT, respectively, and 4) the ratio of the tissue albumin concentration to the plasma albumin concentration, CTA/CMVA(max).

4.3.3 The point at which the total extravascular fluid volume (VTOT) equals 1000 ml.

Staub (13) and Gump et al (48) have found that in most cases where human lungs were subjected to acute edema the total extravascular fluid volume generally reached approximately 1100 ml., approximately one-half of the functional residual capacity of the lung. The patients investigated died under intensive care after severe injury in which it was thought that respiratory failure was the major contributing factor.(48) In this thesis a characteristic point was established below the total extravascular fluid volume of 1100 ml, at a VTOT of 1000 ml. The variables recorded at this characteristic point are: 1) the time to reach a VTOT of 1000 ml, 2) the transepithelial flow, JAS(1000), 3) the EVEA fluid volume, VIS1(1000), and the ratio of the tissue albumin concentration to the plasma albumin concentration, CTA/CMVA(1000).

The behaviour of the exchange system to a perturbation may be

analyzed by comparing the variables between these characteristic points. The change in the rate of alveolar flooding over the course of alveolar edema may be illustrated by comparing the transepithelial flows JAS(max) and JAS(1000). The rapidity with which the fluid accumulates in the extravascular space can be shown by comparing the time to reach the onset of alveolar flooding and the time to reach a VTOT of 1000 ml. Comparison of the EVEA fluid volume, VIS1, at JAS(max) and at a VTOT of 1000 ml indicates the amount of interstitial edema that formed in excess of the EVEA fluid volume at the onset of alveolar flooding given by VTONS. The difference (VTOT-VIS1) at these two characteristic points yields the fluid volume of the air space. Also, comparison of the albumin concentration ratios at the characteristic points illustrates the transient behaviour of the protein concentrations.

4.4 Outline of Simulations for the Alveolar Model

4.4.1 Simulations to study the effect of the parameters introduced with the alveolar model: KAS, SL, VTONS, and B.

The addition of the air space to the lumped compartment model developed by Bert and Pinder (29) introduced several new parameters: KAS, SL, VTONS and B. The epithelial filtration coefficient, KAS, was represented as: 1) KAS=KASO, if VTOT exceeded VTONS, or 2) KAS=NK(VIS1-VTONS), if VIS1 exceeded VTONS. If VTOT in (1) and VIS1 in (2) were less than VTONS, KAS was set equal to zero. Therefore, the expressions for KAS introduced the parameters KASO (for KAS as a

constant value) and NK (for KAS as a variable).

Simulations were performed to study the effect of these parameters on the responses of the microvascular exchange system. The exchange system was subjected to a perturbation that increased the transendothelial flow of fluid and solute. For the simulations conducted for this thesis the perturbation was an elevated circulatory hydrostatic pressure, usually to 50 mmHg.

In Table 10 are listed the simulations that were carried out. For example, when a set of simulations were conducted to study the parameter VTONS, the range of values of VTONS was 414 to 500 ml; the other parameters assumed values as shown in row 4: NK = 0.5 $hr^{-1}mmHg^{-1}$, KASO = 0, SL = $0.25x10^{-2}$ mmHg/ml and B = -3.03 mmHg.

4.4.2 Simulations to study the effect of a maximum lymph flow

In the alveolar model the lymph flow rate is assumed to be given by equation (21), as a function of the EVEA fluid volume, VIS1.

Observations by Drake et al (34) and others, (17,18,49) have shown that the lymph flow reaches a maximum value: 1) during pulmonary edema induced by an elevated circulatory hydrostatic pressure (PMV), 2) during pulmonary edema induced by changes in the endothelial permeability to fluid and solutes. In this thesis simulations will be performed to study the effect of a maximum lymph flow on the responses of the exchange system.

A maximum lymph flow will be represented as JL(max). An EVEA fluid volume, defined as VLMPH, will correspond to JL(max). The point

Table 10: Simulations conducted to study the effect of parameters introduced with the alveolar model*

Parameter value / Varied Parameter		KAS		SL (mmHg/ml)	VTONS (ml)	B (mmHg)
		NK ($hr^{-1}mmHg^{-1}$)	KASO (ml/hr/mmHg)			
KAS	NK	0.05 0.5 5.0 50.0	0	$.25x10^{-2}$	460	-3.03
	KASO	0	1.0 2.5 5.0 10.0	$.25x10^{-2}$	460	-3.03
SL		0.5 50.0	0	$.25x20^{-4}$ $.25x10^{-3}$ $.25x10^{-2}$ $-75x10^{-2}$	460	-3.03
VTONS		0.5	0	$.25x10^{-2}$	414 to 500	-3.03
B		0.05	0	$.25x10^{-2}$	460	-10.0 to 1.0

* Parameters from Table 11 are
PMV = 50 mmHg
KF = KF(normal) = 1.12 ml/hr/mmHg
SIGD = .75
PSA = 3.0 ml/hr
PSG = 1.0 ml/hr
SIGFG = .40
SIGFA = .60

at which the lymph flow becomes a maximum may be specified in reference to the onset of alveolar flooding (17,34); since VTONS is the fluid volume at the onset of alveolar flooding, representing JL(max) by VLMPH will permit easy comparison between these two points.

The value of the maximum lymph flow, JL(max), or its corresponding fluid volume, VLMPH, is not clearly defined. Drake et al (49) performed lymph flow experiments on dog lungs in vivo. Their results showed that maximum lymph flow occurred at a PMV between 20 and 25 mmHg. The corresponding fluid volume for a PMV of 25 mmHg is 414 ml. or 90% of VTONS. Prichard (17) suggested that alveolar flooding occurs shortly after the attainment of a maximum lymph flow, i.e., VLMPH < VTONS. The range of values of VLMPH considered in this study is from approximately 414 ml. (JL(max)=14.8 ml/hr) to an extremely high value (e.g. 5000 ml) which indicates that there is no maximum lymph flow. For VLMPH equal to the fluid volume VTONS(460 ml) the value of JL(max) is 22.6 ml/hr.

4.4.3 Simulations to study the effect of the endothelial permeability parameters, endothelial filtration coefficient, and the circulatory hydrostatic pressure on the alveolar model.

In the interstitial model Bert and Pinder (1984) investigated the effect on the pulmonary microcascular exchange system of changing the endothelial permeability parameters-SIGD, PSA, PSG, SIGFA and SIGFG - the endothelial filtration coefficient, KF, and the circulatory hydrostatic pressure, PMV. One of the objectives of the

current work is to observe the effect of the same parameters on the predictions of the PMVES simulation using the alveolar model.

Table 11 lists the simulations performed. In all three sets of simulations the epithelial filtration coefficient, KAS, is represented as a function of VIS1 (equation (28)). The circulatory hydrostatic pressure (PMV) was raised to 50 mmHg in the simulations investigating KF, and the permeability parameters.

Table 11: Simulations conducted to study the effect of the endothelial permeability parameters and filtration coefficient, and the circulatory hydrostatic pressure on the alveolar model≠

Parameter value Varied Parameter	PMV (mmHg)	KF/KF(normal)	ΔPERM (%) *
PMV	35 to 60	1	0
KF KF(normal)	50	1 to 10	0
ΔPERM	50	1	0 to +100

* The permeability parameters are changed by a specific percent (ΔPERM). If ΔPERM is +50%, then:

	Normal Value	Value after ΔPERM of + 50%
SIGD	0.75	0.375
PSA	3.00	4.50
PSG	1.00	1.50
SIGFA	0.40	.2
SIGFG	0.60	.3

Note that SIGD, SIGFA and SIGFG decrease and PSA and PSG increase.

≠ Parameters from Table 10 were set at:

NK = 0.5 hr^{-1} $mmHg^{-1}$
SL = $.25 \times 10^{-2}$ mmHg/ml
VTONS = 460 ml
B = -3.03 mmHg

RESULTS AND DISCUSSION

5.1 Transient Responses of the Pulmonary Microvascular Exchange System for Constant Epithelial Filtration Coefficient, KAS

The effect of changes in KAS (defined by equation (29)) on the predictions of the PMVES simulation.was studied under the conditions listed in Table 12. In the following section (5.2) the epithelial filtration coefficient was represented by equation (28) as a function of VIS1, which resulted in values for KAS in the range of 0 to 10 ml/hr/mm Hg. Therefore, for the case of a constant epithelial filtration coefficient the values of KAS studied ranged from 1.0 to 10.0 ml/hr/mm Hg. At time zero the PMVES was subjected to a step change in PMV from a normal value of 9.0 mm Hg. to 50 mm Hg.

The time for the onset of alveolar flooding in the simulations conducted for a constant KAS was 2 hrs. Preceding the onset of alveolar flooding the fluid volume, VIS1, rises to a value of VTONS (460 ml), as shown in Figure 19. The transepithelial flow is determined as the product of KAS and (PPMV-PAS). At the onset of alveolar flooding the pressure difference (PPMV-PAS) will be similar for all KAS. Therefore, the value of JAS depends on the value of KAS; Figure 20 shows that as KAS increases, JAS at the onset of alveolar flooding increases. This value of JAS will influence the subsequent responses of variables - such as PAS or VIS1 - predicted by the PMVES simulation.

The alveolar fluid pressure, PAS, is determined as a function of VAS by equation (27). The differential of PAS with respect to time gives:

Table 12

Conditions of PMVES Simulations Conducted to Study Changes in KAS*

KAS = KASO for VTOT > VTONS
KASO = 1.0, 2.5, 5.0 and 10.0 ml/hr/mm Hg

PMV	=	50	mm Hg
KF	=	1.12	ml/hr/mm Hg
ΔPERM	=	0	
SIGD	=	0.75	
PSA	=	3.0	ml/hr
PSG	=	1.0	ml/hr
SIGFA	=	0.4	
SIGFG	=	0.6	
VTONS	=	460.	ml
SL	=	0.25×10^{-2}	mm Hg/ml
B	=	-3.03	mm Hg
**VLMPH	=	5000.	ml

*These are the conditions of the simulations that produced the results illustrated in Figures 19,20,21.

**If VLMPH = 5000 ml, then there is no maximum lumph flow, i.e. JL(max) = N.A.

Figure 19

Transient Responses of VIS1 for Constant KAS (Conditions as in Table 12) - Response continued to time when VTOT = 1000 ml.

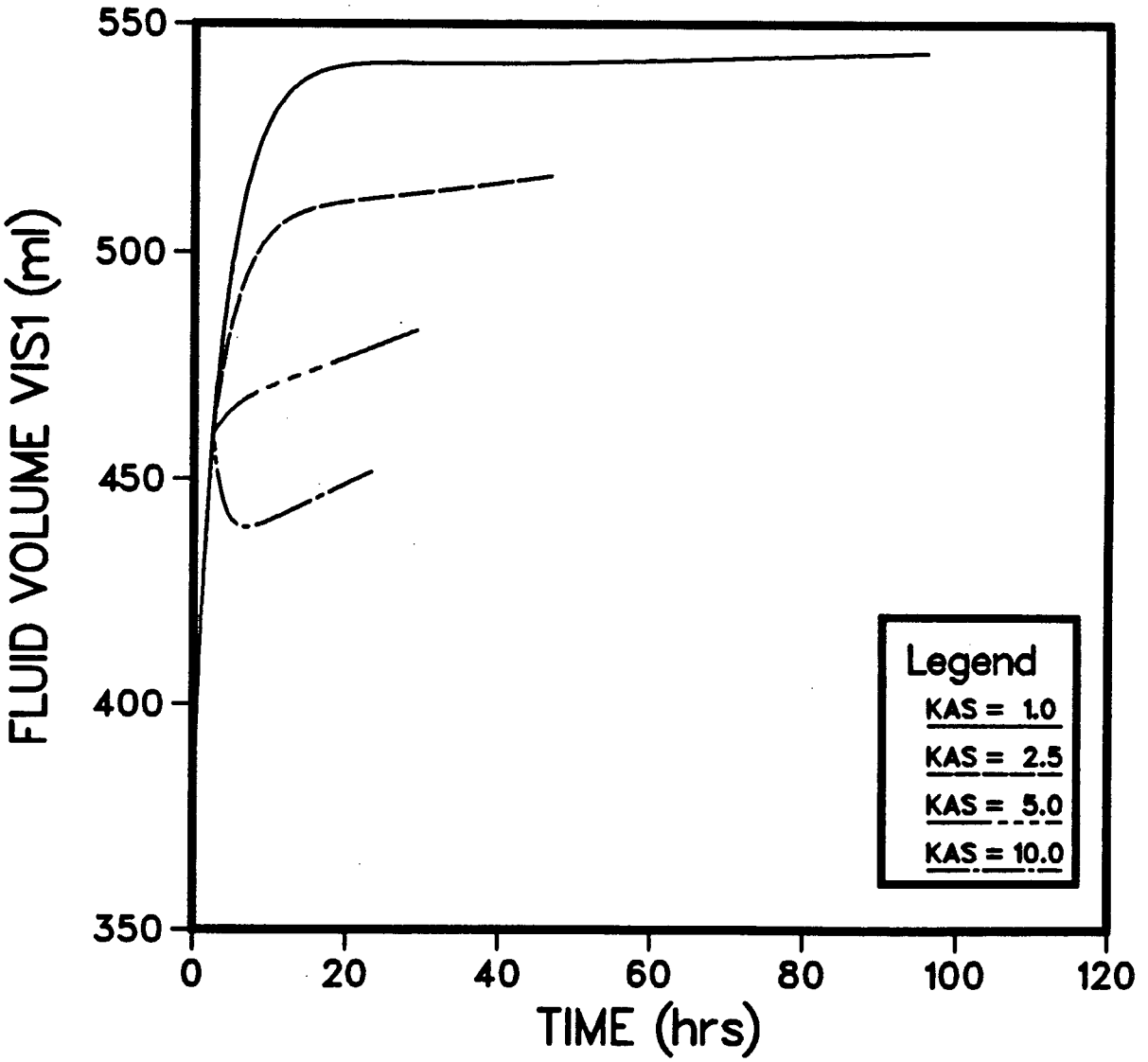

Figure 20

Transient Responses of JAS for Constant KAS (Conditions as in Table 12) - Response continued to time when VTOT = 1000 ml.

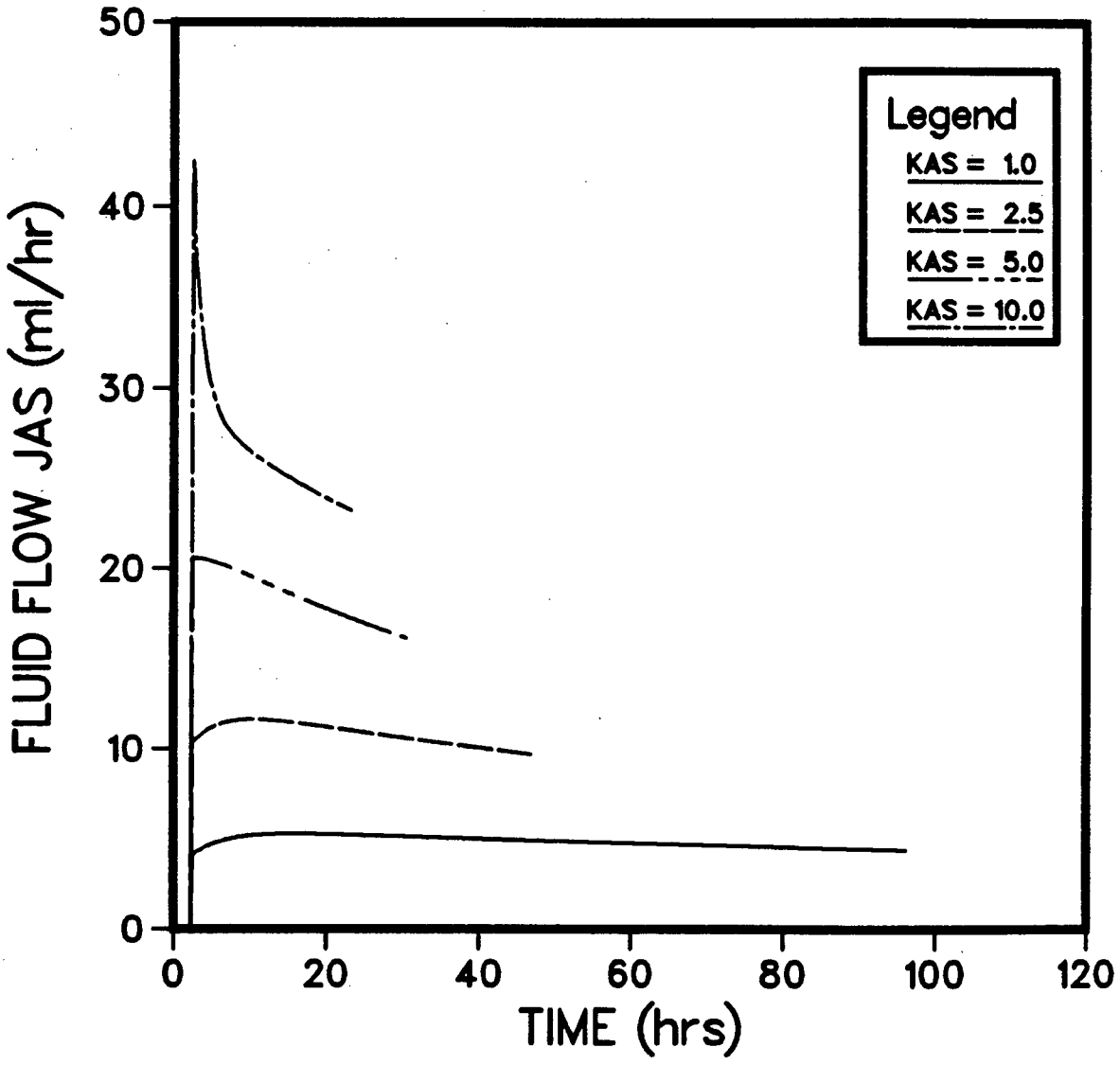

$$\frac{dPAS}{dt} = SL \cdot \frac{dVAS}{dt} \qquad (34)$$

for constant SL and B.

The derivative (dVAS/dt) is equivalent to JAS, so that:

$$\frac{dPAS}{dt} = SL \cdot JAS \qquad (35)$$

Equation (35) illustrates that the slope of the PAS curve from the onset of alveolar flooding depends on the value of JAS, hence KAS. Figure 21 shows that as KAS increases, the slope of the PAS curve increases.

The interstitial fluid pressure (PPMV) is determined as a function of VIS1 through the tissue compliance curve. The derivative of VIS1 is equal to JNET1 by definition, so that:

$$JNET1 = \frac{dVIS1}{dt} = JV - JL - JAS \qquad (36)$$

The value of (dVIS1/dt) depends on the values of JAS, JV and JL. The response of VIS1 immediately after the onset of alveolar flooding is shown in Figure 19. For the case where KAS = 10 ml/hr/mm Hg VIS1 decreases after onset, as JAS is greater than (JV-JL) which causes JNET1 to be negative. Reducing KAS to 5.0 ml/hr/mm Hg and below results in positive values for JNET 1, and a rise in VIS1 following the onset of alveolar flooding.

Following the onset of alveolar flooding the predictions of the PMVES simulation for KAS = 10 ml/hr/mm Hg are as follows: The variable PPMV decreases as VIS1 decreases; the rise in PAS and the decline in PPMV causes a rapid decrease in JAS (Figure 20). As would be expected the lymph flow, JL, decreases as VIS1 decreases.

Figure 21

Transient Responses of PAS for Constant KAS (Conditions as in Table 12) - Response continued to time when VTOT = 1000 ml.

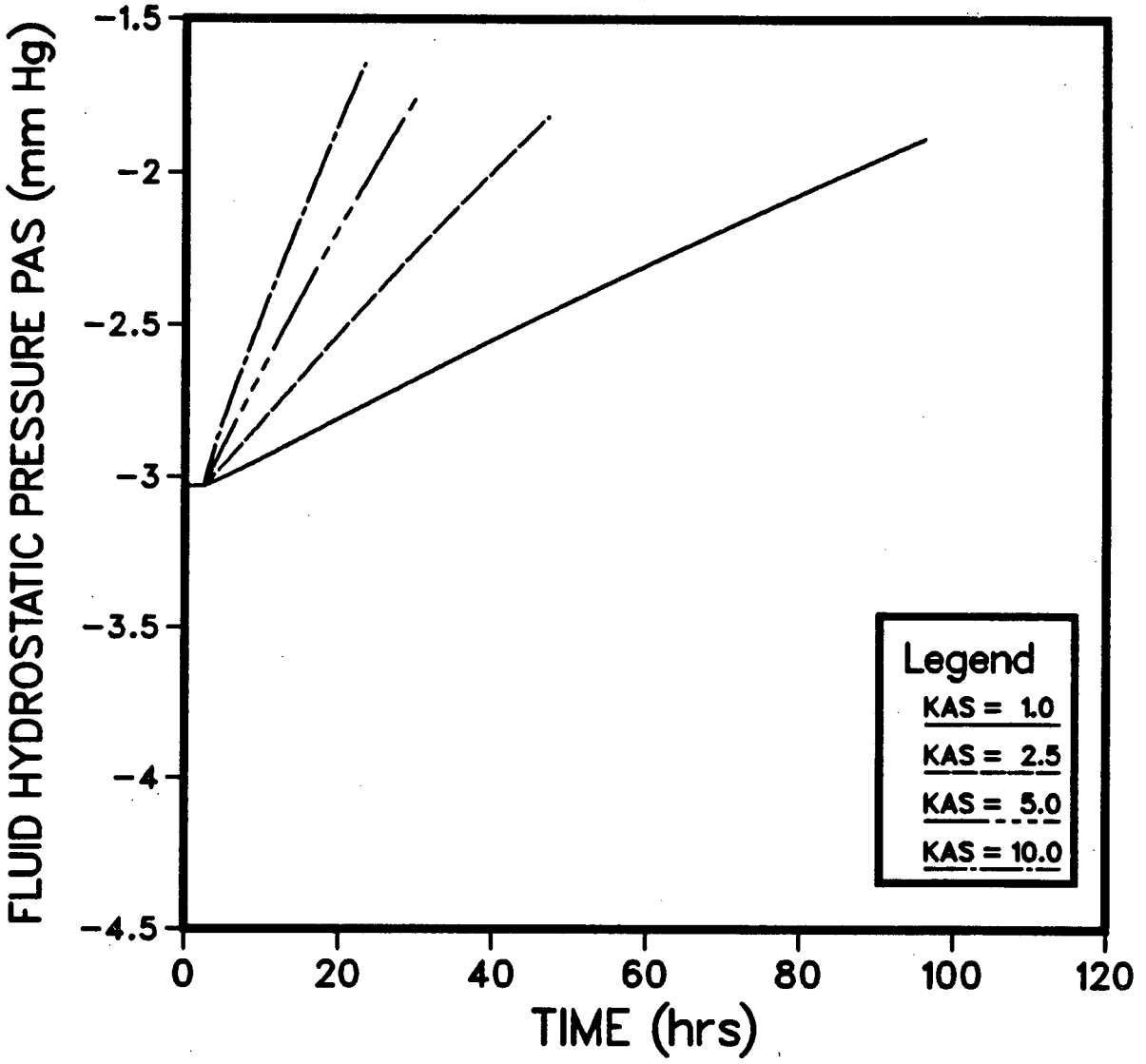

Recalling equation (36), the decrease in JAS and JL leads to an increase in JNET1 (or a decrease in the negativity in JNET1). As the simulation proceeds VIS1 will eventually decrease to a value where JNET1 equals zero; Figure 19 shows that for KAS = 10 ml/hr/mm Hg the fluid volume VIS1 reaches a minimum value. JNET1 then becomes positive and VIS1 increases (Figure 19). PPMV and JL will also increase again. However, the pressure difference (PPMV-PAS) continues to decrease, and as a result JAS decreases (Figure 20). In Figures 19, 20, and 21 the results of the simulation were recorded until a VTOT of 1000 ml. was attained; steady state was not achieved at this point.

For KAS = 10 ml/hr/mm Hg the rate of fluid leaving the interstitium exceeds the rate of fluid entering. The fluid deficit, in this case, was made up by depleting the interstitium of its fluid; the fluid volume VIS1 decreased from its value at the onset of alveolar flooding (Figure 21).

For the case of KAS equal to 5, 2.5 and 1.0 ml/hr/mm Hg, following the onset of alveolar flooding VIS1 continued to rise (Figure 21).

5.2 Transient Responses of the Pulmonary Microvascular Exchange System for Variable Epithelial Filtration Coefficient (KAS)

The variable epithelial filtration coefficient, KAS, is calculated as:

$$KAS = NK(VIS1 - VTONS) \text{ for } VIS1 > VTONS \quad (28)$$

The effect of this representation of KAS on the PMVES was investigated under the conditions given in Table 13 - which were chosen according to the criteria given in the model descriptions. At time zero the PMVES was subjected to a step change in the circulatory hydrostatic pressure from a normal value of 9 mm Hg to 50 mm Hg. In this section the transient responses of the PMVES will be discussed using Figures 22a to 22e.

During the simulation the variables listed in Table 14 will increase from their steady state values at a normal PMV of 9 mm Hg to the initial values given for PMV = 50 mm Hg.

The response of the PMVES proceeds through a phase of interstitial edema followed by alveolar edema. During the transient response a number of variables are integrated over time. These are: the rate of fluid accumulation in the interstitial (and cellular) space (JNET1) and in the air space (JAS), and the rate of accumulation of solutes in the interstitial space (QNETA, QNETG). The integrated variables yield VIS1, VAS, QA and QG, respectively. Figures 22a and 22b show that during the interstitial edema phase (time zero to 2.3 hrs) QA, QG (Figure 22a) and VIS1 (Figure 22b) rise as a result of the positive values of QNETA, QNETG, and JNET1; JAS is zero. The rise in

Table 13

Conditions of the PMVES Simulations for a Variable Epithelial Filtration Coefficient*

$$KAS = NK(VIS1-VTONS) \text{ for } VIS1 > VTONS$$
$$NK = 0.5\ hr^{-1}\ mmHg^{-1}$$

PMV	=	50	mmHg
KF	=	1.12	ml/hr/mmHg
ΔPERM	=	0	
SIGD	=	0.75	
PSA	=	3.0	ml/hr
PSG	=	1.0	ml/hr
SIGFA	=	0.40	
SIGFG	=	0.60	
VTONS	=	460.	ml
SL	=	0.25×10^{-2}	mmHg/ml
B	=	-3.03	mmHg
VLMPH	=	5000.	ml

*These are the conditions of the simulations that produced the results illustrated in Figures 22a-22e.

Table 14

Initial Conditions of PMVES Simulation
at a PMV of 50 mmHg

Variable	Steady State Value at a PMV=9 mmHg	Initial Value at a PMV=50 mmHg
JV (ml/hr)	8.82	54.7
JNET1 (ml/hr)	0.	46.0
QNETA (g/hr)	0.	0.66
QNETG (g/hr)	0.	0.70

Figure 22a

Transient Responses of QA, QG, QNETA and QNETG for Variable KAS with NK = 0.5 hr^{-1} $mmHg^{-1}$ (Conditions as in Table 13)

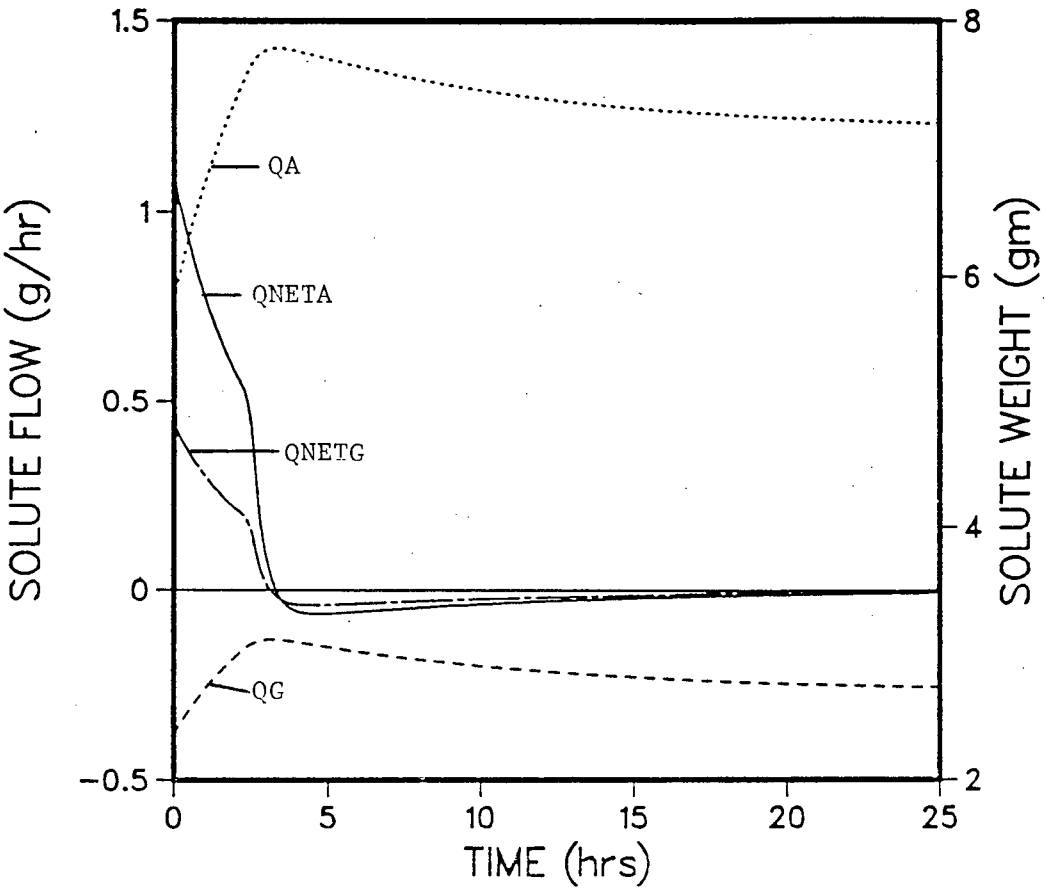

Figure 22b

Transient Responses of JV, JL, JNET1, VIS1, PPMV and PIPMV for Variable KAS with NK = 0.5 hr^{-1} $mmHg^{-1}$ (Conditions as in Table 13)

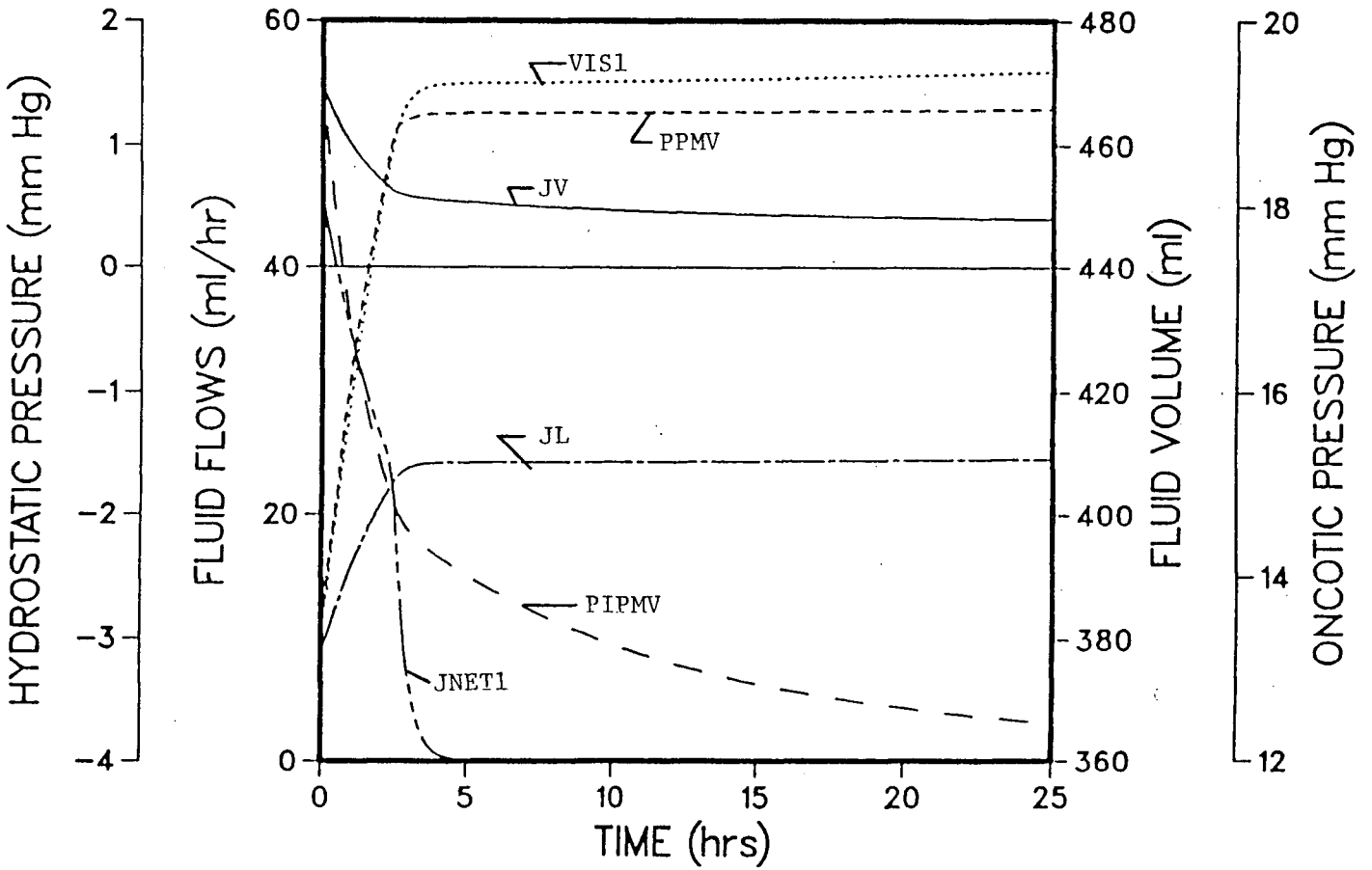

VIS1 results in an increase in PPMV according to the tissue compliance curve, and also an increase in JL according to equation (21). Figure 22b shows these interrelationships. The ratio of the solute weights (QA and QG) to the interstitial volume (VIS=VIS1-VCELL) gives the tissue protein concentrations CTA and CTG. The responses of CTA and CTG are dependent on the rates of change in QA or QG and VIS. As shown in Figure 22c, during the interstitial edema phase CTA and CTG decline. The effective protein concentrations, CAVA and CAVG, also decrease. The tissue oncotic pressure PIPMV, decreases since it is related to the total effective protein concentration (CAVA + CAVG). The decrease in PIPMV and rise in PPMV results in a decrease in JV (Figure 22b). The decrease in JV and increase in JL cause JNET1 to decrease (Figure 22b).

Eventually VIS1 reaches the fluid volume corresponding to the onset of alveolar flooding, VTONS. For the simulation conducted under the conditions given in Table 13 the onset of alveolar flooding occurs at 2.5 hrs. The transepithelial flow, JAS, that results is calculated by equation (25). Whether JAS rises or falls is dependent on the rates of change of PAS, KAS and PPMV:

$$\frac{d(JAS)}{dt} = KAS\ \frac{d(PPMV)}{dt} + (PPMV-PAS)\ \frac{d(KAS)}{dt} - KAS\ \frac{d(PAS)}{dt} \qquad (37)$$

Immediately following the onset of alveolar flooding JAS increases - Figure 22d shows the responses of PPMV, KAS, PAS and JAS.
The rise in JAS results in a further decline in JNET1 (Figure 22e),

Figure 22c

Transient Responses of QA, QG, VIS1, CTA and CTC for Variable KAS with NK = 0.5 hr^{-1} $mmHg^{-1}$ (Conditions as in Table 13)

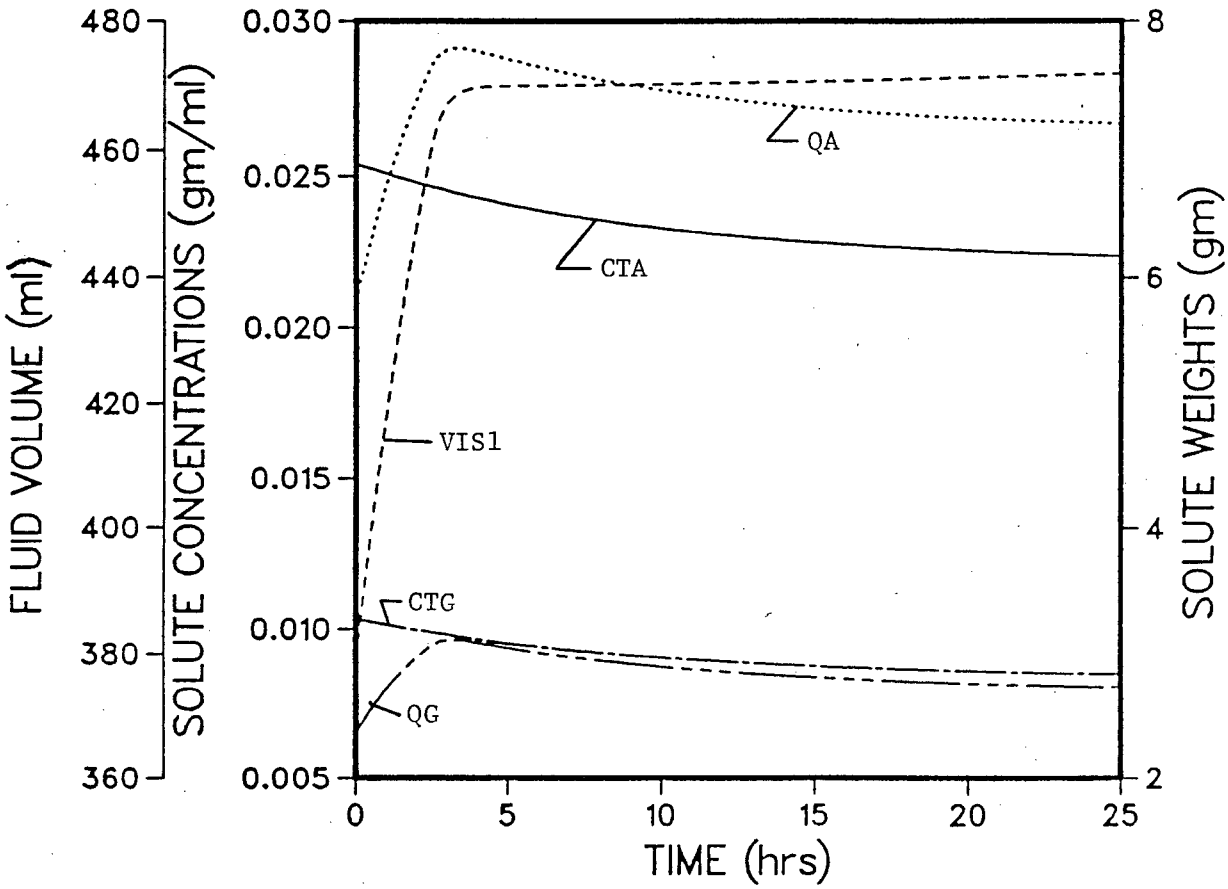

Figure 22d

Transient Responses of JAS, PAS, KAS and PPMV for Variable KAS with NK = 0.5 hr^{-1} $mmHg^{-1}$ (Conditions as in Table 13)

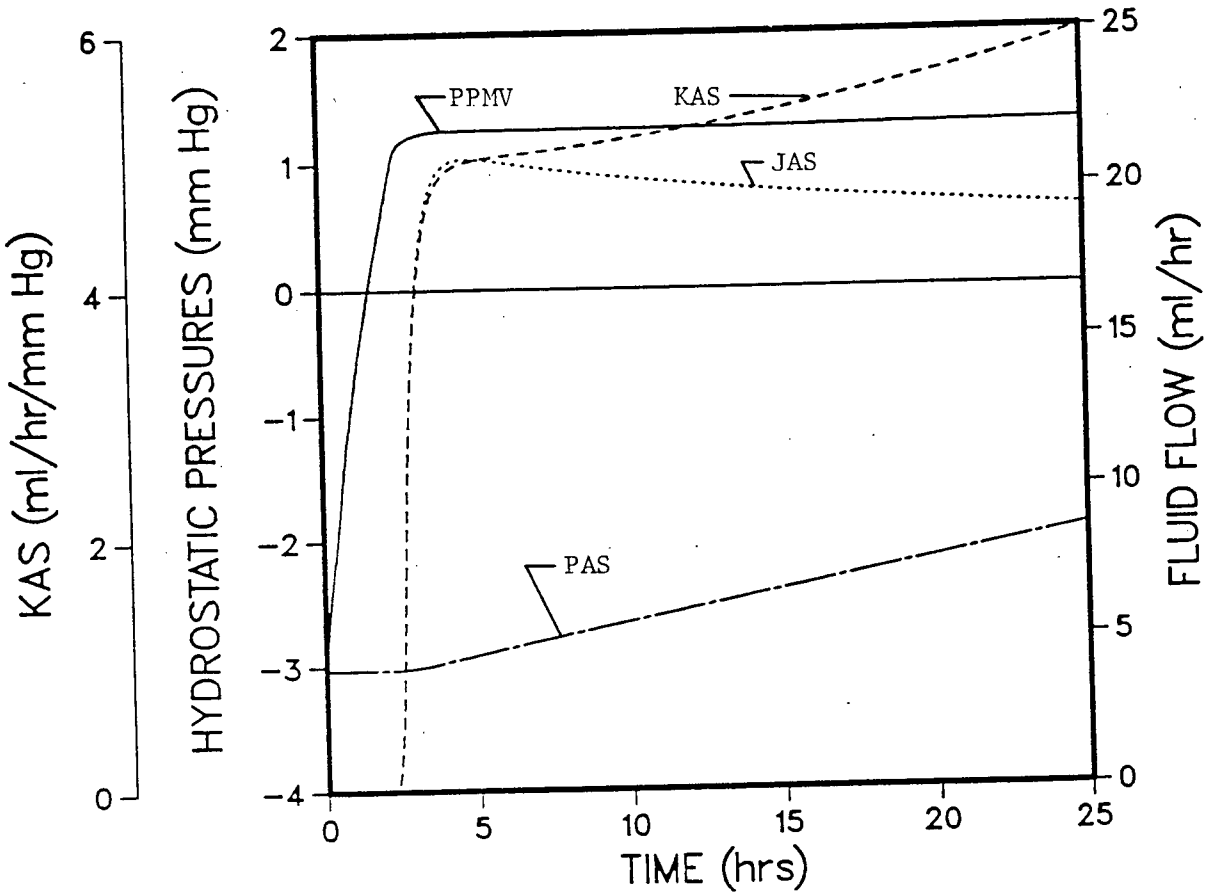

which in turn reduces the rate of increase of VIS1. The reduction in the rate of change of VIS1 diminishes the rate of change of PPMV and KAS. JAS reaches a maximum value (Figure 22d) when JAS equals (JV-JL) or (d(JAS)/dt) equals zero. JAS then declines since the rate of change of PAS exceeds the rates of change of PPMV and KAS (Figure 22d).

As JAS declines, JNET1 increases, which raises VIS1. The rise in VIS1 increases PPMV and JL (Figure 22b). If PPMV increases then JV will decrease (Figure 22b). Figure 22e illustrates the transient responses of JV, JL, JAS and JNET1. Steady state is achieved when JV equals JL, i.e., JNET1 and JAS equal zero.

5.2.1 Transient Response of the Pulmonary Microvascular Exchange System to changes in NK

In the case of a variable epithelial filtration coefficient, NK represents the proportionality between KAS and the fluid volume difference (VIS1-VTONS). The conditions in the PMVES under which NK was studied are listed in Table 15. At time zero the PMVES was subjected to a step change in PMV to 50 mm Hg. Different orders of magnitude of NK were studied, ranging from 0.05 hr^{-1} $mmHg^{-1}$ to 50.0 hr^{-1} $mmHg^{-1}$.

The transient responses of JAS for different NK are illustrated in Figure 23a. The time for the onset of alveolar flooding (JAS > 0) is appoximately 2.5 hrs. After the onset of alveolar flooding JAS in

Figure 22e

Transient Responses of JV, JL, JNET1 and JAS for Variable KAS with NK = 0.5 hr^{-1} $mmHg^{-1}$ (Conditions as in Table 13): Insert illustrates responses up to steady state (approximately 300 hrs).

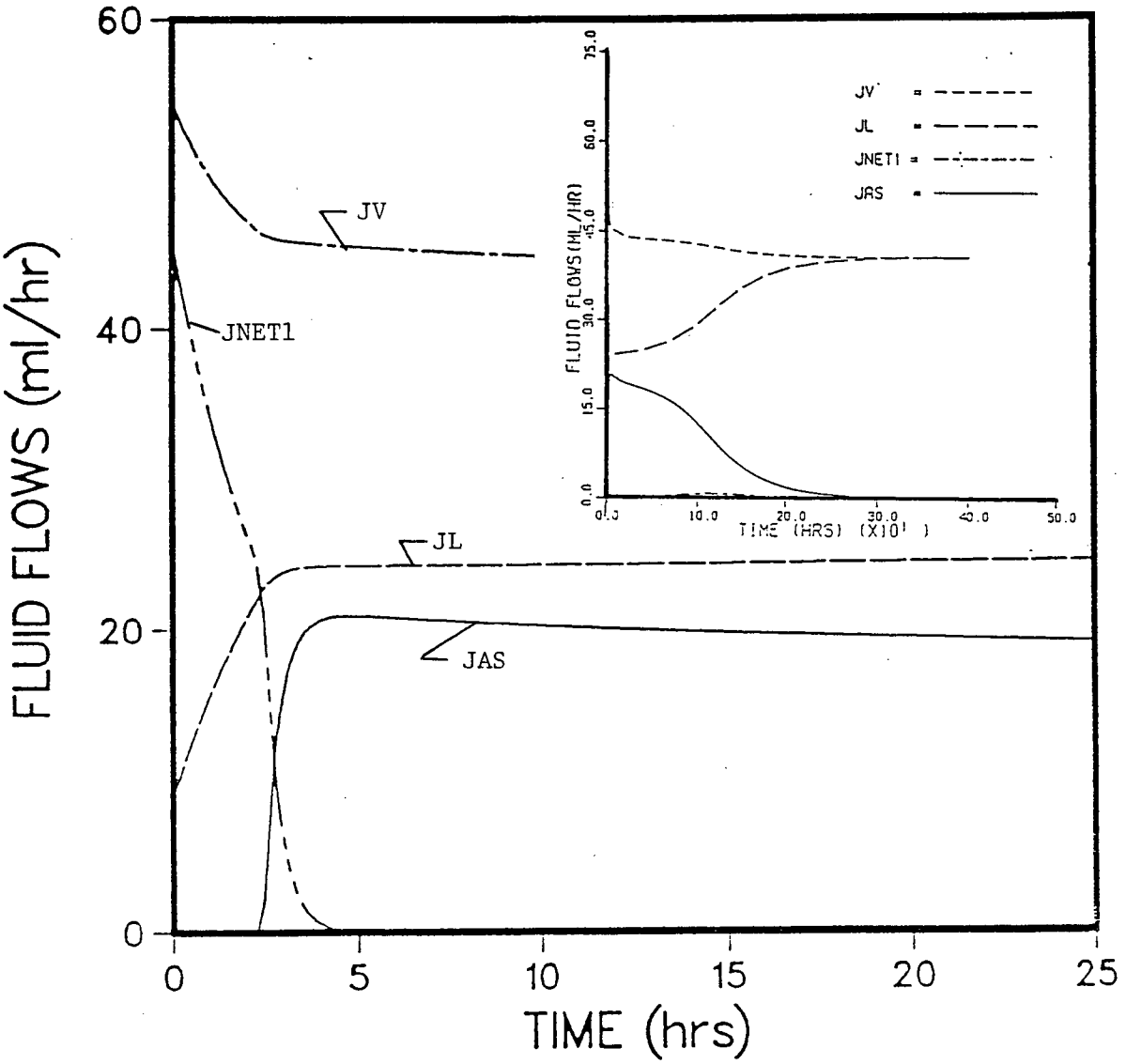

Table 15

Conditions of the PMVES Simulations Conducted to Study Changes in NK*

KAS =NK(VIS1-VTONS) for VIS1 > VTONS

NK = 0.05, 0.5, 5.0 and 50.0 hr^{-1} $mmHg^{-1}$

PMV	=	50	mmHg
KF	=	1.12	ml/hr/mmHg
ΔPERM	=	0	
SIGD	=	0.75	
PSA	=	3.00	ml/hr
PSG	=	1.00	ml/hr
SIGFA	=	0.40	
SIGFG	=	0.60	
VTONS	=	460.	ml
SL	=	0.25×10^{-2}	mmHg/ml
B	=	-3.03	mmHg
VLMPH	=	5000.	ml

*These are the conditions of the simulations that produced the results illustrated in Figures 23a and 23b.

Figure 23a

Transient Responses of JAS for Changes in NK (Conditions as in Table 15) - Response continued to time when VTOT = 1000 ml.

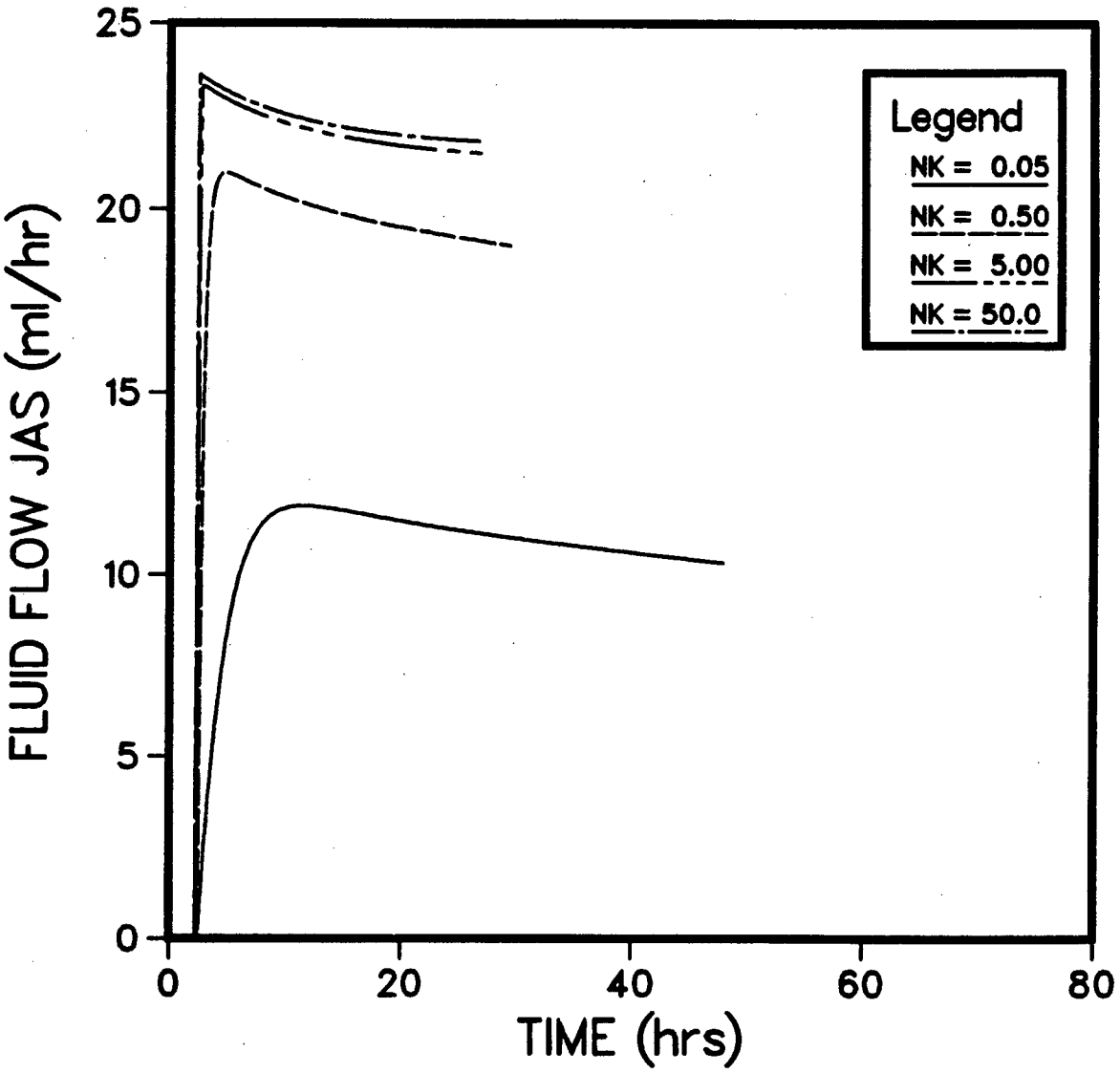

each case rises to a maximum; as NK increases the maximum JAS also increases. The transepithelial flow is determined by the product of KAS and (PPMV-PAS), as shown in equation (25). For the conditions of Table 15 the value of (PPMV-PAS) is 4.12 mm Hg at the onset of alveolar flooding for all cases of NK. Therefore JAS is dependent on the value of KAS which is composed of the product of NK and (VIS1-VTONS). Figure 23b shows that as NK increases (VIS1-VTONS) decreases (VTONS=460 ml). When NK is increased by a factor of 10, from 0.05 to 0.5 hr^{-1} $mmHg^{-1}$, the reduction in (VIS1-VTONS) is less than a factor of 10; JAS increases as NK is raised from 0.05 to 0.5 hr^{-1} $mmHg^{-1}$ (Figure 23a). However, raising NK by a factor of 10, from 5.0 to 50.0 hr^{-1} $mmHg^{-1}$ reduces (VIS1-VTONS) by a factor of almost 10. The benefit of the increase in NK is eliminated and the resulting JAS for NK=5.0 and 50.0 hr^{-1} $mmHg^{-1}$ are almost equal (Figure 23a). Therefore, as NK is increased the sensitivity of the coefficient KAS to (VIS1-VTONS) increases.

It may be surmised that for low values of NK (e.g. NK=.05 hr^{-1} $mmHg^{-1}$) a large increase in VIS1 is required to induce the movement of fluid and solutes across the alveolar membrane. If NK is large (e.g. NK=5.0 or 50.0 hr^{-1} $mmHg^{-1}$) then very little increase in VIS1 is required to induce the movement of fluid and solute across the alveolar membrane. A value of NK=0.5 hr^{-1} $mmHg^{-1}$ was used in the remaining simulations since it allowed some increase in VIS1.

Figure 23b

Transient Responses of VIS1 for Changes in NK (Conditions as in Table 15) - Response continued to time when VTOT = 1000 ml.

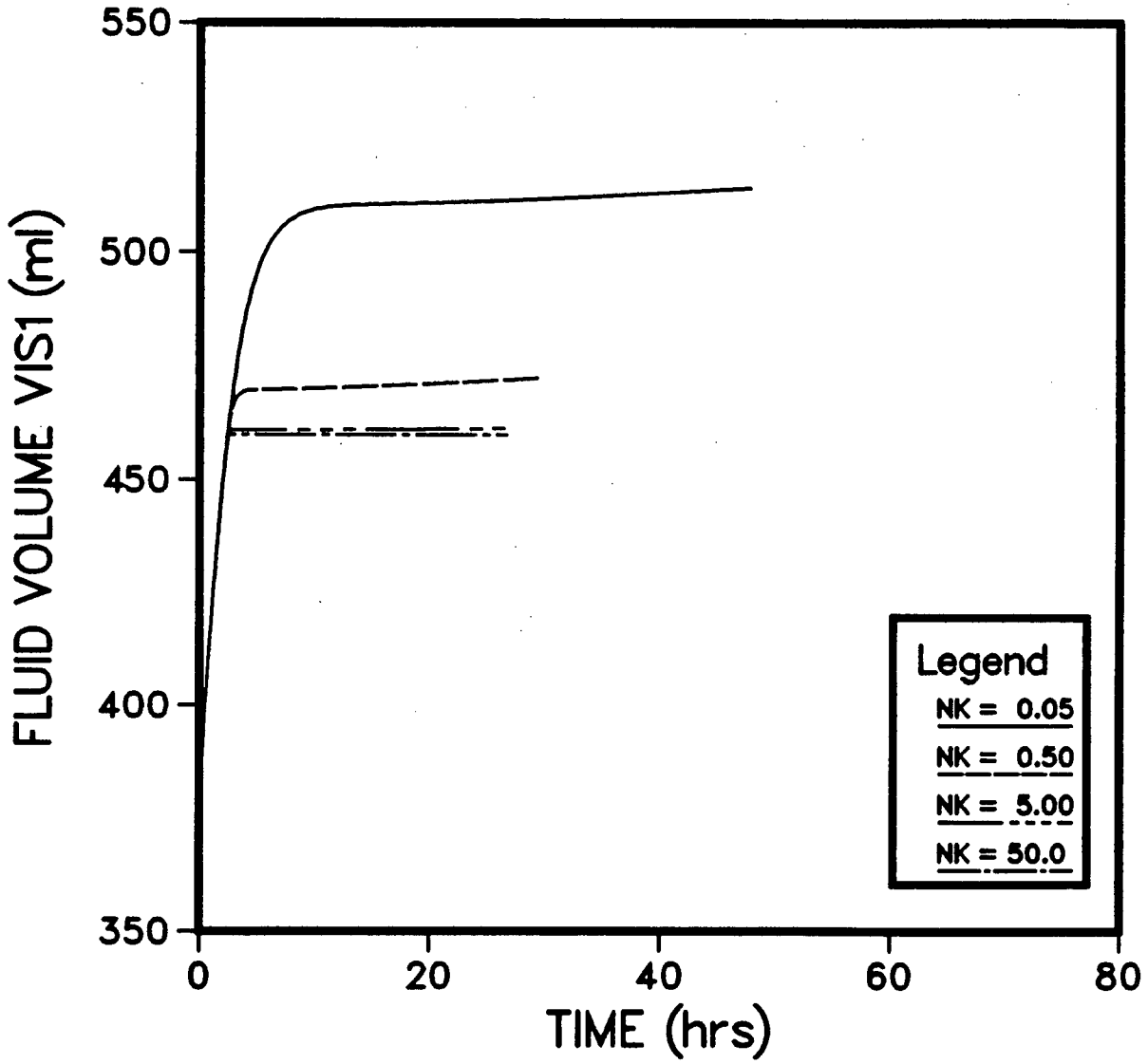

5.3 The Response of the Pulmonary Microvascular Exchange System to changes in the parameter VTONS

The parameter VTONS represents the EVEA fluid volume at the onset of alveolar flooding. The effect of changes in VTONS on the PMVES were studied under the conditions listed in Table 16. At time zero the PMVES was subjected to a step change in PMV from 9 to 50 mmHg. Since a variable epithelial filtration coefficient with an NK of 0.5 hr^{-1} $mmHg^{-1}$ was employed, the shape of the transient responses of the variables is similar to those discussed in Section 5.2.

For VIS1 less than VTONS fluid and solute exchange take place between the circulatory, interstitial and lymphatic compartments only (i.e., interstitial edema is simulated). A simulation of interstitial edema will illustrate that steady state conditions may be achieved for a given perturbation to the PMVES; steady state is established when the transendothelial and lymph flows for both fluid and solutes are equal. If the perturbation is an elevated PMV, then the interstitial (and cellular) fluid volume at steady state (VIS1(ss)) may be obtained for each PMV (Figure 24). The other conditions of the simulation are listed with Figure 24. In the alveolar model, raising VTONS to a very large value, in this case 5000 ml will result in the modelling of interstitial edema. Figure 24 illustrates that at a PMV of 50 mmHg the fluid volume VIS1(ss) is 566 ml.

In the alveolar model a VTONS greater than 566 ml will result in interstitial edema only. The PMVES will reach steady state when VIS1 reaches 566 ml. However, if VTONS is set below a value of 566 ml,

Table 16

Conditions of the PMVES Simulations
to study the changes in VTONS*

VTONS: varied from 410 to 500 ml

$KAS = NK(VIS1 - VTONS)$ for $VIS1 > VTONS$
$Nk = 0.5\ hr^{-1}\ mmHg^{-1}$

PMV	=	50	mmHg
KF	=	1.12	ml/hr
ΔPERM	=	0	
SIGD	=	0.75	
PSA	=	3.0	ml/hr
PSG	=	1.0	ml/hr
SIGFA	=	0.4	
SIGFG	=	0.6	
SL	=	0.25×10^{-2}	mmHg/ml
B	=	-3.03	mmHg
VLMPH	=	5000.	ml

*These are the conditions of the simulations that produced the results illustrated in Figures 25a to 25d.

Figure 24

Steady state values of VIS1 for given PMV for Interstitial Edema (Conditions: VTONS = 5000 ml, VLMPH = 5000 ml, KF = 1.12 ml/hr/mmHg, SIGD = 0.75, PSA = 3.0 ml/hr, PSG = 1.0 ml/hr, SIGFA = 0.4, SIGFG = 0.6)

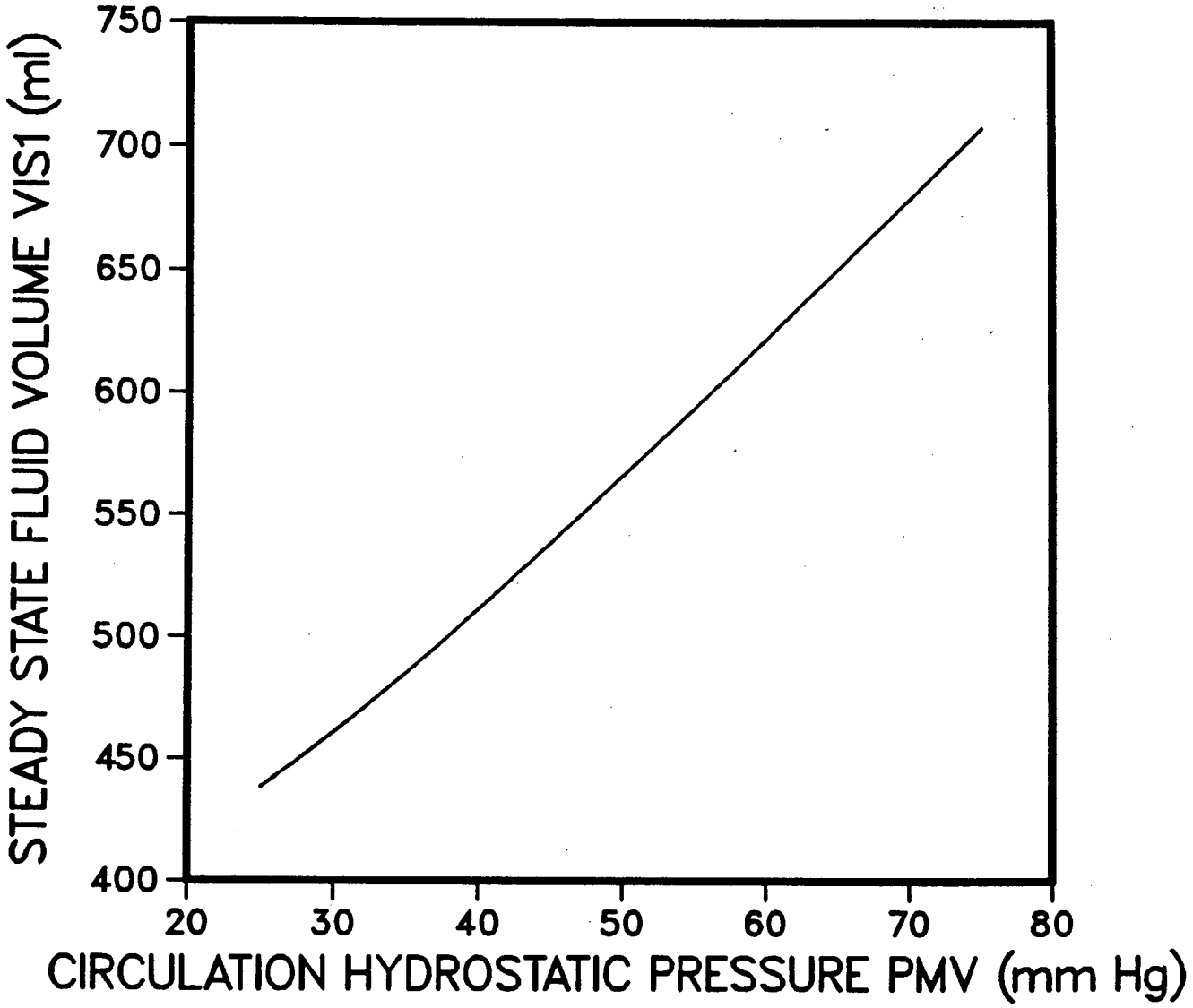

Figure 25a

Transient Responses of (JV-JL) and JAS for VTONS of 420 ml and 500 ml (Conditions as in Table 16) - Response continued to time when VTOT = 1000 ml.

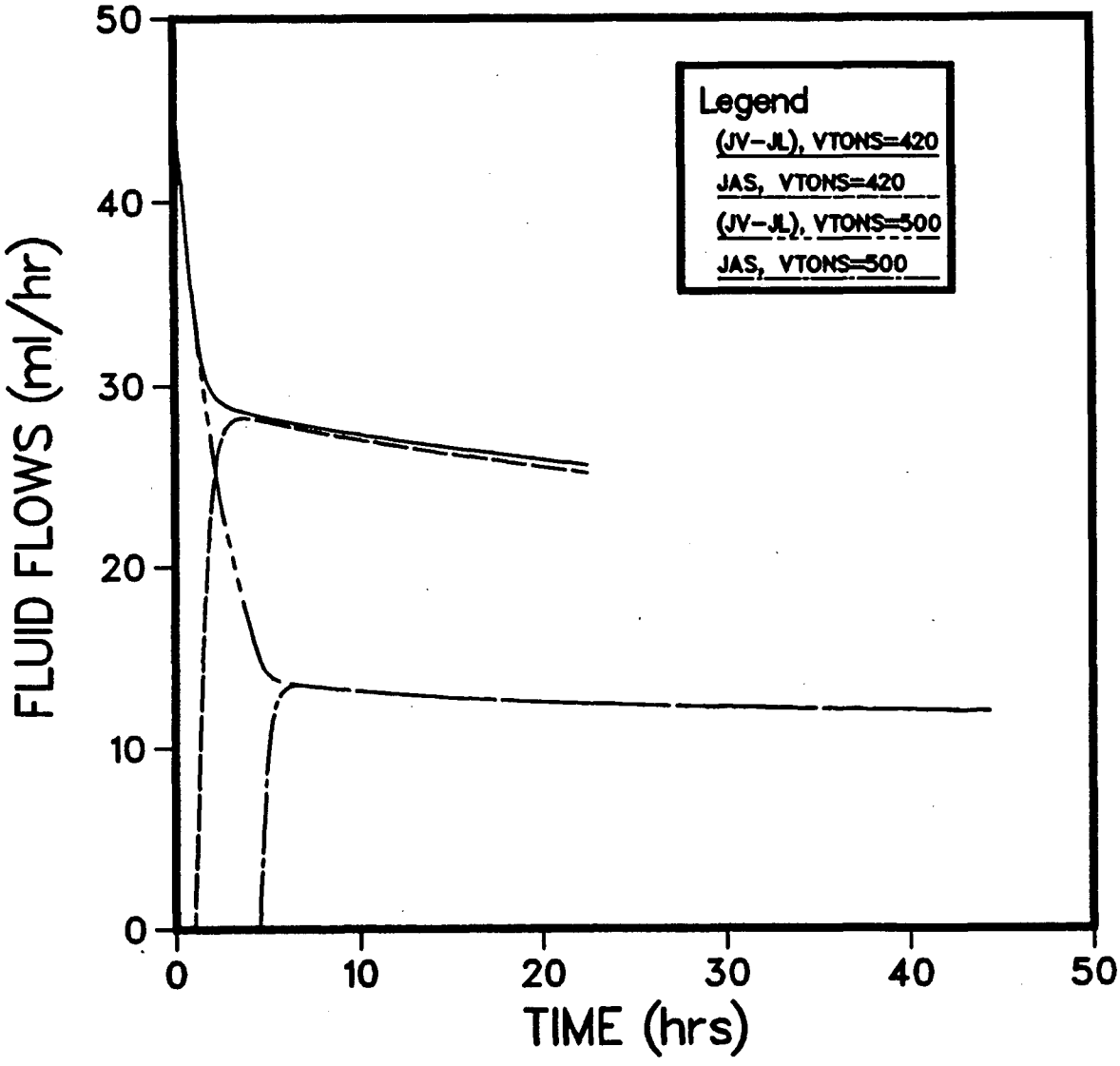

the fluid volume VIS1 will reach a value equal to VTONS and alveolar flooding will occur. As VTONS is reduced from 566 ml the difference between JV and JL at the onset of alveolar flooding increases. Figure 25a shows the transient respone of (JV-JL) up to VTOT=1000 ml for a VTONS of 420 ml and 500 ml; the time for the onset of alveolar flooding is approximately 1.0 and 4.5 hrs., respectively. The value of (JV-JL) is greater for VTONS=420 ml than a VTONS=500 ml. Since (JV-JL) is equivalent to the rate of fluid accumulation in the total extravascular space (interstitial + cellular + alveolar) the time to reach a VTOT of 1000 ml (Figure 25b) and to the onset of flooding are less for the smaller VTONS.

Figure 25a also illustrates that following the onset of alveolar flooding JAS rises to a maximum very rapidly - the shape of the JAS curve was discussed in section 5.2. As (JV-JL) at the onset of alveolar flooding increases, JAS also increases. Therefore, as VTONS is reduced JAS increases (Figure 25c). The transient response of JAS is illustrated in Figure 25c by showing the maximum JAS and the JAS at a VTOT of 1000 ml.

The simulations of the PMVES for changes in VTONS also illustrate that the EVEA fluid volume at a VTOT of 1000 ml increases as VTONS rises (Figure 25d); due to the increase in interstitial fluid accumulation before VIS1 reaches VTONS.

In section 3.4 the upper limit of VTONS experimentally observed was approximately 600 ml. For the simulations conducted in the study of VTONS the upper value of VTONS was only 500 ml. The lower value of

Figure 25b

Time to Reach a VTOT of 1000 ml for Different VTONS (Conditions as in Table 16)

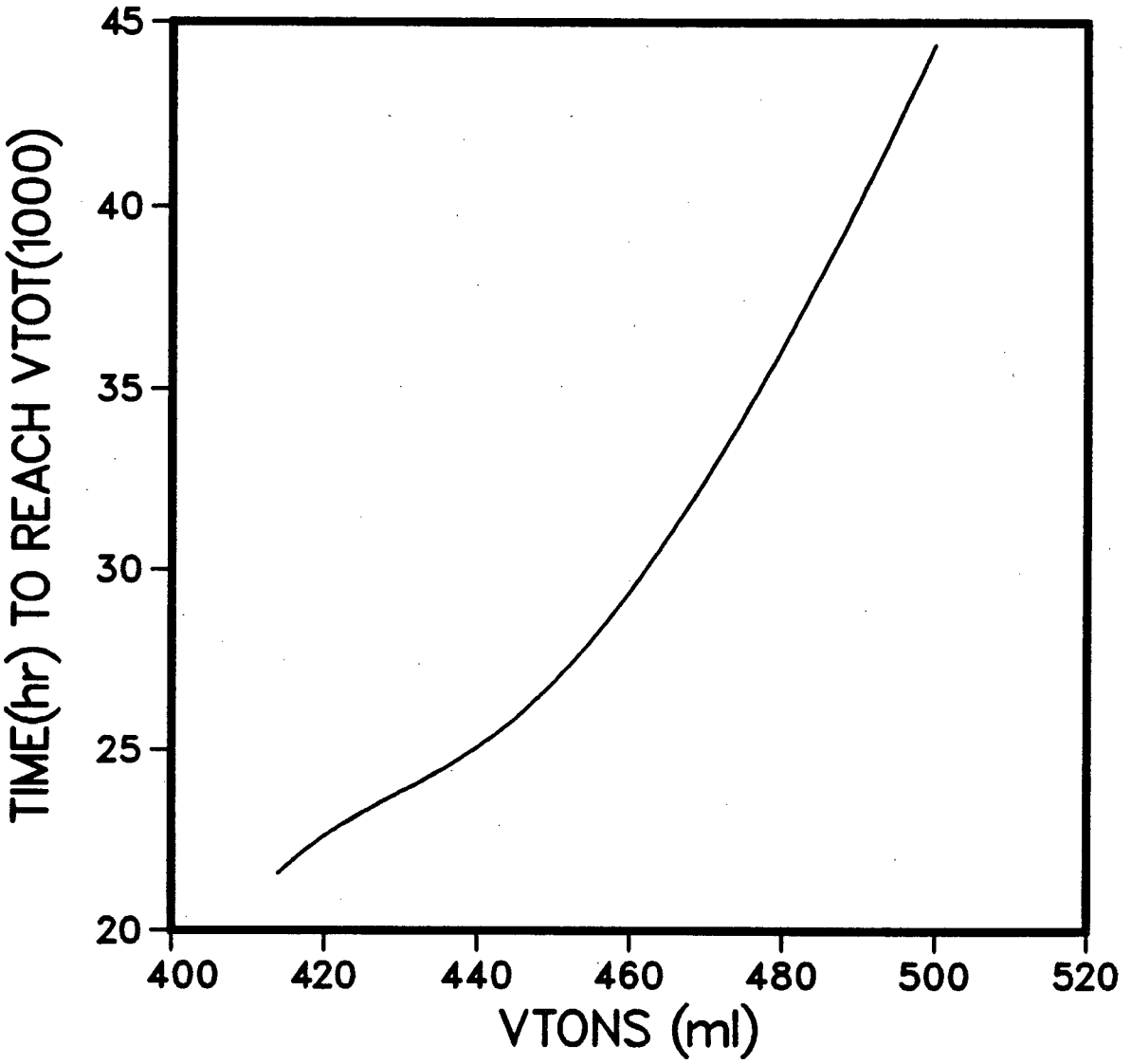

Figure 25c

The Maximum Transepithelial Flow (JAS(max)) and the JAS at a VTOT of 1000 ml for Different VTONS (Conditions as in Table 16)

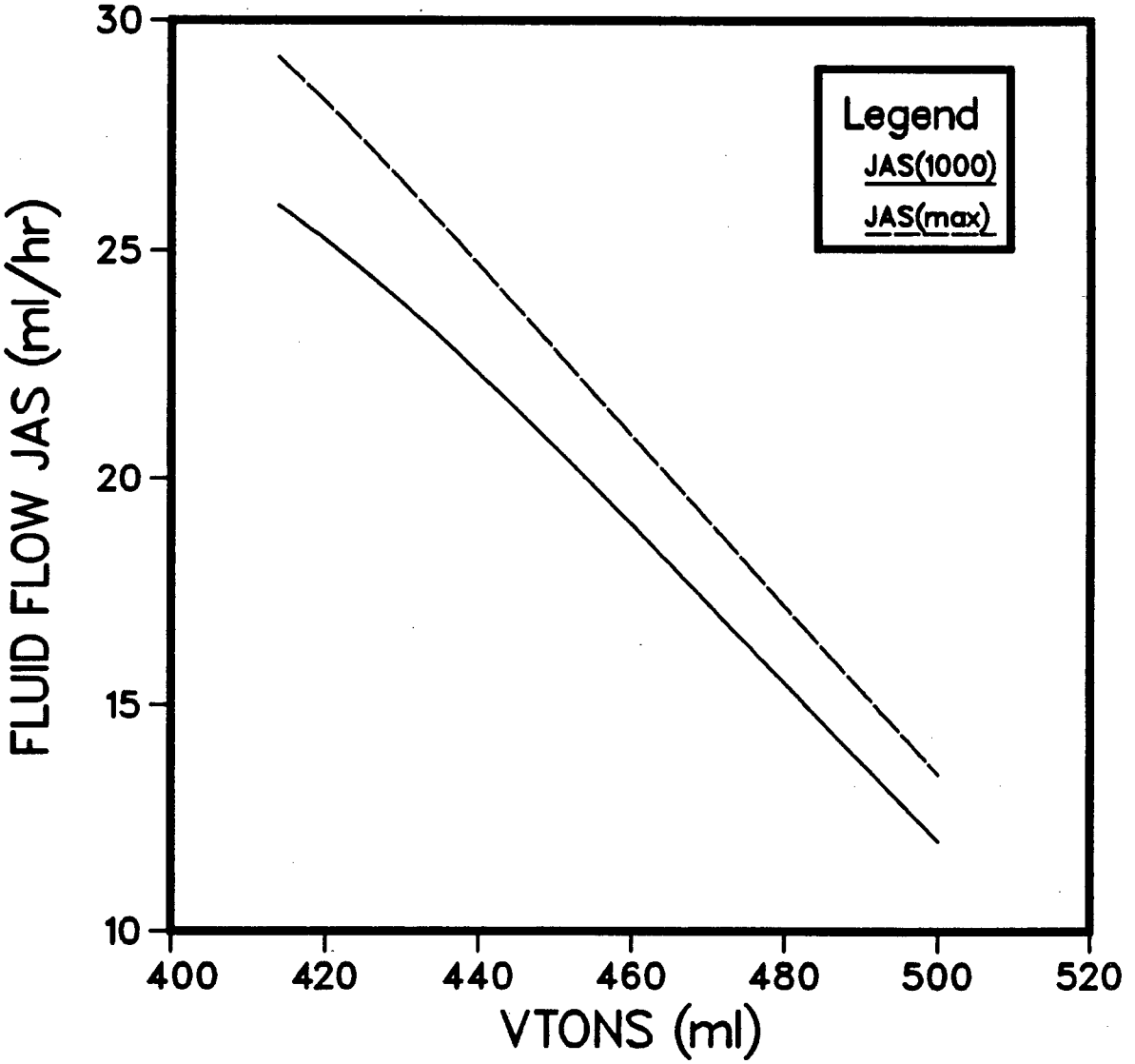

Figure 25d

The Fluid Volume VIS1 at a VTOT of 1000 ml for Different VTONS (Conditions as in Table 16)

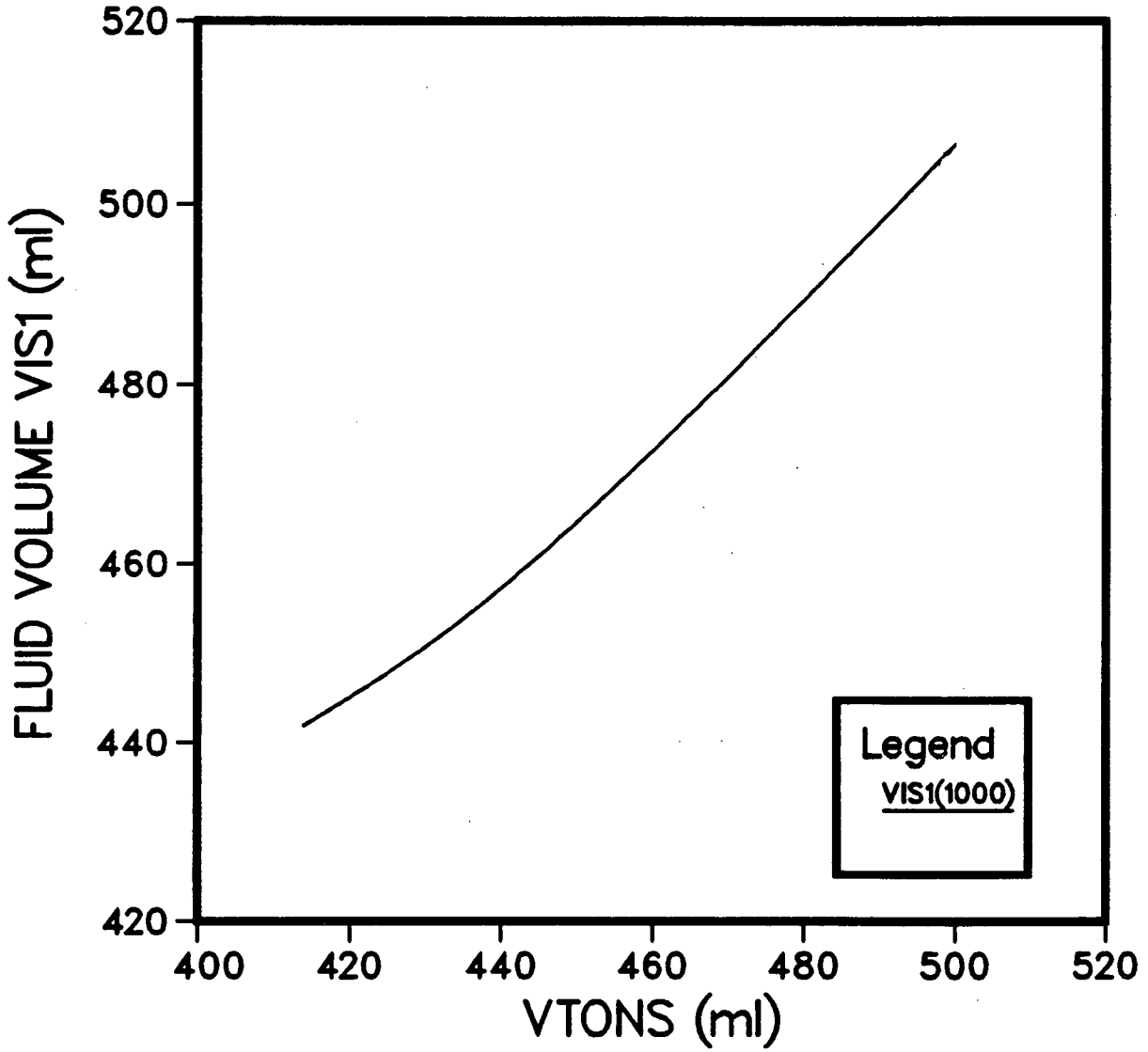

VTONS varies, depending on the origin of the perturbation. As VTONS is lowered the rate of alveolar flooding increases. An interstitial hydrostatic pressure, PPMV (onset), corresponds to the EVEA fluid volume VTONS, as determined by the tissue compliance curve. One may speculate that the alveolar barriers cannot withstand interstitial hydrostatic pressures above PPMV (onset). Guyton et al.(47) suggested that the alveolar barriers cannot withstand positive interstitial pressure. In the remaining simulations VTONS was set at 460 ml, which corresponds to an interstitial hydrostatic pressure of +1.1 mmHg.

5.4 Transient Responses of the Pulmonary Microvascular Exchange System to changes in the Parameter SL

The parameter SL is defined as the slope of the expression relating PAS to VAS - in equation (27). The effect of SL on the PMVES was studied under the conditions shown in Table 17. At time zero the PMVES was subjected to a step change in PMV from a normal value of 9 mmHg to 50 mmHg. Tests were made with values of SL between 0.25×10^{-4} mmHg/ml and 0.75×10^{-2} mmHg/ml.

In the simulations conducted to study changes in SL the alveolar fluid volume at a VTOT of 1000 ml was approximately 500 ml. Using equation (27), the change in the alveolar fluid pressure that corresponds to a change in VAS of 500 ml is 0.0125 mmHg for $SL=0.25 \times 10^{-4}$ mmHg/ml and 3.75 mmHg for $SL=0.75 \times 10^{-2}$ mmHg/ml. For the case of $SL=0.25 \times 10^{-4}$ mmHg/ml the change in PAS is insignificant as compared to the change for $SL=0.75 \times 10^{-2}$ mmHg/ml. The variable PAS

is used in evaluating the pressure gradient that causes fluid flow from the interstitium to the air space (i.e. (PPMV-PAS)); for a given PPMV at a VTOT of 1000 ml and the conditions of Table 17, (PPMV-PAS) decreases as SL increases.

The effect of SL on the PMVES was studied for NK=0.05 hr^{-1}mm Hg^{-1} and NK=50.0 hr^{-1} mm Hg^{-1}.

(i) Simulations with NK=0.05 hr^{-1} mm Hg^{-1}.

Figure 26a shows that following the maximum JAS, the rate of decrease in JAS rises as SL is increased. This is caused by the rise in PAS as SL is increased (Figure 26b). The fluid material balance of equation (32) illustrates that (JNET1 + JAS) equals (JV-JL). As the simulation of the PMVES progresses to steady state conditions (JV-JL) decreases. Following the onset of alveolar flooding the change in (JV-JL) is generally small during non-steady state conditions to a VTOT of 1000 ml. Therefore, as JAS decreases in the period just before a VTOT of 1000 ml, JNET1 will increase. The increase in JNET1 may be reflected by the change in the transient response of VIS1. Since the rate of decline in JAS increases as SL is raised, JNET1 would increase with SL. Figure 26c shows that the increase in VIS1 is more pronounced as SL increases.

(ii) Simulations with NK=50.0 hr^{-1} mm Hg^{-1}.

Following the time of the onset of alveolar flooding (2.5 hrs): for NK=50 hr^{-1} mm Hg^{-1} an increase in SL also increases the alveolar fluid pressure, as seen by Figure 27a. However, the transient responses of JAS, up to the time that VTOT=1000 ml, is not

Table 17

Conditions of the PMVES Simulation
Conducted to Study Changes in SL*

SL = 0.25×10^{-4}, 0.25×10^{-3}, 0.25×10^{-2} and 0.75×10^{-2} mmHg/ml

KAS = NK(VIS1-VTONS) for VISL > VTONS
NK = 0.5, 50. hr^{-1} mm Hg^{-1}

PMV	=	50	mm Hg
KF	=	1.12	ml/hr/mm Hg
ΔPERM	=	0	
SIGD	=	0.75	
PSA	=	3.0	ml/hr
PSG	=	1.0	ml/hr
SIGFA	=	0.40	
SIGFG	=	0.60	
VTONS	=	460	ml
B	=	-3.03	mm Hg
VLMPH	=	5000.	ml

*These are the conditions of the simulations that produced the results illustrated in Figures 26a,b,c and 27 a,b.

Figure 26a

Transient Responses of JAS for Different SL and NK = 0.05 hr^{-1} $mmHg^{-1}$ (Conditions as in Table 17) - Responses continued to time when VTOT = 1000 ml

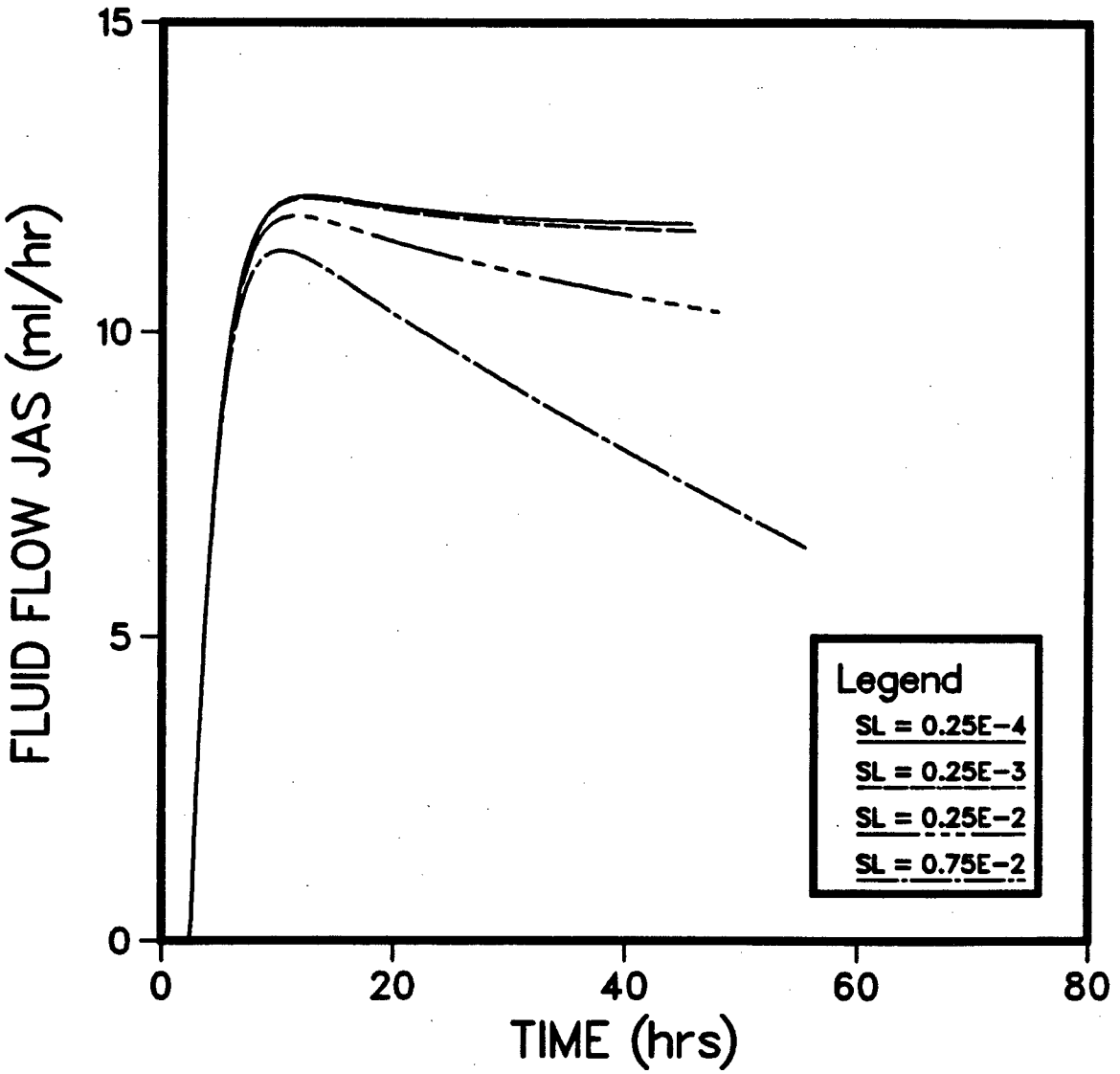

Figure 26b

Transient Responses of PAS for Different SL and NK = 0.05 hr^{-1} $mmHg^{-1}$ (Conditions as in Table 17) - Responses continued to time when VTOT = 1000 ml

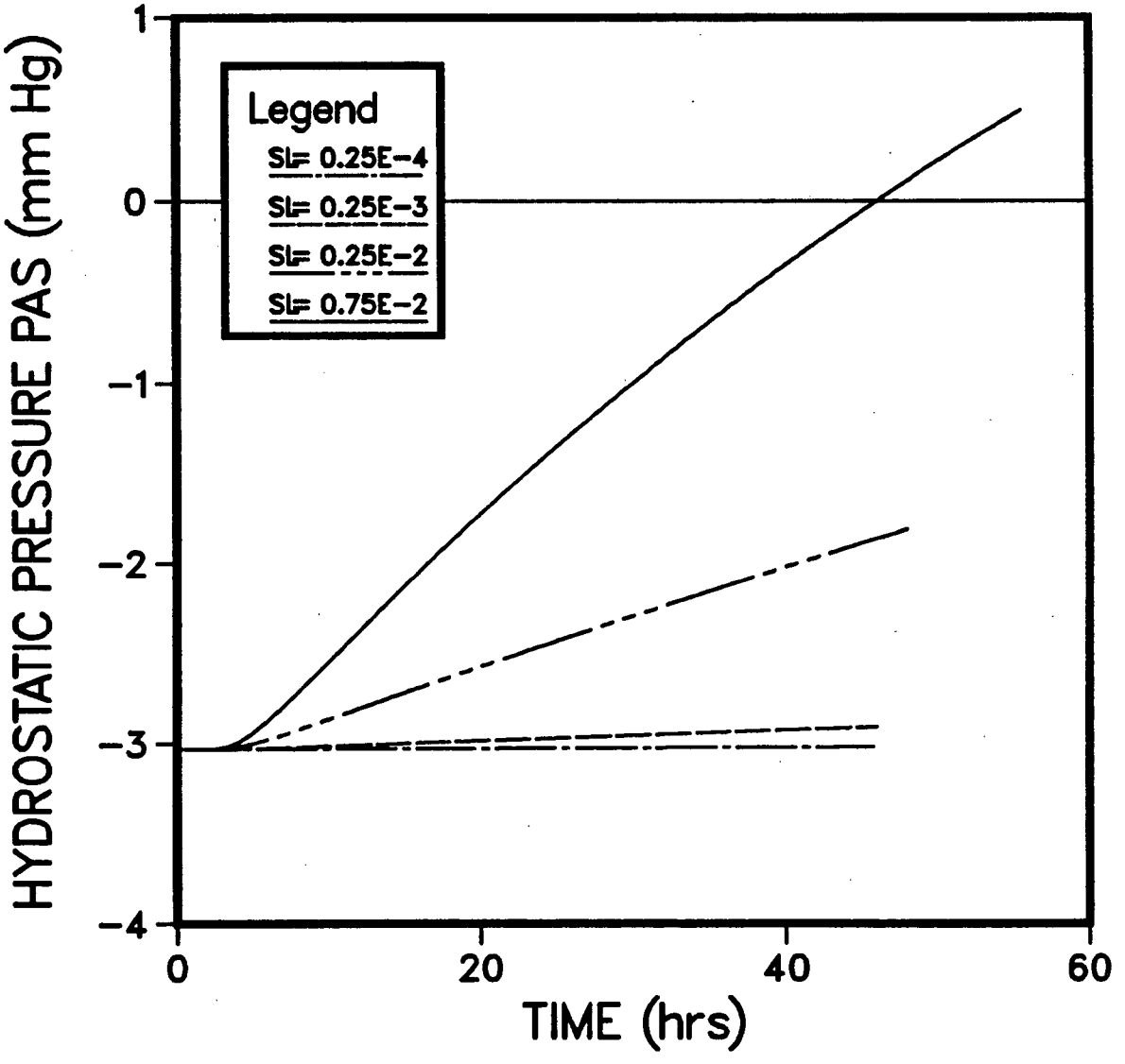

Figure 26c

Transient Responses of VIS1 for Different SL and NK = 0.05 hr^{-1} $mmHg^{-1}$ (Conditions as in Table 17)- Responses continued to time when VTOT = 1000 ml

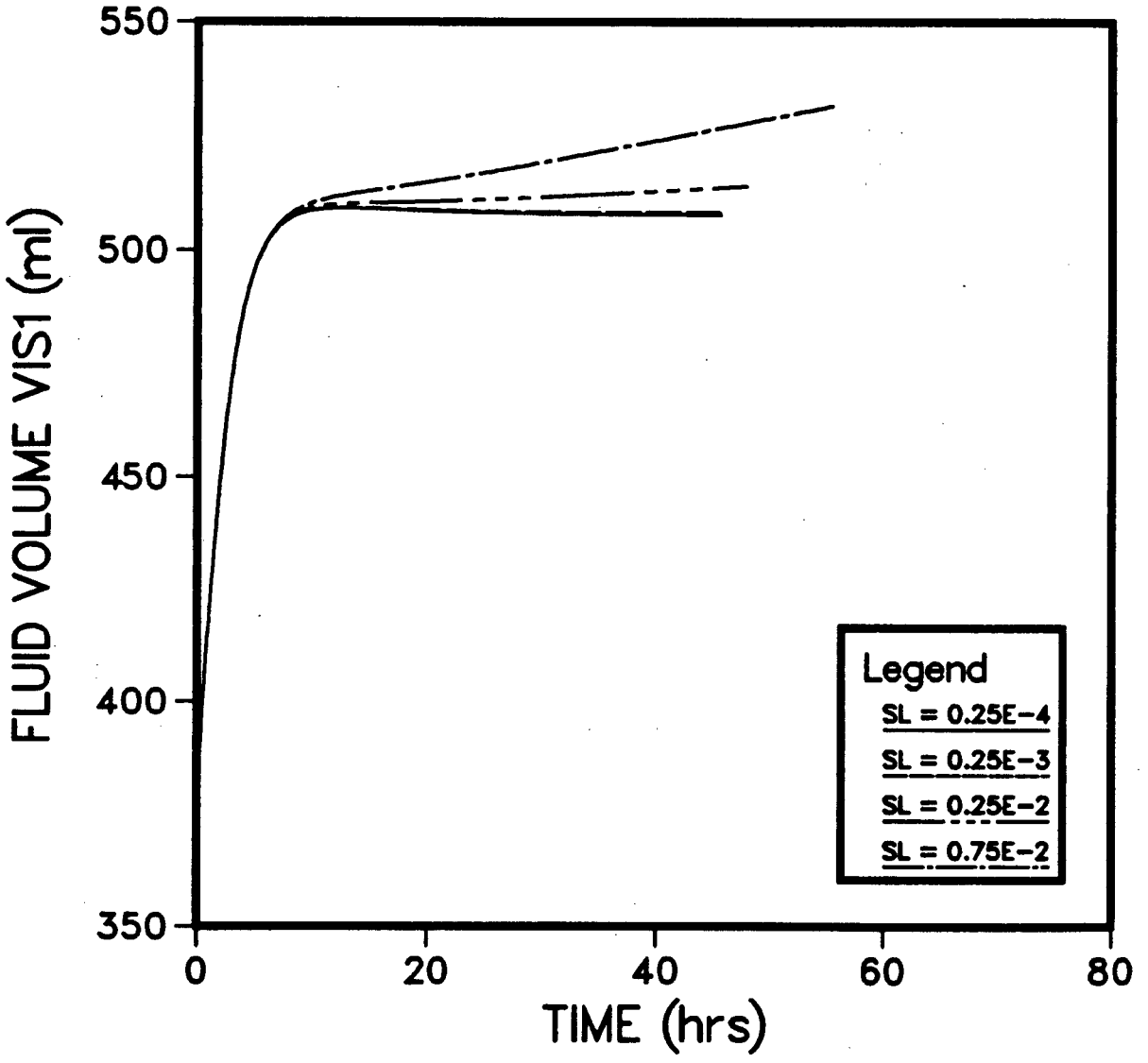

Figure 27a

Transient Responses of PAS for Different SL and NK = 50.0 hr^{-1} $mmHg^{-1}$ (Conditions as in Table 17) - Responses continued to time when VTOT = 1000 ml

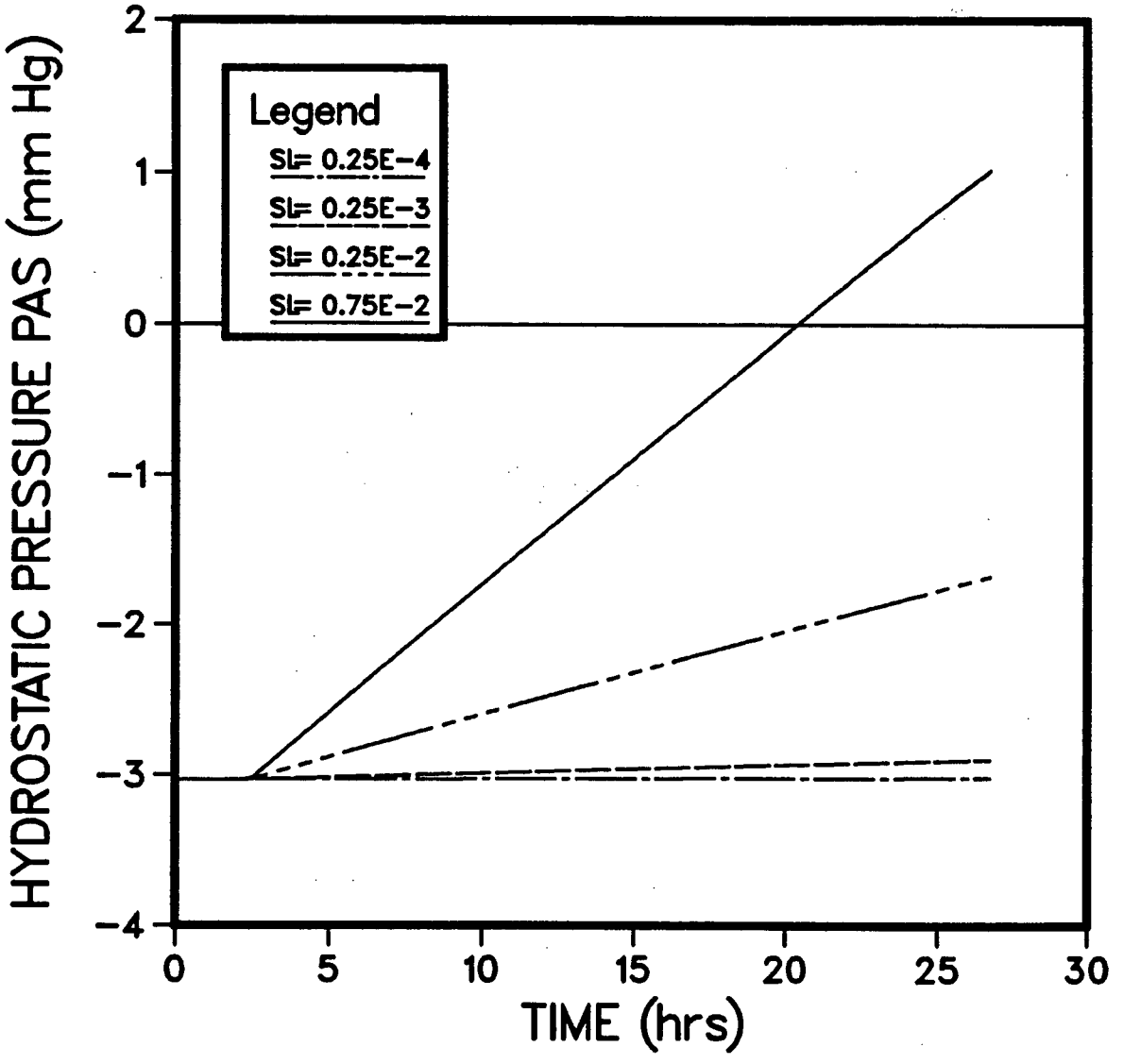

Figure 27b

Transient Responses of JAS for Different SL and NK = 50.0 hr^{-1} $mmHg^{-1}$ (Conditions as in Table 17) - Responses continued to time when VTOT = 1000 ml

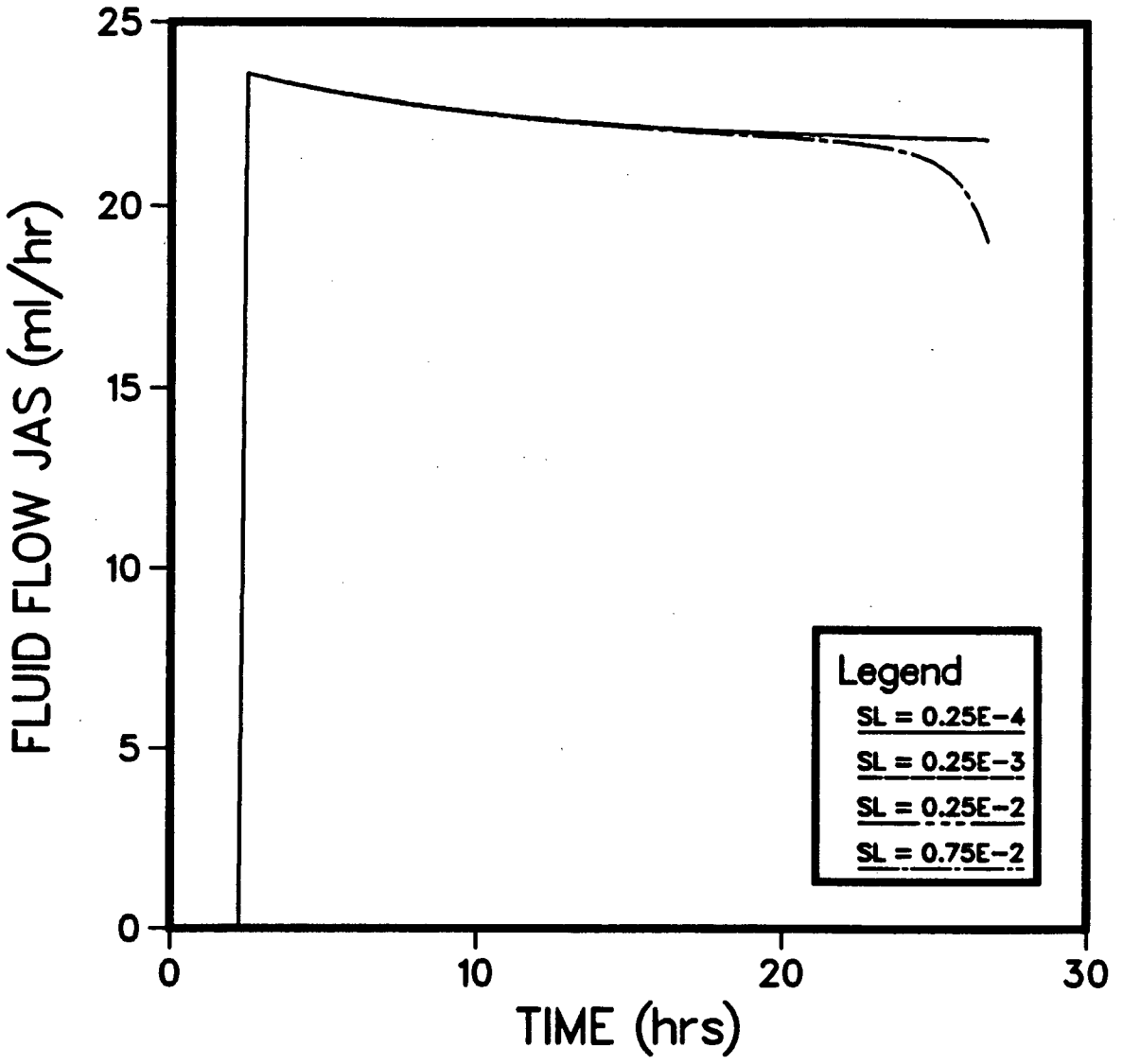

affected by the different values of SL - see Figure 27b. In the determination of JAS the variables VIS1 and PAS exhibit competing effects; the rise in PAS attempts to suppress JAS, while a rise in VIS1 attempts to augment JAS by increasing KAS and PPMV. In the situation where NK=50 hr^{-1} mm Hg^{-1}, the difference (VIS1-VTONS) need only rise by 0.1 ml for a doubling of KAS; JAS is, thus, more responsive to KAS than to PAS.

5.5 Responses of the Pulmonary Microvascular Exchange System to changes in the parameter B.

The parameter B represents the value of the alveolar fluid pressure at the onset of alveolar flooding. The effect of B on the predictions of the PMVES simulation was studied under the conditions listed in Table 18. At time zero the PMVES was subjected to a step change in PMV from 9 mm Hg to 50 mm Hg. For all values of B studied, the time for onset of alveolar flooding is about 2.5 hrs.

Following the onset of alveolar flooding the driving force that causes transepithelial flow is (PPMV-PAS). As B decreases, the initial value of the pressure gradient (PPMV-PAS) will increase. The transient response of JAS may be illustrated by recording the maximum JAS (JAS (max)) and the JAS at a VTOT of 1000 ml (JAS (1000)) for each value of B (Figure 28a); the transient response of JAS between these two points is a gradual decrease from JAS (max) to JAS (1000). Figure 28a illustrates that JAS (max) and JAS (1000) increase as B is reduced from approximately 1.0 mm Hg to -4 mm Hg, but does not change

Table 18

Conditions of the PMVES Simulations Conducted to Study the Changes in B*

B: varied from -10 to 1.0 mm Hg

KAS = NK(VIS1-VTONS) for VIS1 > VTONS
NK = 0.5 hr^{-1} mm Hg^{-1}

PMV	=	50	mm Hg
KF	=	1.12	ml/hr/mm Hg
ΔPERM	=	0	
SIGD	=	0.75	
PSA	=	3.0	ml/hr
PSG	=	1.0	ml/hr
SIGFA	=	0.40	
SIGFG	=	0.60	
VTONS	=	460	ml
SL	=	0.25×10^{-2}	mm Hg/ml
VLMPH	=	5000	ml

*These are the conditions of the simulations that produced the results illustrated in Figures 28a to 28g.

Figure 28a

The maximum transepithelial flow (JAS(max)) and JAS at a VTOT of 1000 ml for Different B (Conditions as in Table 18)

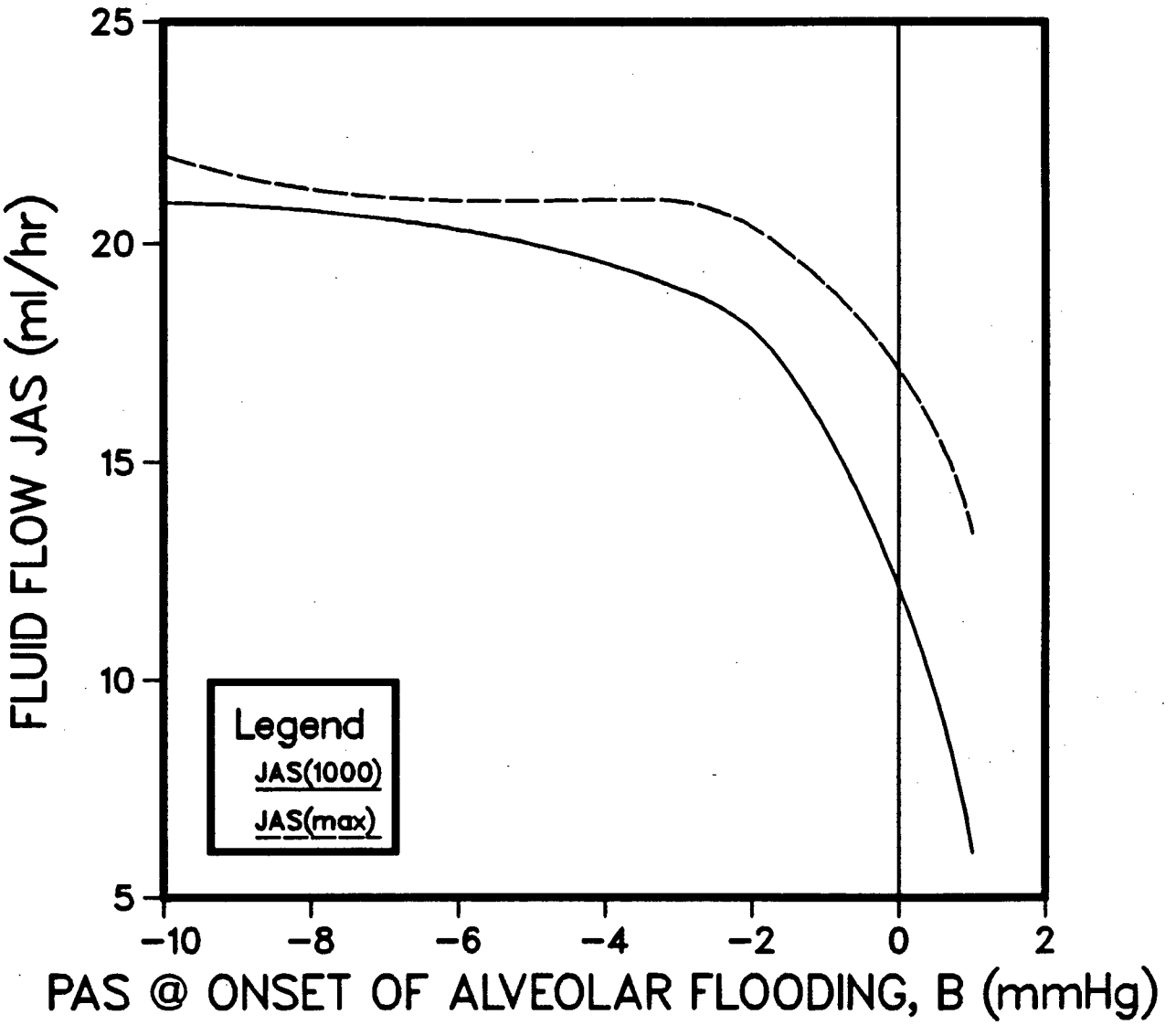

significantly for B less than -4 mm Hg. The following discussion will treat these regions separately.

(i) The region of B less than -4 mm Hg.

JAS is determined by the product of KAS and (PPMV-PAS). Figure 28b illustrates the transient response of (PPMV-PAS) for B=-10 mm Hg and B= -6 mm Hg; the area of interest is for time greater than the time at the onset of alveolar flooding (2.5 hrs). As B is decreased from -6 mm Hg to -10 mm Hg, (PPMV-PAS) increases. Figure 28c shows the transient response of KAS for B= -10 mm Hg and B= -6 mm Hg; as B is decreased from -6 mm Hg to -10 mm Hg, KAS decreases. The factor by which (PPMV-PAS) increases as B is lowered from -6 mm Hg to -10 mm Hg is equivalent to the factor by which KAS decreases as B is lowered from -6 mm Hg to -10 mm Hg. Therefore, the product of KAS and (PPMV-PAS) for B= -6 mm Hg yields a value approximately equal to the product of KAS and (PPMV-PAS) for B= -10 mm Hg. Figure 28a illustrates that JAS(max) and JAS(1000) for B= -6 mm Hg and -10 mm Hg are approximately equal.

Since JAS(1000) is the same for values of B less than -4 mm Hg, the time to reach a VTOT of 1000 ml is also similar (Figure 28d).

(ii) The region of B greater than -4 mm Hg

For the region of B greater than -4 mm Hg the transient responses of (PPMV-PAS) and KAS are illustrated for B= -3 mm Hg and B= 0.5 mm Hg in Figures 28e and 28f respectively. Figure 28e illustrates that following the time of the onset of alveolar flooding (2.5 hrs)

Figure 28b

Transient Responses of (PPMV-PAS) for B = -10 mmHg and B = -6 mmHg (Conditions as in Table 18) - Responses continued to time when VTOT = 1000 ml

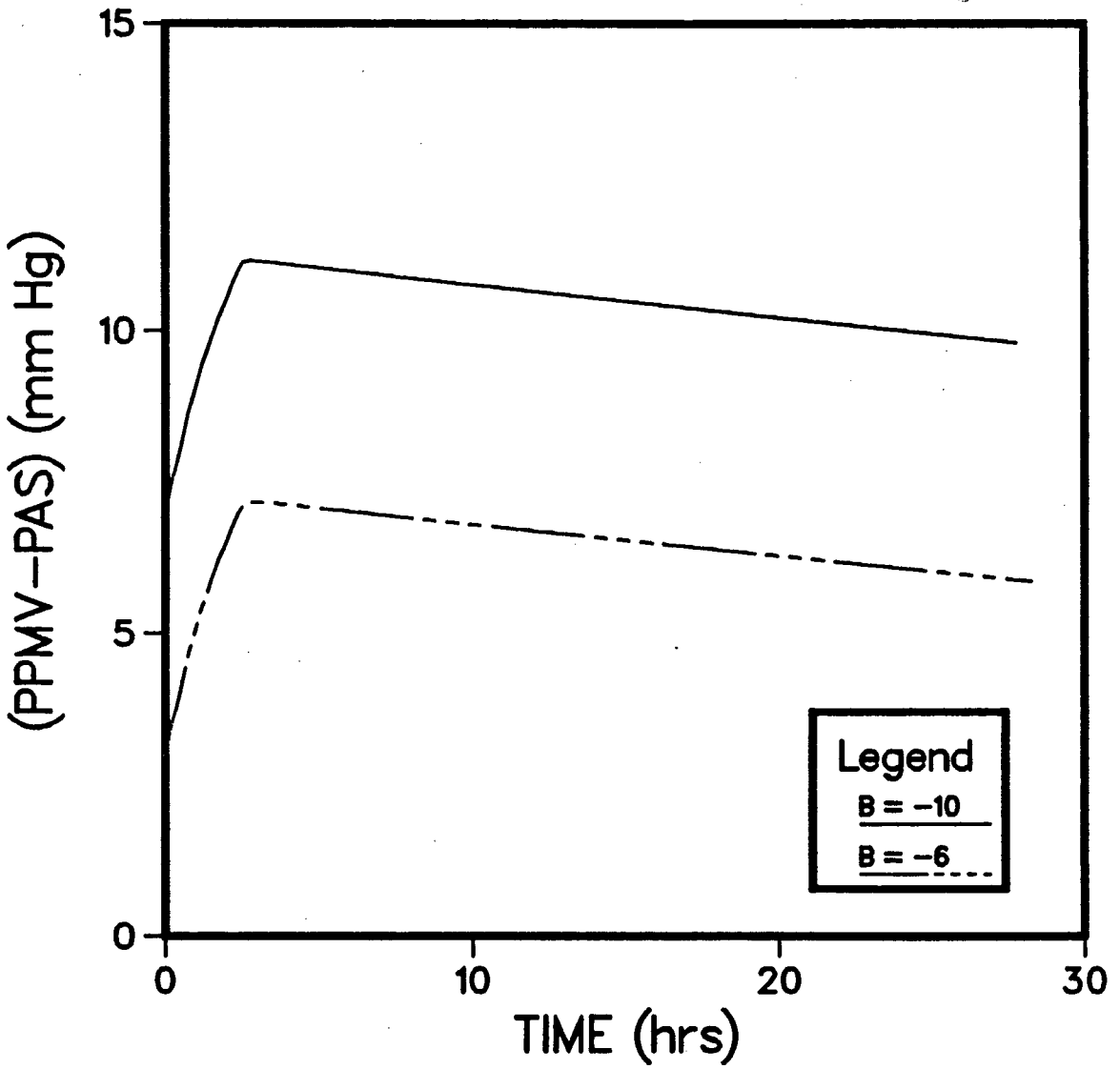

Figure 28c

Transient Responses of KAS for B = -10 mmHg and B = -6 mmHg (Conditions as in Table 18) - Responses continued to time when VTOT = 1000 ml

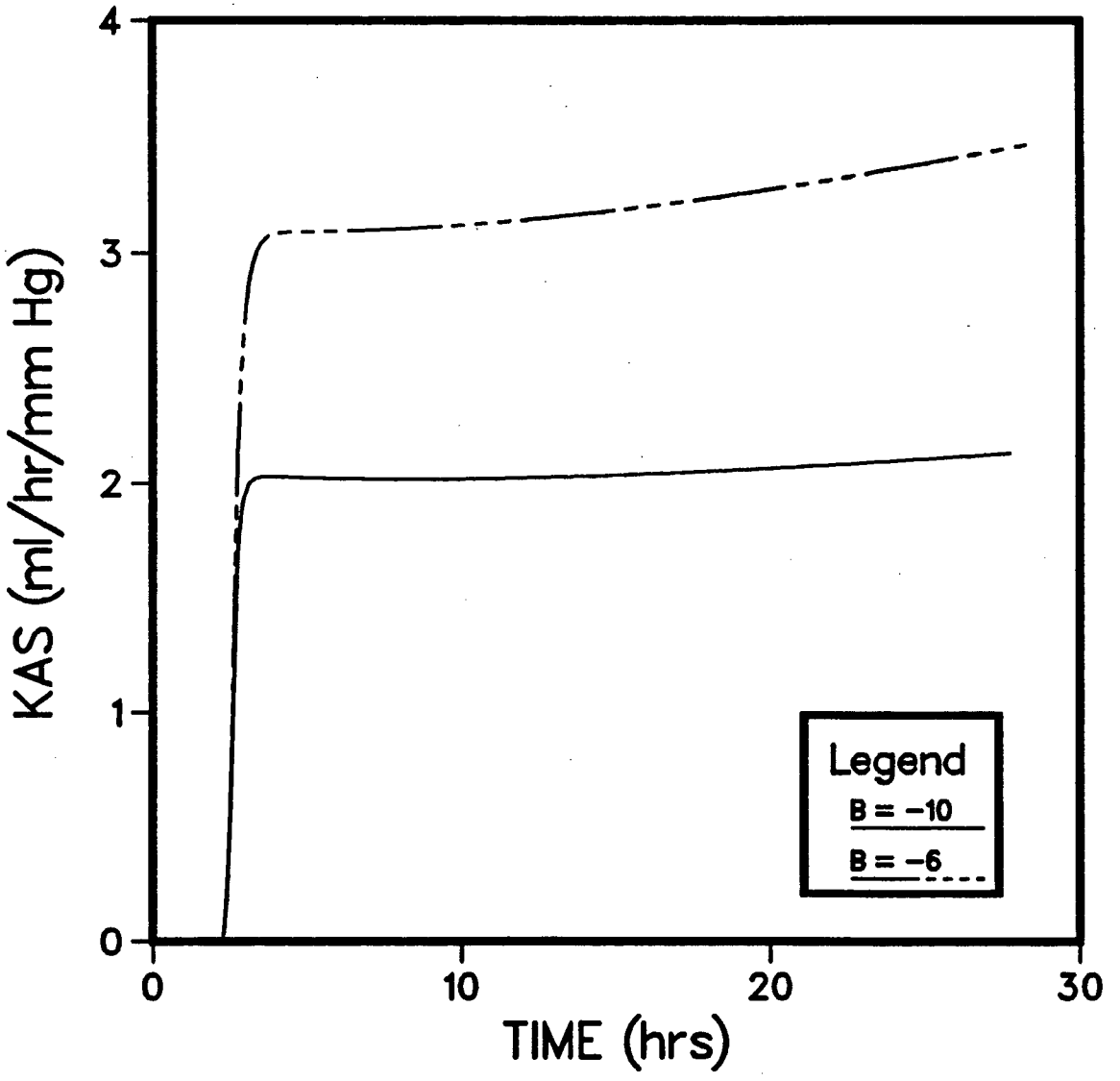

Figure 28d

Time to reach a VTOT of 1000 ml for Different B
(Conditions as in Table 18)

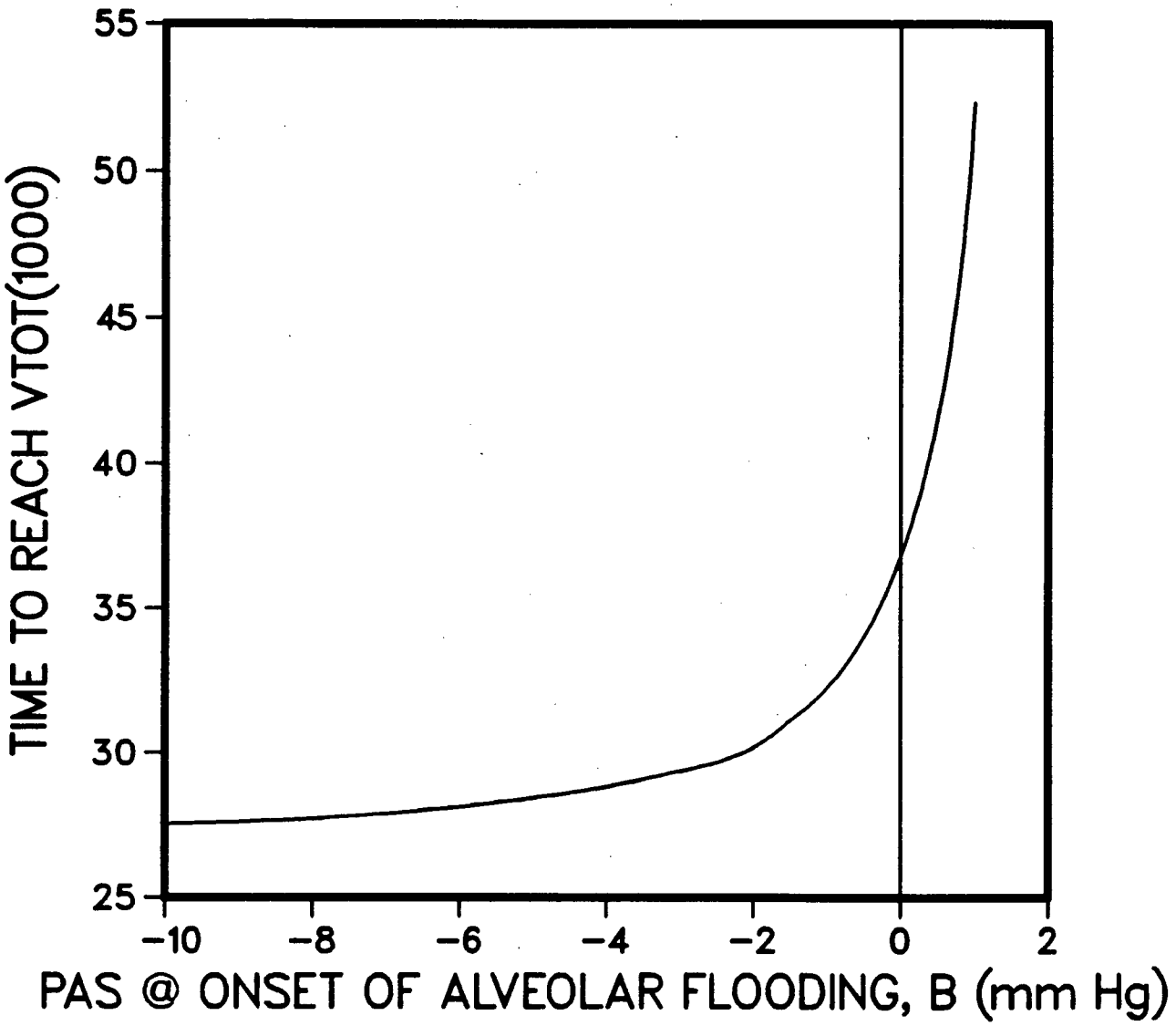

Figure 28e

Transient Responses of (PPMV-PAS) for B = -3 mmHg and B = 0.5 mmHg (Conditions as in Table 18) - Responses continued to time when VTOT = 1000 ml

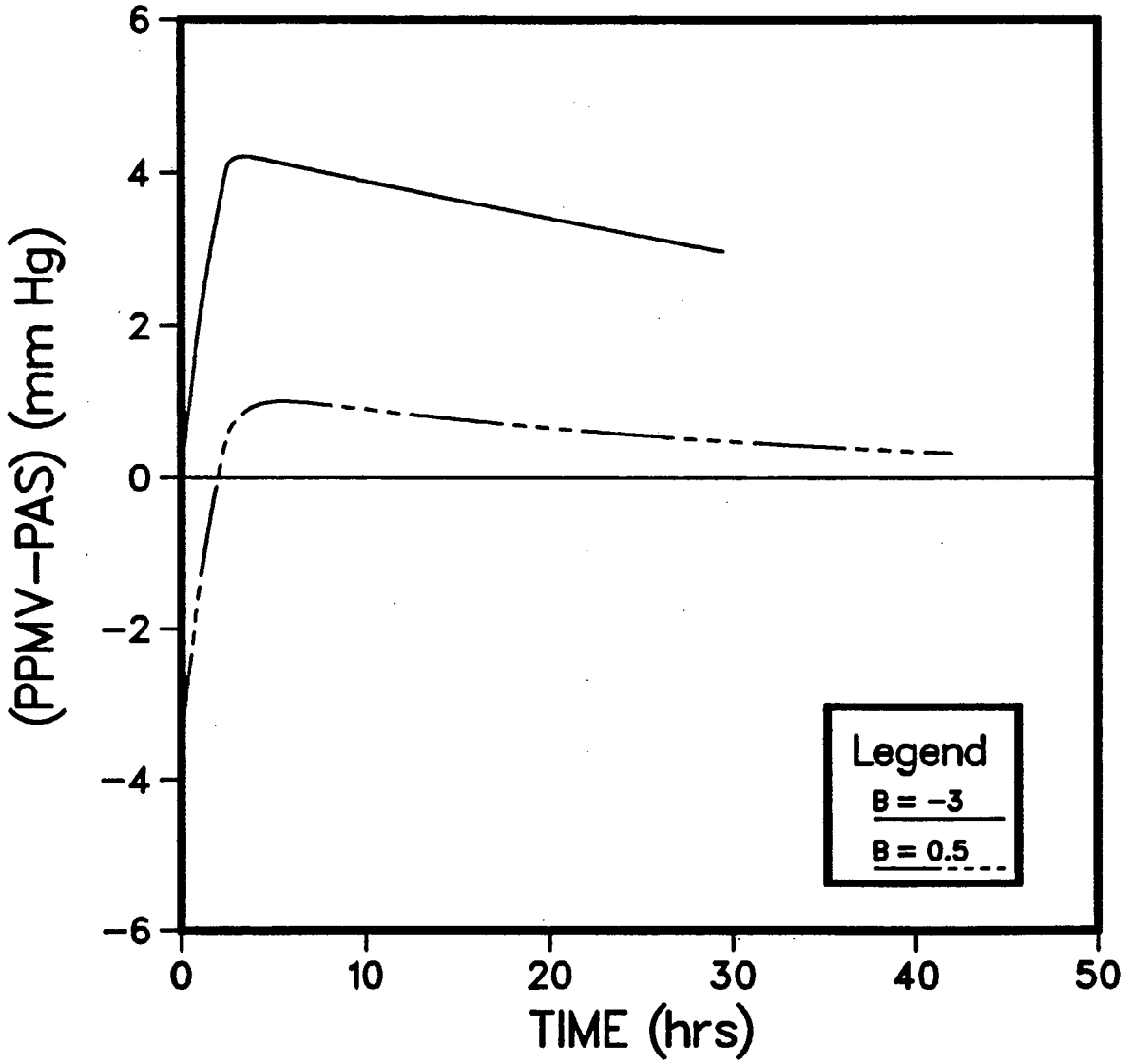

Figure 28f

Transient Responses of KAS for B = -3 mmHg and B = 0.5 mmHg (Conditions as in Table 18) - Responses continued to time when VTOT = 1000 ml

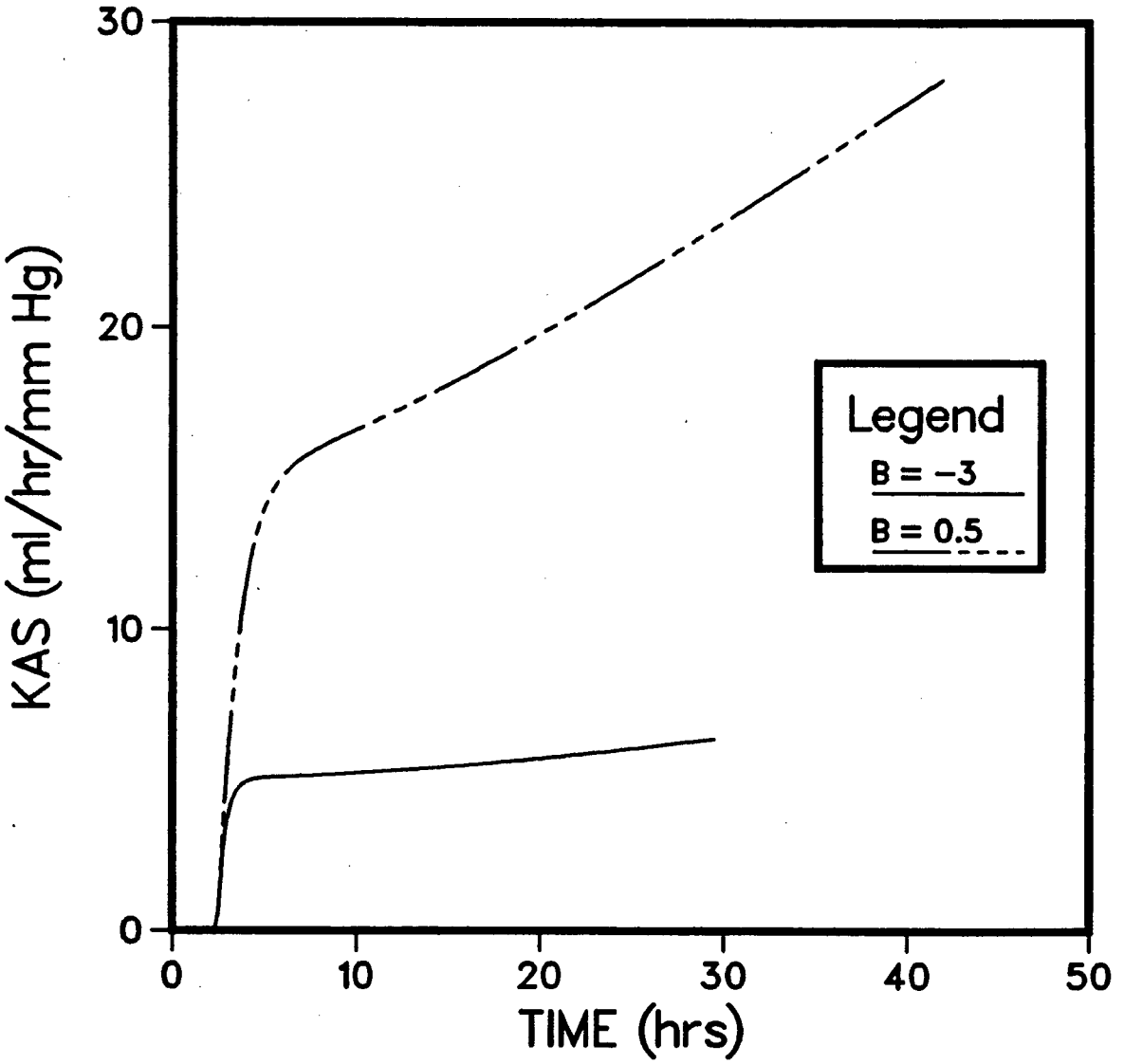

the pressure difference (PPMV-PAS) is less for B = 0.5 mm Hg than for B = -3 mm Hg, while in Figure 28f KAS increases as B is increased from -3 mm Hg to 0.5 mm Hg. After a time of about 7.5 hrs. the slope of the KAS-time curve for B = 0.5 mm Hg is greater than for B = -3 mmHg. However, the product of KAS and (PPMV-PAS) at JAS(max) and at JAS(1000) is less for B = 0.5 mm Hg than for B = -3 mm Hg (Figure 28a). As B is raised from -4 mm Hg, the factor by which (PPMV-PAS) decreases is higher than the factor by which KAS increases. The decline in JAS as B is raised above -4 mm Hg leads to an increase in the time to reach a VTOT of 1000 ml (Figure 28d).

An increase in B also causes a rise in the fluid volume VIS1 at a VTOT of 1000 ml, as shown in Figure 28g. At a PMV of 50 mm Hg and the conditions of Table 18 the steady state VIS1 is 566 ml (as stated in section 5.3). At an EVEA fluid volume of 460 ml (VTONS) the interstitial hydrostatic pressure, PPMV, is 1.09 mm Hg. As B is increased towards 1.09 mm Hg the value of KAS increases; Figure 28f shows that KAS increases when B is raised from -3 mm Hg to 0.5 mm Hg. Corresponding to the increase in KAS is a rise in VIS1. If VIS1 rises to 566 ml, then steady state will be achieved and alveolar flooding terminated. As B approaches 1.09 mm Hg the total extravascular fluid volume (VIS1+VAS) at steady state will decrease; the fluid volume VAS, in particular will decrease. The bulk of the edema fluid is then contained in the interstitial compartment.

If B is elevated to values above 1.09 mm Hg, and conditions remain at those stated in Table 18, then the pressure gradient

Figure 28g

Fluid Volume VIS1 at a VTOT of 1000 ml for Different B (Conditions as in Table 18)

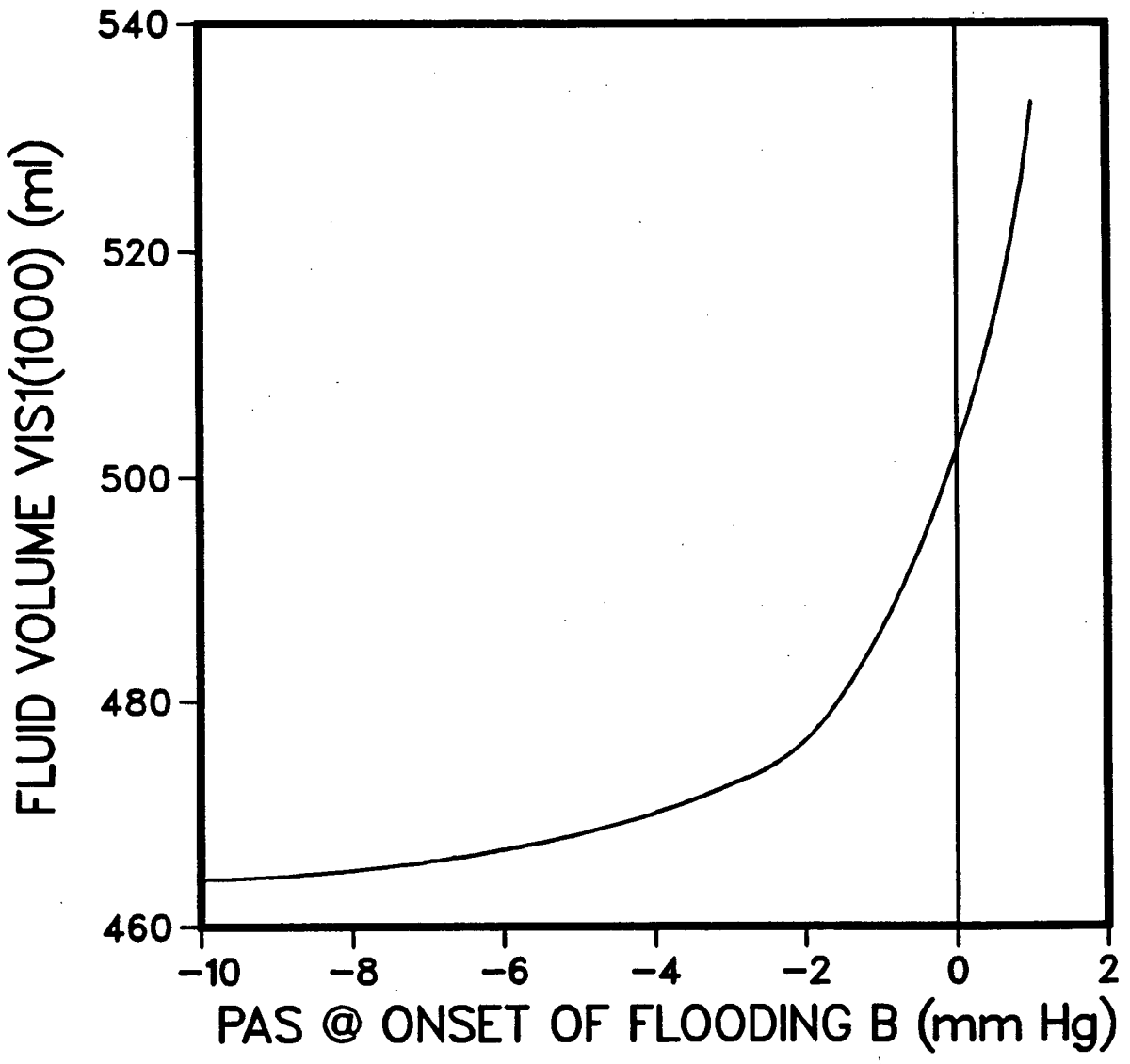

(PPMV-PAS) at the onset of alveolar flooding will become negative, and the transepithelial flow will be initially from the alveolar space to the interstitial space. However, the fluid volume of the air space at the onset of alveolar flooding is zero; a transepithelial flow from the air space to the interstitial space initially will reduce VAS to negative values. Since negative values in VAS are unrealistic, the upper limit of B is 1.09 mm Hg or the interstitial pressure corresponding to a fluid volume of VTONS.

The alveolar fluid pressure (PL=PAS) is related to the gas pressure (PG) according to Laplace's equation, equation (4). Elevation of PG will raise PL. At the onset of alveolar flooding PL is equivalent to B. If B is increased, then the total extravascular fluid volume (VIS1+VAS) at steady state conditions will decrease, i.e. there will be less fluid accumulation in the air space. Clinically, the parameter B may be elevated by applying a positive pressure to the gas space, thus increasing PG, which in turn increases B. Caldini et al. (50) subjected isolated dog lung lobes to continuous positive-pressure ventilation during an increase in the pulmonary microvascular pressure (PMV), i.e., hydrostatic pulmonary edema was induced. If the air space pressure (PG) was maintained above a certain value no "appreciable amount of liquid accumulated in the airways". For PG less than this value "frothy bloody liquid flowed continuously from the endotracheal cannula" during acute pulmonary edema. This set of observations by Caldini et al. (50) supports the significance of the elevation in B.

5.6 The Response of the Pulmonary Microvascular Exchange System to a Maximum Lymph Flow

Lymph flow is related to the fluid volume VIS1 through equation (21). A maximum capacity of the lymphatics may be defined by either JL(max) or equivalently VLMPH. In the computer program the maximum capacity of the lymphatics is related to the EVEA fluid volume VLMPH. JL will be determined by equation (21) until VIS1 reaches VLMPH; further increases in VIS1 will not raise JL. The effect of changes in JL(max) (or VLMPH) on the predictions of the PMVES simulation was studied under the conditions listed in Table 19. The epithelial filtration coefficient was, again, considered to be variable with NK = 0.5 hr^{-1} mm Hg^{-1}. At time zero the PMVES was subjected to a step-change in PMV from 9 mm Hg to 50 mm Hg.

A first estimate of JL(max) as suggested in section 4.4.2, could be the lymph flow corresponding to a fluid volume VTONS (460 ml). Using equation (21) to calculate the lymph flow, JL(max) becomes 22.6 ml/hr. The value of JL(max) was varied above and below 22.6 ml/hr. Figure 29a shows the lymph flow responses, up to a time when VTOT = 1000 ml, for JL(max) equal to 14.8, 22.6 and 24.3 ml/hr, and when no maximum lymph flow exists. When JL(max) is approximately 7% greater than 22.6 ml/hr (i.e., 24.3 ml/hr), Figure 29a illustrates that the response of JL is very close to the response of JL when no maximum lymph flow is defined. Decreasing JL(max) from 22.6 ml/hr by approximately 35% (i.e., 14.8 ml/hr) produces a noticeable change in the lymph flow response, in comparison to the response of JL when no

Table 19

Conditions of the PMVES Simulations Conducted to Study Changes in the Maximum Lymph Flow*

JL(max) varied from 14 to 38 ml/hr corresponds to a VLMPH of 410 to 550 ml.

KAS = NK(VIS1-VTONS) for VIS1 > VTONS
NK = 0.5 hr^{-1} mm Hg^{-1}

PMV	=	50	mm Hg
KF	=	1.12	ml/hr/mm Hg
ΔPERM	=	0	
SIGD	=	0.75	
PSA	=	3.0	ml/hr
PSG	=	1.0	ml/hr
SIGFA	=	0.40	
SIGFG	=	0.60	
VTONS	=	460	ml
SL	=	0.25×10^{-2}	mmHg/ml
B	=	-3.03	mmHg

*These are the conditions of the simulations that produced the results illustrated in Figures 29a to 29c.

Figure 29a

Transient Responses of JL for Different JL(max) (or VLMPH) (Conditions as in Table 19) - Responses continued to time when VTOT = 1000 ml

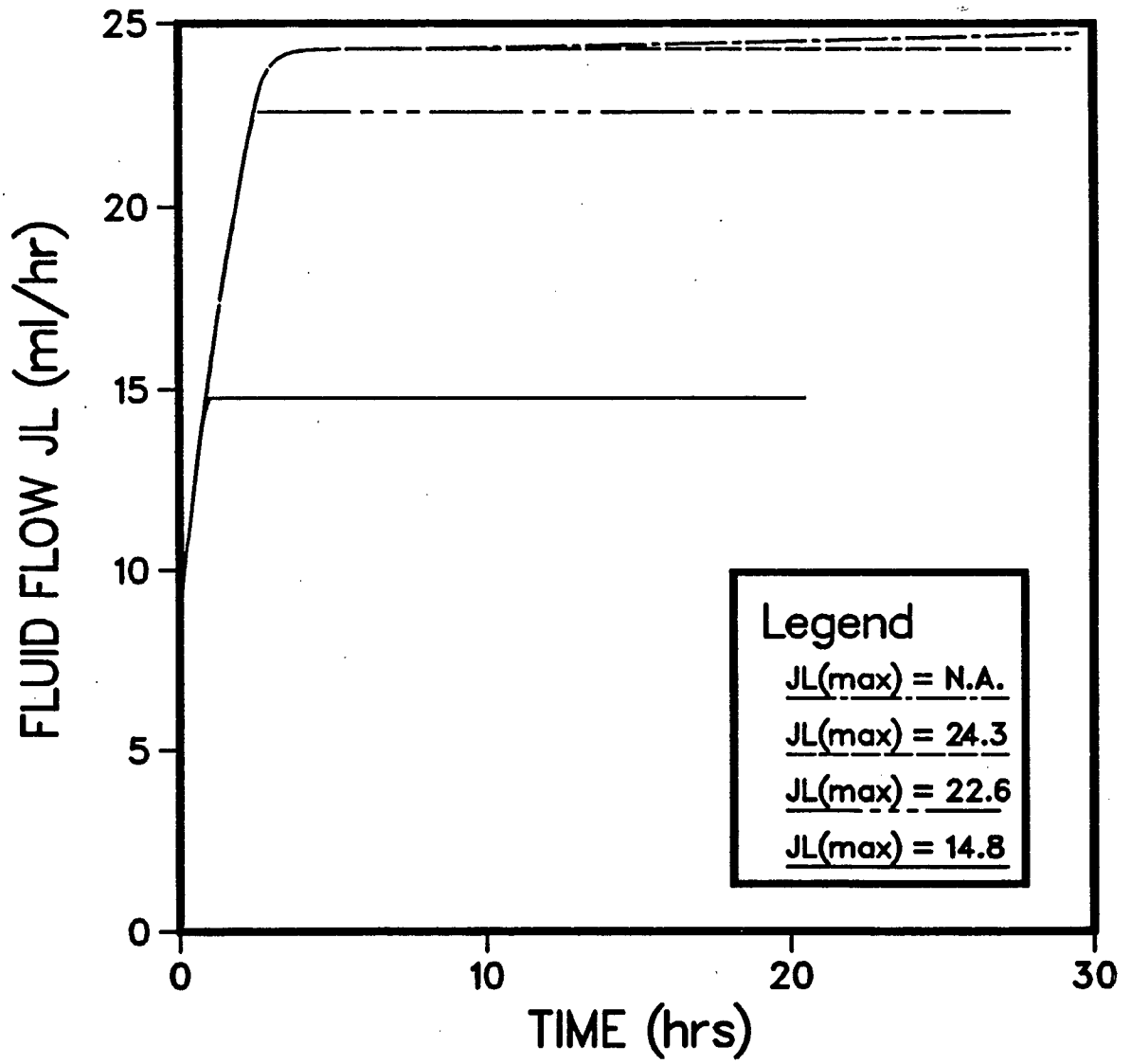

maximum lymph flow is defined.

Figure 29b illustrates the transient responses of (JV-JL) for three maximum lymph flows: 14.8, 22.6 and 29.4 ml/hr. Increasing JL(max) from 22.6 ml/hr to 29.4 ml/hr (a 30% increase) produces a small drop in (JV-JL) that averages 2 ml/hr, while a decrease in JL(max) from 22.6 ml/hr to 14.8 ml/hr (a 35% decrease) produces an average rise in (JV-JL) of about 7.5 ml/hr. Since (JV-JL) represents the rate of fluid accumulation in the total extravascular space, increasing (JV-JL) will lead to a decrease in the time to reach a VTOT of 1000 ml (t(1000)) as shown in Figure 29c. It can be seen that decreasing JL(max) below 22.6 ml/hr yields a rapid decrease in t(1000). For JL(max) above 22.6 ml/hr the increase is less rapid until JL(max) reaches approximately 30 ml/hr, after which t(1000) becomes constant.

From the above discussion one may conclude that if the capacity of the lymphatics is exceeded before the EVEA fluid volume reaches a value of VTONS, then the rate at which fluid accumulates to a VTOT of 1000 ml is accelerated.

Prichard (17) discusses pulmonary edema and lymphatic insufficiency: "Occlusion or partial occlusion of the lymphatic system may be responsible for pulmonary edema in patients with silicosis,..., and possibly shock lung". He suggests that the lymphatic capacity may be reduced by physical alterations of the lymphatic channels or lung tissue. In the alveolar model the lymphatic capacity may be reduced by changes in the parameter VLMPH

Figure 29b

Transient Responses of (JV-JL) for Different JL(max) (Conditions as in Table 19) - Responses continued to time when VTOT = 1000 ml

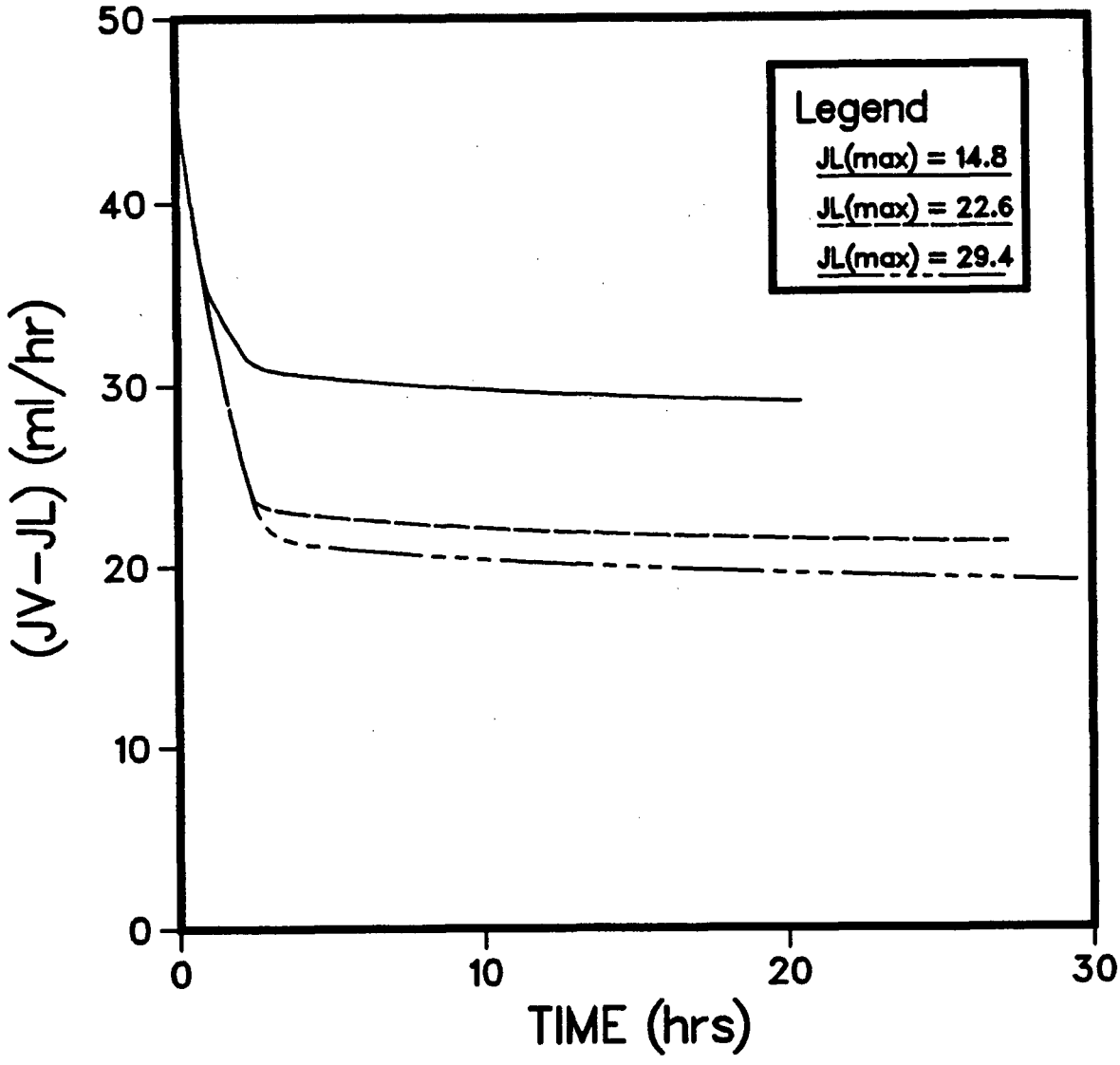

Figure 29c

Time to Reach a VTOT of 1000 ml for Different JL(max) (Conditions as in Table 19)

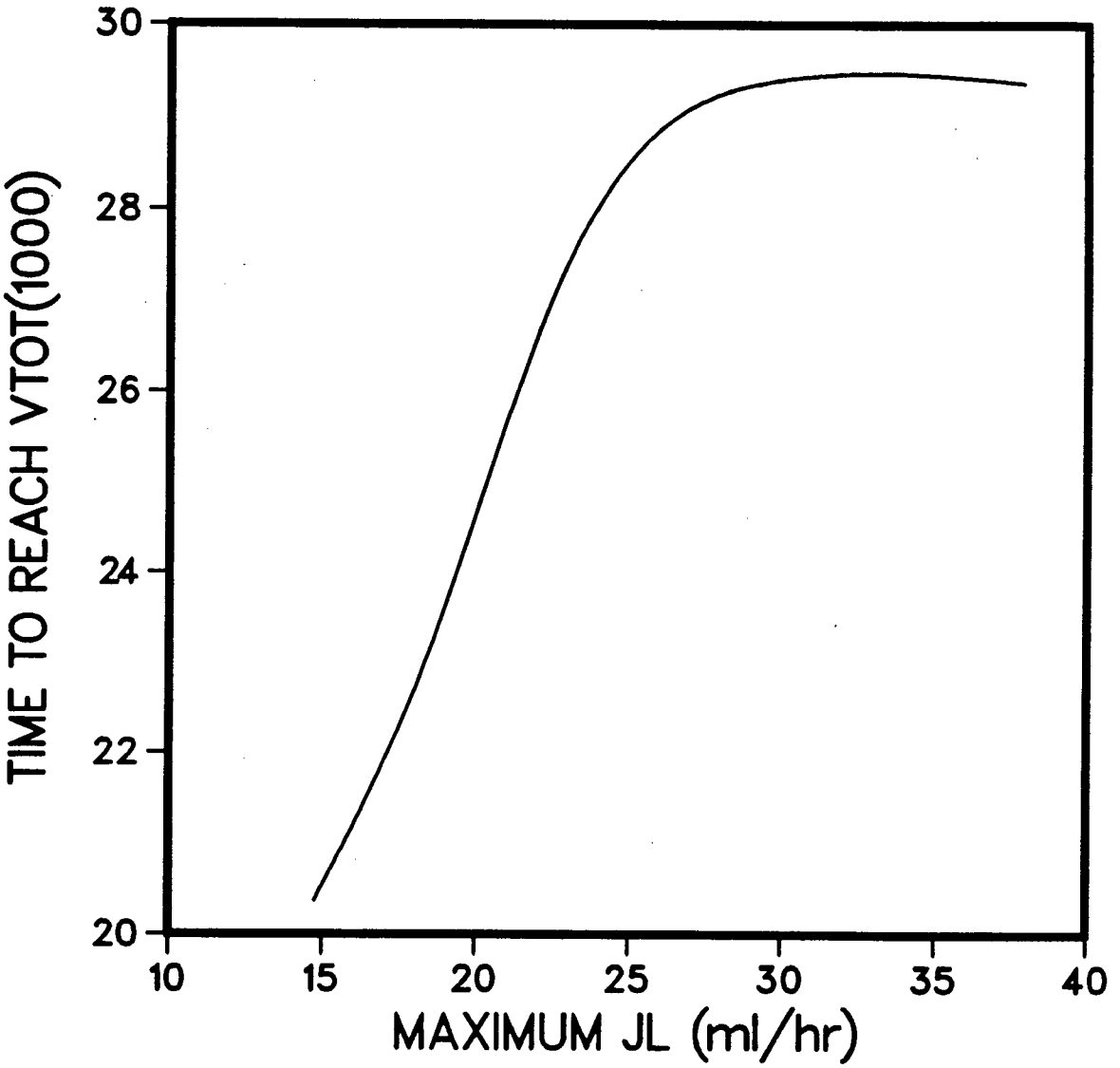

(fluid volume corresponding to JL(max)). The response of the predictions of the PMVES simulation may then be observed.

5.7 The Responses of the Pulmonary Microvascular Exchange System to changes in the value to which PMV is elevated.

In the preceding simulations pulmonary edema was simulated by elevating PMV from 9 mm Hg to 50 mm Hg at time zero. The following discussion will consider step changes in PMV to different values of PMV under the conditions listed in Table 20. The epithelial filtration coefficient was represented as a variable with NK equal to 0.5 hr^{-1} mm Hg^{-1}.

The parameter PMV is introduced in the alveolar model with Starling's Hypothesis, equation (18). From equation (18) one can see that elevating PMV increases the transendothelial flow (JV). The transendothelial flow less the lymph flow equals the rate of fluid accumulation in the total extravascular space. Figure 30a illustrates that increasing PMV from 40 to 60 mm Hg increases (JV-JL). In the interstitial phase VTOT is equivalent to VIS1; therefore as PMV is increased the time for VIS1 to reach the onset of alveolar flooding (t(onset)) decreases (Figure 30b). For PMV=40 mm Hg the value of t(onset) is 3.0 hrs, and for PMV=60 mm Hg the value of t(onset) is 1.5 hrs. Following the onset of alveolar flooding (JV-JL) decreases very slowly (in comparison to before alveolar flooding), as shown in Figure 30a; (JV-JL) for PMV=60 mm Hg is still greater than (JV-JL) for PMV=40 mm Hg. Under the conditions of Table 20 JAS approaches (JV-JL)

Table 20

Conditions of the PMVES Simulations Conducted to Study Changes in PMV*

PMV: varied from 35 to 60 mm Hg

KAS = NK(VIS1-VTONS) for VIS1 > VTONS
NK = 0.5 hr^{-1} mm Hg^{-1}

KF	=	1.12	ml/hr/mm Hg
ΔPERM	=	0	
SIGD	=	0.75	
PSA	=	3.0	ml/hr
PSG	=	1.0	ml/hr
SIGFA	=	0.40	
SIGFG	=	0.60	
VTONS	=	460	ml
SL	=	0.25×10^{-2}	mmHg/ml
B	=	-3.03	mmHg
VLMPH	=	5000	ml

*These are the conditions of the simulations that produced the results illustrated in Figures 30a to 30c.

Figure 30a

Transient Response of (JV-JL) and JAS for Different PMV (Conditions as in Table 20) - Responses continued to a VTOT = 1000 ml

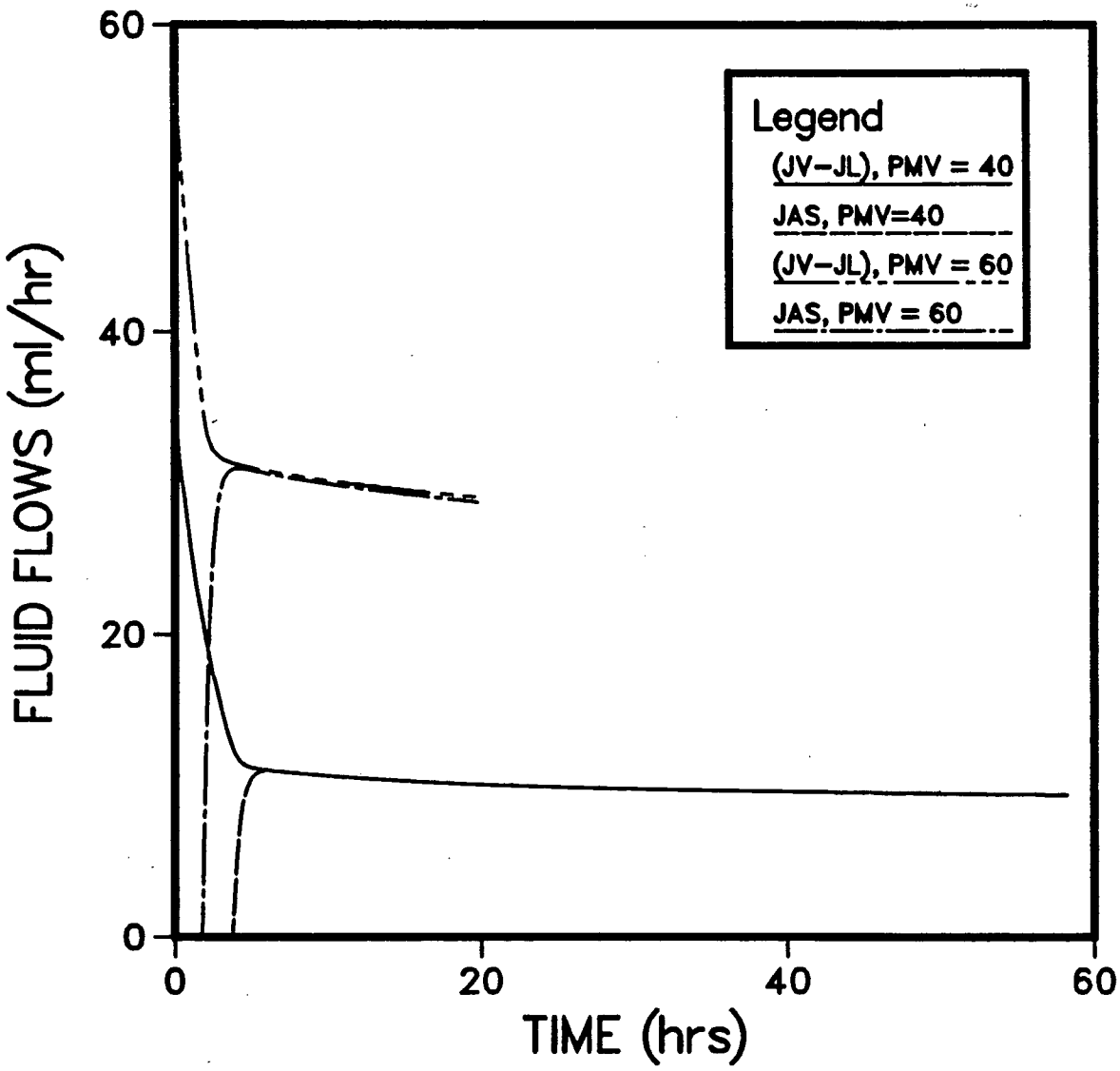

Figure 30b

Time to Reach the Onset of Alveolar Flooding for Different PMV (Conditions as in Table 20)

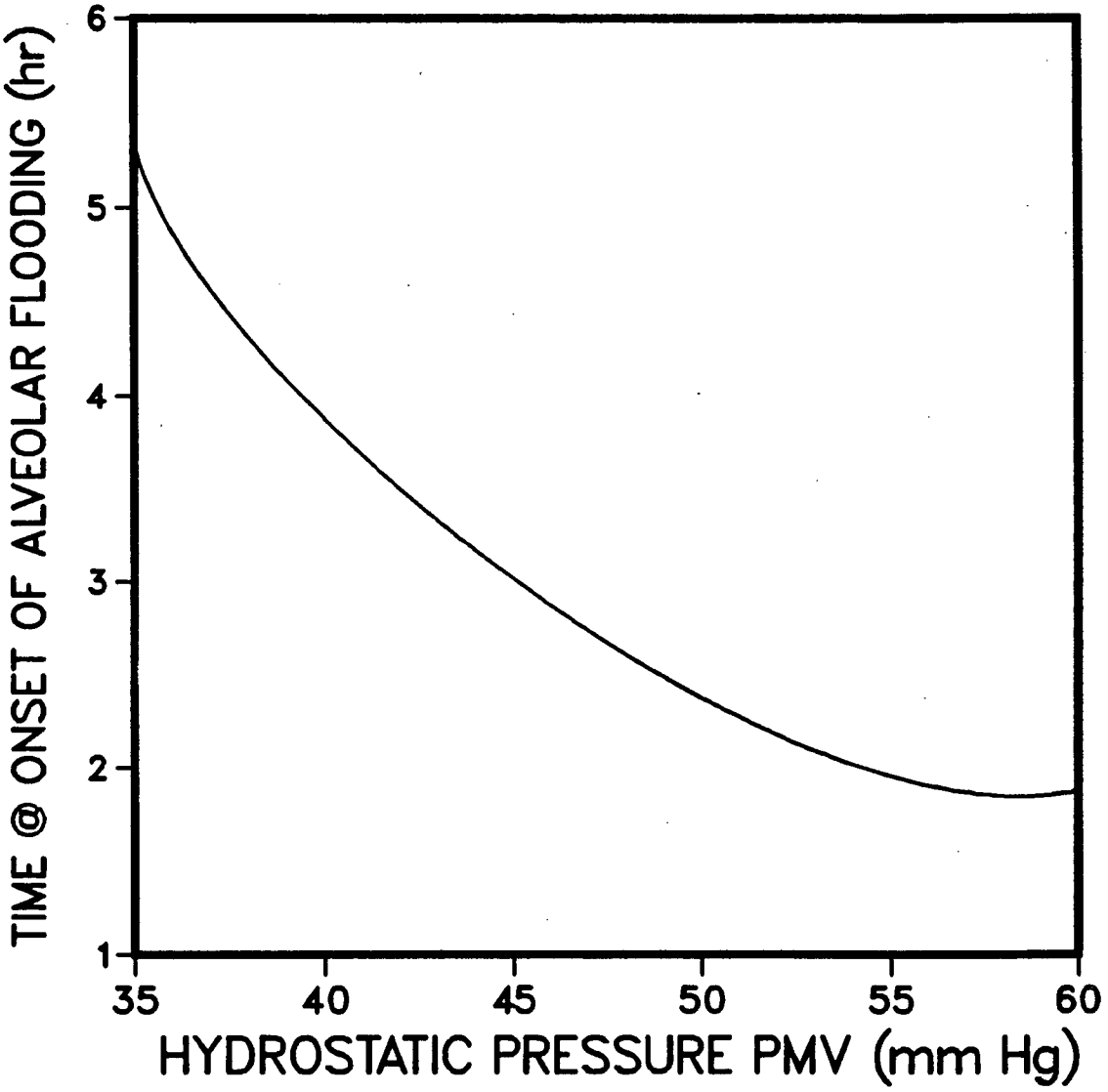

Figure 30c

Time to Reach a VTOT of 1000 ml for Different PMV (Conditions as in Table 20)

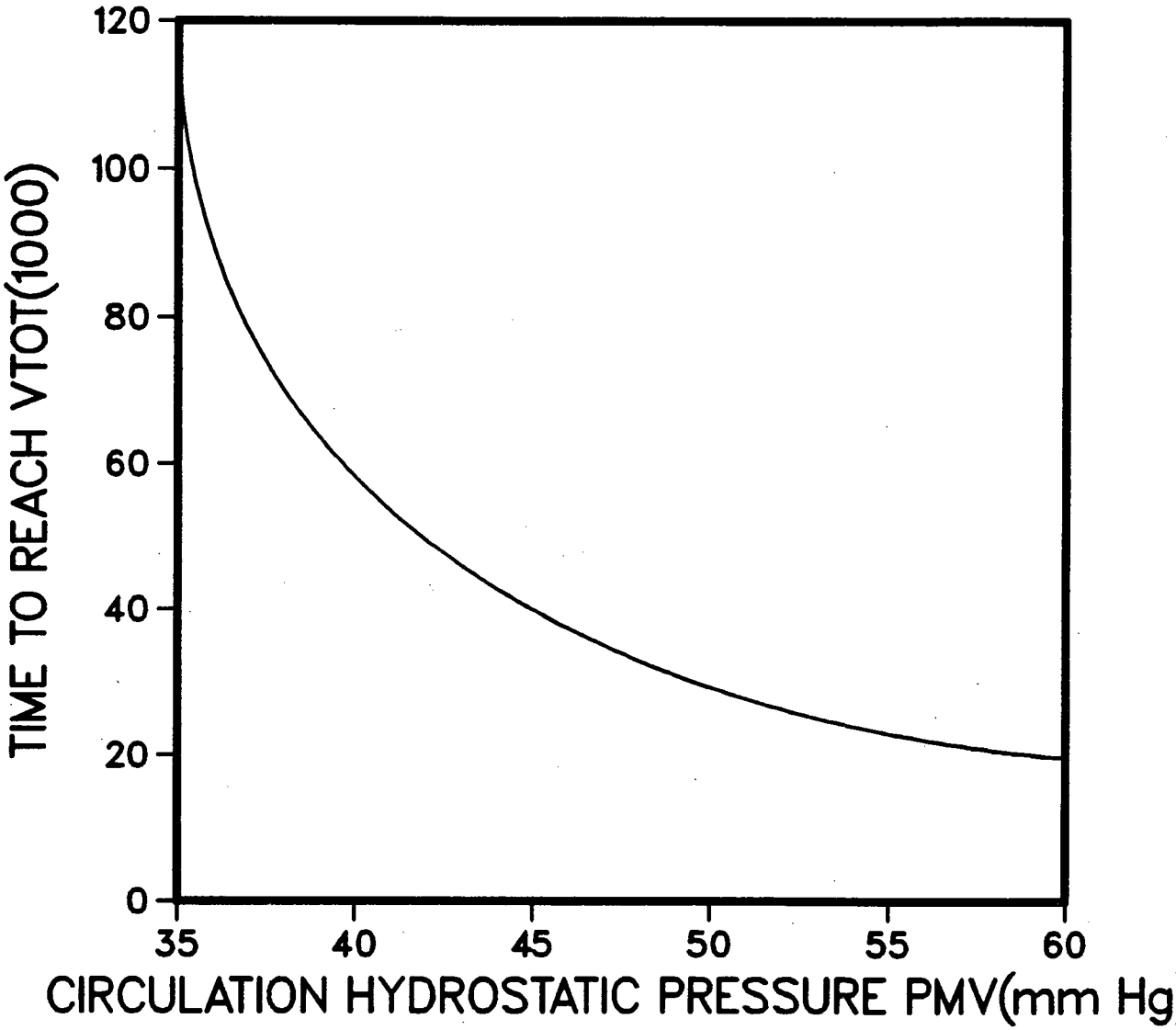

(Figure 30a). The time to reach a VTOT (=VIS1+VAS) of 1000 ml decreases as PMV increases (Figure 30c).

In both Figure 30b and Figure 30c it can be seen that the times, t(onset) and t(1000), respectively, are most sensitive to small increases in PMV above 35 mm Hg and levels off at higher PMV values. If PMV is reduced to 30 mm Hg, no alveolar flooding would occur since at a PMV of 30 mm Hg and for the conditions of Table 20, the steady state VIS1 is 460 ml, which is also equivalent to the assumed VTONS (460 ml). Therefore at a PMV of 30 mm Hg t(onset) and t(1000) would be infinite. Increasing PMV above 30 mm Hg would induce alveolar flooding.

In cardiogenic pulmonary edema the circulatory hydrostatic pressure, PMV, is elevated above its normal value causing an increased transendothelial flow. For the conditions listed in Table 20 increases in PMV up to 30 mm Hg produce only interstitial edema. Raising PMV above 30 mm Hg causes severe pulmonary edema with alveolar flooding.

5.8 The Response of the Pulmonary Microvascular Exchange System to changes in the Endothelial Filtration Coefficient, KF

The effect of changes in KF on the predictions of the PMVES simulation was studied under the conditions listed in Table 21. The perturbation to the exchange system consisted of a step change in the circulatory hydrostatic pressure, at time zero, from 9 mm Hg to 50 mm Hg and changes to the fluid conductivity of the endothelial membrane.

Table 21

Conditions of the PMVES Simulations Conducted to Study Changes in KF*

KF: varied from normal (KF(norm)) to 10 KF(norm)
KF(norm) = 1.12 ml/hr/mm Hg

KAS = NK(VIS1-VTONS) for VIS1 > VTONS
NK = 0.5 hr^{-1} mm Hg^{-1}

PMV	=	50	mm Hg
ΔPERM	=	0	
SIGD	=	0.75	
PSA	=	3.0	ml/hr
PSG	=	1.0	ml/hr
SIGFA	=	0.4	
SIGFG	=	0.6	
VTONS	=	460	ml
SL	=	0.25×10^{-2}	mmHg/ml
B	=	-3.03	mmHg
VLMPH	=	5000	ml

*These are the conditions of the simulations that produced the results illustrated in Figures 31a to 31d.

The endothelial filtration coefficient was introduced into the model with Starling's Hypothesis, equation (18); elevation of KF will result in an increase in the transendothelial flow, JV. The fluid flow difference (JV-JL) is the rate of fluid accumulation in the extravascular fluid space. Figure 31a illustrates that an increase in KF results in an increase in (JV-JL). Therefore the time to reach a total extravascular fluid volume of 1000 ml decreases with an increase in KF (Figure 31b). The time to reach a VTOT of 1000 ml (t(1000)) decreases by approximately two-thirds (29.4 hrs to 9.9 hrs) as KF is doubled to 2KF(normal) and by half (9.9 hrs to 4.3 hrs) when KF is doubled from 2KF(normal) to 4KF(normal). Therefore, t(1000) is most sensitive to the range of KF close to KF(normal).

Increases in the endothelial filtration coefficient also reduces the time to reach the onset of alveolar flooding (Figure 31c). As with t(1000), the time to reach the onset of alveolar flooding is most sensitive to changes in KF near KF(normal).

Following the onset of alveolar flooding the transepithelial flow (JAS) rises to a value close to (JV-JL) (Figure 31a). As KF increases JAS also increases. The rate of fluid accumulation in the interstitial (and cellular) space (JNETI) also increases with KF. The integral over time of JNETI is the fluid volume VISI. In Figure 31d the fluid volume VISI at a VTOT of 1000 ml is seen to increase with KF.

The initial value of (JV-JL) at a KF/KF(normal) of 10 is approximately 200 ml/hr, as compared to 45 ml/hr for KF=KF(norm).

Figure 31a

Transient Responses of (JV-JL) and JAS for Different KF (Conditions as in Table 21) - Responses continued to time when VTOT = 1000 ml

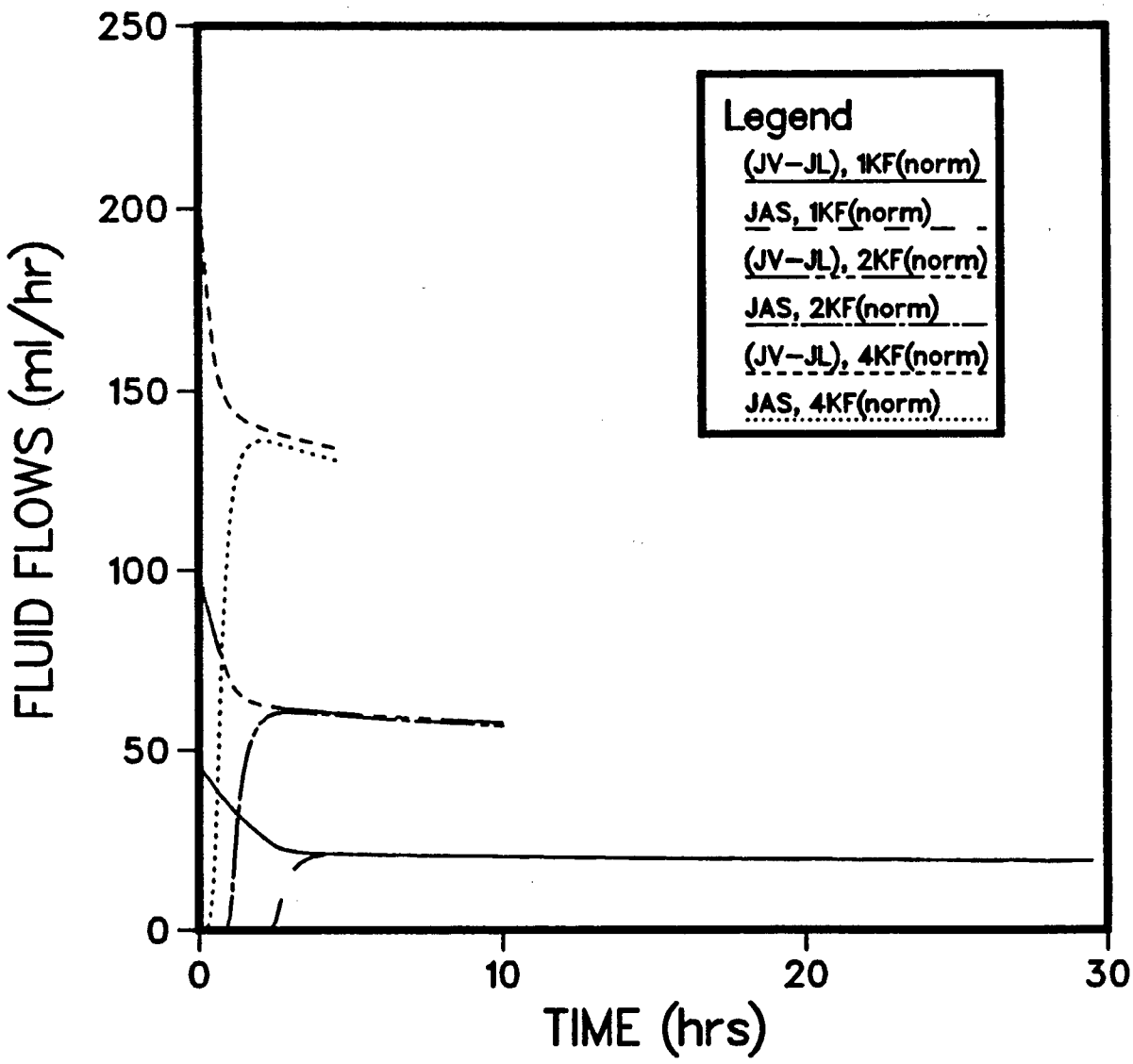

Figure 31b

Time to Reach a VTOT of 1000 ml for Different KF
(Conditions as in Table 21)

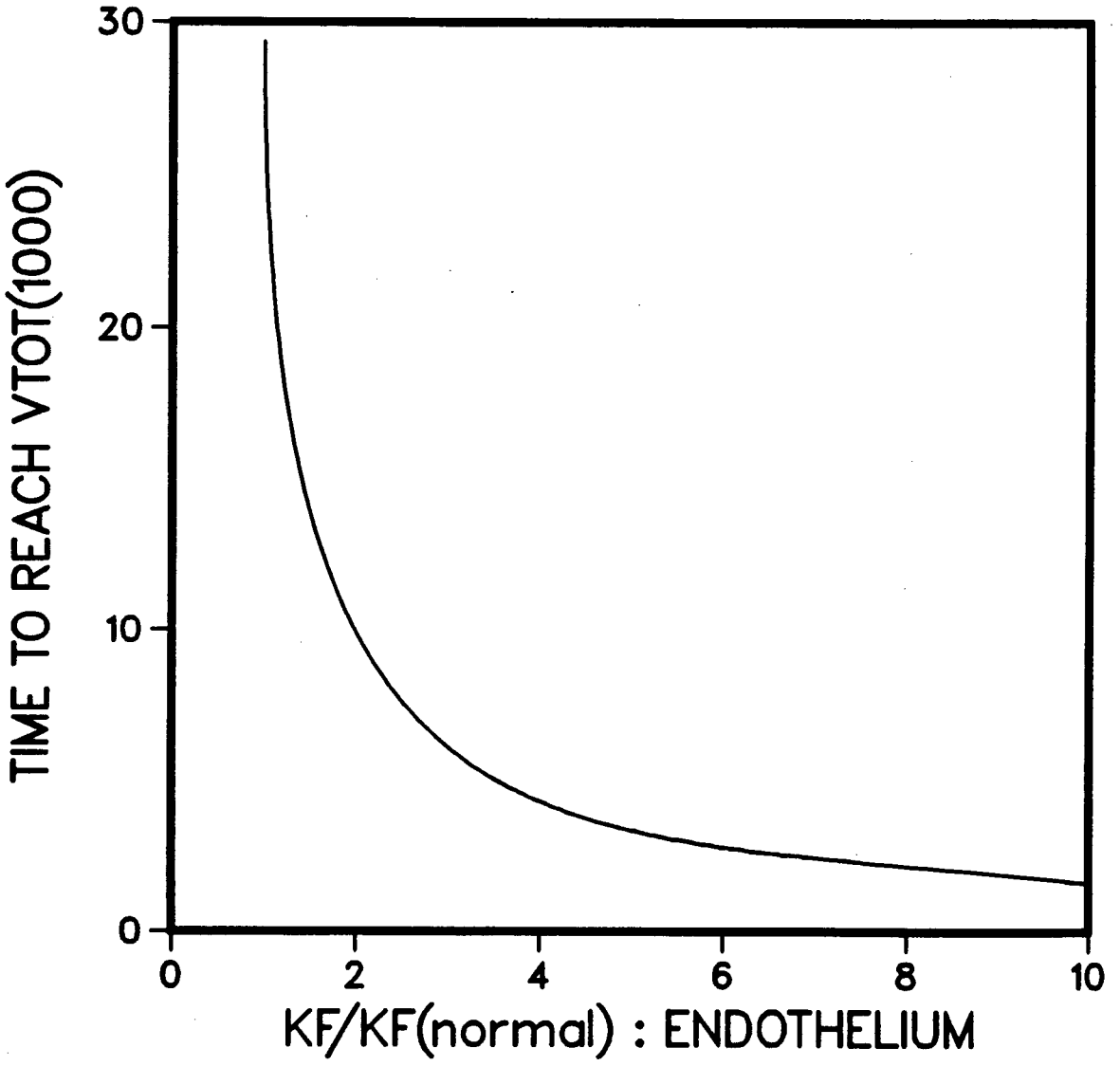

Figure 31c

Time to Reach the Onset of Alveolar Flooding for Different KF (Conditions as in Table 21)

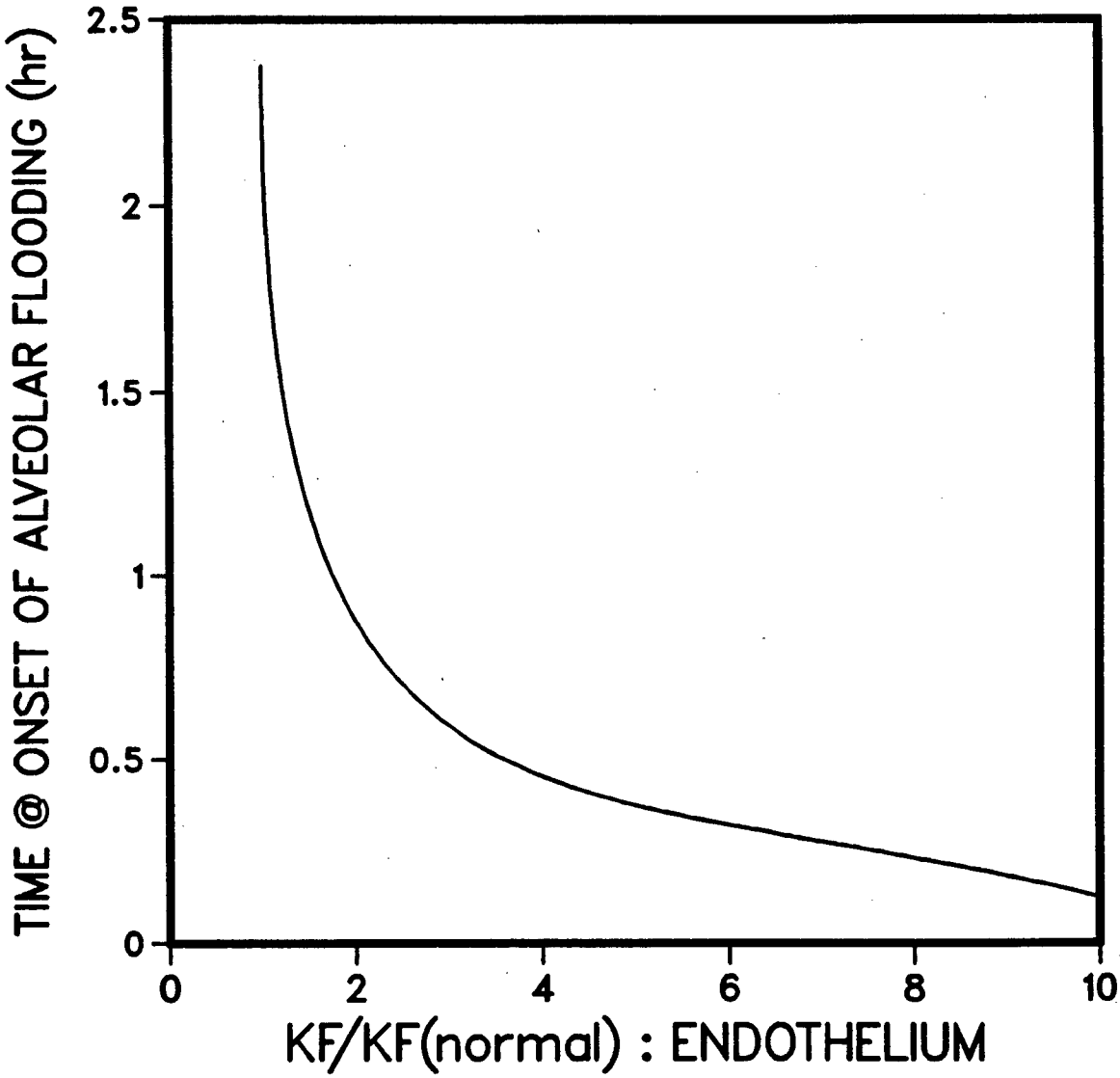

Figure 31d

Fluid Volume VIS1 at a VTOT of 1000 ml for Different KF (Conditions as in Table 21)

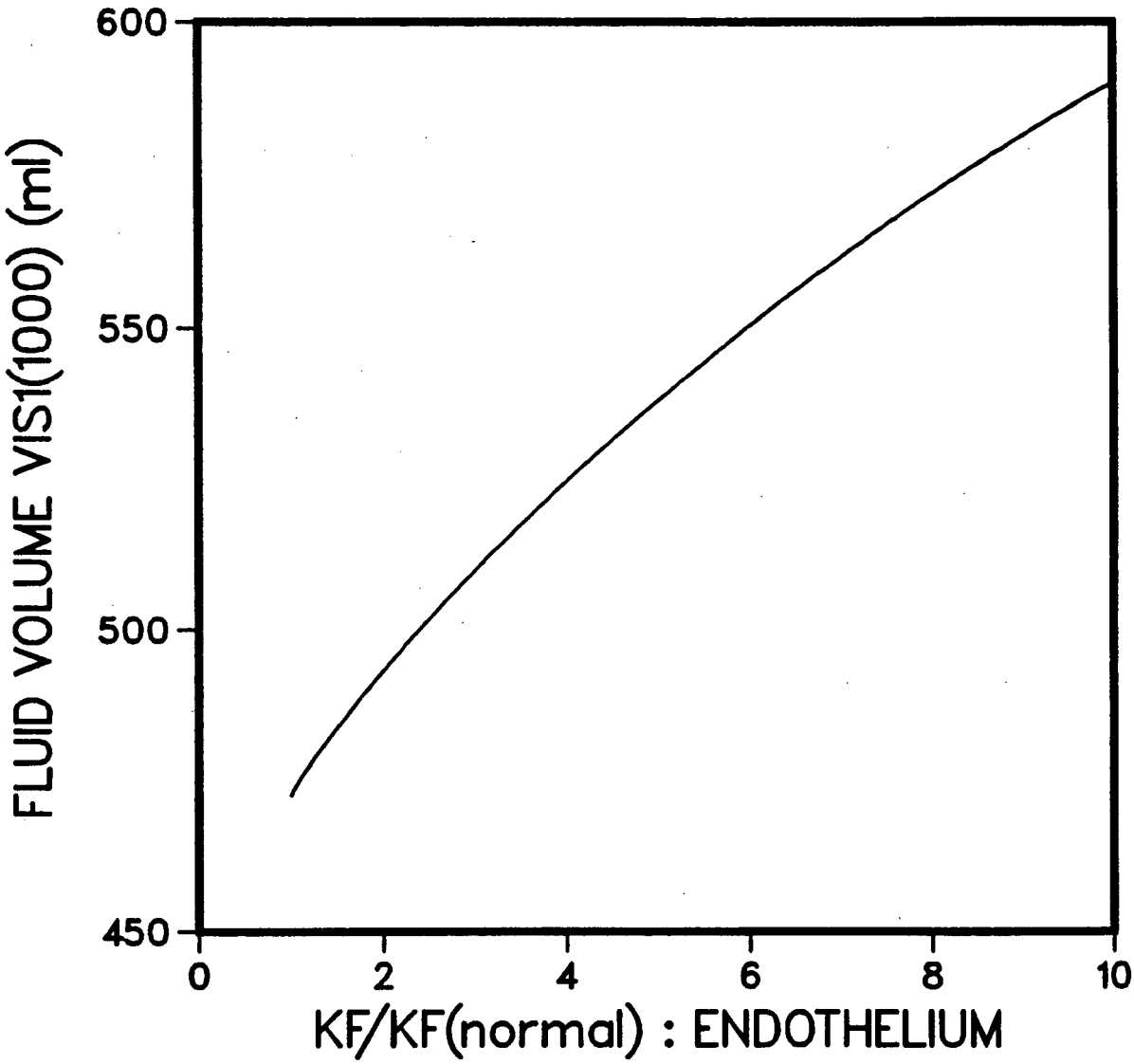

The magnitude of the fluid flow for the condition with KF=10 KF(normal) is large. Experimental results should be obtained to verify this magnitude of transendothelial flow.

Guyton et al. (51) studied hydrostatically-induced pulmonary edema on dog lungs. In cases where alveolar flooding occurred the dogs did not survive past one or two hours after the onset of edema. Paré and Dodek (personal communication,52) stated that alveolar flooding begins within a fraction of an hour following the onset of acute pulmonary edema. Under the conditions shown in Table 21 and with a normal KF the times to reach the onset of alveolar flooding and a VTOT of 1000 ml are 2.3 hrs and 29.4 hrs, respectively. Doubling the value of KF reduces the time to reach the onset of alveolar flooding to 0.9 hrs and the time to reach a VTOT of 1000 ml to 9.9 hrs - much closer to the range of the suggested times.

5.9 The Response of the Pulmonary Microvascular Exchange System to changes in ΔPERM

The plasma protein permeability parameters of the endothelial membrane are:

1) the solute reflection coefficient - SIGD

2) the permeability-surface area product for albumin and globulin-PSA, PSG

3) the solvent drag reflection coefficient for albumin and globulin-SIGFA, SIGFG

Changes in the solute permeability of the endothelium are defined by ΔPERM - this change is expressed as a percent of normal. Increases in ΔPERM refers to increases in PSA and PSG and decreases in SIGD, SIGFA and SIGFG.

The effect of changes in ΔPERM on the predictions of the PMVES simulation was studied under the conditions listed in Table 22. The epithelial filtration coefficient was represented as a function of (VIS1-VTONS) with NK equal to 0.5 hr^{-1} $mmHg^{-1}$. At time zero the PMVES was subjected to a step change in PMV to 50 mmHg. In the cases where ΔPERM was greater than zero the perturbation to the PMVES was an increase in PMV, and an increase in the permeability of the endothelium to solutes.

Solute flow from the circulation to the interstitium is expressed mathematically by the Kedem-Katchalsky (K-K) solute flux equation (equation (20)); the diffusive term includes $(PS)_i$, while the convective term includes $(SIGF)_i$. The interstitial protein concentration used in equation (20) is $(CAV)_i$ - the effective protein concentration. Figure 32a illustrates the transient response of CAVA for changes in ΔPERM from 0 to 100%. For the case of ΔPERM=0 CAVA decreases from 0.038 g/ml at time zero to approximately 0.029 g/ml at which time VTOT = 1000 ml; CAVA is always less than CMVA (.042 g/ml), as shown in Figure 32a. Therefore, for ΔPERM = 0 the values of both the diffusive term and the convective term of equation (20) are positive. In Figure 32b the albumin content in the interstitium (QA) rises to a maximum for ΔPERM = 0 and then declines slowly; initially

Table 22

Conditions for the PMVES Simulations Conducted to Study Changes in ΔPERM*

ΔPERM:	0%	50%	90%	100%
SIGD	0.75	0.375	0.075	0
PSA(ml/hr)	3.0	4.5	5.7	6.0
PSG(ml/hr)	1.0	1.5	1.9	2.0
SIGFA	0.4	0.2	0.04	0
SIGFG	0.6	0.3	0.06	0

KAS = NK(VIS1-VTONS) for VIS1 > VTONS
NK = 0.5 hr^{-1} $mmHg^{-1}$

PMV	=	50	mmHg
KF	=	1.12	ml/hr/mmHg
VTONS	=	460	ml
SL	=	0.25×10^{-2}	mmHg/ml
B	=	-3.03	mmHg
VLMH	=	5000	ml

* These are the conditions of the simulations that produced the results of Figures 32a to 32c.

Figure 32a: Transient Responses of Albumin Protein Concentration CAVA for different ΔPERM (Conditions as in Table 22 - Responses continued to time when VTOT = 1000 ml

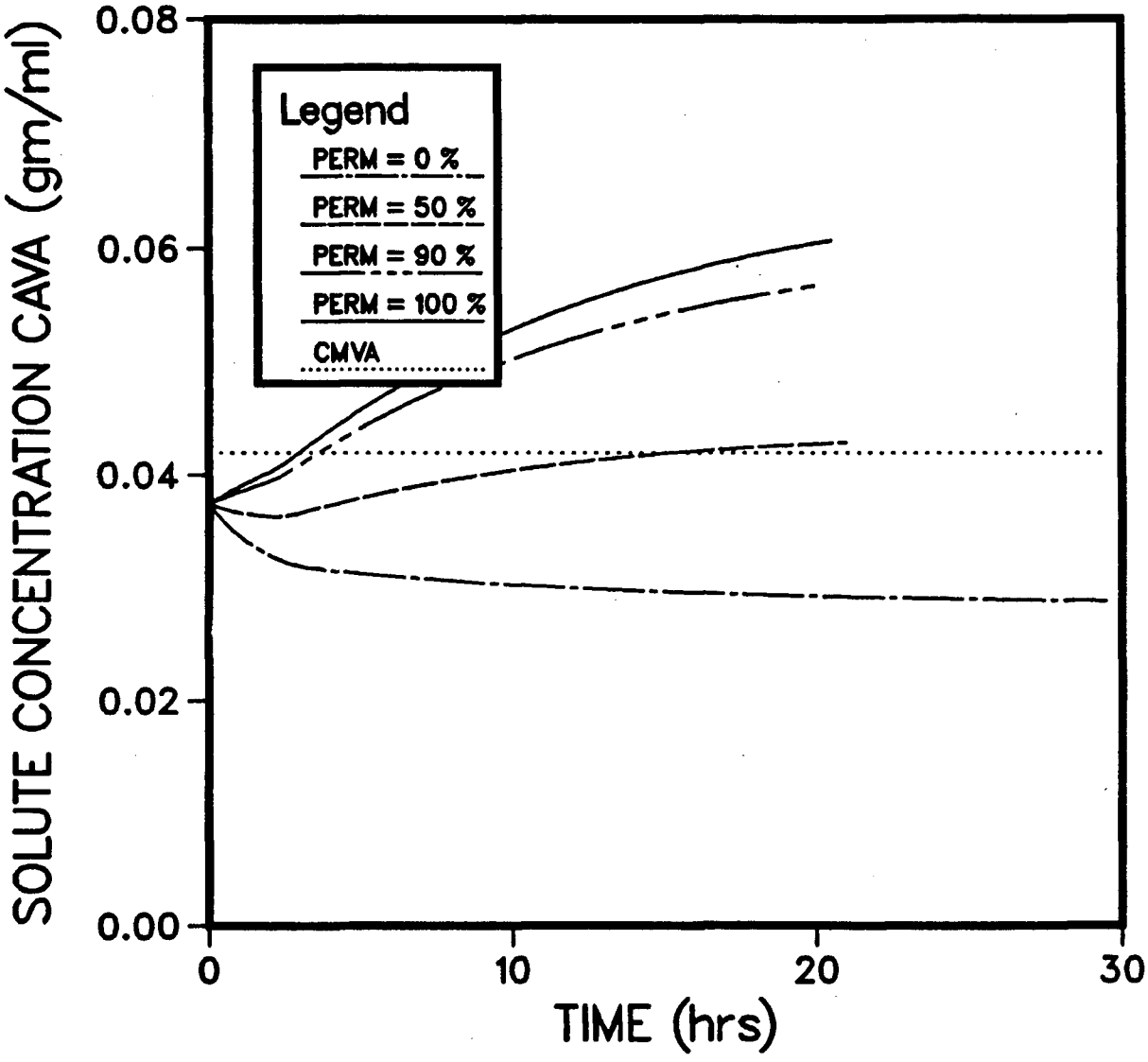

there is a net accumulation of albumin in the interstitium, followed by a net depletion.

An increase in ΔPERM by 50% results in the response of CAVA as shown in Figure 32a; CAVA drops to a minimum and then rises to a value above CMVA by the time VTOT reaches 1000 ml (approximately 21 hrs). Similarly, for the case of ΔPERM = 90% CAVA increases from 0.038 g/ml at time zero to a value greater than CMVA by the time VTOT = 1000 ml (approximately 21 hrs). The time at which CAVA=CMVA is 14.5 hrs. for ΔPERM = 50% and 3.6 hrs. for ΔPERM=90%. Solute concentration is determined by the ratio of solute weight to fluid volume. Following the onset of alveolar flooding (2.5 hrs) the albumin weight in the interstitial fluid rises (Figure 32b); in addition, as ΔPERM increases QA increases. However, the fluid volume VIS1, as shown in Figure 32c, increases very little following the onset of alveolar flooding; as ΔPERM increases the change in VIS1 is also negligible. Therefore, the ratio of QA to VIS1 will rise following the onset of alveolar flooding and as ΔPERM increases. Whether CAVA exceeds CMVA, or not, is dependent on the size of the increase in QA. QA is the integral of QNETA over time, which is determined by equation (33):

$$QNETA = JSA-JL.CTA-JAS.CTA \tag{33}$$

As JSA is increased QA will also increase. For values of CAVA near CMVA, the convective term of equation (20) is dominant in the evaluation of JSA; as SIGFA is reduced (i.e. ΔPERM increased) the value of the convective term increases, and QA rises.

Figure 32b: Transient Responses of Albumin Protein Weight QA for different ΔPERM (Conditions as in Table 22) - Responses continued to time when VTOT = 1000 ml

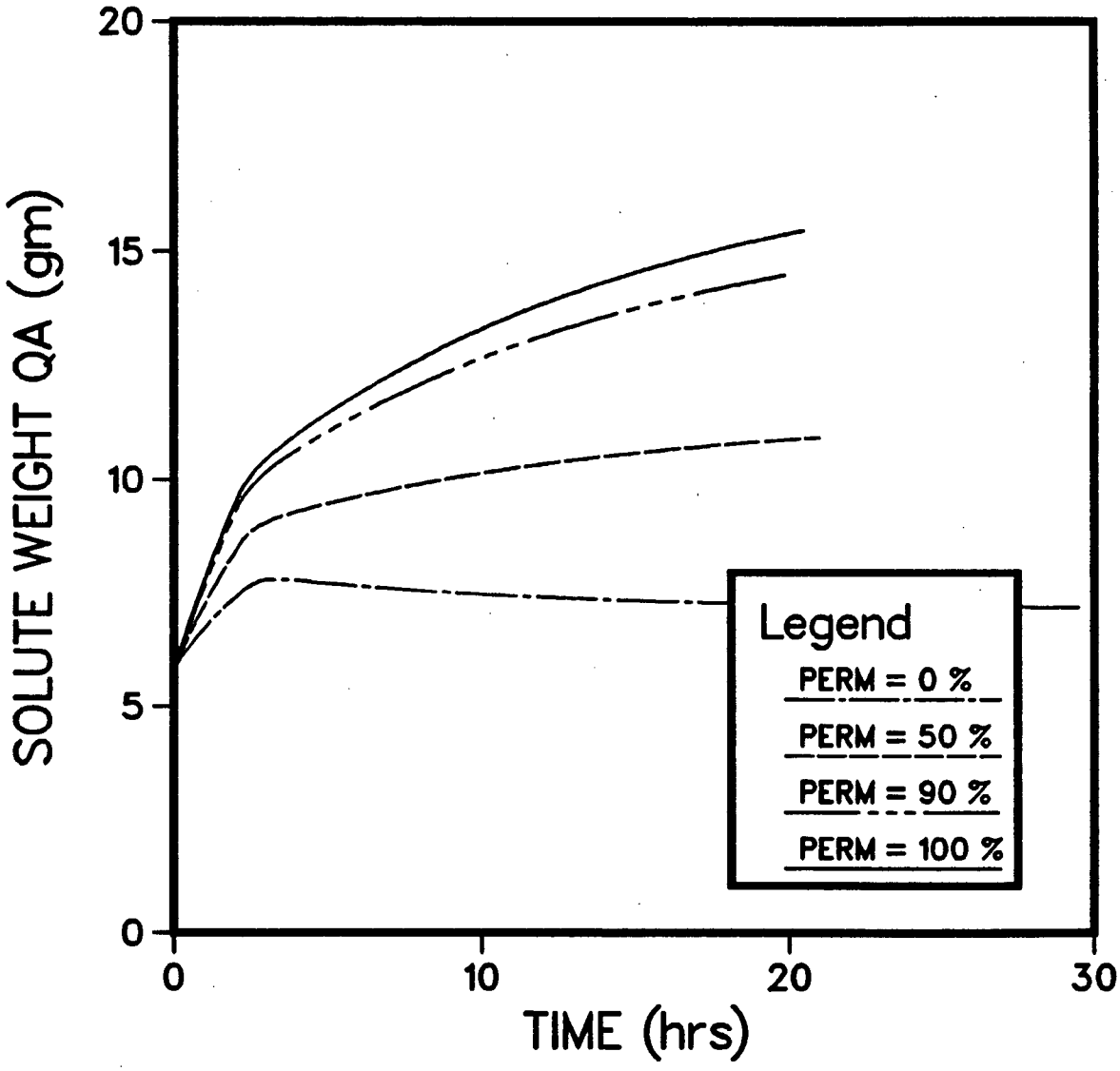

Figure 32c: Transient Responses of Fluid Volume VIS1 for different ΔPERM (Conditions as in Table 22) - Responses continued to time when VTOT = 1000 ml

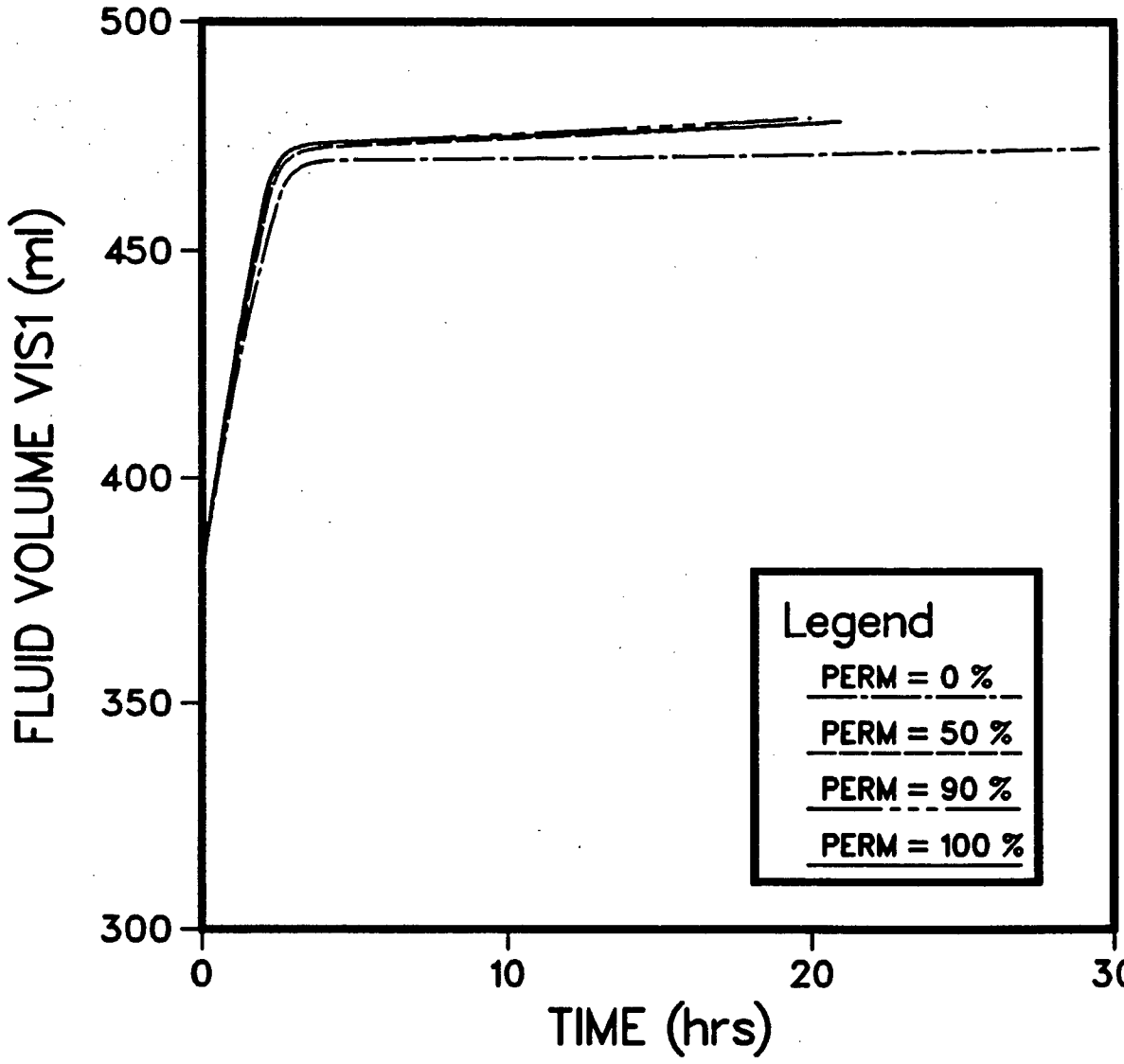

Figure 32d illustrates the time to reach a VTOT of 1000 ml (t(1000)) for changes in ΔPERM; as ΔPERM increases from 0 to approximately 80%, t(1000) decreases from 29 hrs. to 19 hrs. The parameter SIGD is introduced with Starling's Hypothesis and combined with (PIMV-PIPMV) to yield the effective oncotic pressure difference between the circulation and interstitium. As ΔPERM increases SIGD decreases, resulting in a decreasing effective oncotic pressure difference. Therefore the transendothelial flow rate increases. However, the increase in JV is small since the hydrostatic pressure difference (PPMV-PPMV) is dominant when PMV is elevated to 50 mmHg. The primary effect of changes in ΔPERM is on the transmembrane protein movement.

Shirley et al. (53) have carried out tracer studies on the lymph and plasma of dog lungs. They observed that following a large increase in blood volume (which corresponds to a large rise in PMV) the ratio of lymph to plasma solute concentrations rose. From this observation Shirley et al. (53) suggested that the endothelial membrane became more porous during the high PMV - this was classified as the stretched pore model. Figure 32a shows that at an elevated PMV of 50 mmHg the ratio CAVA/CMVA (comparable to the lymph-plasma ratio) may rise if ΔPERM is increased to values such as 50%. However, in the results of Shirley et al. (53) the rise in lymph to plasma solute concentration is primarily due to a drop in the plasma concentration following the infusion of an albumin solution, and not due to a significant rise in lymph solute concentration. In the case of the

simulations of the PMVES where ΔPERM is changed it is the lymph solute concentration that is increased.

5.10 Control of Error in the Numerical Solutions

The numerical integration technique used in the computer program of the alveolar model was the Runge-Kutta-Merson method, supplied as a subroutine by the UBC Computing Centre. In the evaluation of the variables, such as VIS1, because of the approximations used in the calculation there is an error associated with the solution in each integration step. This error was minimized in the computer program by employing a variable time step and setting a tolerance level on the size of the error that was acceptable. If the error in the integrated variables exceeded a tolerance level of 1×10^{-9}, the time step was reduced and the integration was repeated using a smaller time step.

A straight-line interpolation method was used to evaluate PPMV (from VIS1) and the values of variables at the characteristic point such as the time to reach a VTOT of 1000 ml. In this technique the error in the solutions is dependent on the difference in value of the independent variable at the end-points of the interval. Generally, as the time interval of the calculations decreased, the error in the dependent variable decreased. For the calculations of the variables at the characteristic points, this time interval was 0.25 hrs.

Figure 32d: Time to Reach a VTOT of 1000 ml for Different ΔPERM (Conditions as in Table 22)

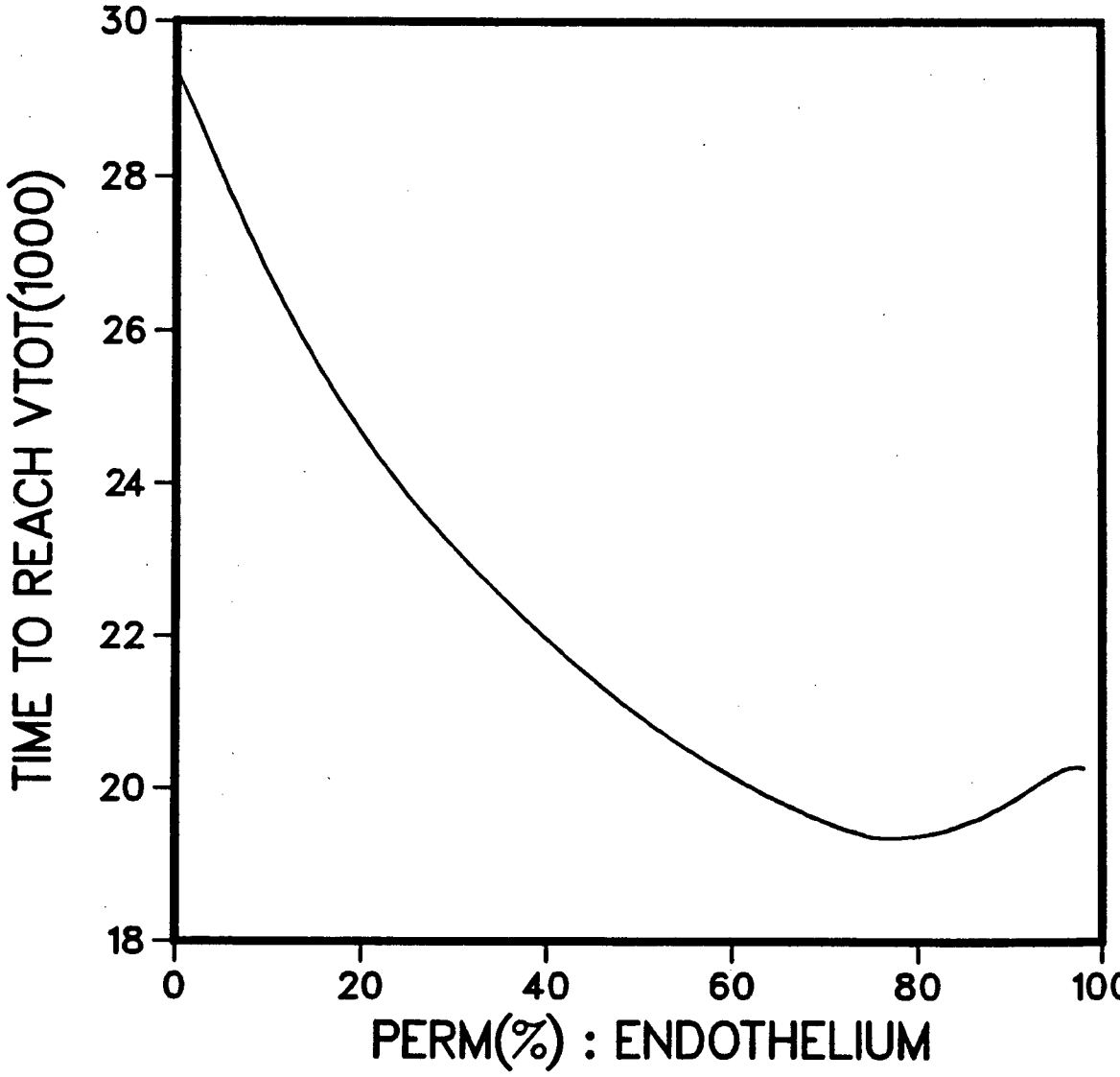

SUMMARY AND CONCLUSIONS

1. The alveolar model describes one way to integrate the air space with the lumped compartment model (interstitial model) of the PMVES as developed by Bert and Pinder (29).

2. Estimates for the parameters introduced with the alveolar model were obtained:

   (a) Epithelial Filtration coefficient, KAS: The coefficient may be represented as a constant or a variable. A variable coefficient appears to be more compatible with literature (33). We suggest a value for the sensitivity parameter NK of 0.5 hr^{-1} $mmHg^{-1}$.

   (b) VTONS: For cases of hydrostatic edema and edema caused by changes to the endothelial permeability, a value of 460 ml is a good estimate. A VTONS of 460 ml corresponds to a PPMV of +1.1 mmHg - a value within the range suggested by Guyton(47).

   (c) SL: No value of SL was found in the literature survey. We suggest a value of 0.25×10^{-2} mmHg/ml.

   (d) B: No value of B was found in the literature survey. We suggest a value of -3.03 mmHg, which corresponds to the expected alveolar fluid pressure at normal conditions.

3. The presence of a maximum lymph capacity may be easily introduced into the model through parameter VLMPH. In the simulations of the PMVES carried out for this thesis a fluid volume VLMPH less than VTONS will accelerate the progression of edema. Values of VLMPH

greater than VTONS have very little effect on the progression of edema (up to the time when VTOT = 1000 ml).

4. In hydrostatically induced pulmonary edema PMV must be raised above a minimum pressure for alveolar flooding to occur. The time to reach the onset of alveolar flooding is most sensitive to small rises in PMV above this minimum value.

5. If PMV is raised above the minimum value specified in (4), then increases in KF will accelerate the progress of edema. The time to reach the onset of alveolar flooding is most sensitive to small increases in KF above its normal value.

6. The interstitial to plasma protein concentration ratio may increase or decrease during the progression of pulmonary edema depending on the size of the change in the endothelial solute permeability parameters.

RECOMMENDATIONS FOR FURTHER WORK

1. To further utilize the computer simulation of the alveolar model experimental data must be obtained to verify the model's predictions, or to suggest alternative ways to integrate the air space with the existing interstitial models of the PMVES.

2. The computer program of the alveolar model should be improved so that it may be more "user friendly". In this way the simulation may be used by the health care profession for teaching purposes.

3. Future development of the alveolar model should incorporate:

   (a) the effects of lung inflation on the PMVES

   (b) the Zone Model of the lung proposed by West, Dollery and Naimark (3)

   (c) the effect of localized pulmonary edema on the PMVES

   (d) a recovery phase following the progression of pulmonary edema.

NOMENCLATURE

B	Alveolar fluid pressure at the onset of alveolar flooding (mmHg)
CAVA,CAVG	The effective interstitial concentration of albumin and globulin respectively (g/ml)
(CL)i	Lymph protein concentration for solute 'i' (g/ml)
CMVA,CMVG	The blood plasma concentration of albumin and globulin, respectively (g/ml)
CP,CPMV,CPPMV	The total protein concentration for blood plasma (CPPMV) and interstitial fluid (CPPMV) (g/ml)
CTA,CTG	The tissue concentration of albumin and globulin, respectively (g/ml)
JAS,JL,JV	The transepithelial, lymph, and transendothelial fluid flows, respectively (ml/hr)
JL(max)	The parameter representing the value of the maximum lymph flow (ml/lhr)
JNETl	The rate of fluid accumulation in the extravascular-extraalveolar space (ml/hr)
JSA,JSG	The transendothelial solute flows for albumin and globulin, respectively (g/hr)
KAS,KF	The fluid filtration coefficient of the epithelium and endothelium, respectively (ml/hr/mmHg)
KASO	The parameter representing a constant epithelial filtration coefficient (ml/hr/mmHg)
LF	The fluid conductivity coefficient of the endothelium (cm/hr/mmHg)
NK	The sensitivity parameter for a variable epithelial filtration coefficient (hr^{-1} $mmHg^{-1}$)
PA	The hydrostatic pressure of the arterial segment of a blood vessel (mmHg)
PALV,PG	The hydrostatic pressure of the gas in the air space (mmHg)
PAS,PL	The alveolar fluid pressure (mmHg)

Continued....

NOMENCLATURE (Cont.d)

PI,PIAS,PIMV,	The colloid osmotic (or oncotic) pressure of the alveolar fluid (PIAS), blood plasma (PIMV), and interstitial fluid (PIPMV) (mmHg)
PLA	The left atrial hydrostatic pressure (mmHg)
PMV	The pulmonary microvascular hydrostatic pressure (mmHg)
PPA	The pulmonary arterial hydrostatic pressure (mmHg)
PPMV,PEA	The hydrostatic pressure of the alveolar and extra-alveolar interstitial fluid, respectively (mmHg)
PSA,PSG	The endothelial permeability-surface area products for albumin and globulin, respectively (ml/hr)
PV	The hydrostatic pressure of the venous segment of a blood vessel (mmHg)
QA,QG	The interstitial solute content of albumin and globulin, respectively (gm)
QNETA,QNETG	The rate of solute accumulation in the interstitium for albumin and globulin respectively (g/hr)
(QO)i	The solute weight in the interstitium for solute 'i' at time zero (gm)
SA	Surface area of pulmonary capillary membrane (cm^2)
SIGD,SIGDAS	The solute reflection coefficient for fluid of the endothelial and epithelial membranes, respectively.
SIGFA,SIGFG	The solvent drag reflection coefficient of the endothelial membrane to albumin and globulin, respectively
SL	The slope of the PAS-VAS curve for the alveolar fluid (mmHg/ml)
VAS	The alveolar fluid volume (ml)
VAVA,VAVG	The available interstitial fluid volume for albumin and globulin, respectively (ml)
VCELL	The cellular fluid volume (ml)
VEXA,VEXG	The excluded fluid volume to albumin and globulin, respectively (ml)

Continued....

NOMENCLATURE (Cont.d)

VIS	The interstitial fluid volume (VIS=VTOT-VAS-VCELL)(ml)
VIS1	The fluid volume of the interstitial (+cellular) space or the extravascular-extraalveolar (EVEA) space (VIS1=VTOT-VAS)(ml)
VIS10	The interstitial (+cellular) fluid volume at time zero (ml)
VLMPH	The interstitial (+cellular) fluid volume corresponding to the maximum lymph flow (ml)
VTONS	The interstitial (+cellular) fluid volume at the onset of alveolar flooding (ml)
VTOT	The total extravascular fluid volume (ml)
r	The radius of curvature: used in Laplace's Equation (cm)
τ	The surface tension of a fluid (dynes/cm)

REFERENCES

1. Guyton, A.C., Human Physiology and Mechanisms of Disease, Third Edition, W.B. Saunders Company, Toronto (1982).

2. Staub, N.C., Pathophysiology of Pulmonary Edema, In: Edema, Edited by N.C. Staub and A.E. Taylor, Raven Press, New York (1984).

3. West, J.B., C.T. Dollery & A. Naimark, Distribution of blood flow in isolated lung; relation to vascular and alveolar pressures. Journal of Applied Physiology 19(4): 713-724, 1964.

4. Low, F.N., Lung Interstitium, In: Lung Water and Solute Exchange, Edited by N.C. Staub, Marcel Dekker, Inc., New York (1978).

5. Wissig, S.L. & A.S. Charonis, Capillary Ultrastructure, In: Edema, Edited by N.C. Staub and A.E. Taylor, Raven Press, New York (1984).

6. Schneeberger, E.E., Barrier Function of Intercellular Junctions in Adult and Fetal Lungs, In: Pulmonary Edema, Edited by A.F. Fishman and E.M. Renkin. American Physiological Society, Baltimore, 1979.

7. Yoffey, J.M. & F.C. Courtice, Lymphatics, Lymph and the Lymphomyeloid Complex. Academic Press, New York, 1970 (p.160-205).

8. Aukland, K. and G. Nicolaysen, Interstitial Fluid Volume: Local Regulatory Mechanisms, Physiological Reviews 61(3): 556-643, 1981.

9. Bert, J.L., J.M. Mathieson & R.H. Pearce, The exclusion of human serum albumin by human dermal collagenous fibres and within human dermis, Biochemical Journal 201: 395-403, 1982.

10. Bert, J.L. & R.H. Pearce, The Interstitium and Microvascular Exchange, In: Handbook of Physiology, section 2: The Cardiovascular System, Volume IV, Microcirculation, Part 1, American Physiological Society, Maryland (1984).

11. Lai-Fook, S.J., Interstitial Fluid Pressure in the Lung, In: Tissue Fluid Pressure and Composition, Edited by A.R. Hargens, Williams & Wilkins, London (1981).

12. Parker, J.C., A.C. Guyton, & A.E. Taylor, Pulmonary interstitial and capillary pressures estimated from intra-alveolar fluid pressures, Journal of Applied Physiology 44(2): 267-276, 1978.

13. Staub, N.C., Pulmonary Edema, Physiological Reviews, 54(3): 678-811, 1974.

14. Howell, J.B.L., S. Permutt, D.F. Proctor, & R.L. Riley, Effect of

Inflation of the lung on different parts of pulmonary vascular bed, Journal of Applied Physiology 16(1): 71-76, 1961.

15. Hida, W., H. Inoue & J Hildebrandt, Lobe weight gain and vascular, alveolar, and peribronchial interstitial fluid pressures, Journal of Applied Physiology 52(1): 173-183, 1982.

16. Goldberg, H.S., Effect of lung volume history on rate of edema formation in isolated canine lobe, Journal of Applied Physiology 45(6): 880-884, 1978.

17. Prichard, J.S., Edema of the Lung, Charles C. Thomas, Publisher. Illinois, USA (1982).

18. Guyton, A.C., A.E. Taylor & H.J. Granger, Circulatory Physiology II: Dynamics and Control of Body Fluids, W.B. Saunders Company, Toronto (1975).

19. Gnepp, D.R., Lymphatics, In: Edema, Edited by N.C. Staub and A.E. Taylor, Raven Press, New York (1984).

20. Egan, E.A., Effect of lung inflation on alveolar permeability to solutes, In: Lung Liquids, American Elsevier, New York (1976).

21. Hills, B.A., Editorial: What is the true role of surfactant in the lung?, Thorax 36: 1-4, 1981.

22. Staub, N.C., The Pathogenesis of Pulmonary Edema. Progress in Cardiovascular Diseases 23(1), 53-80, 1980.

23. Zumsteg, T.A., A.M. Havill, & M.H. Gee, Relationships among lung extravascular fluid compartments with alveolar flooding, Journal of Applied Physiology 53(1): 267-271, 1982.

24. Gee, M.H. & N.C. Staub, Role of bulk fluid flow in protein permeability of the dog lung alveolar membrane. Journal of Applied Physiology 42(2): 144-149, 1977.

25. Egan, E.A., Lung inflation, lung solute permeability and alveolar edema, Journal of Applied Physiology 53(1): 121-125, 1982.

26. Blake, L.H. & N.C. Staub, Pulmonary Vascular Transport in sheep: A Mathematical Model. Microvascular Research 12: 197-220, 1976.

27. Harris, T.R. & R.J. Roselli, A theoretical model of protein, fluid, and small molecule transport in the lung, Journal of Applied Physiology 50(1): 1-14, 1981.

28. Roselli, R.J., R.E. Parker, & T.R. Harris, A model of unsteady-state transvascular fluid and protein transport in the lung, Journal of Applied Physiology 56(5): 1389-1402, 1984.

29. Bert, J.L. & K.L. Pinder, Pulmonary Microvascular Exchange: An Analog Computer Simulation, Microvascular Research 27: 51-70, 1984.

30. Prichard, J.S., B. Rajagopalan, & G. deJ. Lee, Experimental and theoretical studies on the aetiology of adult respiratory distress syndrome. Herz 2(6): 449-458, 1977.

31. Parker, R.E., R.J. Roselli, T.R. Harris, & K.L. Brigham, Effects of graded increases in pulmonary vascular pressures on lung fluid balance in unanesthetized sheep, Circulation Research 49: 1164-1172, 1981.

32. Staub, N.C., The forces regulating fluid filtration in the lung, Microvascular Research 15; 45-55, 1978.

33. Drake, R., K.A. Gaar and A.E. Taylor, Estimation of the filtration coefficient of pulmonary exchange vessels, American Journal of Physiology 234(3): H266-H274, 1978.

34. Drake, R.E., R.L. Scott, & J.C. Gabel, Relationship between weight gain and lymph flow in dog lungs, American Journal of Physiology 245: H125-H130, 1983.

35. Erdmann, A.J., T.R. Vaughan, Jr., K.L. Brigham, W.C. Woolverton, & N.C. Staub, Effect of increased vascular pressure on lung fluid balance in unanesthetized sheep, Circulation Research 37: 271-284, 1975.

36. Parker, J.C., H.J. Falgout, F.A. Grimbert, & A.E. Taylor, The effect of increased vascular pressure on albumin-excluded volume and lymph flow in the dog lung, Circulation Research 47: 866-875, 1980.

37. Taylor, A.E., W.H. Gibson, H.J. Granger, & A.C. Guyton, The interaction between intracapillary and tissue forces in the overall regulation of interstitial fluid volume, Lymphology 6; 192-208, 1973.

38. Mason, G.R. & R.M. Effros, Flow of edema fluid into pulmonary airways, Journal of Applied Physiology 55(4): 1262-1268, 1983.

39. Staub, N.C., H. Nagano, & M.L. Pearce, Pulmonary edema in dogs, especially the sequence of fluid accumulation in lungs, Journal of Applied Physiology 22(2): 227-240, 1967.

40. Macklin, C.C., The pulmonary alveolar mucoid film and the pneumonocytes, Lancet 1: 1099-1104, 1954.

41. Iliff, L.D., Extra-alveolar vessels and edema development in excised dog lungs, Circualtion Research 28: 524-532, 1971.

42. Hughes, J.M.B., J.B. Glazier, J.E. Maloney and J.B. West, Effect of extra-alveolar vessels on distribution of blood flow in the dog lung. Journal of Applied Physiology 25: 701-712, 1968.

43. Vreim, C.E. & N.C. Staub, Protein composition of lung fluids in acute alloxan edema in dogs, American Journal of Physiology 230(2): 376-379, 1976.

44. Vreim, C.E., P.D. Snashall, & N.C. Staub, Protein composition of lung fluids in anesthetized dogs with acute cardiogenic edema, American Journal of Physiology 231(5): 1466-1469, 1976.

45. Guyton, A.C., A.E. Taylor, R.E. Drake & J.C. Parker, Dynamics of subatmospheric pressure in the pulmonary interstitial fluid, In: Lung Liquids, American Elsevier, New York (1976).

46. Tierney, D.F. & R.P. Johnson, Altered surface tension of lung extracts and lung mechanics, Journal of Applied Physiology 20(6): 1253-1260, 1965.

47. Guyton, A.C., J.C. Parker, A.E. Taylor, T.E. Jackson, and D.S. Moffatt, Forces governing water movement in the lung, In: Pulmonary Edema, Edited by A.F. Fishman and E.M. Renkin, American Physiological Society, Baltimore, 1979.

48. Gump, F.E., Y. Mashima, A. Ferenczy, & J.M. Kinney, Pre-and postmortem studies of lung fluids and electrolytes, The Journal of Trauma, 11(6): 474-482, 1971.

49. Drake, R.E., J.H. Smith & J.C. Gabel, Estimation of the filtration coefficient in intact dog lungs. American Journal of Physiology 238(7): H430-H438, 1980.

50. Caldini, P., J.D. Leith, & M.J. Brennan, Effect of continuous positive-pressure ventilation (CPPV) on edema formation in dog lung, Journal of Applied Physiology 39(4): 672-679, 1975.

51. Guyton, A.C., & A.W. Lindsey, Effect of elevated left atrial pressure and decreased plasma protein concentration on the development of pulmonary edema, Circulation Research 7: 649-657, 1959.

52. Paré, P. and P. Dodek, Personal communication.

53. Shirley Jr. H.H., C.G. Wolfram C.G., K. Wasserman and H.S. Mayerson, Capillary Permeability to Macromolecules: stretched pore phenomenon. American Journal of Physiology 190(2): 189-193, 1957.

54. Jacob, S.W. C.A. Francone, and W.J. Lossow, Structure and Function in Man, Fifth Edition, W.B. Saunders Company, Toronto, 1982.

55. Prockop, D.J. Collagen, Elastin and Proteoglycans: Matrix for Fluid Accumulation in the Lung, In: Pulmonary Edema, Edited by A.P. Fishman and E.M. Renkin, American Physiological Society, Baltimore, 1979.

56. Moore, C. UBC RKC: Runge Kutta with Error Control, Computing Centre, The University of British Columbia, 1983.

57. Mair, S.G., UBC PLOT: The UBC plot subroutines and programs. Computing Centre, The University of British Columbia, 1984.

APPENDIX A: The Computer Program

A1.1 Input Files EDA and PDA

The parameters of the input files EDA and PDA were defined in Table 5 and 6, respectively. An example of the numerical values assigned to these parameters is shown in Table 23 for EDA and Table 24 for PDA. (The numerical values must start in column 11 for EDA and column 21 for PDA). The parameters introduced with the alveolar model - VTONS, SL, B, and VLMPH - assume values as stated in section 4.4. In this example the epithelial filtration coefficient is represented as a variable; therefore NK is assigned a value, in this case 0.5 hr^{-1} $mmHg^{-1}$, and KASO is set equal to zero (see Table 24). If KAS is represented as a constant, then NK is set equal to zero and KASO assigned a constant value. The permeability parameters of the endothelium and the endothelial filtration coefficient assume the normal values as selected by Bert and Pinder (29). As shown in file PDA the hydrostatic pressure PMV is set at 50 mmHg, raised from its normal value of 9 mmHg.

The meaning of the parameters TAUMX1, SUBNT1, TAUMX2 and SUBNT2 may be explained as follows: Up to a time of 25 hrs (TAUMX1) the values of the variables listed in Table 9 will be stored every hour (SUBNT1); SUBNT1 must divide evenly into TAUMX1. From a time of 25 hrs (TAUMX1) to 100 hrs (TAUMX2) the values of the variables will be stored every 5 hrs. (SUBNT2); SUBNT2 must divide evenly into TAUMX1 and TAUMX2. A detailed account of the transient response of the PMVES

Table 23: Example of Numerical Values Assigned to Parameters in File EDA

1	VTOTO	=	378.7D0
2	VASO	=	0.0D0
3	QAO	=	5.81D0
4	QGO	=	2.36D0
5	PIMV	=	25.0D0
6	VCELL	=	150.0D0
7	VEXA	=	73.5D0
8	VEXG	=	115.5D0
9	VTONS	=	459.9D0
10	VLMPH	=	5000.0D0
11	B	=	-3.03D0
12	CMVA	=	0.042D0
13	CMVG	=	0.0271D0
14	FPPMV(1)	=	-2.74D0
15	FPPMV(2)	=	-2.40D0
16	FPPMV(3)	=	-1.9D0
17	FPPMV(4)	=	-1.3D0
18	FPPMV(5)	=	-0.8D0
19	FPPMV(6)	=	-0.3D0
20	FPPMV(7)	=	0.15D0
21	FPPMV(8)	=	0.60D0
22	FPPMV(9)	=	1.09D0
23	KF	=	1.12D0
24	SIGD	=	0.750D0
25	PSA	=	3.00D0
26	PSG	=	1.00D0
27	SIGFA	=	0.400D0
28	SIGFG	=	0.600D0

Table 24: Example of Numerical Values Assigned to the Parameters in File PDA

```
 1     PLOTS(Y=1,N=2)      = 2
 2     TABLES 1(Y=1,N=2)   = 1
 3     TABLES 2(Y=1,N=2)   = 1
 4     TAUMX1              =   25.0D0
 5     SUBNT1              =    1.0D0
 6     TAUMX2              =  100.0D0
 7     SUBNT2              =    5.0D0
 8     STEPSZ              =    0.01D0
 9     HMIN                =    0.001D0
10     TOL                 =  0.0000000001D0
11     KAS0                =    0.00
12     NK                  =    0.50
13     SL                  =    0.0025
14     PMV                 =   50.00
15     XS(1)               =    5.875
16     XS(2)               =    7.00
17     YS1(1)              =    7.5625
18     YS2(1)              =    7.1875
19     YS3(1)              =    6.8125
20     YS4(1)              =    6.4375
21     SFT                 =   10.00
22     SFX                 =   15.0
23     SFY                 =  600.0
24     ZMN                 =   -5.0
25     SFZ                 =    5.0
26     SFK                 =   20.0
27     SFR                 =    2.5
28     SFU                 =    0.010
```

simulation is provided from time zero to TAUMX1, as values are recorded every hour. During the interval from TAUMX1 to TAUMX2 the response will be recorded every 5 hrs., and hence less detailed. TAUMX1 was chosen from preliminary tests as the time when all the variables were not changing rapidly with time.

A1.2 The Main Program UBCEDEMA

Following is a copy of the main program UBCEDEMA. Explanations of the contents are presented throughout the program by comment statments.

The numerical integrations of JNET1, JAS, QNETA and QNETG over time to yield VIS1, VAS, QA and QG, respectively, are conducted with the subroutine "DRKC", provided by the University of British Columbia Computing Centre. The definitions of the terms are presented in Table 25.

The tissue compliance curve is required to determine the interstitial hydrostatic pressure PPMV corresponding to the fluid volume VIS1. A subroutine entitled CMPLNC is used to relate PPMV to VIS1 (statement 166 and 683): the terms of CMPLNC are defined in Table 26.

COMPUTER PROGRAM UBCEDEMA

```
Listing of UBCEDEMA at 11:55:23 on MAR 25, 1985 for CCid=HEIJ Page    1

      1            IMPLICIT REAL*8(A-Z)
      2            DIMENSION YIO(5),FIO(5),FPPMV(10),G(5),S(5),T(5)
      3            COMMON/BLCA/SIGD,PSA,PSG,SIGFA,SIGFG
      4            COMMON/BLCB/PIMV,VCELL,VEXA,VEXG,CMVA,CMVG
      5            COMMON/BLCC/FPPMV,VTONS,B,VLMPH,KF,KAS0,NK,SL,PMV
    5.5            COMMON/BLCD/PMV1,PMV2,PTAU1,PTAU2
      6            REAL*4 X1(201),X2(201),X3(201),X4(201),Y1(201),Y2(201),
      7           *Y3(201),Y4(201),Z1(201),Z2(201),Z3(201),R1(201),R2(201),
      8           *S1(201),S2(201),U1(201),U2(201),V1(201),V2(201),W1(201),
      9           *W2(201),TI(201),KA(201),PI(201),XS(2),YS1(2),YS2(2),
     10           *YS3(2),YS4(2)
     11            REAL*4 TMN,SFT,XMN,SFX,YMN,SFY,ZMN,A1,AA1,
     12           *SFZ,RMN,SFR,UMN,SFU,KMN,SFK
     13            INTEGER L,LL,LLL,LLLL,M,N,NN,NNN,NNNN,I,I1,ICHECK,IFLAG,
     14           *II,J,JJ,JJJJ
     15            EXTERNAL FUNC
     16      C
     17      C     INPUT DATA FROM FILE EDA
     18      C
     19            READ(4,1)VTOTO,VASO,QAO,QGO,PIMV
     20          1 FORMAT(4(T11,D13.5,/),T11,D13.5)
     21            READ(4,3)VCELL,VEXA,VEXG,VTONS,VLMPH,
     22           *B
     23          3 FORMAT(5(T11,D13.5,/),T11,D13.5)
     24            READ(4,4)CMVA,CMVG
     25          4 FORMAT(T11,D13.5,/,T11,D13.5)
     26            READ(4,5)(FPPMV(J),J=1,9)
     27          5 FORMAT(8(T11,D13.5,/),T11,D13.5)
     28            READ(4,6)KF,SIGD,PSA,PSG,SIGFA,SIGFG
     29          6 FORMAT(5(T11,D13.5,/),T11,D13.5)
     30      C
     31      C     INPUT DATA FROM FILE PDA
     32      C
     33            READ(5,12)NN
     34            READ(5,12)NNN
     35            READ(5,12)NNNN
     36         12 FORMAT(T21,I1)
     37            READ(5,16)TAUMX1
     38            READ(5,16)SUBNT1
     39            READ(5,16)TAUMX2
     40            READ(5,16)SUBNT2
     41            READ(5,16)STEPSZ
     42            READ(5,17)HMIN
     43            READ(5,17)TOL
     44            READ(5,16)KAS0
     45            READ(5,16)NK
     46            READ(5,16)SL
     47            READ(5,16)PMV
     48         16 FORMAT(T21,D13.6)
     49         17 FORMAT(T21,D19.12)
     50      C
     51      C     PRINTING OF INPUT DATA
     52      C
     53            WRITE(7,401)
     54        401 FORMAT(1H1,10X,'INPUT PARAMETERS FOR RUN',///)
     55            WRITE(7,402)CMVA,CMVG
     56        402 FORMAT(1X,'PLASMA CONCENTRATION : ALBUMIN',8X,'CMVA    = ',
     57           *D13.5,/,24X,'GLOBULIN',7X,'CMVG    = ',D13.5,/)
```

Listing of UBCEDEMA at 11:55:23 on MAR 25, 1985 for CCid=HEIJ Page 2

```
      WRITE(7,403)VCELL,VEXA,VEXG
  403 FORMAT(1X,'CELLULAR VOLUME',23X,'VCELL  = ',D13.5,//,1X,
     *'EXCLUDED VOLUME : ALBUMIN',13X,'VEXA   = ',D13.5,/,19X,
     *'GLOBULIN',12X,'VEXG   = ',D13.5,/)
      WRITE(7,404)SIGD
  404 FORMAT(1X,'REFLECTION COEFFICIENT',16X,'SIGD  = ',D13.5,/)
      WRITE(7,405)PSA,PSG
  405 FORMAT(1X,'PERMEABILITY SURFACE AREA : ALBUMIN',3X,
     *'PSA    = ',D13.5,/,29X,'GLOBULIN  PSG    = ',
     *D13.5,/)
      WRITE(7,406)SIGFA,SIGFG
  406 FORMAT(1X,'REFLECTION COEFFICIENT : ALBUMIN',6X,
     *'SIGFA  = ',D13.5,/,26X,'GLOBULIN',5X,'SIGFG  = ',
     *D13.5,/)
      WRITE(7,407)KAS0,NK,SL
  407 FORMAT(1X,'ALVEOLAR FLOODING CONSTANTS :',9X,'KAS0   = ',
     *D13.5,/,39X,'NK     = ',D13.5,/,39X,'SL     = ',D13.5,/)
      WRITE(7,408)VTONS,VLMPH
  408 FORMAT(1X,'ONSET VOLUME FOR FLOODING',13X,'VTONS  = ',
     *D13.5,//,1X,'VOLUME OF MAXIMUM LYMPH FLOW',10X,'VLMPH  = ',
     *D13.5,/)
      WRITE(7,409)KF,PMV
  409 FORMAT(1X,'ENDOTHELIUM FILTRATION COEFFICIENT    KF     = ',
     *D13.5,//,1X,'PLASMA HYDROSTATIC PRESSURE',11X,'PMV    = ',
     *D13.5,/)
      WRITE(7,410)TAUMX1,SUBNT1,TAUMX2,SUBNT2,STEPSZ,HMIN,TOL
  410 FORMAT(1X,'MAXIMUM TIME OF PRINTING INTERVAL 1',3X,
     *'TAUMX1 = ',D13.5,/,1X,'PRINTING OUTPUT INTERVAL 1',12X,
     *'SUBNT1 = ',D13.5,//,1X,'MAXIMUM TIME OF RUN',19X,
     *'TAUMX2 = ',D13.5,/,1X,'PRINTING OUTPUT INTERVAL 2',12X,
     *'SUBNT2 = ',D13.5,//,1X,'INITIAL STEPSIZE FOR CALCULATIONS',
     *5X,'STEPSZ = ',D13.5,//,1X,'MINIMUM STEPSIZE FOR CALCULATIONS'
     *5X,'HMIN   = ',D13.5,//,1X,'MAXIMUM TOLERANCE',21X,
     *'TOL    = ',D13.5)
C
C     INITIALIZING VARIABLES & COUNTERS
C
      I=0
      ICHECK=1
      IFLAG=1
      L=1
      M=2
      C=0.0
      TAU=0.0
      HSTEP=STEPSZ
      SUBINT=SUBNT1
      QA=QAO
      QG=QGO
      VAS=VASO
      VTOT=VTOTO
      VIS1O=VTOTO-VASO
      VIS1=VIS1O
C
C     ASSIGNING INITIAL VALUES TO ARRAY YIO : NEEDED
C     FOR UBC SUBROUTINE "DRKC"
C
      YIO(1)=VTOTO
      YIO(2)=QAO
```

Listing of UBCEDEMA at 11:55:23 on MAR 25, 1985 for CCid=HEIJ Page 3

```
116           YIO(3)=QGO
117           YIO(4)=VASO
118           YIO(5)=VIS1O
119     C
120     C     ASSIGNING INITIAL VALUES TO VARIABLES THAT ARE TO
121     C     BE DETERMINED AT THE "CHARACTERISTIC POINTS"
122     C
123           JASMAX=0.D0
124           JASLO=0.D0
125           TIMAX=TAU
126           TILO=TAU
127           TAUON=0.D0
128           VTOTLO=VTOT
129           VTOTMX=VTOT
130           VIS1LO=VIS1
131           VIS1MX=VIS1
132           RCAMAX=0.D0
133           CTAON=QA/VIS1
134           CTALO=0.D0
135     C
136     C     DETERMINATION OF THE NUMBER OF INTERVALS (II) OF
137     C     SIZE SUBNT2 IN THE FIRST TIME RANGE OF MAXIMUM
138     C     VALUE TAUMX1
139     C
140           A1=TAUMX1
141           AA1=SUBNT2
142           II=IFIX(A1)/IFIX(AA1)
143     C
144       195 CONTINUE
145     C
146     C     CALCULATION OF INTERSTITIAL VOLUME
147     C
148     C     VIS1=VTOT-VAS
149           VIS=VIS1-VCELL
150     C
151     C     CALCULATION OF ALBUMIN PARAMETERS
152     C
153           CTA=QA/VIS
154           VAVA=VIS-VEXA
155           CAVA=QA/VAVA
156     C
157     C     CALCULATION OF GLOBULIN PARAMETERS
158     C
159           CTG=QG/VIS
160           VAVG=VIS-VEXG
161           CAVG=QG/VAVG
162     C
163     C     CALCULATION OF CENTRAL PARAMETERS
164     C     CALCULATION OF INTERSTITIAL PRESSURE
165     C
166           CALL CMPLNC(VIS1,FPPMV,PPMV)
167     C
168     C     CALCULATION OF INTERSTITIAL ONCOTIC PRESSURE
169     C
170           CP=CAVA+CAVG
171           PIPMV=210.D0*CP+1600.D0*CP*CP+9000.D0*CP*CP*CP
172     C
173     C     CALCULATION OF CAPILLARY FILTRATION RATE
```

Listing of UBCEDEMA at 11:55:23 on MAR 25, 1985 for CCid=HEIJ Page 4

```
174      C
175           JV=KF*((PMV-PPMV)-SIGD*(PIMV-PIPMV))
176      C
177      C
178      C     CALCULATION OF LYMPH FLOW
179      C
180           IF(VIS1.LT.VLMPH)GO TO 203
181      C CALCULATION OF MAXIMUM LYMPH FLOW
182           JL=0.17D0*VLMPH-5.56D1
183           GO TO 204
184        203 JL=0.17D0*VIS1-5.56D1
185      C
186      C     CALCULATION OF RATE OF EXTRAVASCULAR FLUID
187      C     ACCUMULATION
188      C
189        204 JNET=JV-JL
190           FIO(1)=JNET
191      C
192      C     DETERMINATION IF ALVEOLAR FLOODING OCCURS
193      C
194           IF(VTOT.LT.VTONS)GO TO 207
195      C
196      C     CALCULATION OF FILTRATION COEFFICIENT OF
197      C     EPITHELIAL MEMBRANE
198      C
199           KAS=KAS0+NK*(VIS1-VTONS)
200           GO TO 208
201        207 KAS=0.D0
202      C
203      C     CALCULATION OF HYDROSTATIC PRESSURE OF FLUID
204      C     IN THE AIR SPACE
205      C
206        208 PAS=SL*VAS+B
207      C
208      C     CALCULATION OF HYDROSTATIC PRESSURE DIFFERENCE
209      C     (PPMV-PAS) BETWEEN INTERSTITIUM & AIR SPACE
210      C
211           PDIF=PPMV-PAS
212      C
213      C     CALCULATION OF TRANSEPITHELIAL FLUID FLOW RATE
214      C
215           JAS=KAS*(PPMV-PAS)
216           FIO(4)=JAS
217      C
218      C     CALCULATION OF RATE OF ACCUMULATION OF
219      C     INTERSTITIAL FLUID
220      C
221           JNET1=JV-JL-JAS
222           FIO(5)=JNET1
223      C
224      C     CALCULATION OF TRANSENDOTHELIUM ALBUMIN
225      C     FLOW RATE
226      C
227           JSA=PSA*(CMVA-CAVA)+(1.D0-SIGFA)*(CMVA+CAVA)*JV/2.D0
227.3         DIFFUS=PSA*(CMVA-CAVA)
227.6         CONVEC=(1.D0-SIGFA)*(CMVA+CAVA)*JV/2.D0
228      C
229      C     CALCULATION OF RATE OF INTERSTITIAL ALBUMIN
```

Listing of UBCEDEMA at 11:55:23 on MAR 25, 1985 for CCid=HEIJ Page 5

```
      C     ACCUMULATION
      C
            QNETA=JSA-CTA*(JL+JAS)
            FIO(2)=QNETA
      C
      C     CALCULATION OF TRANSENDOTHELIUM GLOBULIN
      C     FLOW RATE
      C
            JSG=PSG*(CMVG-CAVG)+(1.D0-SIGFG)*(CMVG+CAVG)*JV/2.D0
      C
      C     CALCULATION OF RATE OF INTERSTITIAL GLOBULIN
      C     ACCUMULATION
      C
            QNETG=JSG-CTG*(JL+JAS)
            FIO(3)=QNETG
      C
      C     SETTING UP OF TABLES (2) FOR FURTHER CALCULATIONS
      C     USING OTHER PROGRAMS
      C
            IF(NNNN.EQ.2)GO TO 399
            IF(TAU.GT.99.0)GO TO 399
            WRITE(1,310)TAU,JV,JL,JNET1,JAS
        310 FORMAT(5(E12.5,2X))
      C     WRITE(2,320)TAU,VIS1,PPMV,KAS,PAS
      C 320 FORMAT(5(E12.5,2X))
      C     WRITE(3,330)TAU,QA,QG,PIPMV
      C 330 FORMAT(4(E12.5,2X))
      C     CTCMV=CTA/CMVA
      C     WRITE(6,340)TAU,QNETA,QNETG,CTA,CTG
      C 340 FORMAT(5(E12.5,2X))
      C     WRITE(8,350)TAU,DIFFUS,CONVEC,JSA,QNETA
      C 350 FORMAT(5(E12.5,2X))
        399 CONTINUE
      C
      C     DETERMINATION OF THE TIME OF ONSET OF ALVEOLAR
      C     FLOODING (TION) & THE CORRESPONDING ALBUMIN CONCENTR-
      C     -ATION (RCAON)
      C
            IF(IFLAG.GT.1)GO TO 261
            IF(JAS.EQ.0.D0)GO TO 261
            TION=(TAU+TAUON)/2.D0
            RCAON=((CTA+CTAON)/2.D0)/CMVA
            IFLAG=2
      C
      C     DETERMINATION OF MAXIMUM JAS (JASMAX) & CORRESPONDING
      C     TIME (TIMAX),ALBUMIN CONCENTRAION RATIO (RCAMAX),
      C     TOTAL EXTRAVASCULAR FLUID VOLUME (VTOTMX), &
      C     EXTRAVASCULAR-EXTRAALVEOLAR FLUID VOLUME (VIS1MX)
      C
        261 IF(JAS.LT.JASMAX)GO TO 262
            JASMAX=JAS
            TIMAX=TAU
            RCAMAX=CTA/CMVA
            VTOTMX=VTOT
            VIS1MX=VIS1
      C
      C     DETERMINATION OF THE TIME (TIOT) TO REACH A
      C     VTOT OF 1000 ML & THE CORRESPONDING
```

Listing of UBCEDEMA at 11:55:23 on MAR 25, 1985 for CCid=HEIJ Page 6

```
      C     EXTRAVASCULAR-EXTRAALVEOLAR FLUID VOLUME (VIS1OT),
      C     TRANSEPITHELIAL FLUID FLOWRATE (JASOT), SLOPE (JASSLP)
      C     OF THE TRANSEPITHELIAL FLUID FLOWRATE-TIME CURVE AT
      C     VTOT=1000 ML, AND ALBUMIN CONCENTRATION RATIO (RCAOT)
      C
        262 IF(VTOT.LT.1000.D0)GO TO 263
            IF(ICHECK.GT.1)GO TO 264
            FACT=(1000.D0-VTOTLO)/(VTOT-VTOTLO)
            VIS1OT=VIS1LO+FACT*(VIS1-VIS1LO)
            JASOT=JASLO+FACT*(JAS-JASLO)
            JASSLP=(JASLO-JAS)/(TILO-TAU)
            RCAOT=(CTALO+FACT*(CTA-CTALO))/CMVA
            TIOT=TILO+FACT*(TAU-TILO)
            ICHECK=2
            GO TO 264
      C REPLACING OLD VALUES OF DESIGNATED VARIABLES WITH NEW
      C VALUES IF VTOT IS LESS THAN 1000 ML
        263 IF(VTOT.LT.VTOTLO)GO TO 264
            VTOTLO=VTOT
            VIS1LO=VIS1
            JASLO=JAS
            CTALO=CTA
            TILO=TAU
      C
      C     DETERMINATION OF WHETHER A NEW TIME INTERVAL
      C     (I1*SUBINT) FOR PRINTING OF VARIABLES HAS BEEN REACHED.
      C     IF SO, THE VARIABLES ARE STORED IN ARRAY FORM.
      C     IF NOT, TIME ITERATIONS ARE CONTINUED.
      C
        264 IF(C.GE.(FLOAT(I1)*SUBINT)) M=M+1
            IF(M.GT.1)GO TO 260
      C
      C     DETERMINATION OF BEGINNING (A) AND END (C) OF
      C     CALCULATION INTERVAL IN UNITS OF TIME
      C
        210 A=TAU
            C=TAU+0.25D0
            HSTEP=.10D0
            CTAON=CTA
            TAUON=A
      C
      C     UTILIZATION OF UBC SUBROUTINE "DRKC" TO EVALUATE
      C     TIME INTEGRAL OF VARIABLES QA,QG,VAS, & VTOT BETWEEN
      C     CALCULATION INTERVAL BEGINNING AT 'A' & ENDING AT
      C     'C' OF WIDTH 0.25 HR.
      C
            CALL DRKC(5,A,C,YIO,FIO,HSTEP,HMIN,TOL,FUNC,G,S,T)
            VTOT=YIO(1)
            QA=YIO(2)
            QG=YIO(3)
            VAS=YIO(4)
            VIS1=YIO(5)
            TAU=C
            GO TO 195
      C
      C     ARRANGEMENT OF VARIABLES FOR PRINTING AND PLOTTING
      C
        260 I=I+1
```

```
      M=1
C
C SET-UP OF ARRAYS FOR STORAGE OF DIFFERENT VARIABLES
C
      TI(I)=TAU
      X1(I)=JV
      X2(I)=JL
      X3(I)=JNET1
      X4(I)=JAS
      Y1(I)=VTOT
      Y2(I)=VAS
      Y3(I)=VIS1
      Y4(I)=VIS
      Z1(I)=PPMV
      Z2(I)=PAS
      Z3(I)=PDIF
      KA(I)=KAS
      R1(I)=QA
      R2(I)=QG
      S1(I)=VAVA
      S2(I)=VAVG
      U1(I)=CTA
      U2(I)=CTG
      V1(I)=CAVA
      V2(I)=CAVG
      W1(I)=QNETA
      W2(I)=QNETG
      PI(I)=PIPMV
      IF(C.LT.TAUMX1)I1=I
      IF(C.LT.TAUMX1)GO TO 210
      SUBINT=SUBNT2
      II=II+1
      I1=II
      IF(C.GE.TAUMX2)GO TO 267
      GO TO 210
C
C     TERMINATION OF CALCULATIONS
C
  267 CONTINUE
      IF(NNN.EQ.2)GO TO 900
C
C     PRINTING OF TABLES
C
      WRITE(7,414)TION,RCAON
  414 FORMAT(1H1,15X,'ONSET OF ALVEOLAR FLOODING',///,
     *1X,'TIME OF ONSET IS ',D12.5,//,1X,'ALBUMIN',
     *' CONCENTRATION RATIO - CTA/CMVA - IS ',D12.5,////)
      WRITE(7,415)
  415 FORMAT(5X,'VARIABLES AT THE POINT OF THE',
     *' MAXIMUM ALVEOLAR FLOODING RATE',//)
      WRITE(7,420)JASMAX,TIMAX,RCAMAX
  420 FORMAT(1X,'THE MAXIMUM FLUID FLOWRATE INTO',
     *' THE AIR SPACE IS ',D12.5,//,1X,'THE CORRESPONDING',
     *' TIME IS',24X,D12.5,//,1X,'THE ALBUMIN CONCENTRATION',
     *' RATIO - CTA/CMVA - IS  ',D12.5,/)
      WRITE(7,421)VTOTMX,VIS1MX
  421 FORMAT(1X,'THE EXTRAVASCULAR FLUID VOLUME IS ',15X,
     *D12.5,//,1X,'THE INTERSTITIAL AND CELLULAR VOLUME IS ',
```

```
Listing of UBCEDEMA at 11:55:23 on MAR 25, 1985 for CCid=HEIJ Page    8

      *9X,D12.5,////)
       WRITE(7,425)
  425 FORMAT(1X,'THE MAGNITUDE OF VARIABLES AT A TOTAL',
     *' EXTRAVASCULAR FLUID VOLUME OF 1000 ML',//)
       WRITE(7,430)TIOT,VIS1OT,JASOT,JASSLP,RCAOT
  430 FORMAT(1X,'TIME',32X,'TAU       = ',D12.5,//,1X,
     *'INTERSTITIAL AND CELLULAR VOLUME',4X,'VIS1      = ',D12.5,
     *//,1X,'FLUID FLOWRATE INTO THE AIR SPACE   JAS      = ',
     *D12.5,//,1X,'RATE OF CHANGE OF JAS',15X,'DJAS/DT  = ',
     *D12.5,//,1X,'ALBUMIN CONCENTRATION RATIO',9X,'CTA/CMVA = '
     *,D12.5)
       WRITE(7,434)
  434 FORMAT(1H1,18X,'TABLE 1 : OUTPUT OF FLUID FLOWS',//)
       WRITE(7,435)
  435 FORMAT(2X,'TAU(HRS)',6X,'JV(ML/HR)',5X,'JL(ML/HR)',
     *3X,'JNET1(ML/HR)',4X,'JAS(ML/HR)',/)
       WRITE(7,440)(TI(J),X1(J),X2(J),X3(J),X4(J),J=1,I)
  440 FORMAT(5(E12.5,2X))
       WRITE(7,444)
  444 FORMAT(1H1,17X,'TABLE 2 : OUTPUT OF FLUID VOLUMES',//)
       WRITE(7,445)
  445 FORMAT(2X,'TAU(HRS)',6X,'VTOT(ML)',6X,'VAS(ML)',
     *7X,'VIS1(ML)',6X,'VIS(ML)',/)
       WRITE(7,450)(TI(J),Y1(J),Y2(J),Y3(J),Y4(J),J=1,I)
  450 FORMAT(5(E12.5,2X))
       WRITE(7,454)
  454 FORMAT(1H1,1X,'TABLE 3 : OUTPUT OF HYDROSTATIC PRESSURES -',
     *' PPMV,PAS,(PPMV-PAS) -',//,12X,'& EPITHELIUM FILTRATION',
     *' COEFFICIENT - KAS',//)
       WRITE(7,455)
  455 FORMAT(2X,'TAU(HRS)',4X,'PPMV(MM HG)',4X,
     *'PAS(MM HG)',4X,'PDIF(MM HG)',7X,'KAS'/)
       WRITE(7,460)(TI(J),Z1(J),Z2(J),Z3(J),KA(J),J=1,I)
  460 FORMAT(E12.5,2X,E12.5,2X,E12.5,3X,E12.5,1X,E12.5)
       WRITE(7,464)
  464 FORMAT(1H1,5X,'TABLE 4 : OUTPUT OF INTERSTITIAL SOLUTE',
     *'WEIGHTS - QA,QG -',//,16X,'& INTERSTITIAL AVAILABLE',
     *' VOLUMES - VAVA,VAVG',//)
       WRITE(7,465)
  465 FORMAT(2X,'TAU(HRS)',7X,'QA(GM)',8X,'QG(GM)',7X,
     *'VAVA(ML)',6X,'VAVG(ML)',/)
       WRITE(7,450)(TI(J),R1(J),R2(J),S1(J),S2(J),J=1,I)
  470 FORMAT(5(E12.5,2X))
       WRITE(7,474)
  474 FORMAT(1H1,5X,'TABLE 5 : OUTPUT OF INTERSTITIAL - CTA,CTG -',
     *' & AVAILABLE',//,16X,'INTERSTITIAL - CAVA,CAVG - ',
     *'CONCENTRATIONS',//)
       WRITE(7,475)
  475 FORMAT(2X,'TAU(HRS)',5X,'CTA(GM/ML)',4X,
     *'CTG(GM/ML)',4X,'CAVA(GM/ML)',3X,'CAVG(GM/ML)',/)
       WRITE(7,480)(TI(J),U1(J),U2(J),V1(J),V2(J),J=1,I)
  480 FORMAT(5(E12.5,2X))
       WRITE(7,484)
  484 FORMAT(1H1,'TABLE 6 : OUTPUT OF INTERSTITIAL SOLUTE',
     *' ACCUMULATION RATES - QNETA,',//,11X,'QNETG - ',
     *'& INTERSTITIAL ONCOTIC PRESSURE - PIPMV',//)
       WRITE(7,485)
  485 FORMAT(2X,'TAU(HRS)',4X,'QNETA(GM/HR)',2X,
```

Listing of UBCEDEMA at 11:55:23 on MAR 25, 1985 for CCid=HEIJ Page 9

```
      *'QNETG(GM/HR)',3X,'PIPMV(MM HG)',/)
       WRITE(7,490)(TI(J),W1(J),W2(J),PI(J),J=1,I)
  490 FORMAT(4(E12.5,2X))
C
C     TERMINATION OF PRINTING SECTION
C
  900 CONTINUE
       IF(NN.EQ.2)GO TO 1000
C
C     PLOTTING OF GRAPHS
C
C     INPUT DATA FROM FILE PDA FOR SYMBOL LEGEND
C
       READ(5,901)XS(1),XS(2)
  901 FORMAT(T21,E13.5,/,T21,E13.5)
       READ(5,902)YS1(1),YS2(1),YS3(1),YS4(1)
  902 FORMAT(3(T21,E13.5,/),T21,E13.5)
       YS1(2)=YS1(1)
       YS2(2)=YS2(1)
       YS3(2)=YS3(1)
       YS4(2)=YS4(1)
C
C     PLOTTING OF FLUID FLOW RATES
C
       TMN=0.0
       XMN=0.0
C INPUT DATA FROM FILE PDA
       READ(5,903)SFT
       READ(5,903)SFX
  903 FORMAT(T21,E13.5)
       CALL AXIS(2.25,3.,'TIME (HRS)',-10,5.,0.,TMN,SFT)
       CALL AXIS(2.25,3.,'FLUID FLOWS(ML/HR)',18,5.,90.,XMN,SFX)
       CALL DLINE(TI,X1,I,TMN,2.25,SFT,XMN,3.,SFX,.125,.125,.0625)
       CALL DLINE(TI,X2,I,TMN,2.25,SFT,XMN,3.,SFX,.25,.25,.075)
       CALL DLINE(TI,X3,I,TMN,2.25,SFT,XMN,3.,SFX,.15,.0625,.05)
       CALL BBLINE(TI,X4,I,TMN,2.25,SFT,XMN,3.,SFX,2,1,0.1,2)
       CALL LEGEND(PMV,KF,KAS0,NK,SL,SIGD,PSA,PSG,SIGFA,SIGFG)
       CALL PSYM(5.0,7.5,.125,'JV    = ',.0,8)
       CALL PLOT(XS(1),YS1(1),3)
       CALL DASHLN(.125,.0625,.125,.0625)
       CALL PLOT(XS(2),YS1(2),4)
       CALL PSYM(5.0,7.125,.125,'JL    = ',.0,8)
       CALL PLOT(XS(1),YS2(1),3)
       CALL DASHLN(.25,.075,.25,.075)
       CALL PLOT(XS(2),YS2(2),4)
       CALL PSYM(5.0,6.750,.125,'JNET1 = ',.0,8)
       CALL PLOT(XS(1),YS3(1),3)
       CALL DASHLN(.15,.05,.0625,.05)
       CALL PLOT(XS(2),YS3(2),4)
       CALL PSYM(5.0,6.375,.125,'JAS   = ',.0,8)
       CALL LINE(XS,YS4,2,1)
       CALL PLOT(12.0,0.,-3)
C
C     PLOTTING OF FLUID VOLUMES
C
       YMN=0.0
C INPUT DATA FROM FILE PDA
       READ(5,903)SFY
```

```
Listing of UBCEDEMA at 11:55:23 on MAR 25, 1985 for CCid=HEIJ Page   10

      CALL AXIS(2.25,3.,'TIME (HRS)',-10,5.,0.,TMN,SFT)
      CALL AXIS(2.25,3.,'FLUID VOLUMES(ML)',17,5.,90.,YMN,SFY)
      CALL BBLINE(TI,Y1,I,TMN,2.25,SFT,YMN,3.,SFY,2,1,0.1,2)
      CALL DLINE(TI,Y2,I,TMN,2.25,SFT,YMN,3.,SFY,.125,.125,.0625)
      CALL DLINE(TI,Y3,I,TMN,2.25,SFT,YMN,3.,SFY,.15,.0625,.05)
      CALL LEGEND(PMV,KF,KAS0,NK,SL,SIGD,PSA,PSG,SIGFA,SIGFG)
      CALL PSYM(5.0,7.50,.125,'VTOT = ',.0,7)
      CALL LINE(XS,YS1,2,1)
      CALL PSYM(5.0,7.125,.125,'VIS1 = ',.0,7)
      CALL PLOT(XS(1),YS2(1),3)
      CALL DASHLN(.125,.0625,.125,.0625)
      CALL PLOT(XS(2),YS2(2),4)
      CALL PSYM(5.0,6.750,.125,'VAS  = ',.0,7)
      CALL PLOT(XS(1),YS3(1),3)
      CALL DASHLN(.15,.05,.0625,.05)
      CALL PLOT(XS(2),YS3(2),4)
      CALL PLOT(12.0,0.,-3)
C
C     PLOTTING OF HYDROSTATIC PRESSURES
C
C INPUT DATA FROM FILE PDA
      READ(5,903)ZMN
      READ(5,903)SFZ
      CALL AXIS(2.25,3.,'TIME (HRS)',-10,5.,0.,TMN,SFT)
      CALL AXIS(2.25,3.,'HYDROSTATIC & OSMOTIC PRESSURES(MM HG)',
     *38,5.,90.,ZMN,SFZ)
      CALL BBLINE(TI,Z1,I,TMN,2.25,SFT,ZMN,3.,SFZ,2,1,0.1,2)
      CALL DLINE(TI,PI,I,TMN,2.25,SFT,ZMN,3.,SFZ,.15,.0625,.05)
      CALL DLINE(TI,Z2,I,TMN,2.25,SFT,ZMN,3.,SFZ,.125,.125,.0625)
      CALL LEGEND(PMV,KF,KAS0,NK,SL,SIGD,PSA,PSG,SIGFA,SIGFG)
      CALL PSYM(5.0,7.50,.125,'PIPMV = ',.0,8)
      CALL PLOT(XS(1),YS1(1),3)
      CALL DASHLN(.15,.05,.0625,.05)
      CALL PLOT(XS(2),YS1(2),4)
      CALL PSYM(5.0,7.125,.125,'PPMV  = ',.0,8)
      CALL LINE(XS,YS2,2,1)
      CALL PSYM(5.0,6.750,.125,'PAS   = ',.0,8)
      CALL PLOT(XS(1),YS3(1),3)
      CALL DASHLN(.125,.0625,.125,.0625)
      CALL PLOT(XS(2),YS3(2),4)
      CALL PLOT(12.0,0.,-3)
C
C     PLOTTING OF EPITHELIUM FILTRATION COEFFICIENT
C
      KMN=0.0
C INPUT DATA FROM FILE PDA
      READ(5,903)SFK
      CALL AXIS(2.25,3.,'TIME (HRS)',-10,5.,0.,TMN,SFT)
      CALL AXIS(2.25,3.,'KAS (ML/HR/MM HG)',17,5.,90.,KMN,SFK)
      CALL BBLINE(TI,KA,I,TMN,2.25,SFT,KMN,3.0,SFK,2,1,0.1,2)
      CALL LEGEND(PMV,KF,KAS0,NK,SL,SIGD,PSA,PSG,SIGFA,SIGFG)
      CALL PLOT(12.0,0.,-3)
C
C     PLOTTING OF SOLUTE WEIGHTS
C
      RMN=0.0
C INPUT DATA FROM FILE PDA
      READ(5,903)SFR
```

Listing of UBCEDEMA at 11:55:23 on MAR 25, 1985 for CCid=HEIJ Page 11

```
      CALL AXIS(2.25,3.,'TIME (HRS)',-10,5.,0.,TMN,SFT)
      CALL AXIS(2.25,3.,'SOLUTE WEIGHTS(GM)',18,5.,90.,RMN,SFR)
      CALL BBLINE(TI,R1,I,TMN,2.25,SFT,RMN,3.,SFR,2,1,0.1,2)
      CALL DLINE(TI,R2,I,TMN,2.25,SFT,RMN,3.,SFR,.125,.125,.0625)
      CALL LEGEND(PMV,KF,KAS0,NK,SL,SIGD,PSA,PSG,SIGFA,SIGFG)
      CALL PSYM(5.0,7.50,.125,'QA = ',.0,5)
      CALL LINE(XS,YS1,2,1)
      CALL PSYM(5.0,7.125,.125,'QG = ',.0,5)
      CALL PLOT(XS(1),YS2(1),3)
      CALL DASHLN(.125,.0625,.125,.0625)
      CALL PLOT(XS(2),YS2(2),4)
      CALL PLOT(12.0,0.,-3)
C
C     PLOTTING OF SOLUTE CONCENTRATIONS
C
      UMN=0.0
C INPUT DATA FROM FILE PDA
      READ(5,903)SFU
      CALL AXIS(2.25,3.,'TIME (HRS)',-10,5.,0.,TMN,SFT)
      CALL AXIS(2.25,3.,'SOLUTE CONCENTRATIONS(GM/ML)',28,5.,
     *90.,UMN,SFU)
      CALL BBLINE(TI,U1,I,TMN,2.25,SFT,UMN,3.,SFU,2,1,0.1,2)
      CALL DLINE(TI,U2,I,TMN,2.25,SFT,UMN,3.,SFU,.125,.125,.0625)
      CALL LEGEND(PMV,KF,KAS0,NK,SL,SIGD,PSA,PSG,SIGFA,SIGFG)
      CALL PSYM(5.0,7.50,.125,'CTA = ',.0,6)
      CALL LINE(XS,YS1,2,1)
      CALL PSYM(5.0,7.125,.125,'CTG = ',.0,6)
      CALL PLOT(XS(1),YS2(1),3)
      CALL DASHLN(.125,.0625,.125,.0625)
      CALL PLOT(XS(2),YS2(2),4)
C
C     TERMINATION OF PLOTTING SECTION
C
      CALL PLOTND
 1000 STOP
      END
C
C
C     SUBROUTINE CMPLNC : FOR THE CALCULATION OF
C      INTERSTITIAL PRESSURE USING THE INTERSTITIAL
C      COMPLIANCE CURVE
C
      SUBROUTINE CMPLNC(VIS1,PPMV,PPMV)
C
      IMPLICIT REAL*8(A-Z)
      DIMENSION PPMV(10)
      REAL*4 SVIS1
      INTEGER MLO,MHI
      IF(VIS1.LT.460.D0)GO TO 610
      PPMV=0.017D0*VIS1-6.73D0
      GO TO 650
  610 IF(VIS1.GE.380.0D0)GO TO 620
      PPMV=0.227D0*VIS1-89.0D0
      GO TO 650
C INTERPOLATION OVER CURVED PORTION OF COMPLIANCE
  620 DVIS1=(VIS1-380.D0)/10.D0
      SVIS1=DVIS1
      MLO=INT(SVIS1)+1
```

Listing of UBCEDEMA at 11:55:23 on MAR 25, 1985 for CCid=HEIJ Page 12

```
      MHI=MLO+1
      PPMVLO=FPPMV(MLO)
      PPMVHI=FPPMV(MHI)
      PPMV=(1.D0+DVIS1-DFLOAT(MLO))*(PPMVHI-PPMVLO)+PPMVLO
  650 CONTINUE
      RETURN
      END
C
C
C     SUBROUTINE FUNC : TO BE USED IN CONJUNCTION WITH
C      SUBROUTINE DRKC FOR THE EVALUATION OF THE DERIVATIVES
C      (FIO) OF DEPENDENT VARIABLES (YIO)
C
      SUBROUTINE FUNC(TIME,YIO,FIO)
C
      IMPLICIT REAL*8(A-H,O-Z)
      REAL*8 JAS,JL,JNET,JNET1,JSA,JSG,JV,KF,KAS,NK,KAS0
      DIMENSION YIO(5),FIO(5)
      COMMON/BLCA/SIGD,PSA,PSG,SIGFA,SIGFG
      COMMON/BLCB/PIMV,VCELL,VEXA,VEXG,CMVA,CMVG
      COMMON/BLCC/FPPMV(10),VTONS,B,VLMPH,KF,KAS0,NK,SL,PMV
      COMMON/BLCD/PMV1,PMV2,PTAU1,PTAU2
      VTOT=YIO(1)
      QA=YIO(2)
      QG=YIO(3)
      VAS=YIO(4)
      VIS1=YIO(5)
C
C     CALCULATION OF INTERSTITIAL VOLUME
C
C     VIS1=VTOT-VAS
      VIS=VIS1-VCELL
C
C     CALCULATION OF ALBUMIN PARAMETERS
C
      CTA=QA/VIS
      VAVA=VIS-VEXA
      CAVA=QA/VAVA
C
C     CALCULATION OF GLOBULIN PARAMETERS
C
      CTG=QG/VIS
      VAVG=VIS-VEXG
      CAVG=QG/VAVG
C
C     CALCULATION OF CENTRAL PARAMETERS
C     CALCULATION OF INTERSTITIAL PRESSURE
C
      CALL CMPLNC(VIS1,FPPMV,PPMV)
C
C     CALCULATION OF INTERSTITIAL ONCOTIC PRESSURE
C
      CP=CAVA+CAVG
      PIPMV=210.D0*CP+1600.D0*CP*CP+9000.D0*CP*CP*CP
C
C     CALCULATION OF CAPILLARY FILTRATION RATE
C
      JV=KF*((PMV-PPMV)-SIGD*(PIMV-PIPMV))
```

Listing of UBCEDEMA at 11:55:23 on MAR 25, 1985 for CCid=HEIJ Page 13

```
      C
      C
      C     CALCULATION OF LYMPH FLOW
      C
            IF(VIS1.LT.VLMPH)GO TO 203
            JL=0.17D0*VLMPH-5.56D1
            GO TO 204
        203 JL=0.17D0*VIS1-5.56D1
      C
      C     CALCULATION OF RATE OF EXTRAVASCULAR FLUID
      C     ACCUMULATION
      C
        204 JNET=JV-JL
            FIO(1)=JNET
      C
      C     DETERMINATION IF ALVEOLAR FLOODING OCCURS
      C
            IF(VTOT.LT.VTONS)GO TO 207
      C
      C     CALCULATION OF FILTRATION COEFFICIENT OF
      C     EPITHELIAL MEMBRANE
      C
            KAS=KAS0+NK*(VIS1-VTONS)
            GO TO 208
        207 KAS=0.D0
      C
      C     CALCULATION OF HYDROSTATIC PRESSURE OF FLUID
      C     IN THE AIR SPACE
      C
        208 PAS=SL*VAS+B
      C
      C     CALCULATION OF TRANSEPITHELIAL FLUID FLOW RATE
      C
            JAS=KAS*(PPMV-PAS)
            FIO(4)=JAS
      C
      C     CALCULATION OF RATE OF ACCUMULATION OF
      C     INTERSTITIAL FLUID
      C
            JNET1=JV-JL-JAS
            FIO(5)=JNET1
      C
      C     CALCULATION OF TRANSENDOTHELIUM ALBUMIN
      C     FLOW RATE
      C
            JSA=PSA*(CMVA-CAVA)+(1.D0-SIGFA)*(CMVA-CAVA)*JV/2.D0
      C
      C     CALCULATION OF RATE OF INTERSTITIAL ALBUMIN
      C     ACCUMULATION
      C
            QNETA=JSA-CTA*(JL+JAS)
            FIO(2)=QNETA
      C
      C     CALCULATION OF TRANSENDOTHELIUM GLOBULIN
      C     FLOW RATE
      C
            JSG=PSG*(CMVG-CAVG)+(1.D0-SIGFG)*(CMVG+CAVG)*JV/2.D0
      C
```

Listing of UBCEDEMA at 11:55:23 on MAR 25, 1985 for CCid=HEIJ Page 14

```
      C     CALCULATION OF RATE OF INTERSTITIAL GLOBULIN
      C     ACCUMULATION
      C
            QNETG=JSG-CTG*(JL+JAS)
            FIO(3)=QNETG
            RETURN
            END
      C
      C
      C     SUBROUTINE LEGEND : FOR THE PRINTING OF CONSTANTS
      C      ON PLOTS
      C
            SUBROUTINE LEGEND(PMV,KF,KAS0,NK,SL,SIGD,PSA,PSG,SIGFA,SIGFG)
      C
            REAL*8 PMV,KF,KAS0,NK,SL,SIGD,PSA,PSG,SIGFA,SIGFG
            CALL PSYM(2.00,1.875,.125,'PMV (MM HG)         = ',.0,21)
            CALL NUMBER(4.25,1.875,.125,PMV,.0,2)
            CALL PSYM(2.00,1.60,.125,'KF (ML/HR/MM HG)    = ',.0,21)
            CALL NUMBER(4.25,1.60,.125,KF,.0,4)
            CALL PSYM(2.00,1.325,.125,'KAS0 (ML/HR/MM HG) = ',.0,21)
            CALL NUMBER(4.25,1.325,.125,KAS0,.0,5)
            CALL PSYM(2.00,1.050,.125,'NK (/HR/MM HG)      = ',.0,21)
            CALL NUMBER(4.25,1.050,.125,NK,.0,5)
            CALL PSYM(2.00,0.775,.125,'SL (MM HG/ML)       = ',.0,21)
            CALL NUMBER(4.25,0.775,.125,SL,.0,5)
            CALL PSYM(5.25,1.875,.125,'SIGD          = ',.0,14)
            CALL NUMBER(6.75,1.875,.125,SIGD,.0,5)
            CALL PSYM(5.25,1.6,.125,'PSA (ML/HR)   = ',.0,15)
            CALL NUMBER(6.75,1.6,.125,PSA,.0,4)
            CALL PSYM(5.25,1.325,.125,'PSG (ML/HR)   = ',.0,15)
            CALL NUMBER(6.75,1.325,.125,PSG,.0,4)
            CALL PSYM(5.25,1.05,.125,'SIGFA        = ',.0,14)
            CALL NUMBER(6.75,1.05,.125,SIGFA,.0,5)
            CALL PSYM(5.25,.775,.125,'SIGFG        = ',.0,14)
            CALL NUMBER(6.75,.775,.125,SIGFG,.0,5)
            RETURN
            END
```

Table 25: Explanation of Subroutine DRKC (56)

CALL DRKC(N,X,Z,Y,F,H,HMIN,E,FUNC,G,S,T)

where:

N is an INTEGER variable or constant. On entry, it contains the number of differential equations to be solved.

X is a REAL*8 variable. On entry, it contains the input value of the independent variable. On exit, it contains the final value of the independent variable.

Z is a REAL*8 variable or constant. On entry, it contains the final value of the independent variable at the end point of integration.

Y is a REAL*8, one-dimensional array, of dimension ≥N. On entry, Y(I)I=1,...,N contain the initial values of the dependent variables. On exit, Y contains the values of the dependent variables at the end point of integration.

F is a REAL*8, one-dimensional array, of dimension ≥N. On exit, it contains the output vector of derivatives Y'(X) at X=Z.

H is a REAL*8 variable. On entry, it contains the input step-size. H is changed by DRKC to contain the step-size used at the current integration step. For maximum accuracy in single precision, H≈(Z-X)/64.

HMIN is a REAL*8 variable or constant. On entry, it contains a lower bound for the step-size in order to prevent infinite cycling. For difficult problems (e.g. the orbit problem—see the sample problem in UBC DIFSY) DRKC may require HMIN≈10^{-4}*H. Usually HMIN=10^{-2}*H is adequate. See subsection (c), below, for a method to detect when HMIN has been reached.

Table 25: (cont'd.)

E is a REAL*8 variable or constant. On entry, it contains an error tolerance. If $E \geq 1$, the original step-length will be maintained throughout the integration. In single precision, $E \geq .5 \times 10^{-5}$.

FUNC is the name of a SUBROUTINE subprogram which is coded by the user to evaluate the derivatives. FUNC must be declared EXTERNAL in the user's calling program. Typically this subroutine would look like:

```
SUBROUTINE FUNC (X,Y,F)
IMPLICIT REAL*8(A-H,O-Z)
DIMENSION Y(1),F(1)
F(1)= f1(X,Y(1),...,Y(N))
.
.
.
F(N)= fN(X,Y(1),...,Y(N))
RETURN
END
```

where:

X is a REAL*8 variable which contains the current value of the independent variable.

Y is a REAL*8, one-dimensional array, which contains the current values of the dependent variables.

F is a REAL*8, one-dimensional array. On exit from FUNC it contains the values of the derivatives.

G, S, T are REAL*8, one-dimensional arrays, dimensioned ≥N. They are work areas required internally.

Table 26: Explanation of Subroutine CMPLNC

CALL	CMPLNC (VIS1, FPPMV, PPMV)
VIS1	is a REAL*8 variable, on entry VIS1 is the EVEA fluid volume to which the corresponding interstitial pressure is required
FPPMV	is a REAL*8 array, containing the interstitial hydrostatic pressures listed in Table 3 - the curved portion of the compliance curve.
PPMV	is a REAL*8 variable, on exit it contains the interstsitial pressure corresponding to VIS1.

A1.3 Plotting Section of Main Program UBCEDEMA

The plotting section of the simulation is executed from within the program UBCEDEMA, starting on line 466. Plots will be drawn if parameter NN in file PDA [PLOTS(Y=1,N=2)] is set equal to 1. The plots drawn are of the time variation of: 1) the fluid flows JV, JL, JNET1 and JAS, 2) the fluid volumes VTOT, VIS1 and VAS, 3) the epithelial filtration coefficient KAS, 4) the protein content (albumin and globulin) in the interstitium QA and QG and 5) the tissue protein concentration (albumin and globulin) CTA and CTG.

For each set of plots a number of subroutines are called: AXIS, PLOT, PLOTND, LINE, DASHLN, PSYM, DLINE, BBLINE, NUMBER and LEGEND. These subroutines are explained in Tables 27 through 36.

Table 27: Explanation of subroutine AXIS (57)

AXIS

Purpose

AXIS draws an axis with tick marks every inch, places scale values near the tick marks, and identifies the axis with a label.

This subroutine was not designed for use in the metric system and does not give pleasing results if metric units are used. Users who prefer to work in metric are advised to use subroutine AXPLOT, described on a following page. AXPLOT also gives the user more control over the plotting of an axis.

How To Use

CALL AXIS(X,Y,BCD,N,S,THETA,XMIN,DX)

where:

(X,Y) are the coordinates of the start of the axis.

BCD is a Hollerith literal (nHxxx... or 'xxx...') or an array containing BCD information to be used as the axis label.

N is positive if the label is to be written on the counterclockwise side of the axis, and negative if the label is to be written on the clockwise side. The absolute value of N is the number of characters in BCD.

S is the length of the axis in floating-point units. This value will be rounded up to the nearest whole unit.

THETA is the direction of the axis in floating-point degrees. For an x axis, THETA is usually 0.0, and for a y axis, 90.0.

XMIN is the value to be assigned to the origin (i.e. the value of the annotation opposite the first tick on the axis).

DX is the scale increment (number of units per inch or centimetre). The scale annotations at each successive tick of the axis will be XMIN, XMIN+DX, XMIN+2*DX, etc.

Note: XMIN and DX may be calculated using subroutine SCALE.

Table 28: Explanation of subroutine PLOT (57)

PLOT

Purpose

This subprogram is the basic plot subroutine. It generates the pen movements required to move the pen in a straight line from its present position to the position indicated in the call. It is also used to relocate the origin of the plotter coordinate system in the x direction.

How To Use

CALL PLOT(X,Y,IPEN)

where:

X,Y are the coordinates of the point to which the pen is to move. Y must be between -0.5 and 34.5 inches (-1.27 and 87.63 centimetres). X must be between -1.0 and 200.0 inches (-2.54 and 508.0 cm). If the y coordinate is larger than 10.5 inches (26.67 cm), the plot will automatically be directed to large paper when it is queued.

IPEN specifies whether the pen is to be up or down during its move to (X,Y). The values for IPEN are:

+1 for no change. If the pen is down before the call, it will remain down.

+2 for pen down. If the pen is up before the call, the pen will be lowered before the movement to (X,Y) is made. If down, it will remain down.

+3 for pen up. If the pen is down before the call, it will be raised before it is moved to (X,Y). If up, it will remain up.

+4 for pen dashed. While the pen is moved to (X,Y) it will be raised and lowered to produce dashed lines in accordance with the last call to the subroutine DASHLN.

Important

The subroutine PLOT is also used to relocate the origin on the graph paper in the x direction. If IPEN = -1, -2, or -3, the pen is moved to the (X,0.0) position on the paper (regardless of the y coordinate specified), and this position then becomes the new origin (0.0,0.0). The origin of the y coordinate may not be relocated. The origin of the x coordinate is relocated when a series of graphs is to be drawn.

Table 29: Explanation of subroutine PLOTND (57)

PLOTND

Purpose

To terminate plotting.

How To Use

CALL PLOTND

Comments

To ensure that a complete plot is received, terminate your plotting with a call to PLOTND, or a call to PLOT with a negative IPEN value. If PLOTND is used, it must be the last plotter subprogram called. No other calls to the plot routines are allowed after PLOTND. PLOTND will print the following message:

*** UBC Plot Subroutines - End of Plotting ***

Number of plot frames generated = n
If this plot is queued for plotting it will take approximately m minutes to plot at an approximate cost of d.dd dollars (University rates) and use I inches of paper. Approximately p% of the time will be spent plotting with the pen raised.

The numbers given are approximate and are intended to give the user some idea of how much it will cost to produce the plot. "n" is the number of frames in the plotfile, "m" is the number of minutes to draw the plot on the plotter, "d.dd" is the approximate cost in dollars at academic rates, and "i" is the number of inches of paper required. "p", the pen-up time, is included as a measure of efficiency of the plot.

When the plot is copied to *PLOT* the time actually used in drawing the plot will be calculated and your account charged.

A user will receive only part of his plot if the last call to a plotter subprogram is not to PLOTND, or to PLOT with a negative IPEN value. He may receive an error message at the time the plot is queued indicating a missing PEND record.

Table 30: Explanation of subroutine LINE (57)

LINE

Purpose

To draw a line through a series of points.

How To Use

CALL LINE(ARRAYX,ARRAYY,N,J)

where:

ARRAYX	contains the x coordinates of N data points.
ARRAYY	contains the y coordinates of the points.
N	is the number of points through which the line is to be drawn.
J	should be set to -1 if the pen is to be down when moving to the first point; otherwise, it should be set to +1. If J is +1, the line may be drawn backwards if this is more efficient. This means that the pen may not always finish at the coordinates of the last point in the line; it will sometimes finish at the coordinates of the first point. If J is set to -1, the line is always drawn forward.

Table 31: Explanation of subroutine DASHLN (57)

DASHLN

Purpose

To set a pattern for dashed line pen movements (IPEN=4).

How To Use

CALL DASHLN(DASH1,SPAC1,DASH2,SPAC2)

where:

DASH1 is the length of the first dash.

SPAC1 is the length of the first space.

DASH2 is the length of the second dash.

SPAC2 is the length of the second space.

These values should be entered as positive REAL*4 variables, indicating the lengths in user units. Zero values are not allowed.

If DASHLN has been called, a call to PLOT with an IPEN value of 4 will result in a dashed line being drawn. The first dash will be DASH1 inches or centimetres in length, the first space will be SPAC1 inches or centimetres in length, and similarly for the second dash and space. Then the pattern will repeat itself. By using a variety of parameters, many types of dashed lines may be created.

If dashing is discontinued, for example, in ordef to draw a symbol, and the pen is then returned to the same position where dashing was discontinued, the dashes will be correctly connected.

Comments

The lengths of dashes and spaces at angles of 45 degrees will be approximately 1.4 times their length as specified in the call. This difference is rarely noticeable in a finished plot.

Table 32: Explanation of subroutine PSYM (57)

PSYM

Purpose

PSYM produces text on a plot. This routine is used for all character sets. See the description of PALPHA for information on alternative character sets.

How To Use

```
CALL PSYM(X,Y,HEIGHT,STRING,ANGLE,LENGTH,&RC4)
```

where:

X,Y	are the floating-point (REAL*4) coordinates of the first character to be drawn. For most character sets, including the standard one, this is the lower-left corner of the first character. If either coordinate is -0.0 (hexadecimal 80000000), PSYM continues from the end of the last character string drawn.
HEIGHT	is the floating-point (REAL*4) height in inches at which the string is drawn.
STRING	is the character string to be drawn.
ANGLE	is the floating-point (REAL*4) angle in degrees of the character string (using a positive counterclockwise convention).
LENGTH	is the fullword integer (INTEGER*4) number of characters in STRING.
&RC4	is the exit taken for an unsuccessful return; STRING is not drawn. Either the parameters are in error (for instance, calling PSYM for the first time with X or Y equal to -0.0), or there is an error in a user-defined character set.

Table 33: Explanation of subroutine DLINE

CALL DLINE(XY,N,XO,SX,SFX,YO,YS,SFY,D1,D2,DB)

where:

X	real array of independent x-values
Y	real array of dependent y-values
N	integer number of pairs of (x,y) points
XO	real starting value of x-axis (units)
XS	real starting location of x-axis (inches)
SFX	real x-axis scale factor (units/inch)
YO	real starting value of y-axis (units)
YS	real starting location of y-axis (inches)
SFY	real y-axis scale factor (units/ inch)
D1	length of first dash (inches)
D2	length of second dash (inches)
D3	length of space between dashes (inches)

Subroutine plots a smooth dashed curve.

COMPUTER PROGRAM OF SUBROUTINE DLINE

Listing of DLINE at 11:55:38 on MAR 25, 1985 for CCid=HEIJ Page 1

```
      1            SUBROUTINE DLINE(X,Y,N,X0,XS,SFX,Y0,YS,SFY,D1,D2,DB)
      2            DIMENSION X(N),Y(N)
      3            COMMON/BLKA/XP(101),YP(101),M,MM
      4            M=N
      5            MM=M-1
      6            DO 10 I=1,N
      7            XP(I)=XS+(X(I)-X0)/SFX
      8            YP(I)=YS+(Y(I)-Y0)/SFY
      9       10   CONTINUE
     10            CALL SPLINE
     11            XI=XP(1)
     12            YI=YP(1)
     13            CALL PLOT(XI,YI,3)
     14            IFLAG=1
     15       20   ITER=1
     16            GO TO (30,40,50,60), IFLAG
     17       30   D=D1
     18            IPEN=2
     19            GO TO 70
     20       40   D=DB
     21            IPEN=3
     22            GO TO 70
     23       50   D=D2
     24            IPEN=2
     25            GO TO 70
     26       60   D=DB
     27            IPEN=3
     28       70   XF1=XI+D/2.
     29       80   XF=XF1-FX(XF1,XI,YI,D)/DFX(XF1,XI,YI,D)
     30            IF(XF.LE.XI) GO TO 85
     31            IF(ABS((XF1-XF)/XF).LT.0.00001) GO TO 90
     32            ITER=ITER+1
     33            IF(ITER.GT.20) GO TO 90
     34            XF1=XF
     35            GO TO 80
     36       85   X1=XI
     37            FX1=FX(X1,XI,YI,D)
     38            DX=D/2.
     39       86   XF=X1+DX
     40            IF(DX.LT.0.00001) GO TO 90
     41            DX=DX/2.
     42            FXF=FX(XF,XI,XI,D)
     43            IF(FX1*FXF.LT.0.) GO TO 86
     44            X1=XF
     45            FX1=FXF
     46            GO TO 86
     47       90   IF(XF.GT.XP(N)) XF=XP(N)
     48            YF=F(XF)
     49            CALL PLOT(XF,YF,IPEN)
     50            IF(XF.EQ.XP(N)) RETURN
     51            XI=XF
     52            YI=YF
     53            IFLAG=IFLAG+1
     54            IF(IFLAG.EQ.5) IFLAG=1
     55            GO TO 20
     56            END
     57       C
     58            SUBROUTINE SPLINE
```

Listing of DLINE at 11:55:38 on MAR 25, 1985 for CCid=HEIJ Page 2

```
      C
      C     Interpolation using cubic splines with fitted end points.
      C     Input:  X  Array of independent x-values
      C             Y  Array of dependent y-values
      C             N  Number of data points
      C             NM N-1
      C     Output: Q,R,S Coefficients of cubic spline equations
      C
            COMMON/BLKA/X(101),Y(101),N,NM
            COMMON/BLKB/Q(100),R(101),S(100)
            DIMENSION H(100),A(101),B(101),C(101),D(101),COEFF(4,5)
      C
      C     Coefficient matrices for end point cubics
      C
            INTEGER FLAG
            M=4
            IS=0
            FLAG=0
            MP=M+1
            MM=M-1
   10       DO 20 I=1,M
            II=I+IS
            COEFF(I,MP)=Y(II)
            COEFF(I,1)=1.
            DO 20 J=2,M
   20       COEFF(I,J)=COEFF(I,J-1)*X(II)
      C
      C     Gauss elimination to find A4 and B4
      C
            DO 30 K=1,MM
            KP=K+1
            DO 30 I=KP,M
            DO 30 J=KP,MP
   30       COEFF(I,J)=COEFF(I,J)-COEFF(I,K)*COEFF(K,J)/COEFF(K,K)
            IF(FLAG.NE.0) GO TO 40
            A4=COEFF(M,MP)/COEFF(M,M)
            FLAG=1
            IS=N-M
            GO TO 10
   40       B4=COEFF(M,MP)/COEFF(M,M)
      C
      C     Calculate H(I)
      C
            DO 50 I=1,NM
   50       H(I)=X(I+1)-X(I)
      C
      C     Coefficients of tridiagonal equations
      C
            A(1)=0.0
            B(1)=-H(1)
            C(1)=H(1)
            D(1)=3.*H(1)*H(1)*A4
            DO 60 I=2,NM
            IP=I+1
            IM=I-1
            A(I)=H(IM)
            B(I)=2.*(H(IM)+H(I))
            C(I)=H(I)
```

Listing of DLINE at 11:55:38 on MAR 25, 1985 for CCid=HEIJ Page 3

```
117       60    D(I)=3.*((Y(IP)-Y(I))/H(I)-(Y(I)-Y(IM))/H(IM))
118             A(N)=H(NM)
119             B(N)=-H(NM)
120             C(N)=0.0
121             D(N)=-3.*H(NM)*H(NM)*B4
122       C
123       C     Call Thomas algorithm to solve tridiagonal set
124       C
125             CALL TDMA(A,B,C,D,R,N)
126       C
127       C     Determine Q(I) and S(I)
128       C
129             DO 70 I=1,NM
130             IP=I+1
131             Q(I)=(Y(IP)-Y(I))/H(I)-H(I)*(2.*R(I)+R(IP))/3.
132       70    S(I)=(R(IP)-R(I))/(3.*H(I))
133             RETURN
134             END
135       C
136             SUBROUTINE TDMA(A,B,C,D,X,N)
137       C
138       C     Thomas algorithm
139       C
140             DIMENSION A(N),B(N),C(N),D(N),X(N),P(101),Q(101)
141             NM=N-1
142             P(1)=-C(1)/B(1)
143             Q(1)=D(1)/B(1)
144             DO 10 I=2,N
145             IM=I-1
146             DEN=A(I)*P(IM)+B(I)
147             P(I)=-C(I)/DEN
148       10    Q(I)=(D(I)-A(I)*Q(IM))/DEN
149             X(N)=Q(N)
150             DO 20 II=1,NM
151             I=N-II
152       20    X(I)=P(I)*X(I+1)+Q(I)
153             RETURN
154             END
155       C
156             FUNCTION F(Z)
157       C
158       C     Spline interpolation function.  Interpolation interval found
159       C     by bisection.
160       C
161             COMMON/BLKA/X(101),Y(101),N,NM
162             COMMON/BLKB/Q(100),R(101),S(100)
163             I=1
164             IF(Z.LT.X(1)) GO TO 30
165             IF(Z.GE.X(NM)) GO TO 20
166             J=NM
167       10    K=(I+J)/2
168             IF(Z.LT.X(K)) J=K
169             IF(Z.GE.X(K)) I=K
170             IF(J.EQ.I+1) GO TO 30
171             GO TO 10
172       20    I=NM
173       30    DX=Z-X(I)
174             F=Y(I)+DX*(Q(I)+DX*(R(I)+DX*S(I)))
```

Listing of DLINE at 11:55:38 on MAR 25, 1985 for CCid=HEIJ Page 4

```
175             RETURN
176             END
177       C
178             FUNCTION FX(Z,X0,Y0,D)
179             COMMON/BLKA/X(101),Y(101),N,NM
180             COMMON/BLKB/Q(100),R(101),S(100)
181             I=1
182             IF(Z.LT.X(1)) GO TO 30
183             IF(Z.GE.X(NM)) GO TO 20
184             J=NM
185          10 K=(I+J)/2
186             IF(Z.LT.X(K)) J=K
187             IF(Z.GE.X(K)) I=K
188             IF(J.EQ.I+1) GO TO 30
189             GO TO 10
190          20 I=NM
191          30 DX=Z-X(I)
192             FX=(Z-X0)**2+(Y(I)-Y0+DX*(Q(I)+DX*(R(I)+DX*S(I))))**2-D*D
193             RETURN
194             END
195       C
196             FUNCTION DFX(Z,X0,Y0,D)
197             COMMON/BLKA/X(101),Y(101),N,NM
198             COMMON/BLKB/Q(100),R(101),S(100)
199             I=1
200             IF(Z.LT.X(1)) GO TO 30
201             IF(Z.GE.X(NM)) GO TO 20
202             J=NM
203          10 K=(I+J)/2
204             IF(Z.LT.X(K)) J=K
205             IF(Z.GE.X(K)) I=K
206             IF(J.EQ.I+1) GO TO 30
207             GO TO 10
208          20 I=NM
209          30 DX=Z-X(I)
210             DFX=2.*(Z-X0)+2.*(Y(I)-Y0+DX*(Q(I)+DX*(R(I)+DX*S(I))))*
211            1 (Q(I)+DX*(2.*R(I)+DX*3.*S(I)))
212             RETURN
213             END
```

Table 34: Explanation of subroutine BBLINE

SUBROUTINE BBLINE (X,Y,N,XO,XS,SFX,YO,YS,SFY,L,J,H,K)

where:

X	real array of independent x-values
Y	real array of dependent y-values
N	integer number of pairs of (x,y) points
XO	real starting value of x-axis (units)
XS	real starting location of x-axis (inches)
SFX	real x-axis scale factor (units/inch)
YO	real starting value of y-axis (units)
YS	real starting location of y-axis (inches)
SFY	real y-axis scale factor (units/inch)
L	integer line type control parameter
	L=0 symbols plotted only
	L=1 curved line plotted with symbols
	L=2 curved line plotted without symbols
	L=-1 straight line plotted with symbols
	L=-2 straight line plotted without symbols
J	integer symbol control parameter
H	real symbol height
K	integer orientation parameter
	K>0 y is single-valued function of x
	K<0 x is single-valued function of y

- Subroutine plots a smooth curve

COMPUTER PROGRAM OF SUBROUTINE BBLINE

Listing of BBLINE at 11:55:46 on MAR 25, 1985 for CCid=HEIJ Page 1

```
      SUBROUTINE BBLINE(X,Y,N,X0,XS,SFX,Y0,YS,SFY,L,J,H,K)
C
C     PARAMETERS:
C         X  real array of independent x-values
C         Y  real array of dependent y-values
C         N  integer number of pairs of (x,y) points
C        X0  real starting value of x-axis (units)
C        XS  real starting location of x-axis (inches)
C       SFX  real x-axis scale factor (units/inch)
C        Y0  real starting value of y-axis (units)
C        YS  real starting location of y-axis (inches)
C       SFY  real y-axis scale factor (units/inch)
C         L  integer line type control parameter
C            L=0  symbols plotted only
C            L=1  curved line plotted with symbols
C            L=2  curved line plotted without symbols
C            L=-1 straight line plotted with symbols
C            L=-2 straight line plotted without symbols
C         J  integer symbol control parameter
C         H  real symbol height
C         K  integer orientation parameter
C            K>0  y is single-valued function of x
C            K<0  x is single-valued function of y
C
      DIMENSION X(N),Y(N)
      COMMON/BLKA/XP(101),YP(101),M,MM
      M=N
      MM=M-1
      DO 10 I=1,N
      XP(I)=XS+(X(I)-X0)/SFX
      YP(I)=YS+(Y(I)-Y0)/SFY
      IF(K.GT.0.OR.L.LE.0) GO TO 10
      TEMP=XP(I)
      XP(I)=YP(I)
      YP(I)=TEMP
   10 CONTINUE
      IF(L.LE.0) GO TO 40
      CALL SPLINE
      IF(K.GT.0) CALL PLOT(XP(1),YP(1),3)
      IF(K.LT.0) CALL PLOT(YP(1),XP(1),3)
      IF(K.GT.0.AND.L.EQ.1) CALL SYMBOL(XP(1),YP(1),H,J,0.,-1)
      IF(K.LT.0.AND.L.EQ.1) CALL SYMBOL(YP(1),XP(1),H,J,0.,-1)
      DO 30 I=2,N
      IM=I-1
      DX=(XP(I)-XP(IM))/20.
      DO 20 JJ=1,20
      XX=XP(IM)+JJ*DX
      YY=P(XX)
      IF(K.GT.0) CALL PLOT(XX,YY,2)
      IF(K.LT.0) CALL PLOT(YY,XX,2)
   20 CONTINUE
      IF(K.GT.0.AND.L.EQ.1) CALL SYMBOL(XP(I),YP(I),H,J,0.,-1)
      IF(K.LT.0.AND.L.EQ.1) CALL SYMBOL(YP(I),XP(I),H,J,0.,-1)
   30 CONTINUE
      RETURN
   40 CALL PLOT(XP(1),YP(1),3)
      IF(L.EQ.0.OR.L.EQ.-1) CALL SYMBOL(XP(1),YP(1),H,J,0.,-1)
      DO 50 I=2,N
      IF(L.LT.0) CALL PLOT(XP(I),YP(I),2)
      IF(L.EQ.0) CALL PLOT(XP(I),YP(I),3)
      IF(L.EQ.0.OR.L.EQ.-1) CALL SYMBOL(XP(I),YP(I),H,J,0.,-1)
   50 CONTINUE
      RETURN
      END
```

Table 35: Explanation of subroutine NUMBER (57)

NUMBER

Purpose

This subroutine will plot a floating-point number.

How To Use

CALL NUMBER(X,Y,HT,FLOAT,THETA,N)

where:

(X,Y) are the coordinates of the lower left-hand corner of the number.

HT is the height of the number. (For more information, refer to the SYMBOL routine description.)

FLOAT is the floating-point number to be drawn.

THETA is the angle.

N specifies the number of decimal digits to the right of the decimal point. N=0 puts a decimal point at the end of the number, N=-1 suppresses the decimal point. N should not be larger than 3. The number is truncated, not rounded. For example, if FLOAT=-17.795 and

N= 3, the characters -17.795 are drawn;
N= 0, the characters -17. are drawn;
N=-1, the characters -17 are drawn.

Example

This example would plot the number 12.3 at (5.3,6.2):

```
X=12.3
CALL NUMBER(5.3,6.2,0.21,X,0.0,1)
```

Restrictions

1. The integer portion of the number to be plotted must not exceed 7 characters.

2. NUMBER may not be used to plot integers directly. The integer must be converted to floating-point form and plotted with N=-1.

Table 36: Explanation of subroutine LEGEND

LEGEND (PMV,KF,KASO,NK,SL,SIGD,PSA,PSG,SIGFA,SIGFG)

- terms are parameters used in the computer program UBCEDEMA

A1.4 Operation of Computer Program

1) The computer programs UBCEDEMA, BBLINE and DLINE are compiled as follows:

```
#RUN   *FTN  SCARDS=UBCEDEMA+BBLINE+DLINE
```

The compiled programs are then stored under the temporary name - LOAD.

2) Execution of the programs using the data files EDA and PDA is as follows:

```
#RUN  -LOAD  4=EDA  5=PDA  7=-TABLES  9=-PLOTS
```

The tabulated and graphical output is stored in the temporary files - TABLES and - PLOTS, respectively.